Contract No. N62269-85-R-0278
Report No. NADC-91069-60

FINAL REPORT FOR THE CH-46 & OH-58 TRANSMISSION STRESS WAVE ANALYSIS

David B. Board
DIAGNOSTIC EQUIPMENT DEVELOPMENT, INC.
6899 N.E. 7th Ave.
Boca Raton, FL 33487

30 DECEMBER 1990

FINAL REPORT

Approved for Public Release; Distribution is Unlimited

Prepared for
Air Vehicle and Crew Systems Technology Department (Code 6061)
NAVAL AIR DEVELOPMENT CENTER
Warminster, PA 18974-5000

Sponsoring Organization
Power Systems Division (Code 2720)
DAVID TAYLOR RESEARCH CENTER
Annapolis, MD 21402-5067

NOTICES

REPORT NUMBERING SYSTEM — The numbering of technical project reports issued by the Naval Air Development Center is arranged for specific identification purposes. Each number consists of the Center acronym, the calendar year in which the number was assigned, the sequence number of the report within the specific calendar year, and the official 2-digit correspondence code of the Command Officer or the Functional Department responsible for the report. For example: Report No. NADC-88020-60 indicates the twentieth Center report for the year 1988 and prepared by the Air Vehicle and Crew Systems Technology Department. The numerical codes are as follows:

CODE	OFFICE OR DEPARTMENT
00	Commander, Naval Air Development Center
01	Technical Director, Naval Air Development Center
05	Computer Department
10	AntiSubmarine Warfare Systems Department
20	Tactical Air Systems Department
30	Warfare Systems Analysis Department
40	Communication Navigation Technology Department
50	Mission Avionics Technology Department
60	Air Vehicle & Crew Systems Technology Department
70	Systems & Software Technology Department
80	Engineering Support Group
90	Test & Evaluation Group

PRODUCT ENDORSEMENT — The discussion or instructions concerning commercial products herein do not constitute an endorsement by the Government nor do they convey or imply the license or right to use such products.

Reviewed By: _____ Date: _____
Contracting Officer's Technical Representative (COTR)
or
Point Of Contact (POC)

Reviewed By: _____ Date: _____
Branch Head

Reviewed By: _____ Date: _____
Division Head

REPORT DOCUMENTATION PAGE

Form Approved
OMB No 0704-0188

1. AGENCY USE ONLY (Leave blank)	2. REPORT DATE	3. REPORT TYPE AND DATES COVERED
	30 Dec. 1990	Final

4. TITLE AND SUBTITLE
FINAL REPORT FOR THE CH-46 & OH-58 TRANSMISSION STRESS WAVE ANALYSIS

5. FUNDING NUMBERS
Contract No.
N62269-85-R-0278

6. AUTHOR(S)
David B. Board

7. PERFORMING ORGANIZATION NAME(S) AND ADDRESS(ES)
DIAGNOSTIC EQUIPMENT DEVELOPMENT, INC.
6899 N.E. 7th Ave.
Boca Raton, FL 33487

8. PERFORMING ORGANIZATION REPORT NUMBER

9. SPONSORING/MONITORING AGENCY NAME(S) AND ADDRESS(ES)
Air Vehicle and Crew Systems Technology Department
(Code 6061)
NAVAL AIR DEVELOPMENT CENTER
Warminster, PA 18974-5000

10. SPONSORING/MONITORING AGENCY REPORT NUMBER
NADC-91069-60

11. SUPPLEMENTARY NOTES
Approved for Public Release; Distribution is Unlimited

12a. DISTRIBUTION/AVAILABILITY STATEMENT

12b. DISTRIBUTION CODE

13. ABSTRACT (Maximum 200 words)

This report documents the results of testing on two types of helicopter transmissions. The analysis of high frequency stress wave data indicates various types of problems that were detected with gears and bearings in both CH-46 and OH-58 gear boxes. The types of discrepancies detected include shaft misalignment as a function of flight loads; planet gear/bearing assembly damage, sun gear damage, wear-in phenomena, and the presence of particulate debris in the lubrication system.

14. SUBJECT TERMS	15. NUMBER OF PAGES
	16. PRICE CODE

17. SECURITY CLASSIFICATION OF REPORT	18. SECURITY CLASSIFICATION OF THIS PAGE	19. SECURITY CLASSIFICATION OF ABSTRACT	20. LIMITATION OF ABSTRACT
Unclassified	Unclassified	Unclassified	SAR

STRESS WAVE ANALYSIS OF CH-46 & OH-58 HELICOPTER TRANSMISSIONS

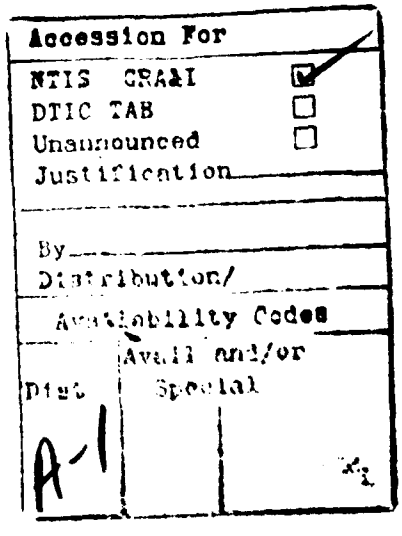

LIST OF FIGURES

LIST OF FIGURES

LIST OF FIGURES

LIST OF TABLES

1.0 EXECUTIVE SUMMARY

This report documents the results of testing on two types of helicopter transmissions. The analysis of high frequency stress wave data indicates various types of problems that were detected with gears and bearings in both CH-46 and OH-58 gearboxes. The types of discrepancies detected include shaft misalignment as a function of flight loads; planet gear/bearing assembly damage, sun gear damage, wear-in phenomena, and the presence of particulate debris in the lubrication system.

The OH-58 data analyzed in this report was obtained from a test cell transmission operated by NASA Lewis as part of a program to evaluate advanced lubricants. The high frequency stress wave sensors and tape recorders were provided by NADC Warminster but were installed and data recorded by NASA Lewis personnel.

2.0 INTRODUCTION

This section will discuss the operating principles of Stress Wave Analysis and define some of the terms associated with its use. It will also describe the objectives of this project and the instrumentation system used to record and analyze the stress wave data.

2.1 Stress Wave Analysis

Stress Wave ANalysis (SWAN) is an instrumentation technique for the direct measurement of friction and shock in rotating machinery. This technique is relatively insensitive to background levels of sound and vibration, and has shown the ability, in a test environment, to detect impending failure of gears and bearings in helicopter transmissions and drive shaft bearings. The SWAN technique provides a quantitative measure of friction and shock energy which is related to the amount of damage in gears and bearings (see Figures 1 & 2).

This computed Stress Wave Energy (SWE) can be recorded for trending. When SWE increases dramatically, it signifies a distressed operating condition and possible impending failure. This allows maintenance personnel to trend SWE readings and schedule their corrective actions for both maximum efficiency and minimum downtime. Early detection of abnormal Stress Wave Energy levels can provide significant benefits by:

1.) Avoiding unscheduled downtime due to unforseen bearing and gear failures.

2.) Eliminating unnecessary preventive maintenance (such as time based precautionary overhauls.

3.) Alerting maintenance personnel to situations which cause premature failure (such as misalignment and contaminated lubricant).

4.) Avoiding catastrophic failure resulting in serious secondary damage and safety hazards.

SWAN can also be an effective tool at the depot level. Here it can be used to localize damaged components within a gearbox prior to disassembly, and to provide a final check of overhauled units, thus reducing infant mortality rates. This fault location can be accomplished by using the time history of stress wave amplitude, or stress wave pulse train. The stress wave pulse train can be analyzed to determine its spectral content (pulse amplitudes as a function of the repetitive frequencies at which they occur). This type of algorithm is called the Stress Wave Power Spectral Density (SWPSD).

STRESS WAVE ANALYSIS (SWAN)

Stress Wave Analysis is an electronic means of detecting and analyzing sounds traveling through a machine's structure at ultrasonic frequencies. This structure borne ultrasound (or "Stress Wave") is caused by friction and shock events between the moving parts of a machine. It is detected, separated from background sources of noise and vibration, and then analyzed by a digital processor (see figure 1).

The digital analysis consists of computing both the amplitude and the energy content of the detected stress waves. The amplitude (or peak level) of a stress wave, is a function of the intensity of a single friction or shock event. The Stress Wave Energy is a computed value which considers the amplitude, shape, duration, and rates of all friction and shock events that occur during a reference time interval.

In a spalled ball bearing for example, the peak level of the detected stress waves is primarily a function of spall depth, while the Stress Wave Energy is a function of spall area (size), as shown in figure 2.

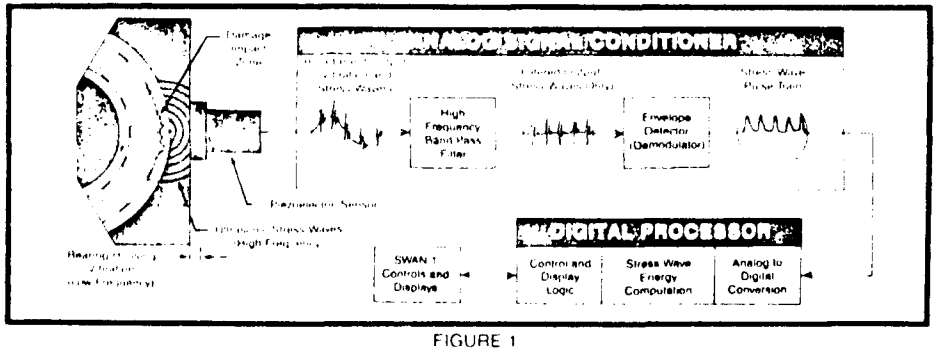

FIGURE 1
SWAN - 1 SCHEMATIC

STRESS WAVE ANALYSIS TECHNIQUE

Stress waves are detected by a specially designed sensor which must be firmly mounted onto a machine's structure. The stress waves enter the sensor and excite a piezoelectric crystal which converts them into an electrical signal. This signal is then amplified and filtered (to remove unwanted sound and vibration components) by the Analog Signal Conditioner (ASC) in the SWAN-1. The output of the ASC is a series of stress wave pulses that represent a time history of individual friction and shock events in the monitored machine. This Stress Wave Pulse Train is then analyzed by the SWAN-1 digital processor to determine the peak level and the energy content of the detected stress waves. The computed Stress Wave Energy is digitally displayed on the SWAN-1 control panel, so that it can be recorded for comparison with identical machines, or for trending over a period of time. When the Stress Wave Energy increases to between 5 and 10 times its normal value, it signifies a distressed operating condition and possible impending failure.

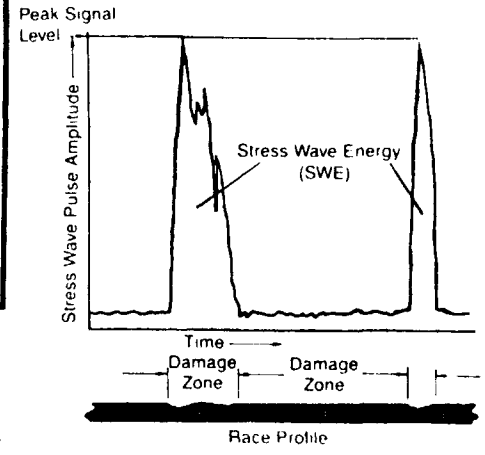

Where
Peak Signal Level is a Function of
- Impact Velocity
- Damage Depth

And
Stress Wave Energy is a Function of
- Impact Velocity
- Damage Depth
- Damage Size/Area

FIGURE 2
STRESS WAVE PULSE AMPLITUDE
& ENERGY CONTENT

Report No. NADC-91069-60
Contract No. N62269-85-R-0278

Both SWE and SWPSD have been successfully used to diagnose the condition of gears and bearings in numerous types of mechanical drive trains, including automotive and helicopter transmissions. SWE has the advantage of being a highly trendable symptom that can be employed to both detect and quantify a broad range of damage levels in gear/bearing systems. It is also highly sensitive to lubrication quality, lubricant contamination, and abnormal preloads due to such causes as misalignment or improper build-up during overhaul/repair. SWPSD has the advantage of being extremely sensitive to very small (early) levels of damage and the capability to localize the fault to a particular gear or bearing, and even to an individual race or rolling element within a bearing.

2.2 Test objectives

The original objective of this project was to collect and analyze stress wave data from 6 CH-46 aircraft over a period of several months for two purposes:

1.) To investigate some anomalous stress wave data previously acquired from the aft transmission input pinion of an aircraft at Cherry Point.

2.) Obtain sufficient baseline data to establish caution and warning thresholds on selected critical drive train components.

After several years of attempting to gather data from operational aircraft, data had been obtained from only two aircraft. It was decided that the baseline data collection objective was not feasible within the program budget. The data from two H-46 aircraft was employed to investigate the input pinion anomaly.

In place of the baseline data from operational aircraft, sensors were installed and data collected from an OH-58 main rotor transmission under test for just over 183 operating hours in a load cell. This testing was being conducted under separate funding for the evaluation of advanced lubricants.

The objective of this OH-58 data collection and analysis effort was to see if the Stress Wave Analysis parameters of Stress Wave Energy (SWE) and Stress Wave Power Spectral Density (SWPSD) could be correlated with naturally occurring gear and bearing damage. The stress wave analysis was conducted "in-the-blind" with no information provided on discrepant conditions encountered during the testing and data collection.

Thus the revised program objectives became:

1.) To investigate some anomalous stress wave data previously acquired from the aft transmission input pinion of an

H-46 aircraft at Cherry Point.

2.) To see if the Stress Wave Analysis parameters could be correlated with naturally occurring gear and bearing damage.

2.3 Instrumentation

All the data collection efforts and instrumentation for this project were supplied by government personnel.

The same basic instrumentation was used for data collection on both of the H-46 aircraft and from the H-58 transmission in the test cell. This data collection hardware consisted stress wave sensors with built-in amplifiers powered by an external power supply and a Wide Band Group II FM tape recorder capable of recording data from DC to 62,000 Hz.

For some unknown reason, data collection personnel changed the gain of the tape recorder between CH-46 aircraft #01 and #04. This was done for all channels except the one used for recording the sensor located on the transmission input pinion. This means that making a direct comparison between SWE levels on these two aircraft is not valid for any sensor location other than the transmission input pinion. This data collection procedural change does not significantly effect the spectral analysis of the stress wave pulse train, nor the relative levels of SWE as a function of torque on aircraft #01.

Data was analyzed by playing the taped stress wave sensor signal into a SWAN-1 BEARING/GEAR ANALYZER which computed the Stress Wave Energy and provided the filtered and demodulated Stress Wave Pulse Train signal for spectral analysis. The SWE data was processed by a personal computer spreadsheet, and the SWPT was processed into the frequency domain using a 400 line digital FFT spectrum analyzer.

3.0 CH-46 Aft Transmission and Mix Box Data Analysis

3.1 Test Description and Sensor Locations.

As previously mentioned, the H-46 testing was intended to determine whether or not abnormal fatigue stresses were being generated on the aft rotor transmission input pinion or its associated quill shaft between the mix box and the aft rotor transmission. Data was acquired from only two aircraft at 11 different sensor locations. Only five of the sensor locations provided data relevant to quill shaft loading question and only data from these five sensor locations has been analyzed under this contract. The five sensor locations are:

1. the left side (#1) input pinion to the mix box (engine combining transmission) (sensor location #7),

2. the right side (#2) input pinion to the mix box (engine combining transmission) (sensor location #5),

3. the left side (#1) mix box idler gear shaft (sensor location #8),

4. the right side (#2) mix box idler gear shaft (sensor location #6), and

5. the aft rotor transmission input pinion housing (sensor location #1).

Data at all sensor locations on both aircraft was acquired at 8 different flight conditions with corresponding torque levels that ranged from 17% to 68% of maximum torque. These 8 Flight conditions are described as follows:

1. Ground flat pitch - 17% torque

2. Light on gear - 28% torque

3. Hover in ground effect - 68% torque

4. Rolling with nose gear on ground - 25% torque

5. Rolling with nose gear off the ground - 42% torque

6. Forward flight at 20 knots - 60% torque

7. Forward flight at 60 knots - 50% torque

8. Forward flight at 100 knots - 58% torque

3.2 Data Analysis

Data analysis consisted of calculating the mean and standard deviation for computed SWE values on each aircraft, at each torque level, at each of the five sensor locations previously described. Tables I through V provide a summary listing of this SWE statistical analysis. Data analysis also included plotting one or more Power Spectral Density plots for each sensor location and torque combination on each of the aircraft. All the CH-46 spectral data is contained in Appendix A to this report.

3.2.1 Previous Experience

As discussed above in section 2.2, some anomalous stress wave data had been acquired, using the SWAN-1 analyzer, from an aircraft at Cherry Point, prior to this project. Figure 3 summarizes the anomaly encountered during that prior effort (in this report the aircraft is assigned an ID number of "00").

The data acquired from aircraft 00 was limited to SWE readings at three sensor locations: the two mixbox input pinions and the aft transmission input pinion. Data was acquired at three torque levels: 17%, 49%, and 57%. These torque levels correspond to a flat pitch ground run (17%), light on gear with nose gear off the ground (49%), and hover In Ground Effect (IGE) at a torque of 57%. The torque mismatch between engines did not exceed 2% and did not contribute significantly to differences in SWE readings.

The differences that do exist between the #1 and #2 input pinions are small in terms of the SWE variation that would indicate significant gear or bearing degradation. These differences are associated with the normal variations in gear, bearing, and build-up tolerances.

The "peaking" of the transmission pinion SWE at 49% torque, relative to its lower values at 17% and 57% is unusual. It would be expected to increase smoothly with increasing torque levels, as did the SWE at both of the input pinions. The source of this elevated SWE is unknown but may be indicative of an undesirable operating condition.

The data acquired under this effort from aircraft 01 and 04 was analyzed to see if the "peaking" of the transmission pinion SWE at less than max torque was present, and if so, what SWPSD changes could be associated with this phenomenon.

3.2.2 Aircraft 01 and 04

3.2.2.1 Stress Wave Energy Measurements

Figures 4 and 5 show the SWE vs. Torque for the same sensor locations on aircraft #01 and #04. These figures show that aircraft #04 did exhibit a "peaking" characteristic of the

XDCR	COND.	SENS.	T-X	A/C 04 STRESS WAVE ENERGY MEAN	A/C 04 STRESS WAVE ENERGY SIGMA	A/C 04 STRESS WAVE ENERGY M + 3 SIG	A/C 04 STRESS WAVE ENERGY SIG/MEAN	A/C 01 STRESS WAVE ENERGY MEAN	A/C 01 STRESS WAVE ENERGY SIGMA	A/C 01 STRESS WAVE ENERGY M + 3 SIG	A/C 01 STRESS WAVE ENERGY SIG/MEAN
1.	1 C		17	72434	1224	76107	0.0169	125944	2437	133254	0.0193
		4	25	118277	2134	124678	0.0180	121356	2954	130219	0.0243
		2	28	101171	2330	108162	0.0230	130512	2164	137003	0.0166
		5	42	135795	65237	331505	0.4804	111563	934	114363	0.0084
		7	50	50359	2695	58445	0.0535	118980	2053	125139	0.0173
		8	58	55074	7130	76465	0.1295	101161	2062	107346	0.0204
		6	60	38143	2140	44563	0.0561	87171	10257	117942	0.1177
		3	68	41556	1344	45589	0.0323	88965	1947	94806	0.0219

TABLE I

CH-46 STATISTICAL SWE DATA, SENSOR #1

XDCR	COND.	SENS.	T-%	A/C 04 STRESS WAVE ENERGY MEAN	A/C 04 STRESS WAVE ENERGY SIGMA	A/C 04 STRESS WAVE ENERGY M + 3 SIG	A/C 04 STRESS WAVE ENERGY SIG/MEAN		A/C 01 STRESS WAVE ENERGY MEAN	A/C 01 STRESS WAVE ENERGY SIGMA	A/C 01 STRESS WAVE ENERGY M + 3 SIG	A/C 01 STRESS WAVE ENERGY SIG/MEAN
5	1 B	17	31656	979	34592	0.0309	31656		3380	503	4889	0.1489
		4	25	45579	282	46424	0.0062		2584	348	3628	0.1346
		2	28	40326	1918	46078	0.0476		1967	525	3544	0.2671
		5	42	31391	457	32763	0.0146	31391	1163	185	1717	0.1588
		7	50	28451	244	29182	0.0086		601	66	800	0.1100
		8	58	30759	1145	34196	0.0372		437	24	508	0.0538
		6	60	38203	1849	43750	0.0484		512	26	590	0.0508
		3	68	34832	758	37107	0.0218	34832	361	23	430	0.0641
5	1 C	17		242093	9477	270523	0.0391		58869	2680	66909	0.0455
		4	25	318626	1560	324205	0.0058		55402	2598	63196	0.0469
		2	28	295005	13595	335788	0.0461		49987	4599	63783	0.0920
		5	42	229296	2894	237980	0.0126		44402	1633	49302	0.0368
		7	50	211350	1634	216253	0.0077		34106	990	37077	0.0290
		8	58	221571	5736	239779	0.0259		31977	407	33198	0.0127
		6	60	263105	9853	292663	0.0374		33689	476	35116	0.0141
		3	68	248022	4072	260238	0.0164		31135	275	31959	0.0088

TABLE II

CH-46 STATISTICAL SWE DATA, SENSOR #5

XDCR	COND.	SENS.	T-X	A/C 04 STRESS WAVE ENERGY MEAN	SIGMA	M + 3 SIG	SIG/MEAN	A/C 01 STRESS WAVE ENERGY MEAN	SIGMA	M + 3 SIG	SIG/MEAN
6	1 B		17	14799	276	15626	0.0186	19925	3158	29398	0.1585
		4	25	21387	536	22996	0.0251	12107	3565	22802	0.2945
		2	28	21330	717	23481	0.0336	20154	3688	31218	0.1830
		5	42	18608	368	19711	0.0198	6158	1364	10249	0.2215
		7	50	21177	213	21817	0.0101	3316	731	5507	0.2203
		8	58	21511	360	22590	0.0167	3632	405	4846	0.1114
		6	60	18993	255	19759	0.0134	2791	946	5630	0.3392
		3	68	20343	509	21870	0.0250	796	241	1519	0.3027
6	1 C		17	129058	1399	133255	0.0108	148337	17798	201731	0.1200
		4	25	163853	3770	175163	0.0230	113720	19473	172140	0.1712
		2	28	166643	4377	179773	0.0263	152350	19481	210794	0.1279
		5	42	149133	2078	155366	0.0139	75638	7581	98381	0.1002
		7	50	163611	1204	167224	0.0074	57310	5128	72693	0.0895
		8	58	165203	1911	170636	0.0110	60988	3023	70072	0.0497
		6	60	150984	1303	154892	0.0086	55815	5503	72322	0.0986
		3	69	158074	2127	164454	0.0135	40381	1875	46005	0.0464

TABLE III

CH-46 STATISTICAL SWB DATA, SENSOR #6

XDCR	COND.	SENS.	T-k	A/C 04 STRESS WAVE ENERGY MEAN	SIGMA	M + 3 SIG	SIG/MEAN	A/C 01 STRESS WAVE ENERGY MEAN	SIGMA	M + 3 SIG	SIG/MEAN
7	1 B		17	16656	382	17803	0.0229	859	31	951	0.0358
		4	25	30073	767	32373	0.0255	1748	184	2299	0.1051
		2	28	35763	791	38135	0.0221	1947	169	2514	0.0972
		5	42	45360	1448	49702	0.0319	3126	100	3427	0.0321
		7	50	34711	773	37031	0.0223	3178	96	3467	0.0302
		8	58	30996	1185	34549	0.0382	3090	85	3344	0.0274
		6	60	29285	1146	32722	0.0391	3174	196	3760	0.0616
		3	68	26016	687	28078	0.0264	2524	1491	6997	0.5907
7	1 C		17	131606	2000	137607	0.0152	40976	408	42200	0.0100
		4	25	210123	4108	222447	0.0196	50803	1283	54666	0.0253
		2	28	239925	4336	252933	0.0181	52637	747	54879	0.0142
		5	42	297035	8369	322143	0.0282	58884	741	61106	0.0126
		7	50	237985	4456	251354	0.0187	58870	511	60404	0.0087
		8	58	217223	6894	237906	0.0317	56545	495	60031	0.0085
		6	60	207509	6036	225618	0.0291	59024	1389	63190	0.0235
		3	68	189075	3713	200215	0.0196	55573	732	57769	0.0132

TABLE IV

CH-46 STATISTICAL SWE DATA, SENSOR #7

XDCR	COND.	SENS.	T-X	A/C 04 STRESS WAVE ENERGY MEAN	SIGMA	M + 3 SIG	SIG/MEAN	A/C 01 STRESS WAVE ENERGY MEAN	SIGMA	M + 3 SIG	SIG/MEAN
8	1	8	17	17410	217	18060	0.0125	2096	561	3778	0.2676
		4	25	21172	1026	24251	0.0485	7009	817	9460	0.1166
		2	28	20576	2394	27757	0.1163	7684	770	9993	0.1002
		5	42	19171	417	20423	0.0218	3907	1023	6974	0.2618
		7	50	21463	424	22734	0.0197	4258	668	6262	0.1568
		8	58	22404	317	23356	0.0142	4043	247	4785	0.0612
		6	60	21376	771	23689	0.0361	3739	576	5467	0.1541
		3	68	20318	1696	25405	0.0835	1469	256	2237	0.1744
8	1	C	17	97606	45753	234865	0.4688	47614	14813	92055	0.3111
		4	25	164370	6086	182628	0.0370	80808	4737	95019	0.0586
		2	28	160741	13900	202442	0.0865	84949	4244	97680	0.0500
		5	42	151825	2366	158923	0.0156	62841	5915	80585	0.0941
		7	50	166044	2151	172496	0.0130	64246	4807	78666	0.0748
		8	58	171548	1503	176058	0.0088	63969	1274	67792	0.0199
		6	60	163135	3690	174174	0.0226	62044	3339	72061	0.0538
		3	68	157509	9730	186697	0.0618	48543	1725	53717	0.0355

TABLE V

CH-46 STATISTICAL SWE DATA, SENSOR #8

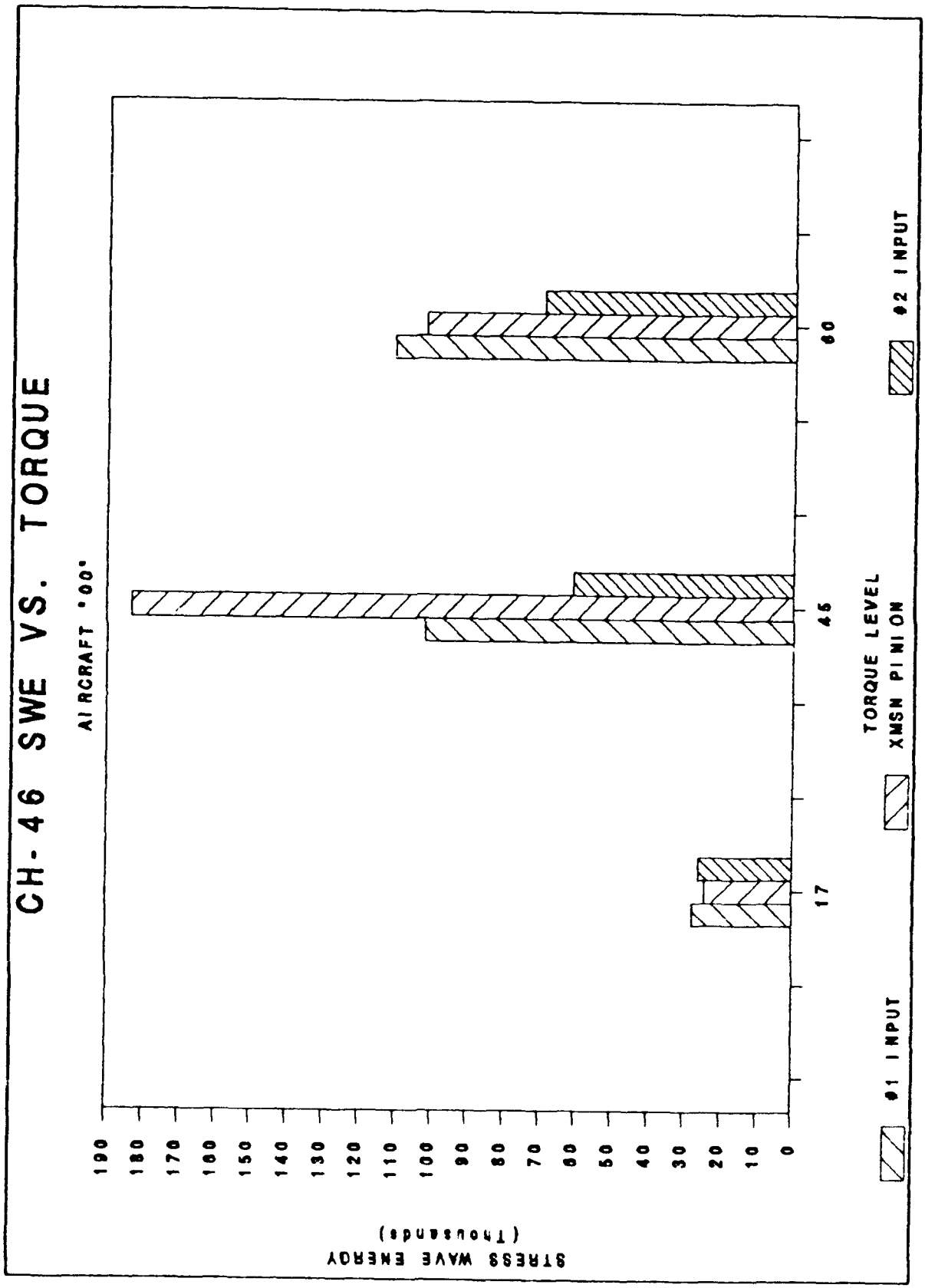
CH-46 SWE VS. TORQUE
AIRCRAFT '00'
STRESS WAVE ENERGY
(Thousands)
190
180
170
160
150
140
130
120
110
100
90
80
70
60
50
40
30
20
10
0
60
45
17
TORQUE LEVEL
XMSN PINION
#1 INPUT
#2 INPUT

Figure 3

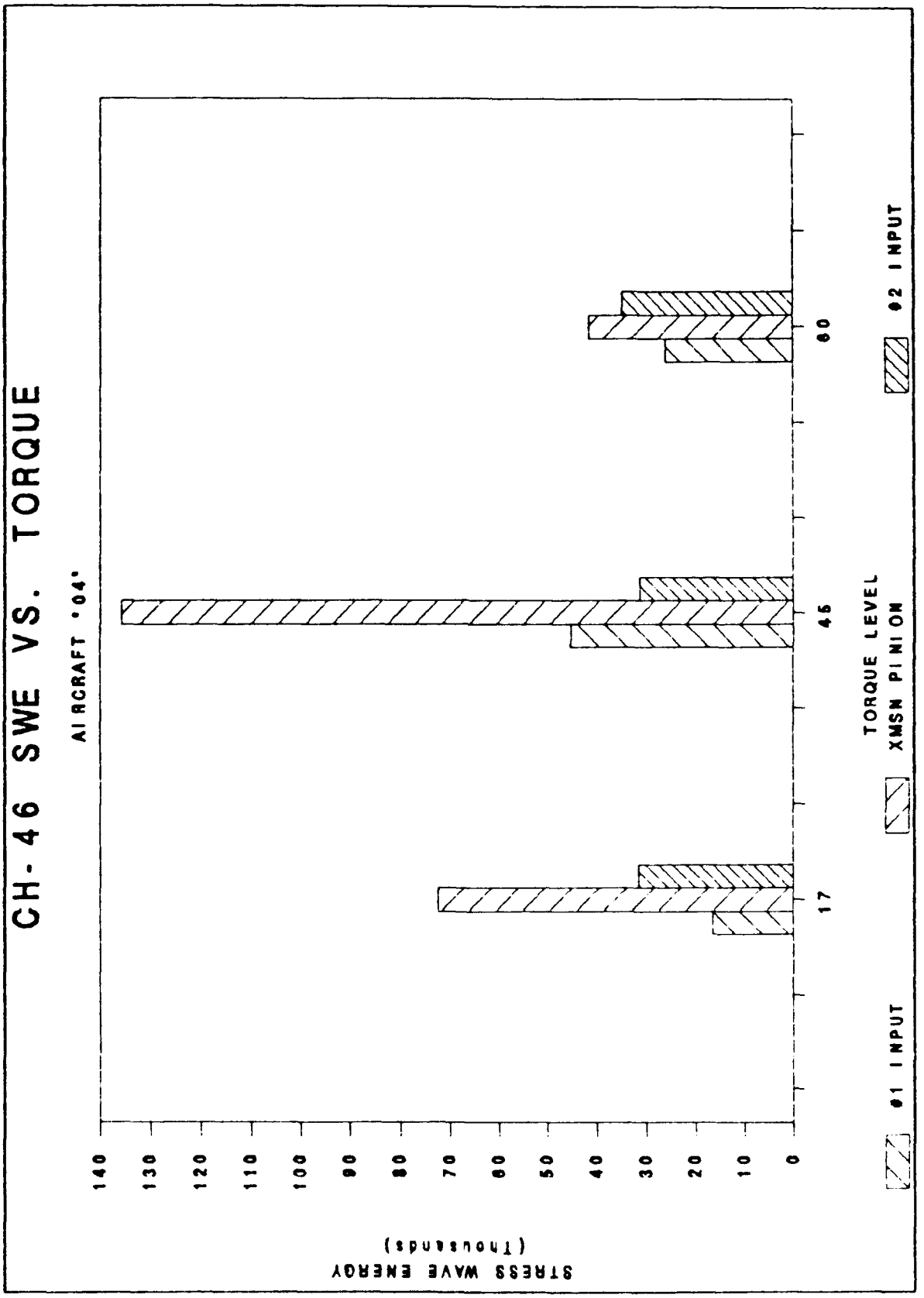
CH-46 SWE VS. TORQUE
AIRCRAFT '04'
STRESS WAVE ENERGY
(Thousands)
140
130
120
110
100
90
80
70
60
50
40
30
20
10
0
17
45
60
TORQUE LEVEL
XMSN PINION
#1 INPUT
#2 INPUT

Figure 4

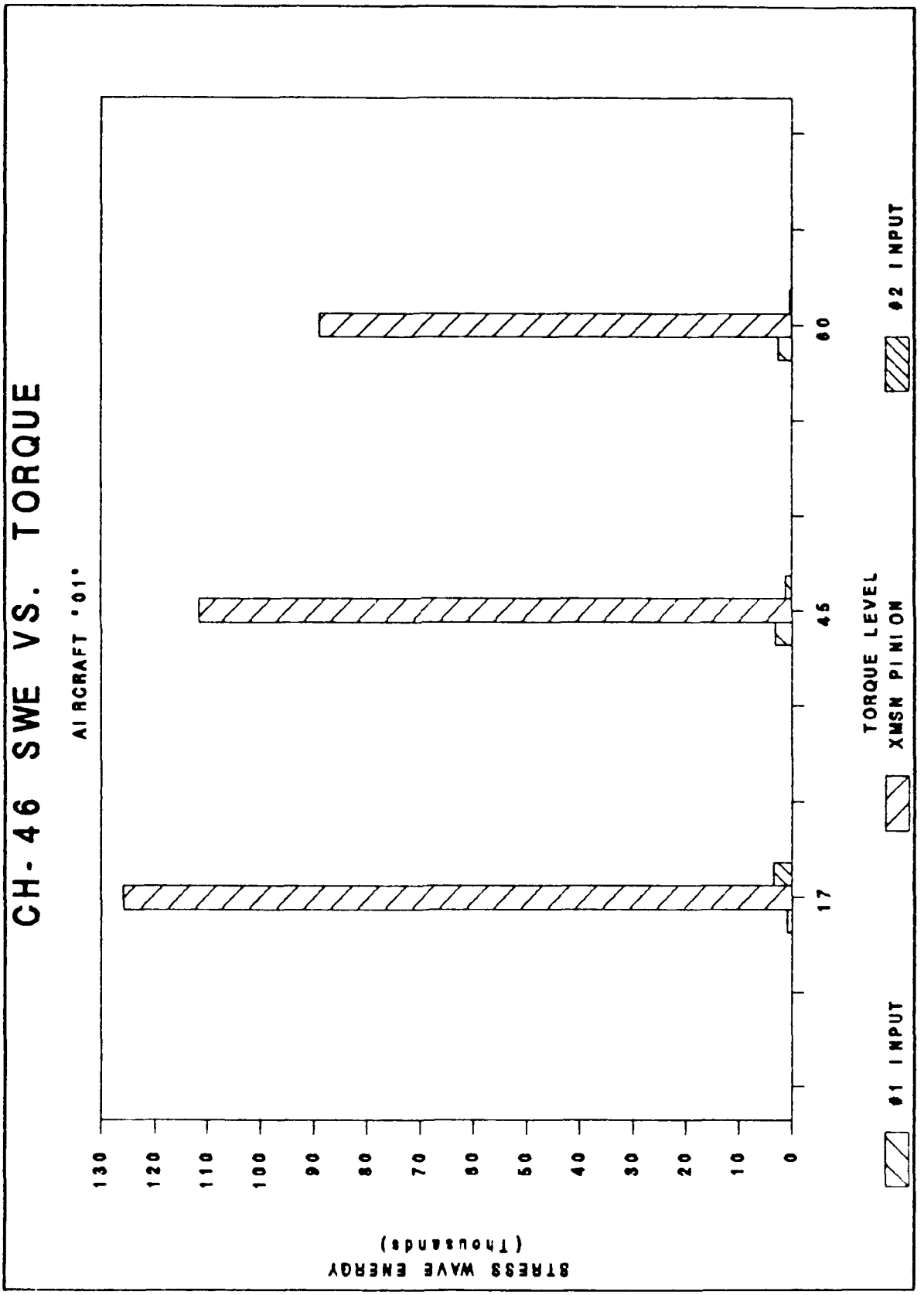
CH-46 SWE VS. TORQUE
AIRCRAFT '01'
STRESS WAVE ENERGY
(Thousands)
130
120
110
100
90
80
70
60
50
40
30
20
10
0
17
45
60
TORQUE LEVEL
XMSN PINION
#1 INPUT
#2 INPUT

Figure 5

transmission pinion SWE when the aircraft was taxiing with the nose gear off the ground, but that aircraft #01 did not. Aircraft #01 had its maximum transmission pinion SWE at its minimum torque, which is just as odd as having it at a mid-level torque. In addition, due to an erroneous gain setting on the instrumentation tape recorder, the SWE values for the mixbox input pinions of aircraft #01 are significantly less than the corresponding values on aircraft #00 and #04.

Figures 6 through 10 provide a more detailed picture of the SWE vs. torque characteristics at each sensor location on both aircraft. Figure 6 shows the mean SWE reading obtained from the sensor located on the transmission input pinion housing at each flight condition/torque level. The first notable feature in this bar graph is that the SWE for both aircraft is highest at the lower levels of torque. This characteristic is most apparent on aircraft #01. The SWE fluctuations from one torque level to another, are most pronounced on aircraft #04 which has its highest SWE at 42% torque when the aircraft is taxiing with its nose gear approximately 3 feet off the ground. Aircraft #04 has SWE highs that are more than 3.5 times as much as its lows. Finally it should be noted that aircraft #01 had generally higher SWE readings than aircraft #04. This is particularly evident at torques of 50% or more, where aircraft 01 generates slightly more than twice as much SWE at the transmission input pinion sensor location.

Figures 7 and 8 illustrate the mean SWE readings obtained from the sensors located on the input pinion housings of the mixbox engine combining transmission. Data was acquired from these sensor locations at two sensitivity settings on the SWAN-1 instrument, but the readings at sensitivity C are probably most accurate since the recorded stress wave signals were closest to the middle of the instruments dynamic range for both aircraft. Figure 7 shows the SWE detected on the #1 input pinion and Figure 8 shows the SWE detected on the #2 input pinion.

The difference between SWE levels on aircraft #01 and #04 is primarily due to the difference in tape recorder gain settings. However, it is clear that the aircraft #04 SWE fluctuated more dramatically as a function of torque, than it did on aircraft #01. It should also be noted that the maximum and minimum values of SWE occur at different torque levels on each input pinion, and that this is true for both aircraft.

Figures 9 and 10 show the mean SWE readings obtained from the sensors located on the idler gear housings of the mixbox. Data was also acquired from these sensor locations at two sensitivity settings on the SWAN-1 instrument, but the readings at sensitivity C are probably most accurate due to the previously mentioned dynamic range considerations. Figure 9 shows the SWE detected on the #1 idler gear and Figure 10 shows the SWE detected on the #2 side of the mixbox.

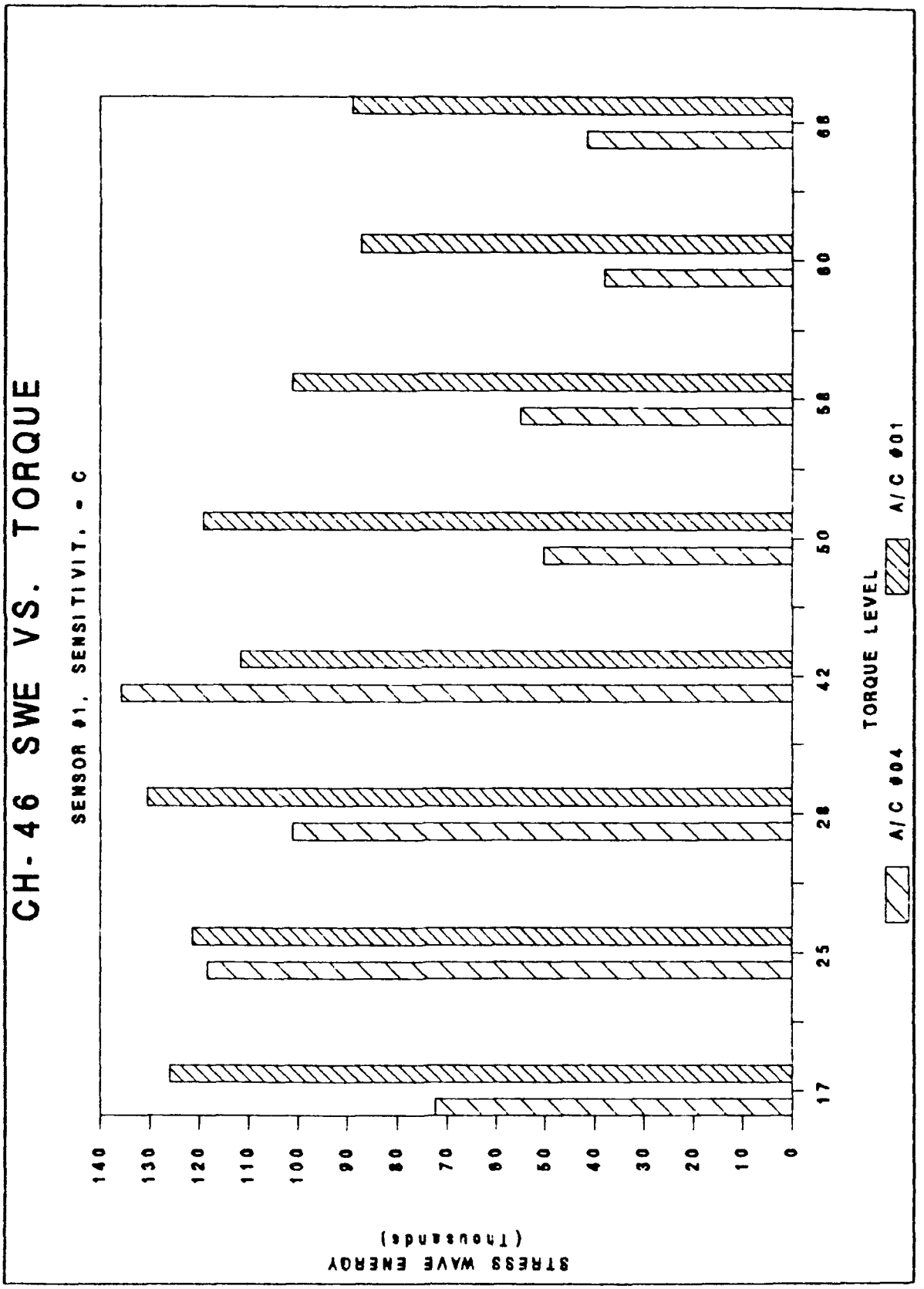

Figure 6 - AFT ROTOR TRANSMISSION INPUT PINION HOUSING

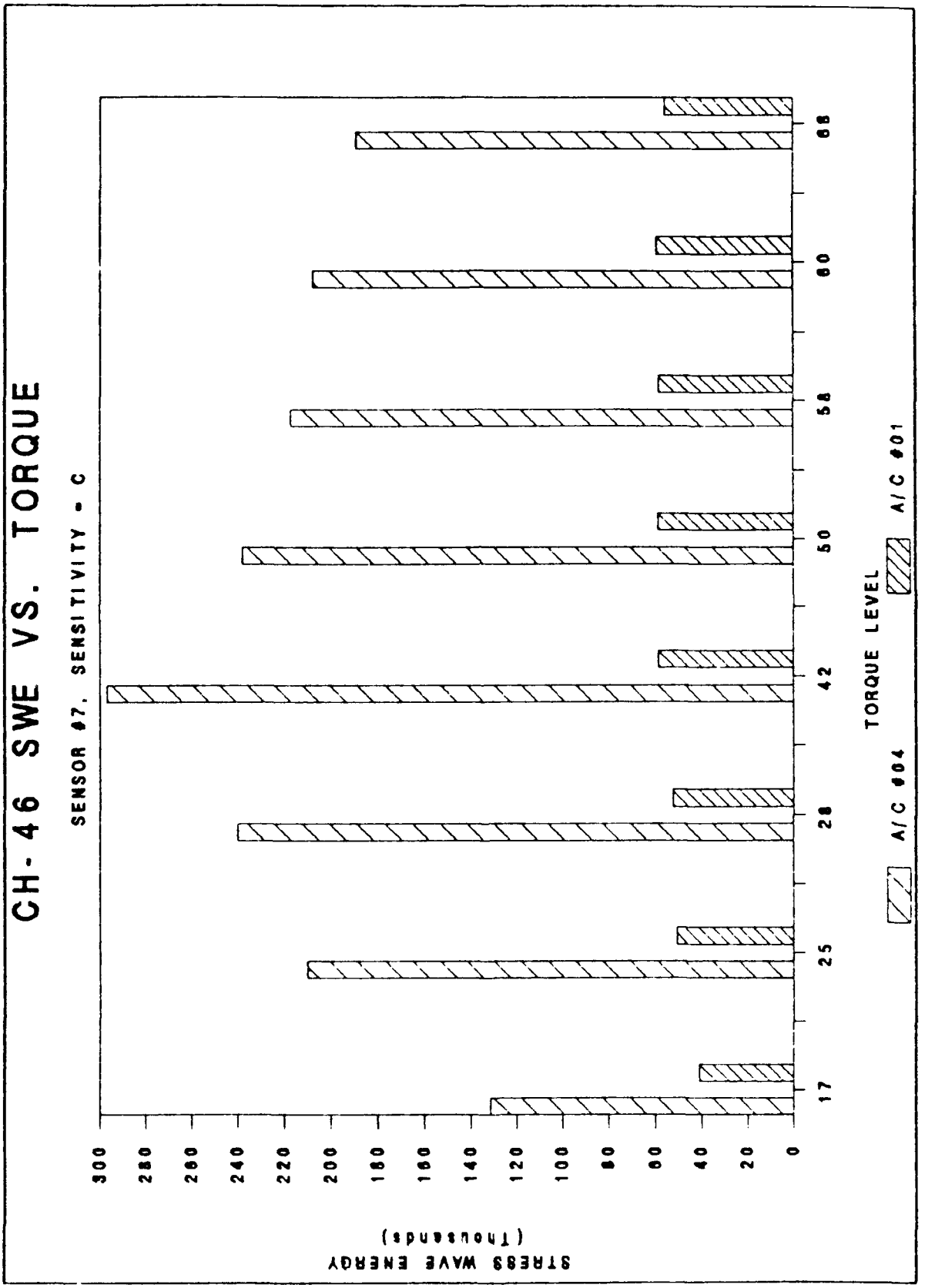

Figure 7A - MIX BOX #2 ENGINE INPUT PINION HOUSING

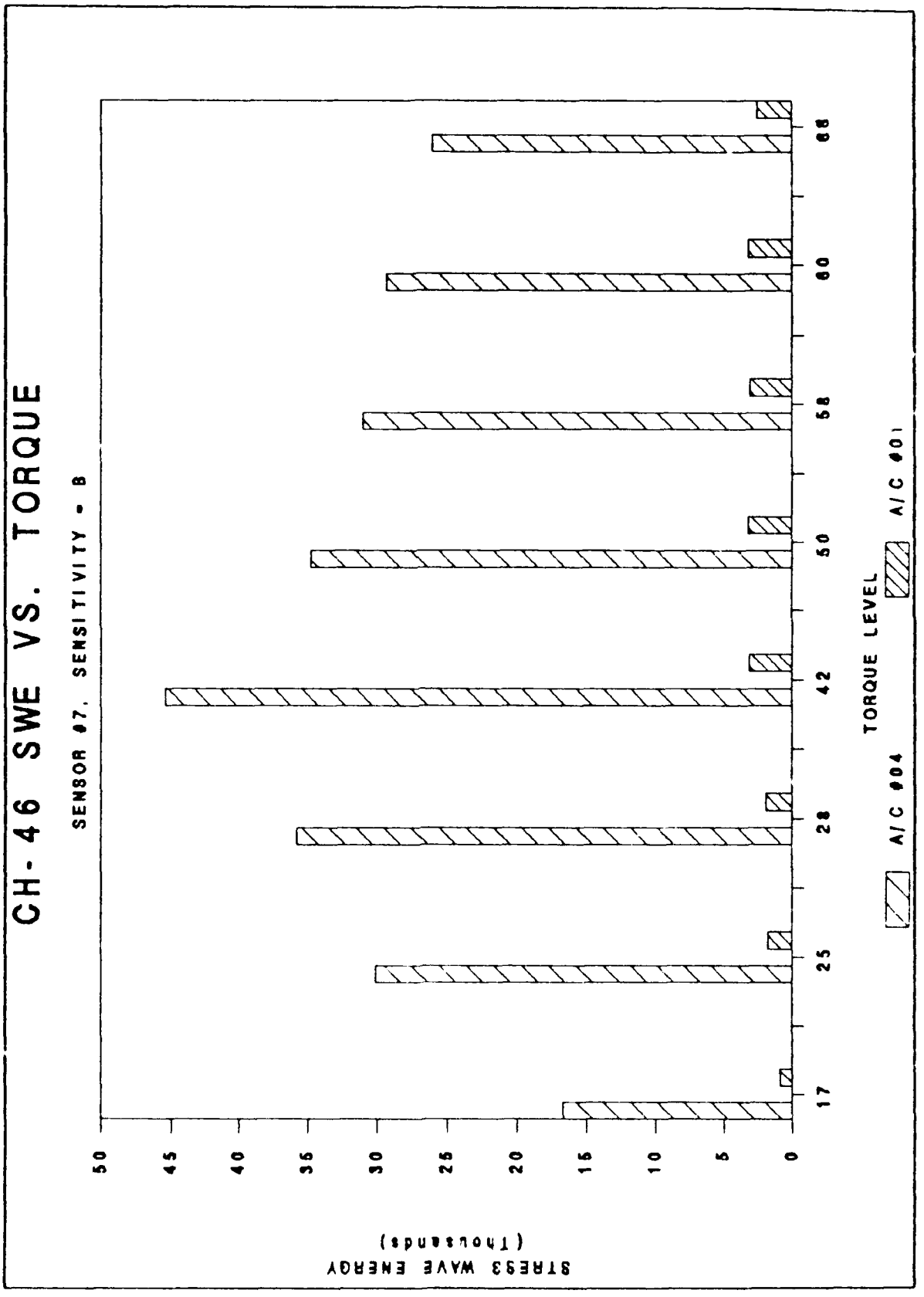

Figure 7B - MIX BOX #1 ENGINE INPUT PINION HOUSING

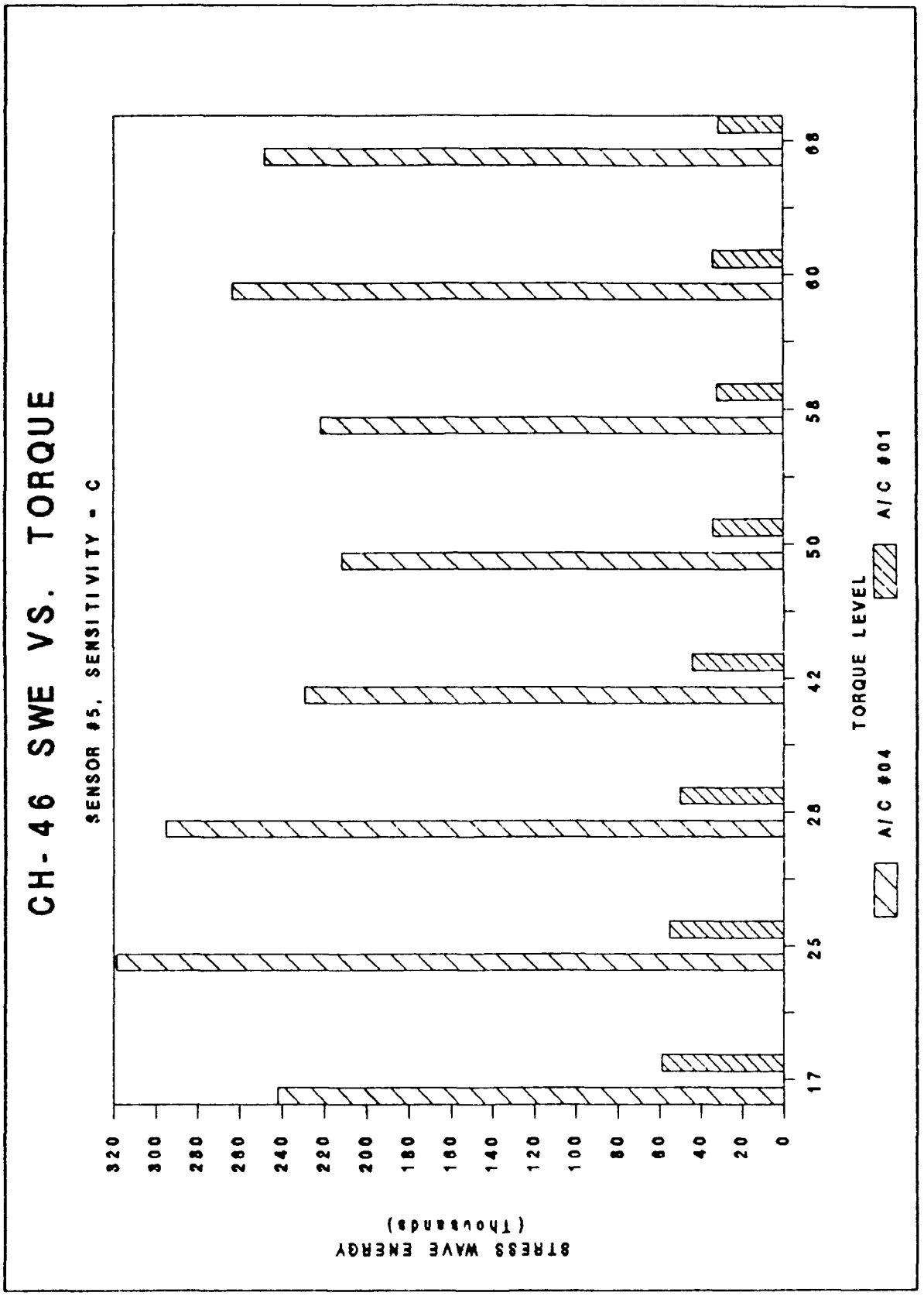

Figure 8A - MIX BOX #2 ENGINE INPUT PINION HOUSING

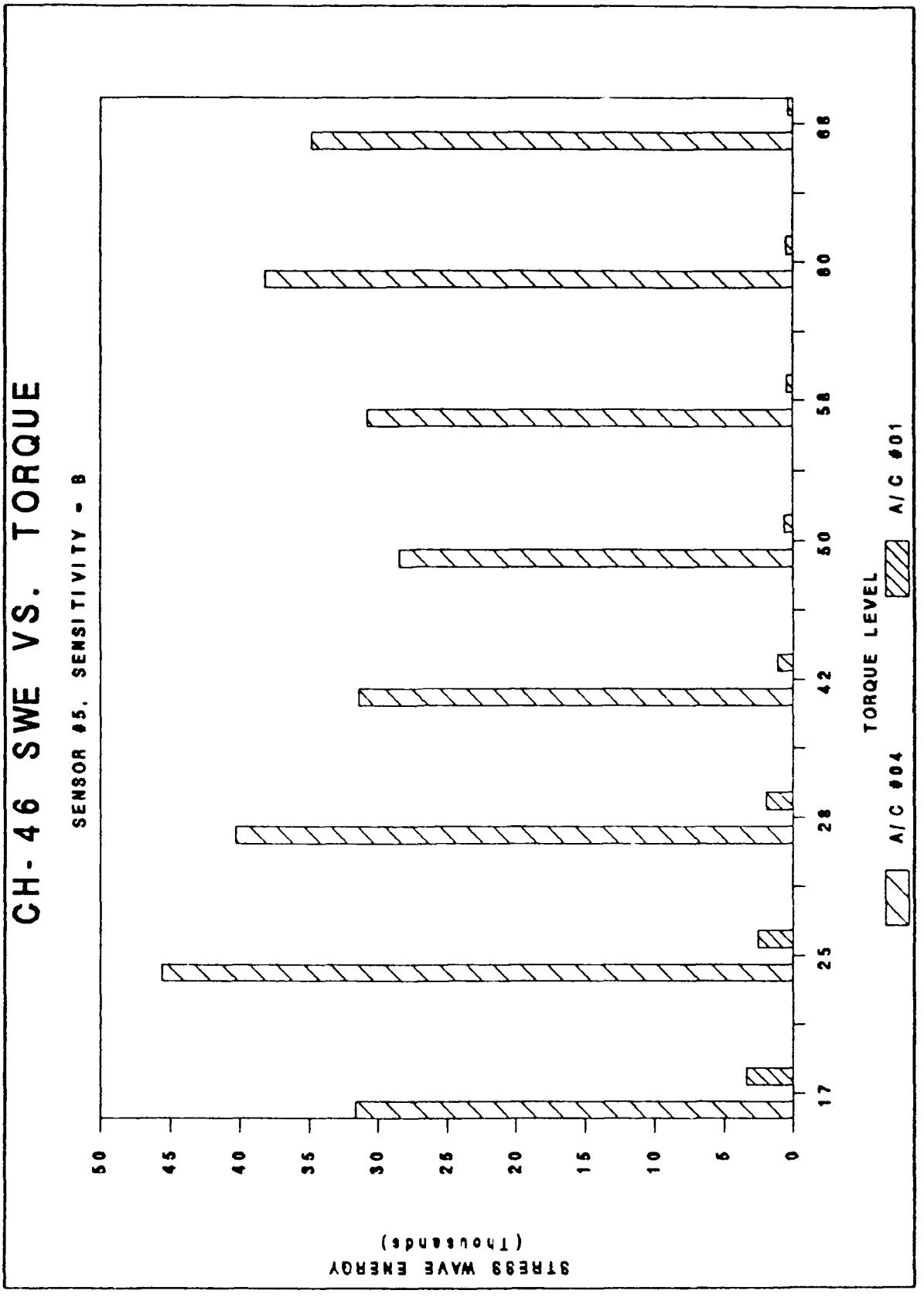

Figure 88 - MIX BOX #2 ENGINE INPUT PINION HOUSING

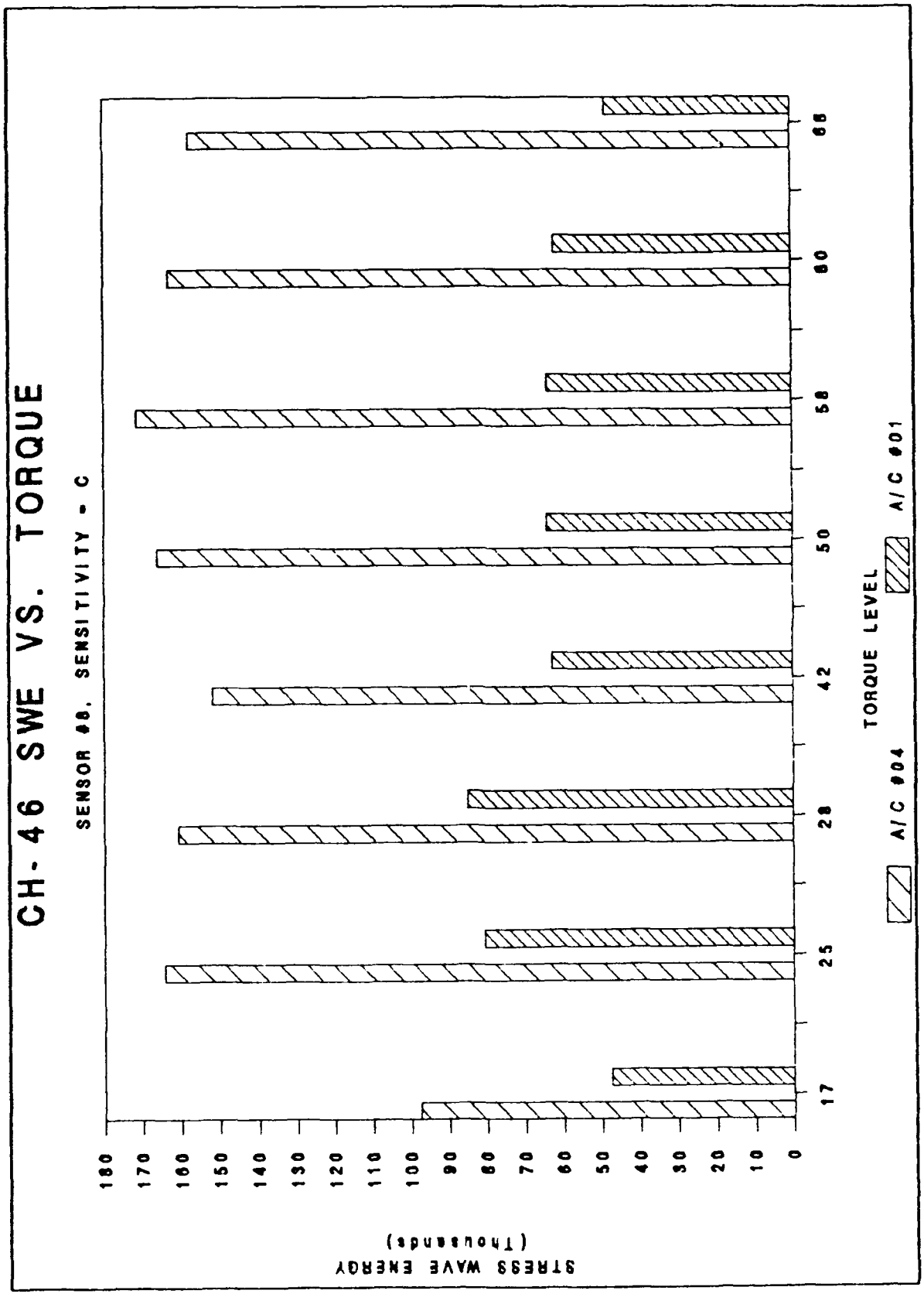

Figure 9A - MIX BOX #1 IDLER GEAR HOUSING

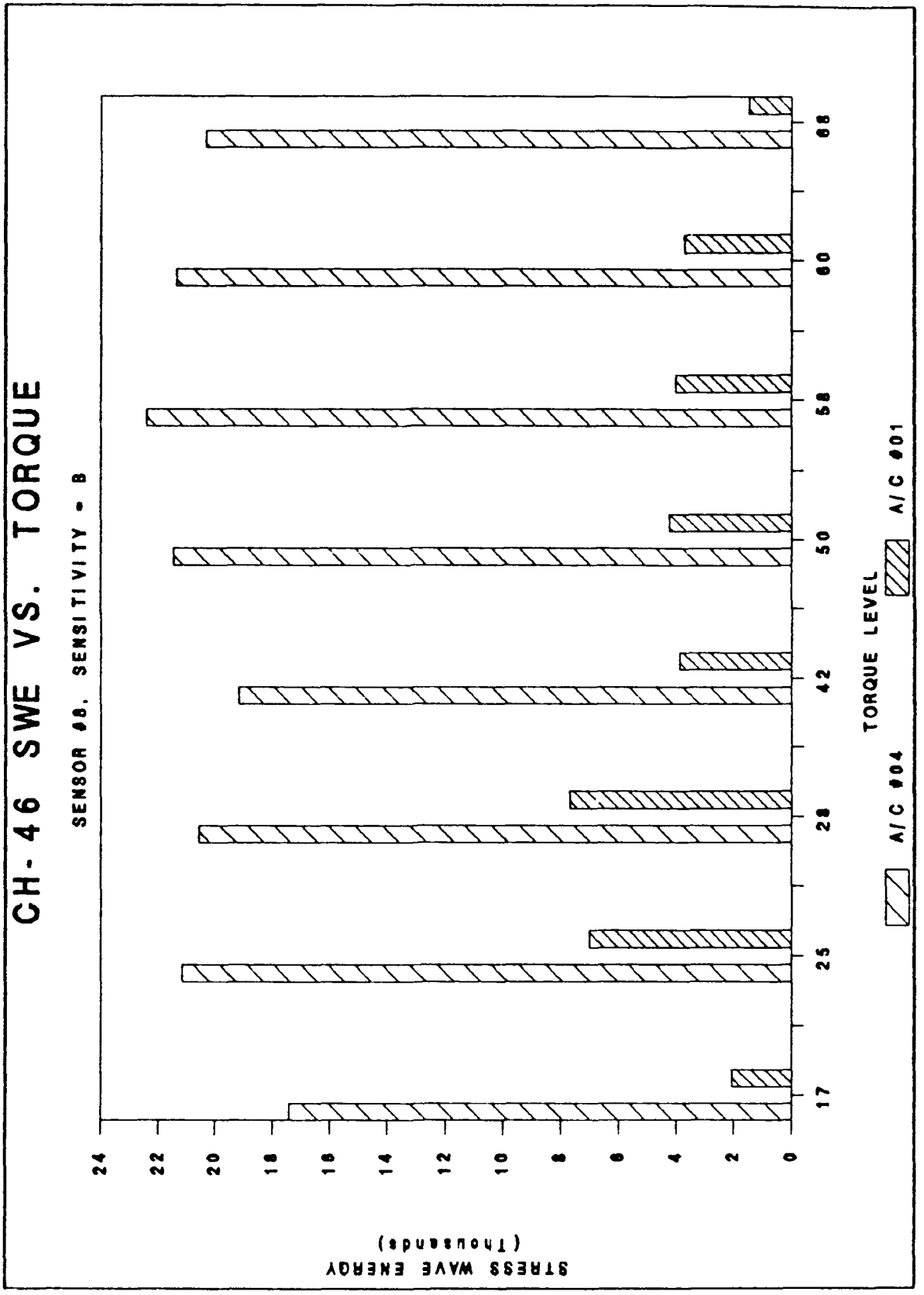

Figure 9B - MIX BOX #1 IDLER GEAR HOUSING

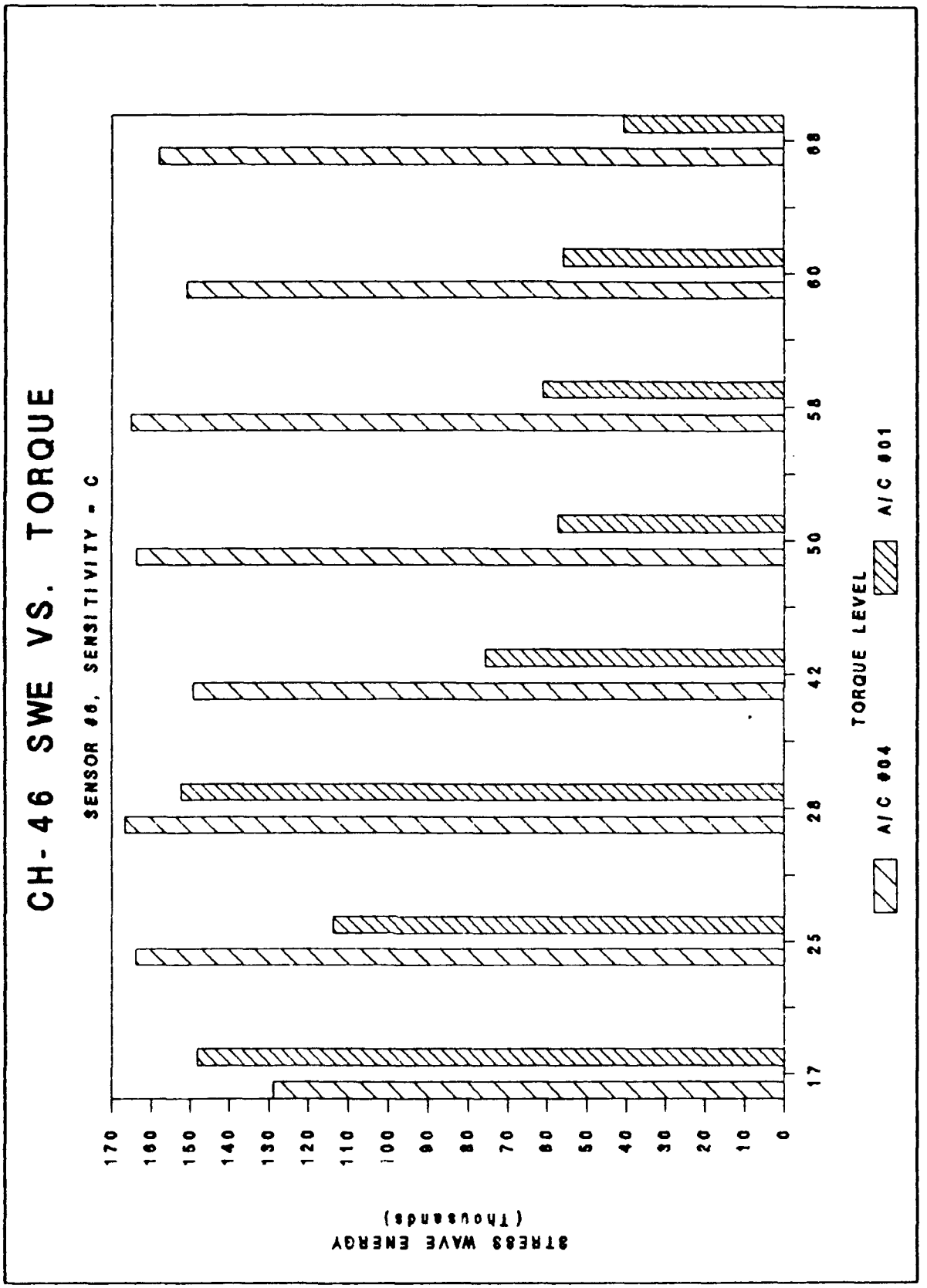

Figure 10A - MIX BOX #2 IDLER GEAR HOUSING

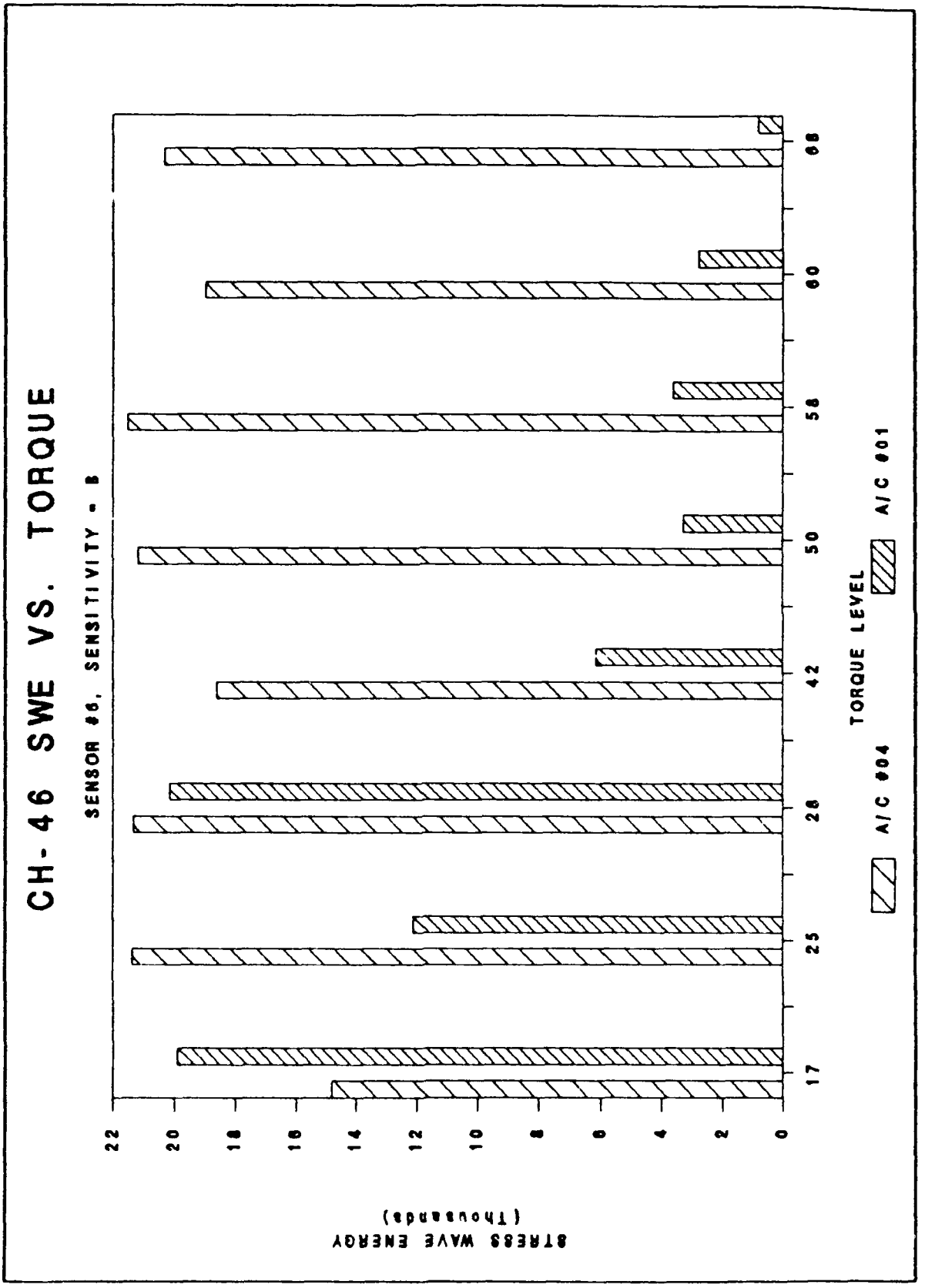

Figure 108 - MIX BOX #2 IDLER GEAR HOUSING

Again, the difference between SWE levels on aircraft #01 and #04 is primarily due to the difference in tape recorder gain settings. Aircraft #01 exhibits the largest range of SWE levels over the 17%-68% torque range. This is evident in Figure 10a, which shows the SWE levels measured on the #2 side idler gear housing. Aircraft #01 has SWE highs that are more than 3.5 times as much as its lows.

3.2.2.2 Stress Wave Power Spectral Density Measurements

Figures 11, 12, and 13 illustrate the gear and bearing characteristic frequencies in the H-46 drive train and the stress wave sensor locations. When spectral lines are present with amplitudes more than 10 db above background levels, they are often close to one of these frequencies or their harmonics.

Transmission Input Pinion (Sensor Location #1)

No significant (>10 db above background) spectral lines were observed at any torque level on aircraft #1. Figures 14, 15, and 16 are representative spectra at 17%, 42%, and 68% torque.

On aircraft #04, a 126 Hz spectral line of slightly more than 10 db amplitude appeared during data acquisition at 42% torque (nose high taxi) but then decayed to an insignificant amplitude. At the same time that the PSD changed, the SWE dropped suddenly from a mean value of 164,389 to 53444. This is illustrated in Figures 14, 15, and 16. The 126 Hz frequency could be caused by either the blower drive or one of the idler gears in the mix box. It is likely that this abrupt change in the stress wave energy and spectral content was due to the pilot putting the nose gear back down on the ground, although this was not noted on the voice track of the tape recorded data. Figures 17, 18, and 19 are representative spectra at 17%, 42%, and 68% torque.

Mix Box #2 Input Pinion (Sensor Location #5)

No significant spectral lines more than 10 db above background levels were observed at any torque level on either aircraft. The only clearly distinguishable spectral line is at the 1/rev and harmonics of the mix box input pinion gear. This characteristic is most evident on aircraft #01, where it is present at all torque levels. Figures 20, 21, and 22 are representative spectra at 17%, 42%, and 68% torque.

Mix Box #1 Input Pinion (Sensor Location #7)

No significant spectral lines more than 10 db above background levels were observed at any torque level on aircraft #04. The only clearly distinguishable spectral lines on this aircraft are at the 1/rev of the mix box input pinion gear and at 75 Hz which may be related to the aft transmission oil scavenge pump (refer to item 16 in Figure 11). Aircraft #01 exhibits strong spectral lines

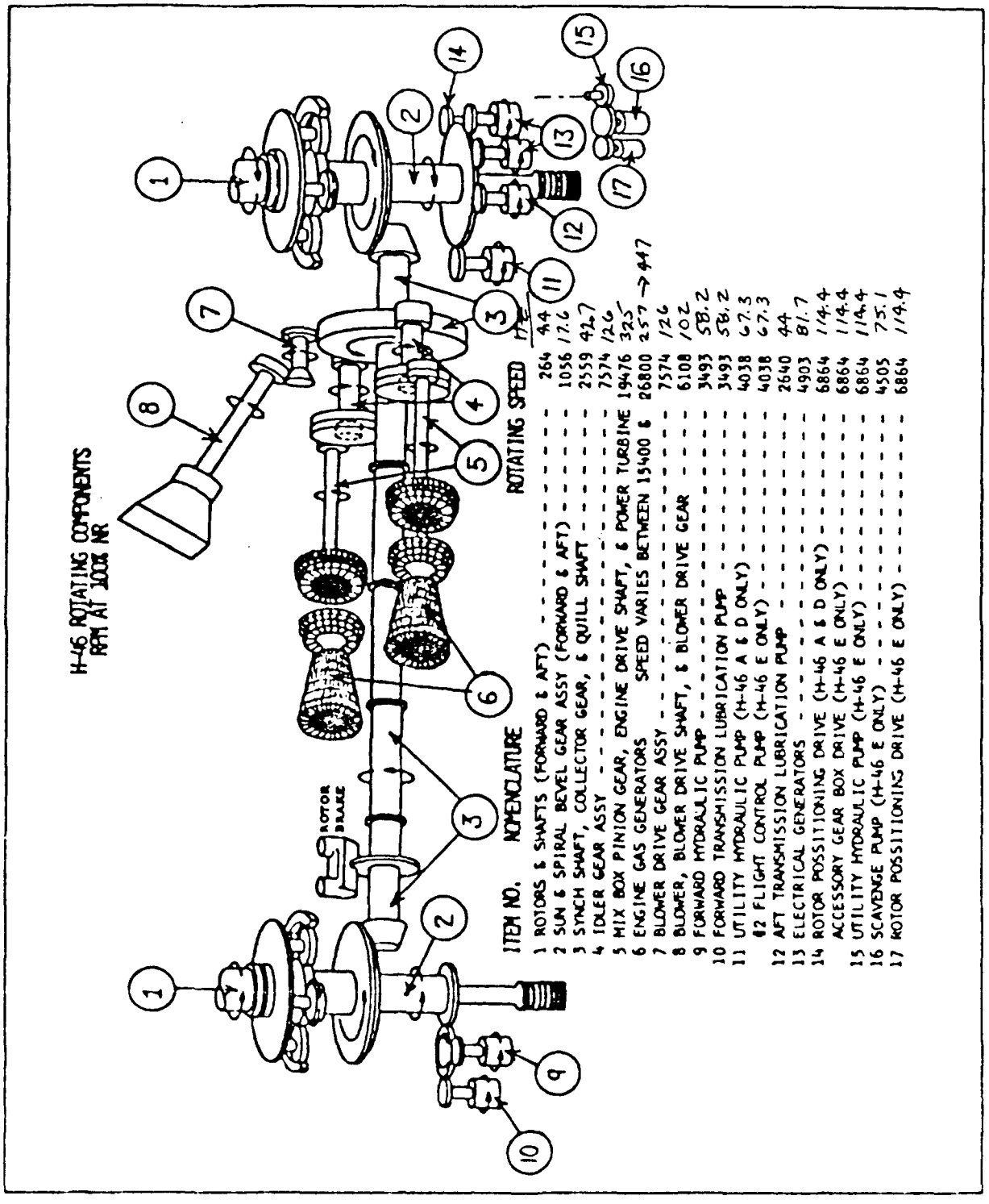

Figure 12A

H-46 COMPONENT 1/REV FREQUENCIES

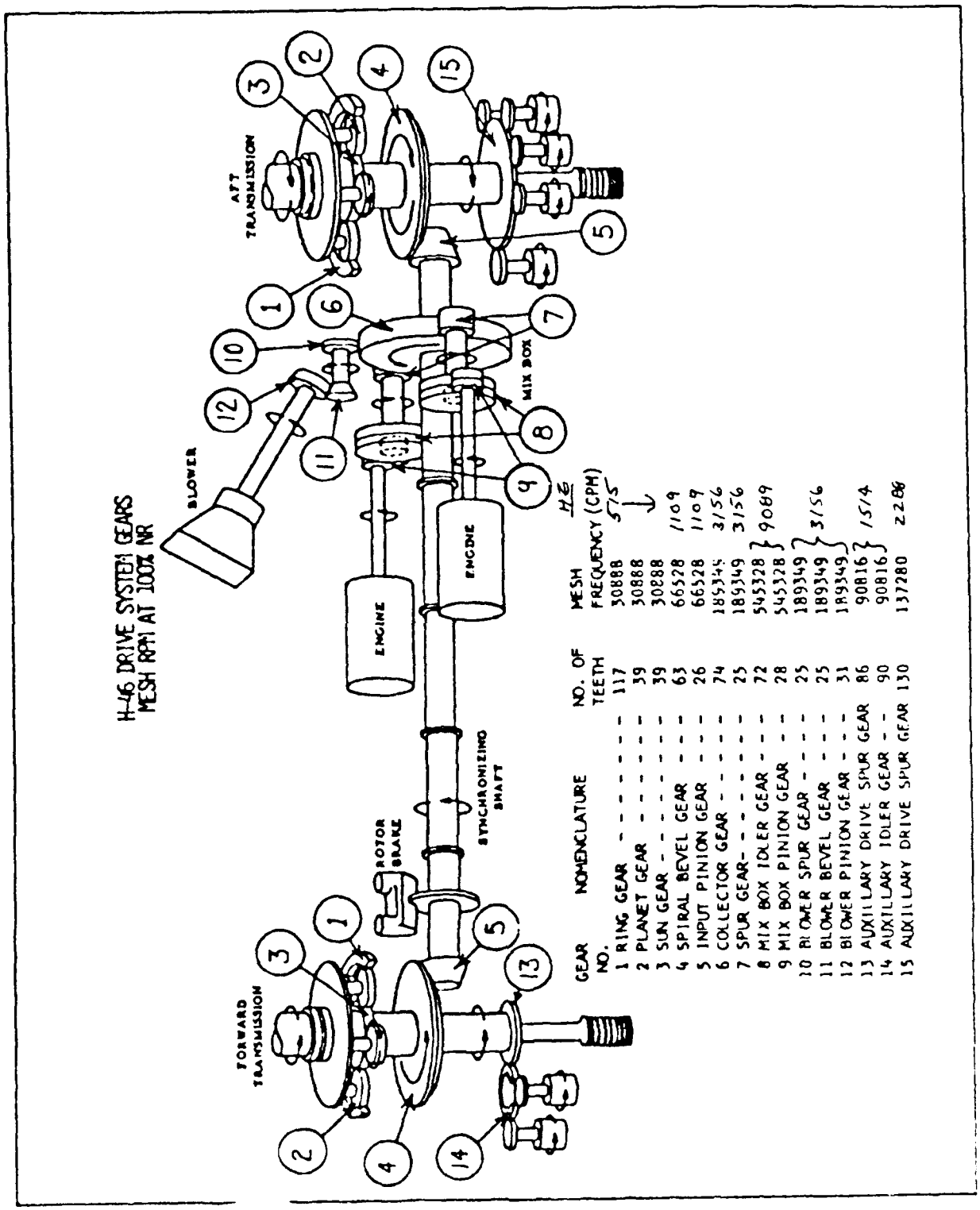

Figure 12

H-46 GEAR MESH FREQUENCIES

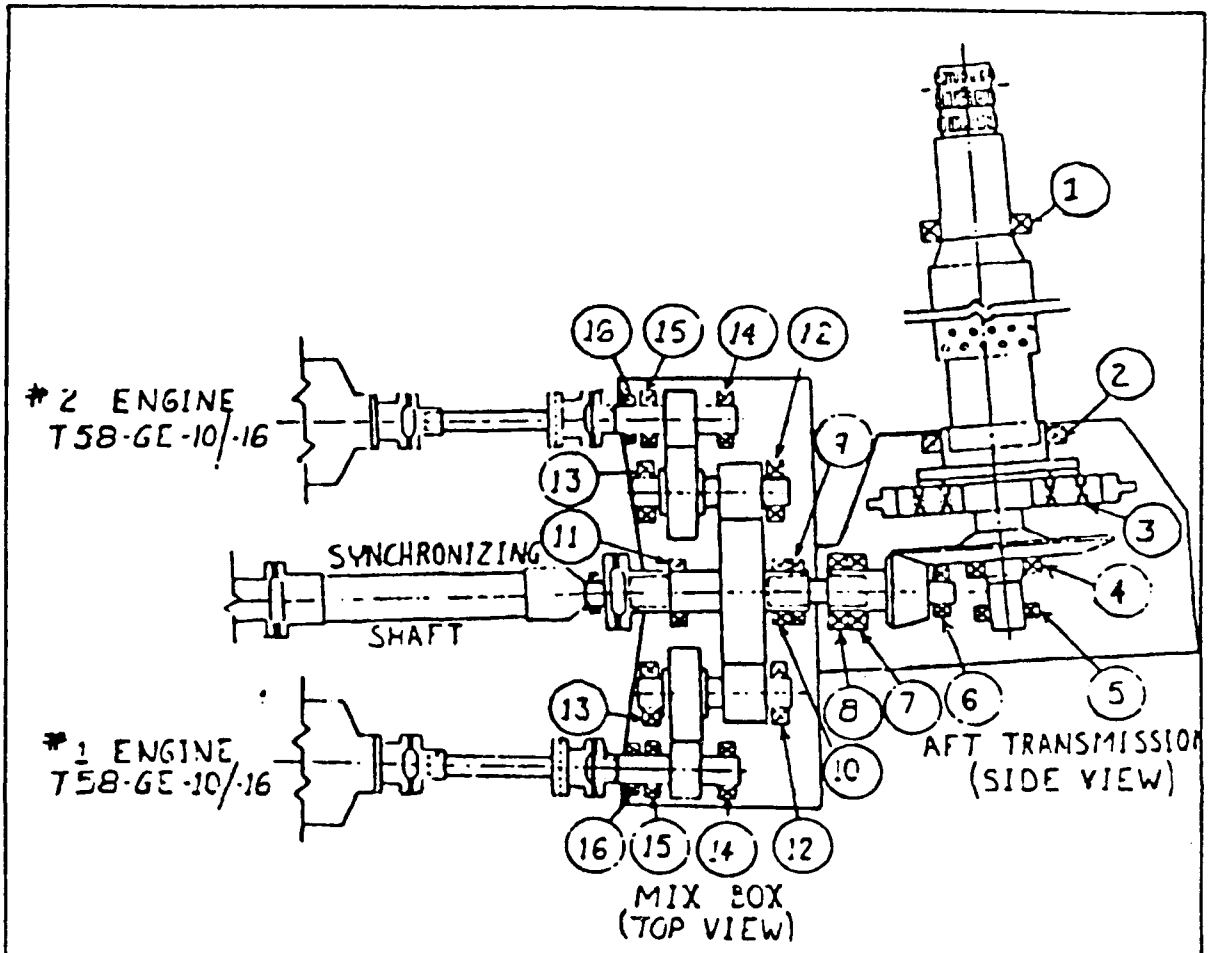

BEARING NO.	CAGE RPM		BEARING PASS OUTER RACE (CPM)		BEARING PASS INNER RACE (CPM)		BEARING DEFECT FREQUENCY (CPM)	
		HZ		HZ		HZ		HZ
1	115	1.92	2538	42.3	3269	60.5	2076	34.6
2	123	2.05	3078	51.3	3521	58.7	3918	65.3
3	293	4.88	4103	68.4	6103	101.7	4014	66.9
4	464	7.73	9744	162	12432	207.2	8413	140.2
5	478	7.97	12908	215	15604	260	10736	179
6	1038	17.3	14533	242	21291	355	16215	270
7	1134	18.9	26091	435	32761	546	21650	361
8	1050	17.5	14694	245	21130	352	12995	217
9	1145	19.1	27473	458	33938	566	24039	401
10	1108	18.5	15510	259	20314	339	18739	312
11	1131	18.9	24878	415	31415	524	21739	362
12	3069	51.1	42972	716	63064	1051	38537	642
13	3051	50.1	36615	610	54273	905	37512	625
14	7875	131	94450	1574	139212	2320	93074	1635
15	7641	127	91686	1528	142026	2367	86227	1437
16	8013	134	80129	1335	114631	1911	106438	1775

Figure 12B

H-46 BEARING FREQUENCIES

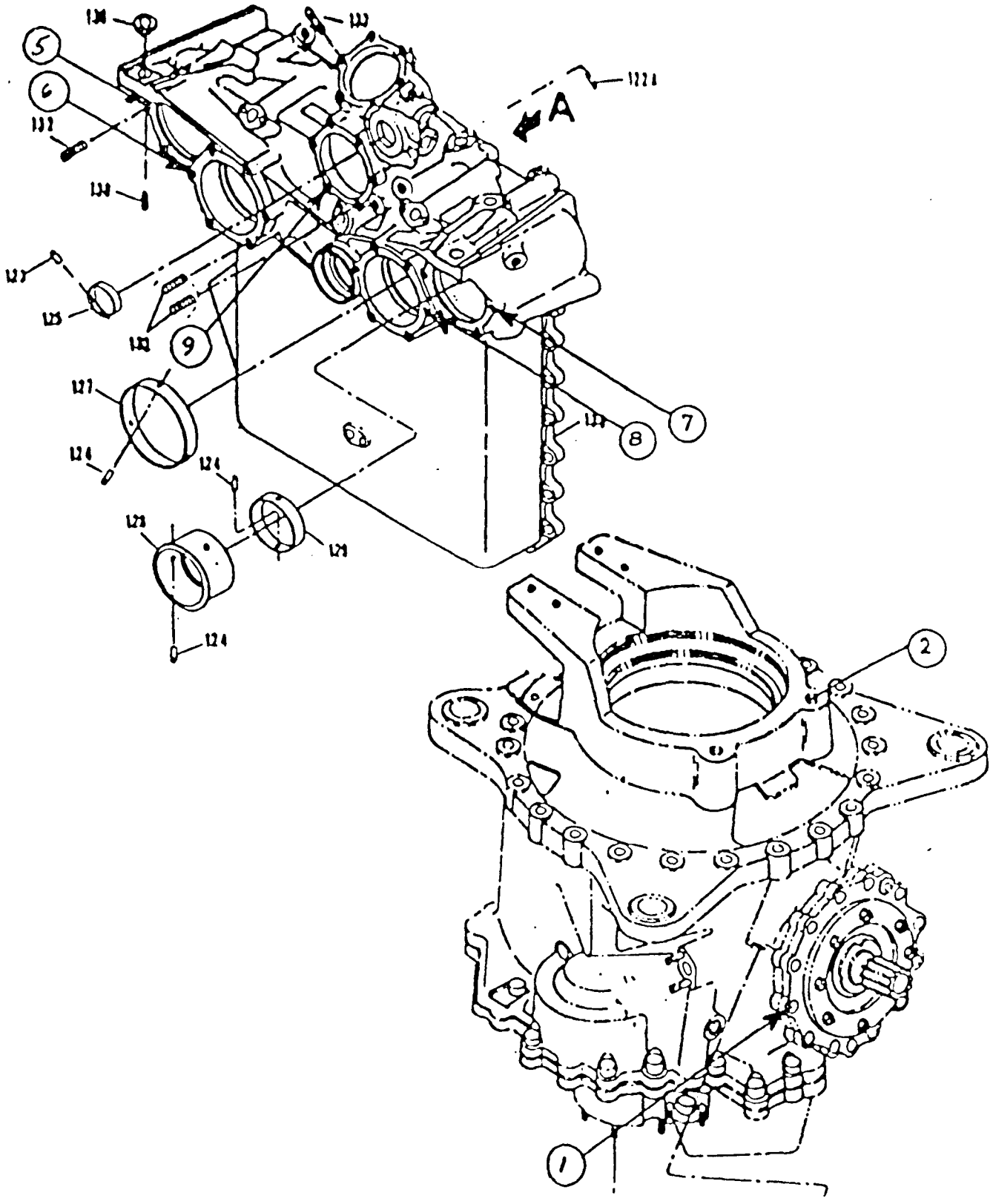

FIGURE 13

H-46 STRESS WAVE SENSOR LOCATIONS

Table VI

H-46 Power Spectral Density Identification Code

At the top of each Power Spectral Density sheet is an identification code of the form:

H46011711.3

This code can be interpreted as follows:

Character No.	Meaning
1-3	H46 = aircraft type
4&5	01 = aircraft number
6&7	17 = operating torque
8	1 = flight condition
9	1 = sensor number
10	.3 = spectral range

The spectral range code is as follows:

.1 = 50 Hz
.2 = 250 Hz
.3 = 1250 Hz
.4 = 5000 Hz

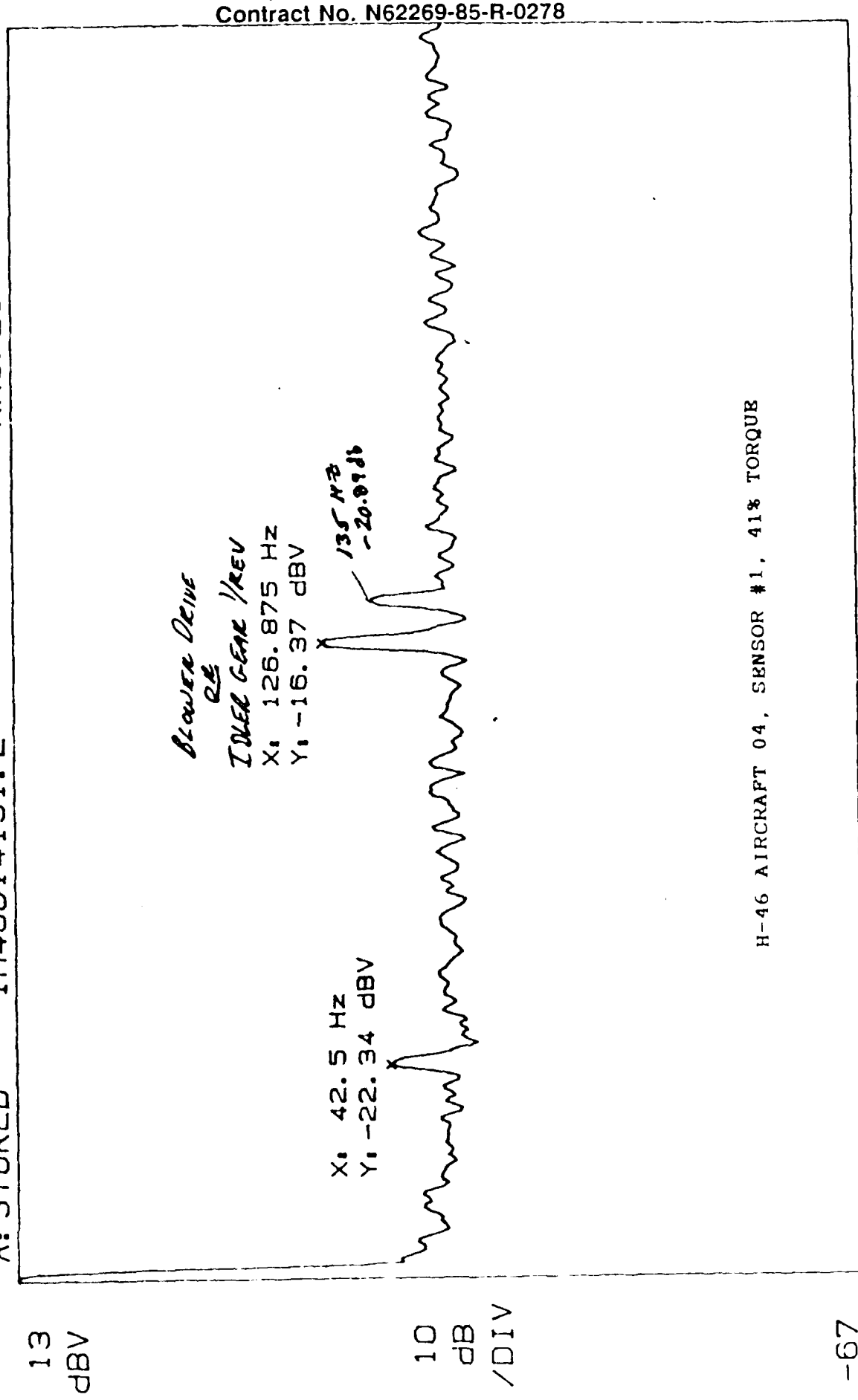
A: STORED
1H4604 4151.2
RANGE: -21 dBV
STATUS: PAUSED
RMS: 25
Blower Once
&
Idler Gear 1/Rev
X: 126.875 Hz
Y: -16.37 dBV
135 Hz
-20.9 dB
X: 42.5 Hz
Y: -22.34 dBV
H-46 AIRCRAFT 04, SENSOR #1, 41% TORQUE
13
dBV
10
dB
/DIV
-67
START: 0 Hz
X: 126.875 Hz
BW: 2.3871 Hz
Y: -16.37 dBV
STOP: 250 Hz

Figure 14

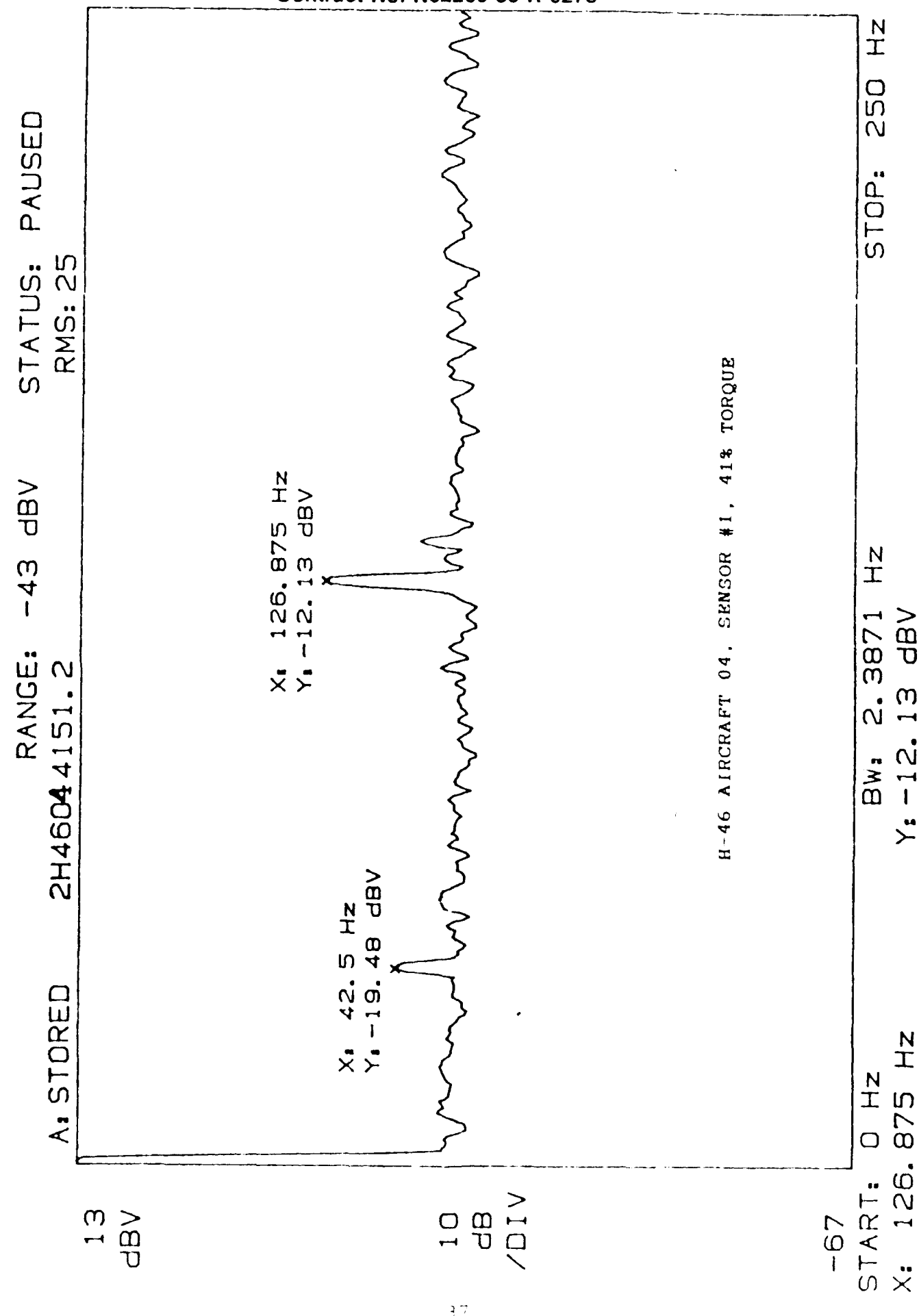
A: STORED 2H46044151.2
RANGE: -43 dBV
STATUS: PAUSED
RMS: 25
X: 126.875 Hz
Y: -12.13 dBV
X: 42.5 Hz
Y: -19.48 dBV
H-46 AIRCRAFT 04, SENSOR #1, 41% TORQUE
13 dBV
10 dB /DIV
-67
START: 0 Hz
X: 126.875 Hz
BW: 2.3871 Hz
Y: -12.13 dBV
STOP: 250 Hz

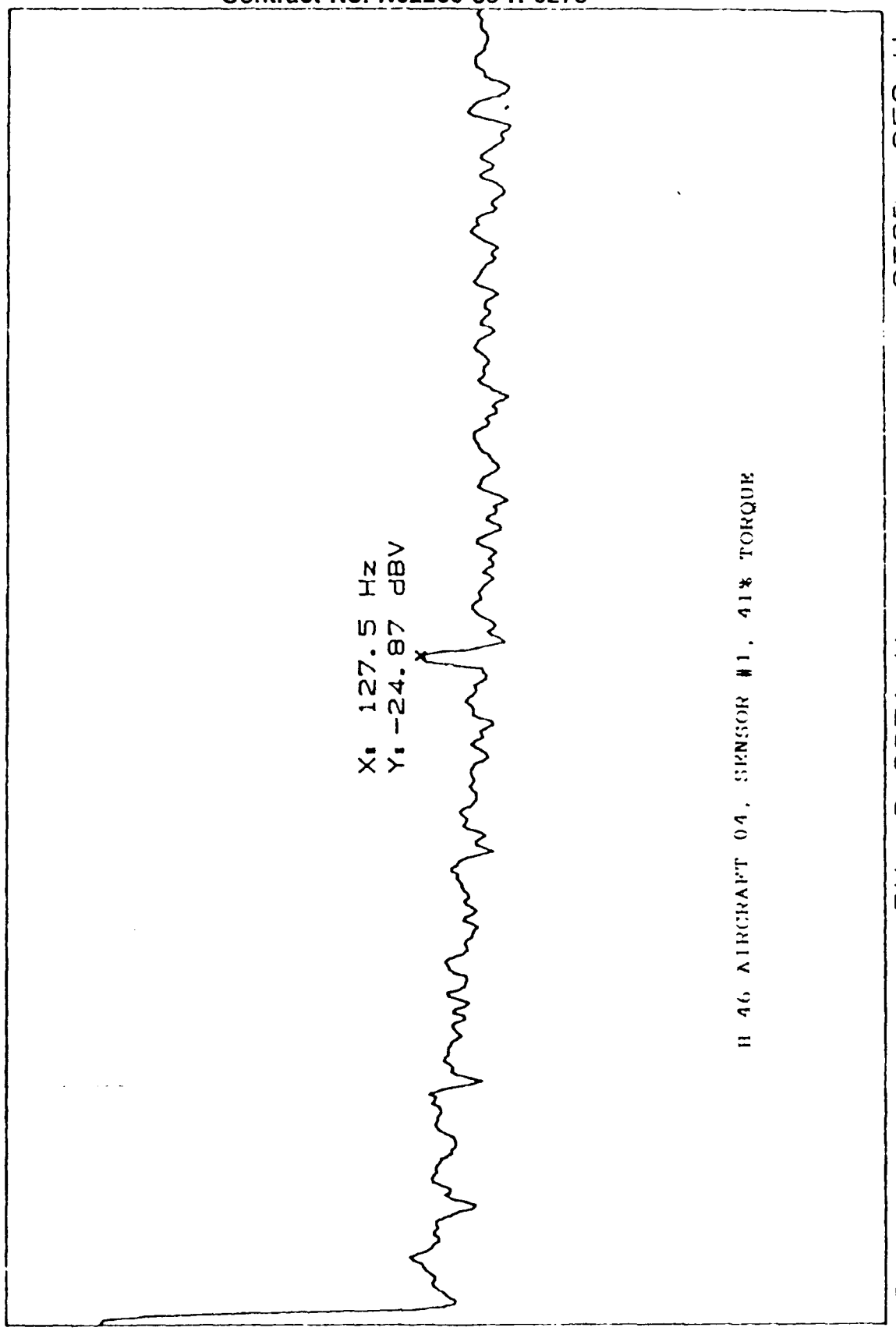
RANGE: -43 dBV
STATUS: PAUSED
A: STORED
3H46044151.2
RMS: 25
X: 127.5 Hz
Y: -24.87 dBV
H 46 AIRCRAFT 04, SENSOR #1, 41% TORQUE
13
dBV
10
dB
/DIV
-67
START: 0 Hz
STOP: 250 Hz
X: 127.5 Hz
BW: 2.3871 Hz
Y: -24.87 dBV

Figure 16

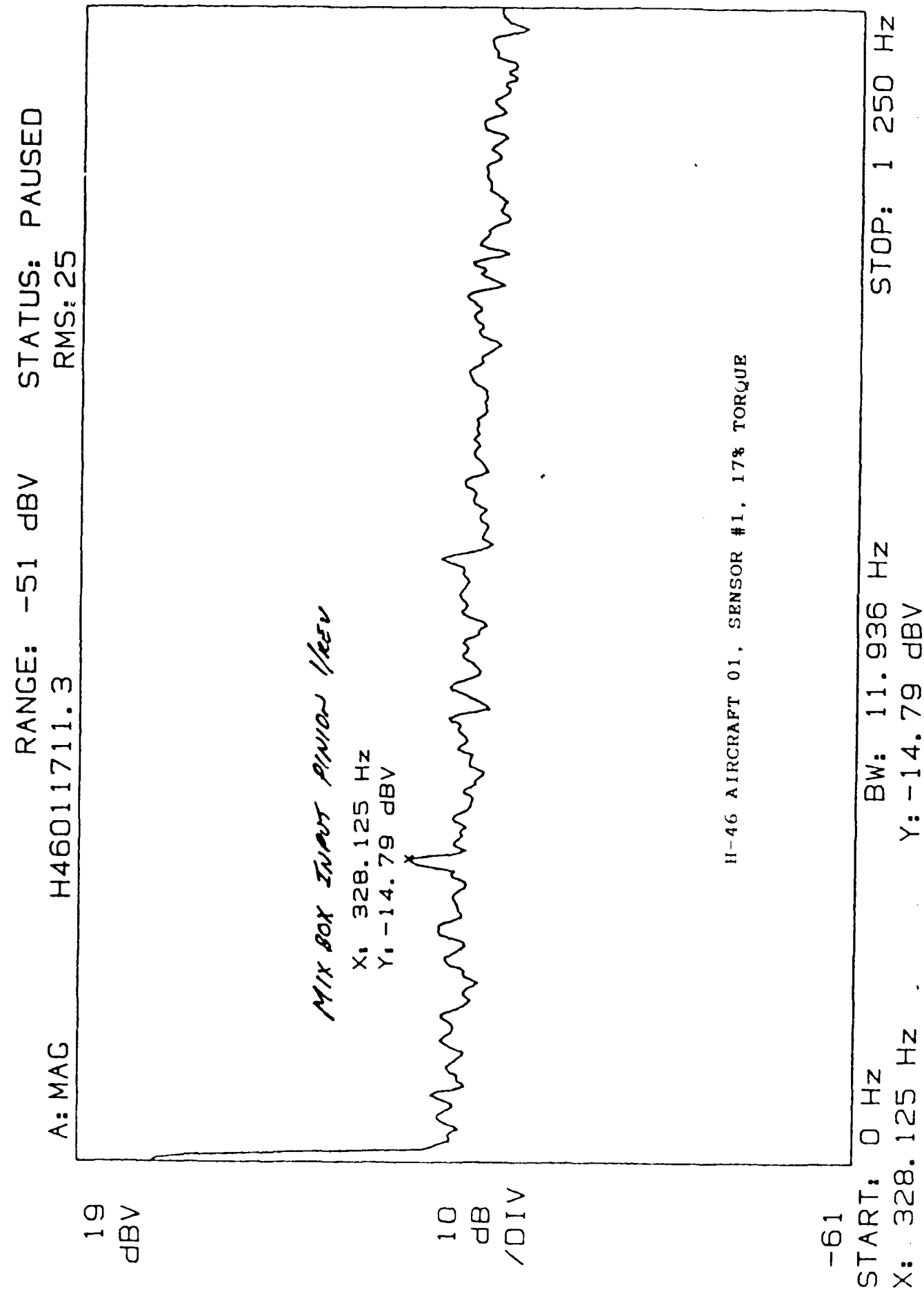
A: MAG
RANGE: -51 dBV
H46011711.3
STATUS: PAUSED
RMS: 25
MIX BOX INPUT PINION 1/REV
X: 328.125 Hz
Y: -14.79 dBV
H-46 AIRCRAFT 01, SENSOR #1, 17% TORQUE
19
dBV
10
dB
/DIV
-61
START: 0 Hz
X: 328.125 Hz
BW: 11.936 Hz
Y: -14.79 dBV
STOP: 1 250 Hz

Figure 17A

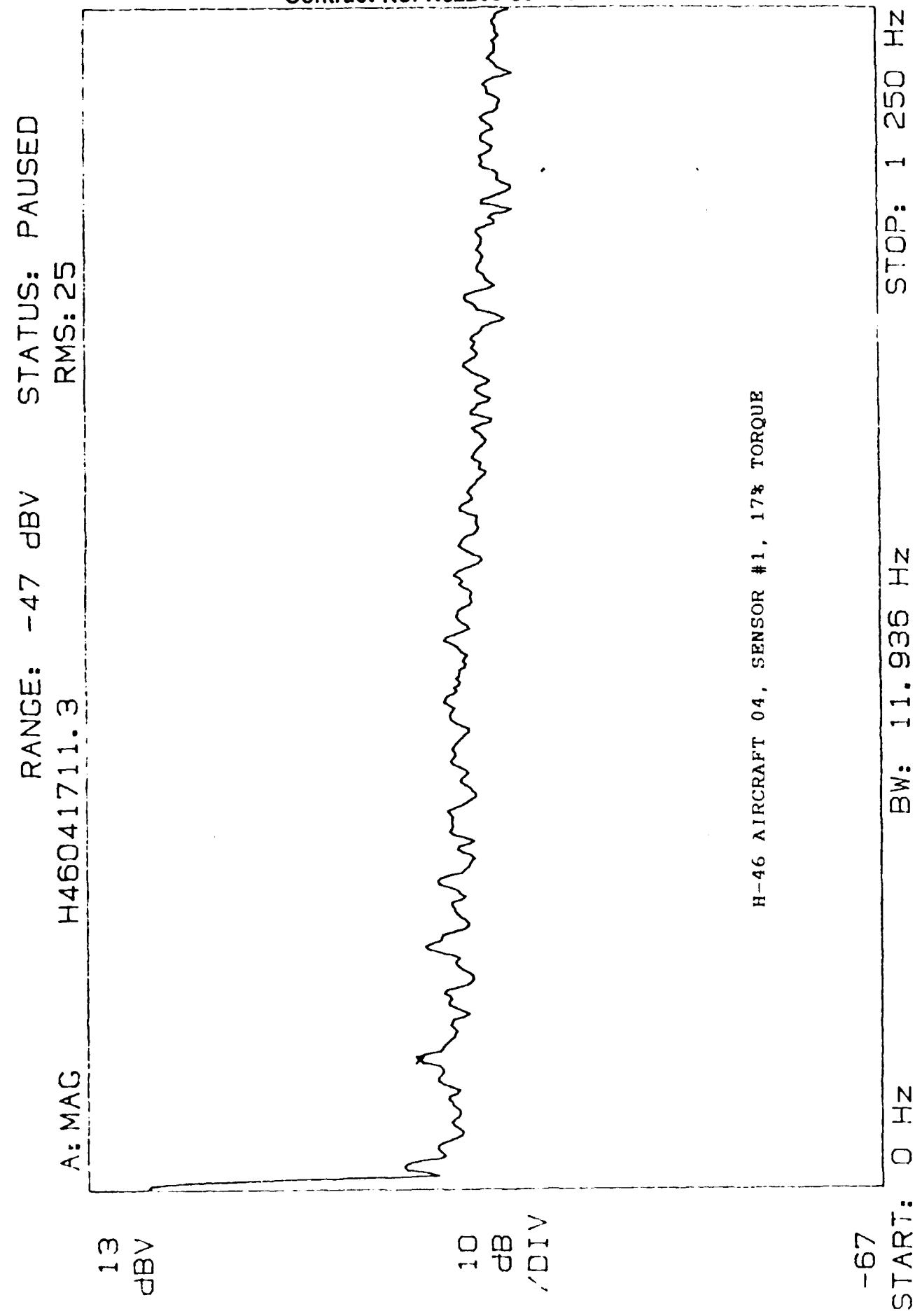
A: MAG
H46041711.3
RANGE: -47 dBV
STATUS: PAUSED
RMS: 25
13
dBV
10
dB
/DIV
-67
START: 0 Hz
X: 134.375 Hz
BW: 11.936 Hz
Y: -20.45 dBV
STOP: 1 250 Hz
H-46 AIRCRAFT 04, SENSOR #1, 17% TORQUE

Figure 17B

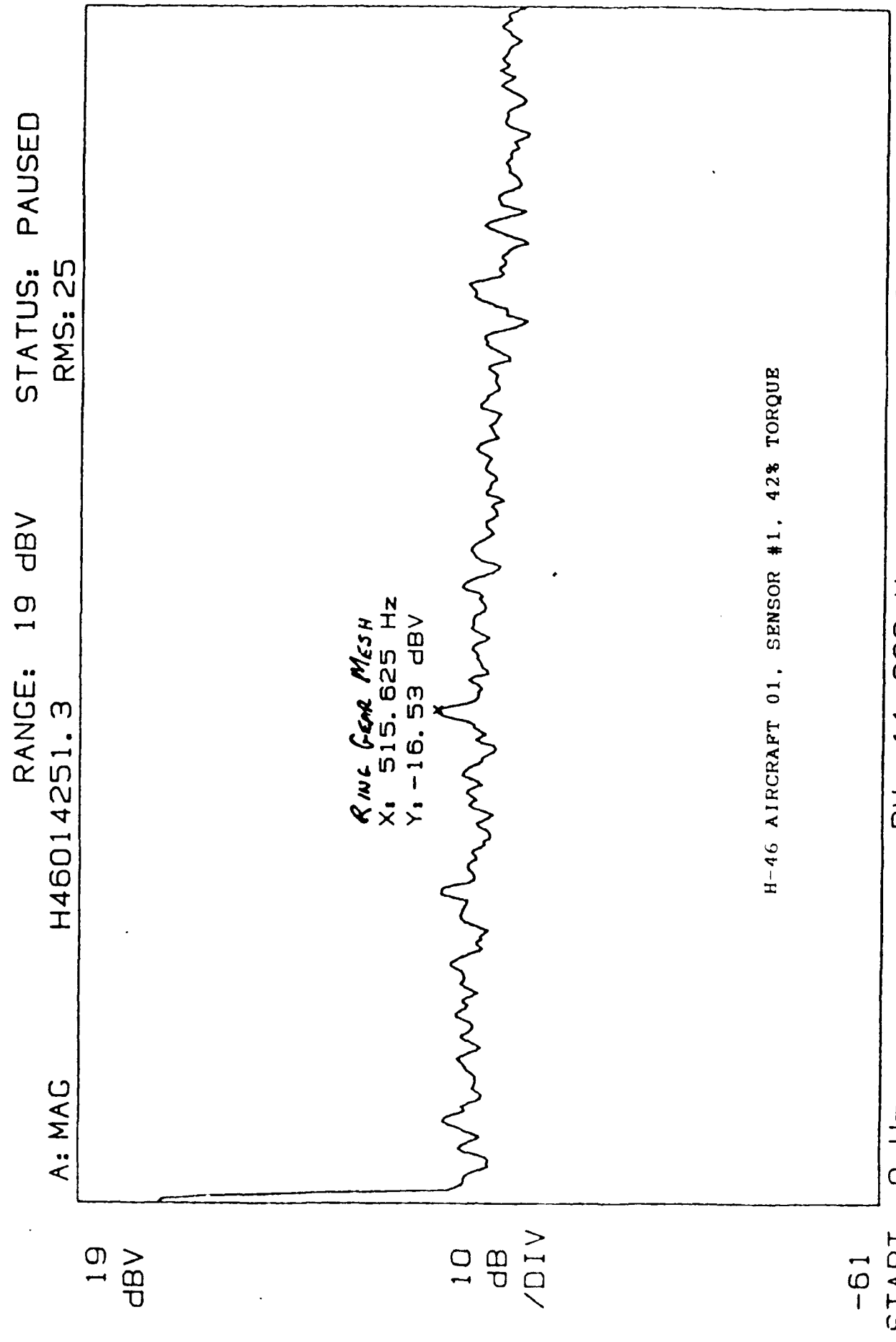
A: MAG
RANGE: 19 dBV
H46014251.3
STATUS: PAUSED
RMS: 25
Ring Gear Mesh
X: 515.625 Hz
Y: -16.53 dBV
H-46 AIRCRAFT 01, SENSOR #1, 42% TORQUE
19
dBV
10
dB
/DIV
-61
START: 0 Hz
X: 515.625 Hz
BW: 11.936 Hz
Y: -16.53 dBV
STOP: 1 250 Hz

Figure 18A

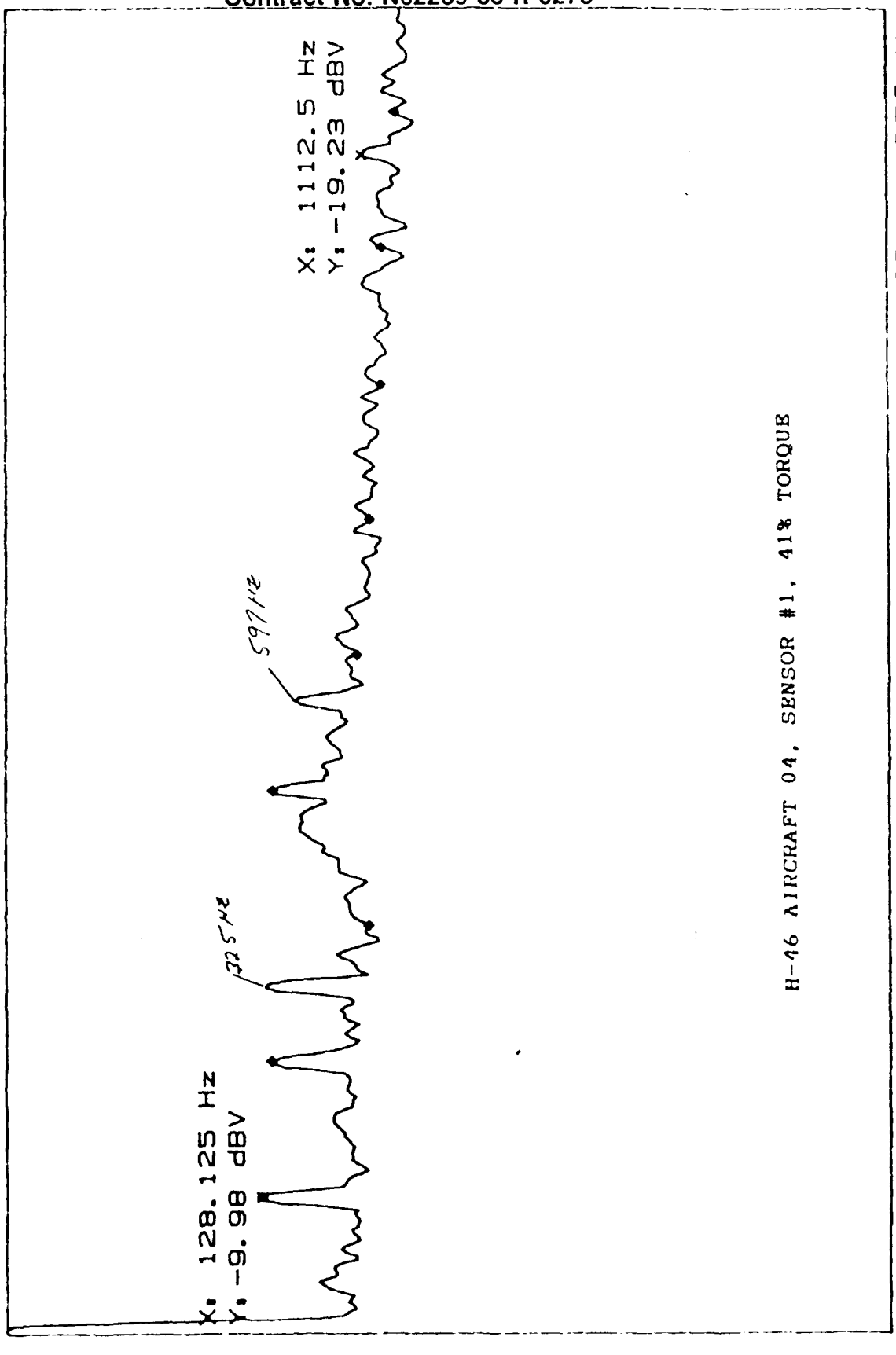
A: STORED
RANGE: -51 dBV
2H4604151.3
STATUS: PAUSED
RMS: 25
X: 128.125 Hz
Y: -9.98 dBV
X: 1112.5 Hz
Y: -19.23 dBV
225 Hz
597 Hz
H-46 AIRCRAFT 04, SENSOR #1, 41% TORQUE
13 dBV
10 dB /DIV
-67
START: 0 Hz
X: 128.125 Hz
BW: 11.936 Hz
Y: -9.98 dBV
STOP: 1 250 Hz
THD: 3.37 dB

Figure 18B

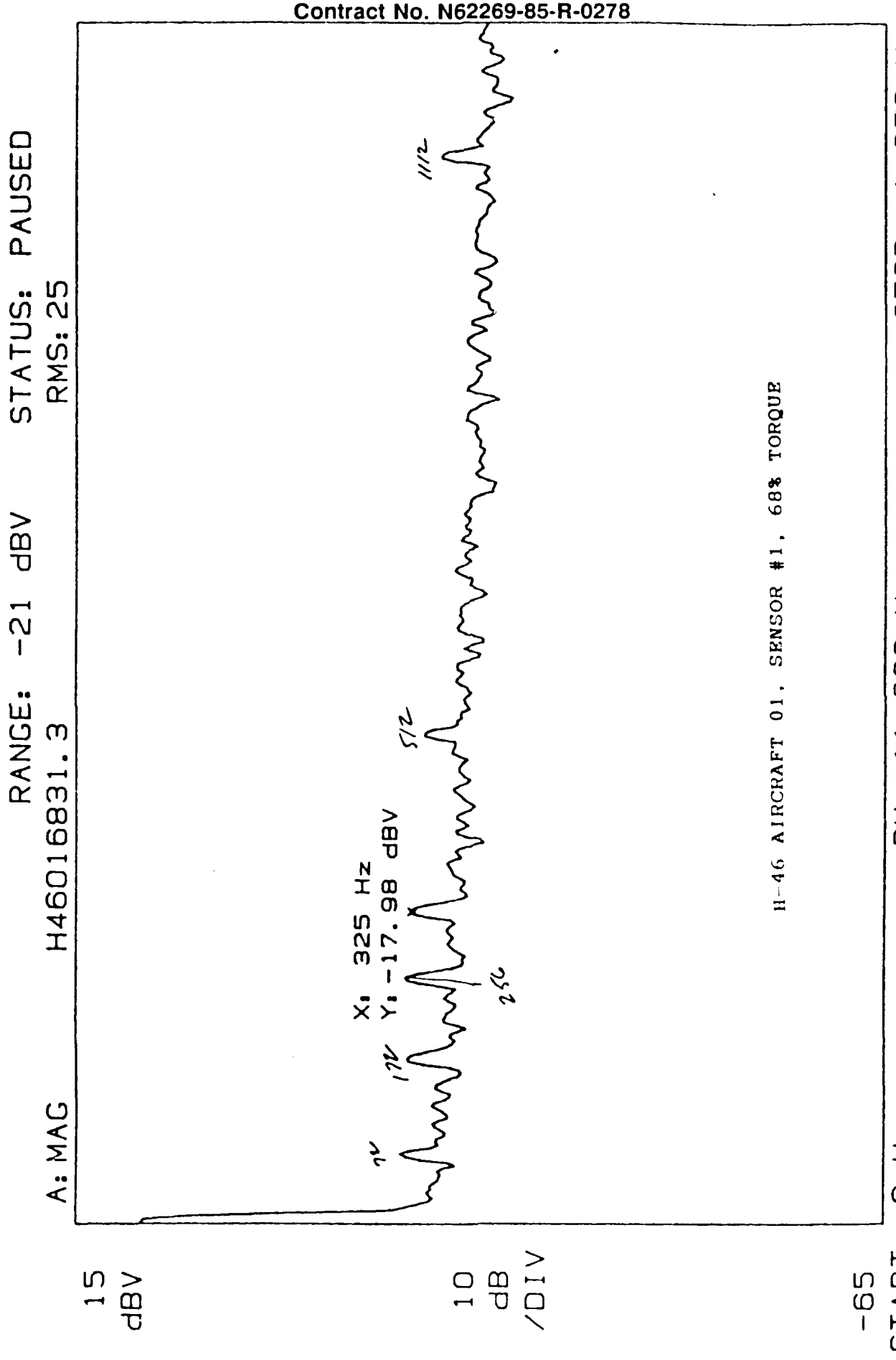
A: MAG
H46016831.3
RANGE: -21 dBV
STATUS: PAUSED
RMS: 25
X: 325 Hz
Y: -17.98 dBV
1/2
1/2
1/2
1/2
15
dBV
10
dB
/DIV
-65
START: 0 Hz
X: 325 Hz
BW: 11.936 Hz
Y: -17.98 dBV
STOP: 1 250 Hz
H-46 AIRCRAFT 01, SENSOR #1, 68% TORQUE

Figure 19A

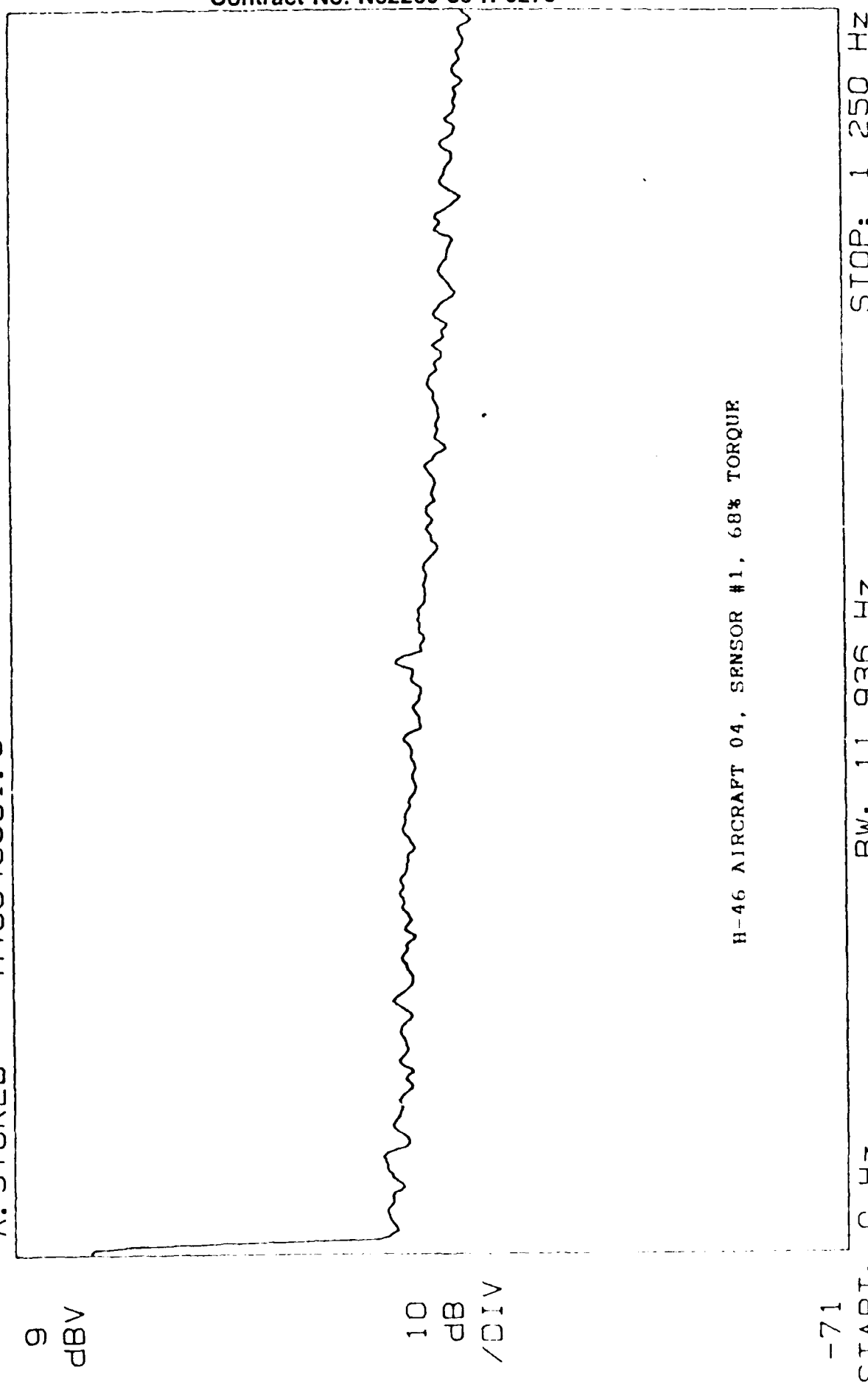
A: STORED
H46046831.3
RANGE: -51 dBV
STATUS: PAUSED
RMS: 100
9
dBV
10
dB
/DIV
-71
START: 0 Hz
BW: 11.936 Hz
STOP: 1 250 Hz
H-46 AIRCRAFT 04, SENSOR #1, 68% TORQUE

Figure 19B

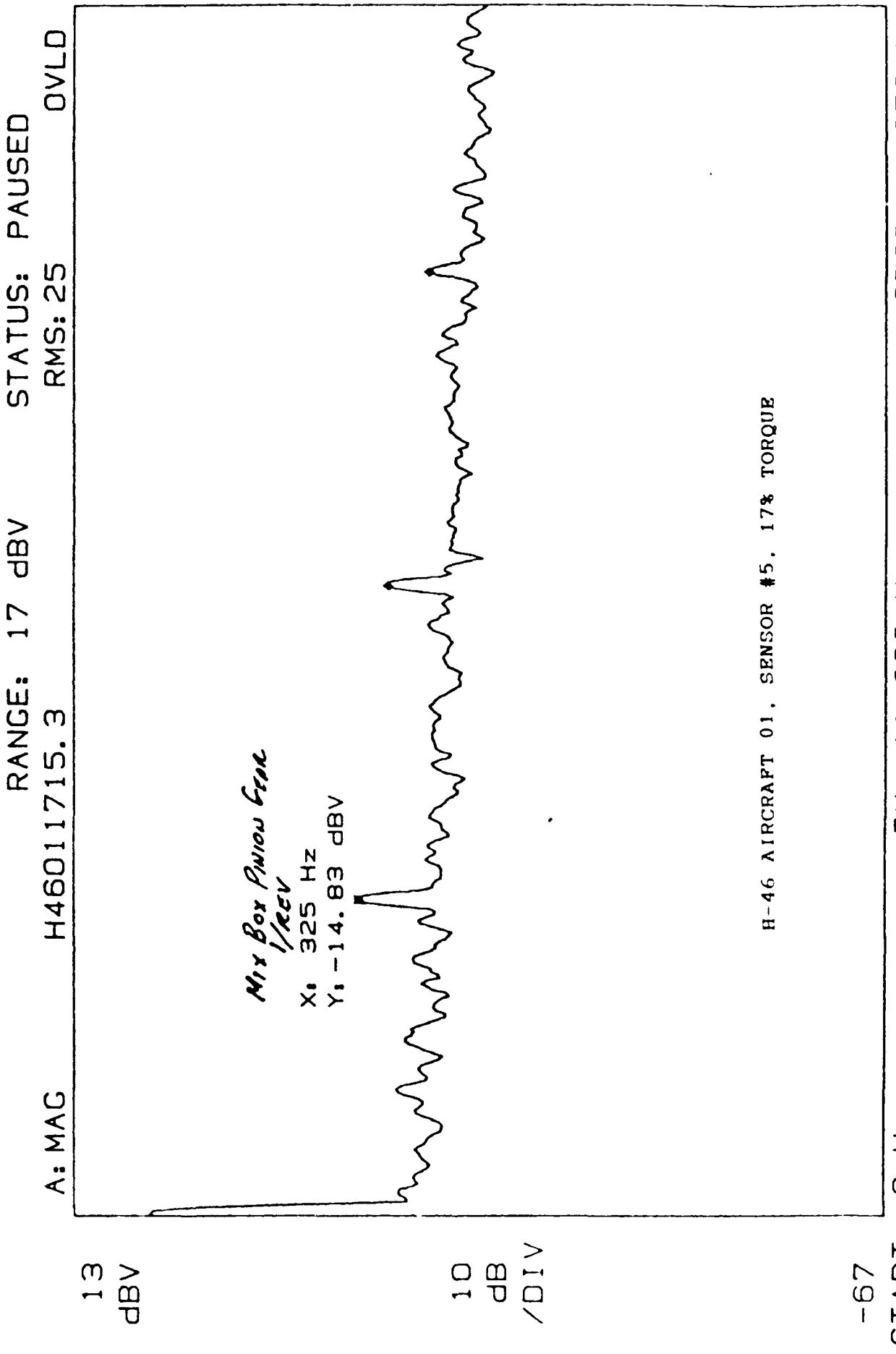
A: MAG
RANGE: 17 dBV
H46011715.3
STATUS: PAUSED
RMS: 25
OVLD
Mix Box Pinion Gear
1/REV
X: 325 Hz
Y: -14.83 dBV
H-46 AIRCRAFT 01, SENSOR #5, 17% TORQUE
13
dBV
10
dB
/DIV
-67
START: 0 Hz
X: 325 Hz
BW: 11.936 Hz
Y: -14.83 dBV
STOP: 1 250 Hz
THD: -1.44 dB

Figure 20A

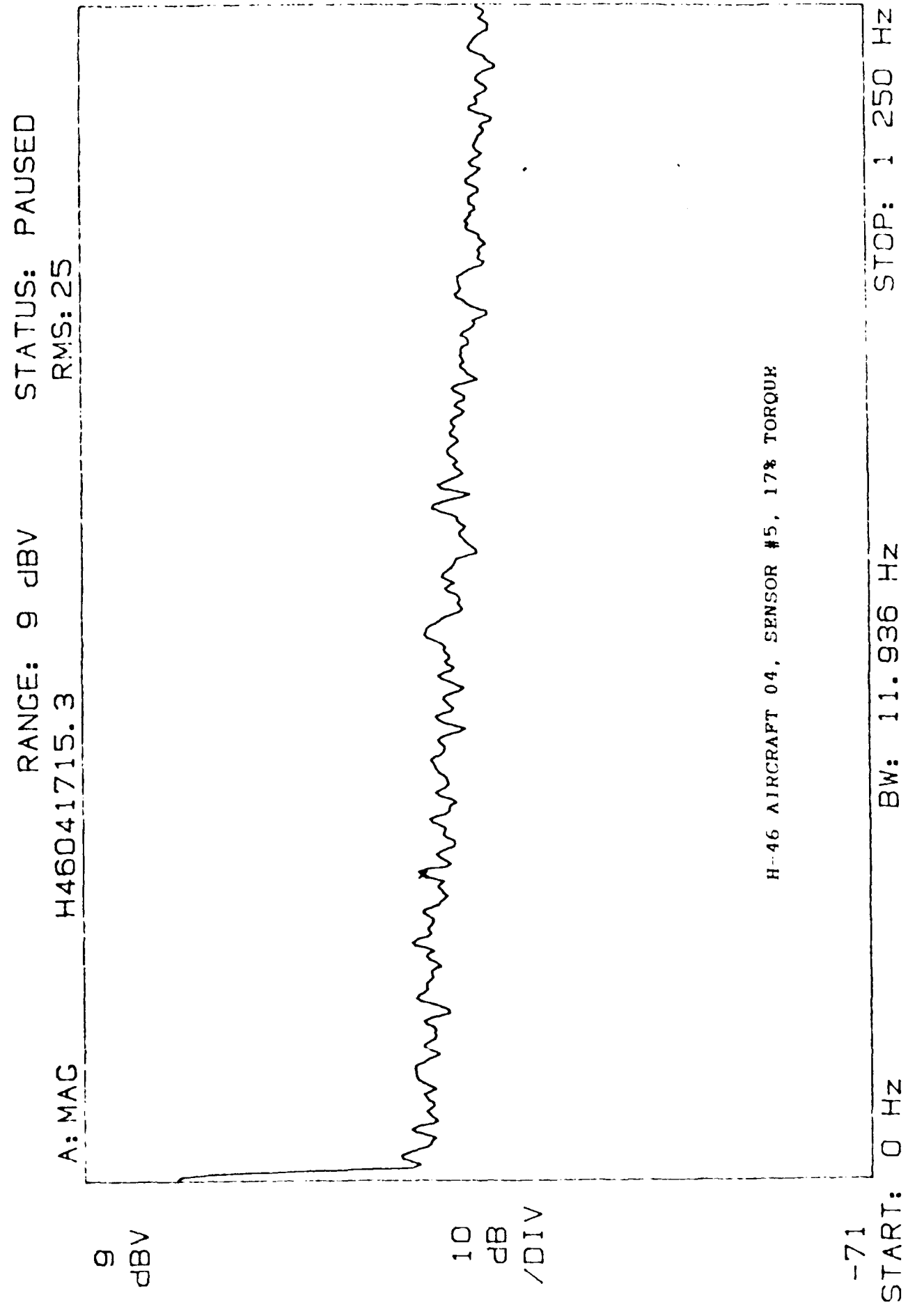
A: MAG
H46041715.3
RANGE: 9 dBV
STATUS: PAUSED
RMS: 25
9
dBV
10
dB
/DIV
-71
START: 0 Hz
X: 325 Hz
BW: 11.936 Hz
Y: -25.53 dBV
STOP: 1 250 Hz
H-46 AIRCRAFT 04, SENSOR #5, 17% TORQUE

Figure 20B

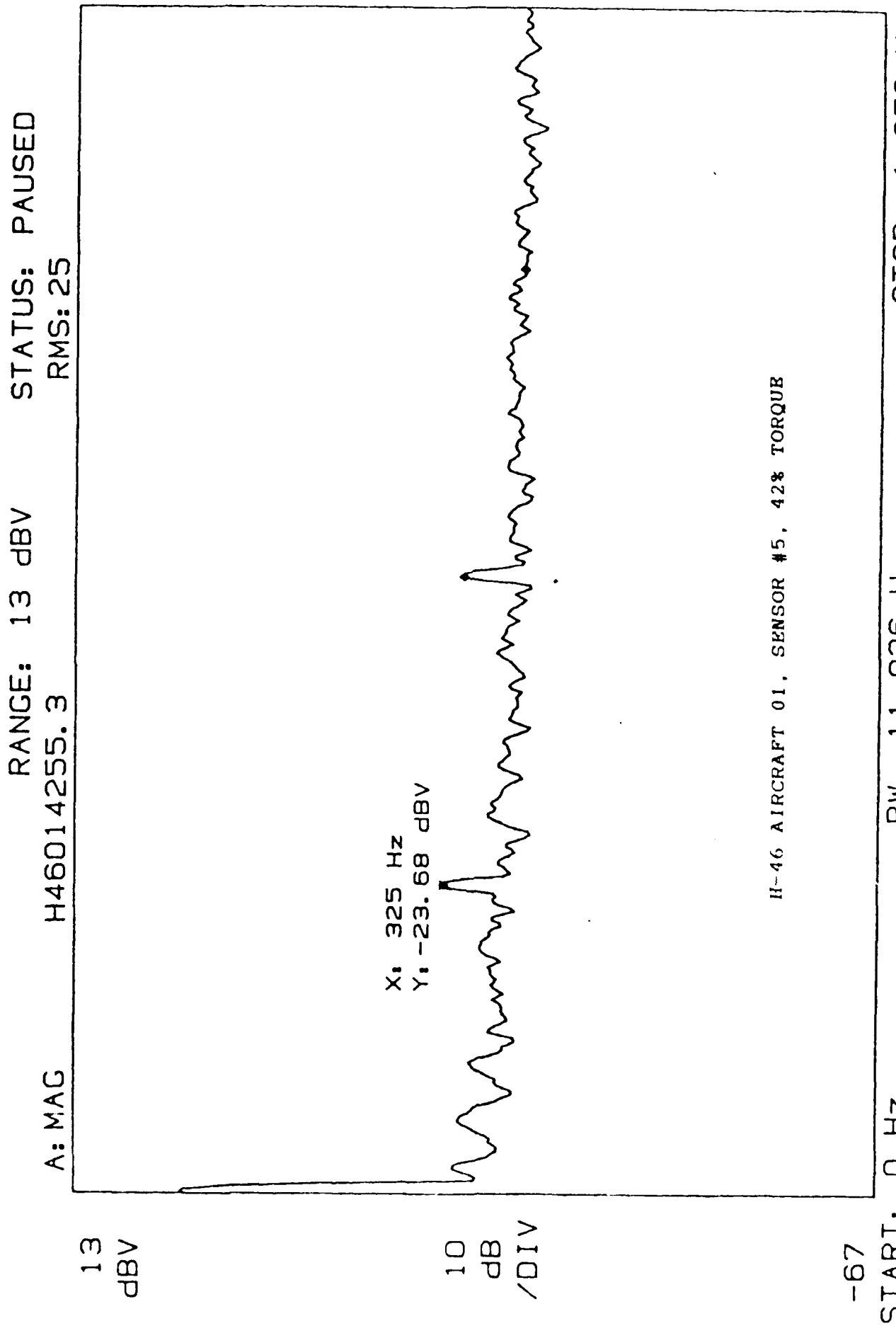
A: MAG
RANGE: 13 dBV
H46014255.3
STATUS: PAUSED
RMS: 25
X: 325 Hz
Y: -23.68 dBV
H-46 AIRCRAFT 01, SENSOR #5, 42% TORQUE
13
dBV
10
dB
/DIV
-67
START: 0 Hz
X: 325 Hz
BW: 11.936 Hz
Y: -23.68 dBV
STOP: 1 250 Hz
THD: -0.93 dB

Figure 21A

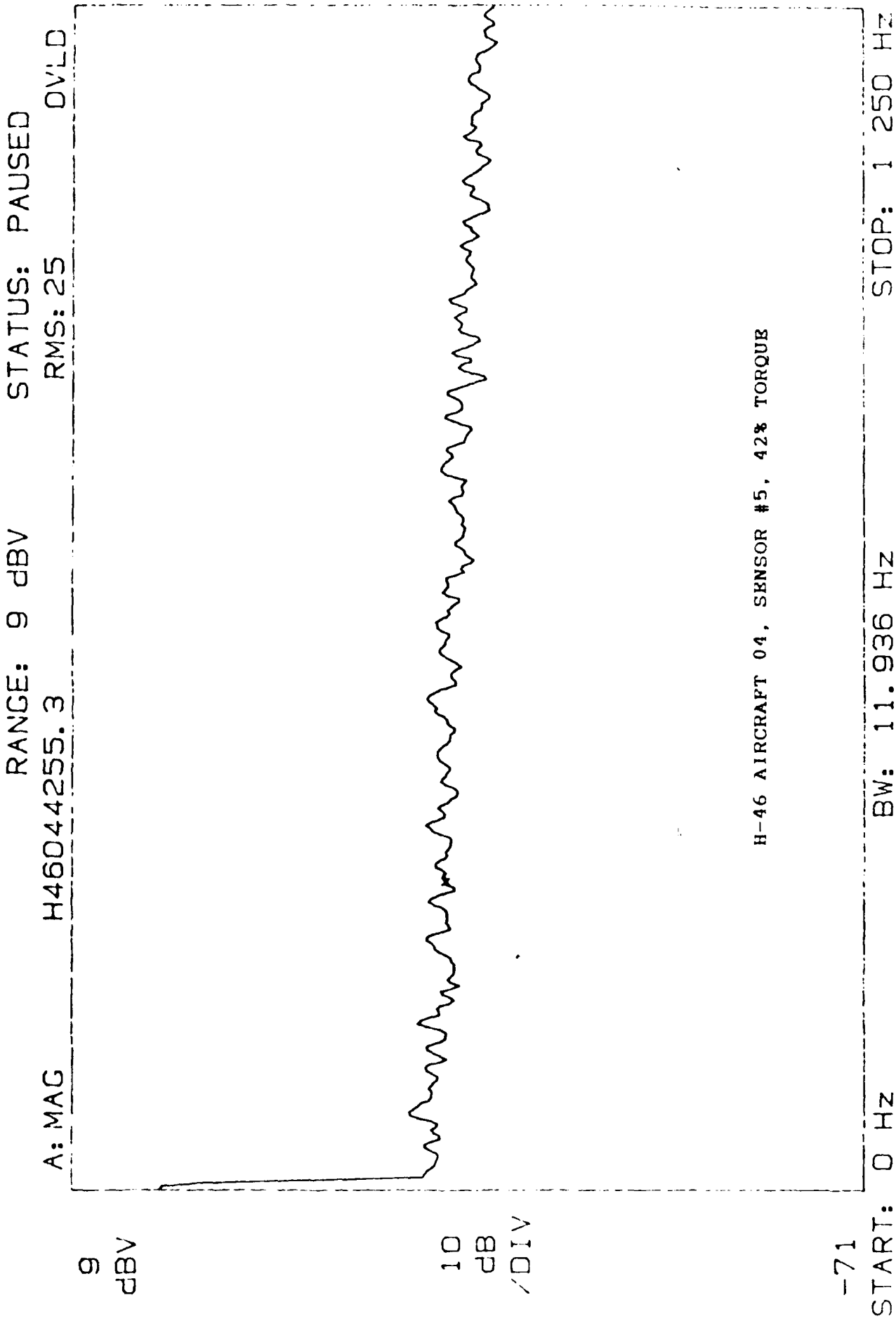
RANGE: 9 dBV
STATUS: PAUSED
A: MAG
H46044255.3
RMS: 25
OVLD
9 dBV
10 dB /DIV
-71
START: 0 Hz
STOP: 1 250 Hz
X: 325 Hz
BW: 11.936 Hz
Y: -28.63 dBV
H-46 AIRCRAFT 04, SENSOR #5, 42% TORQUE

Figure 21B

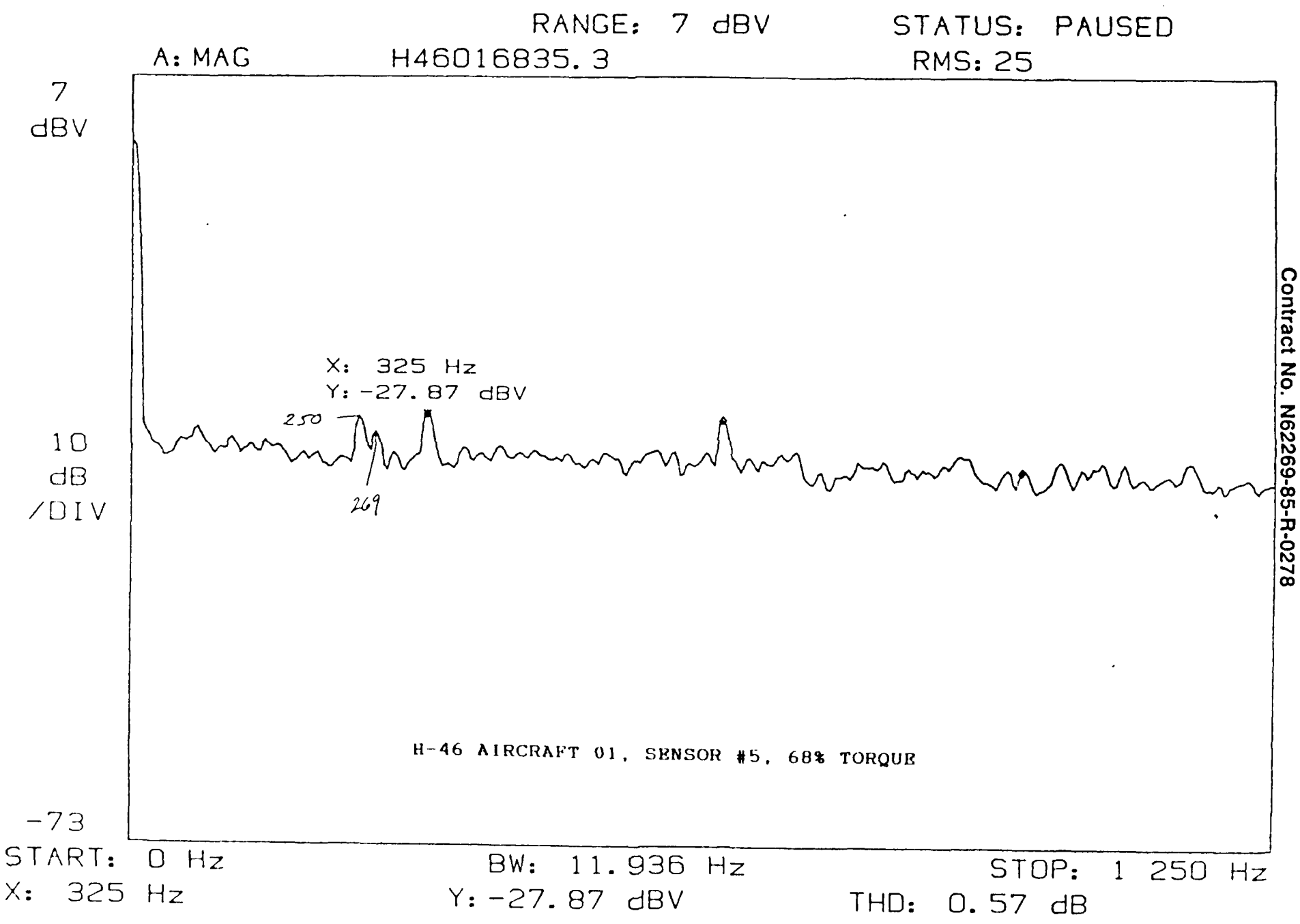

Figure 22A

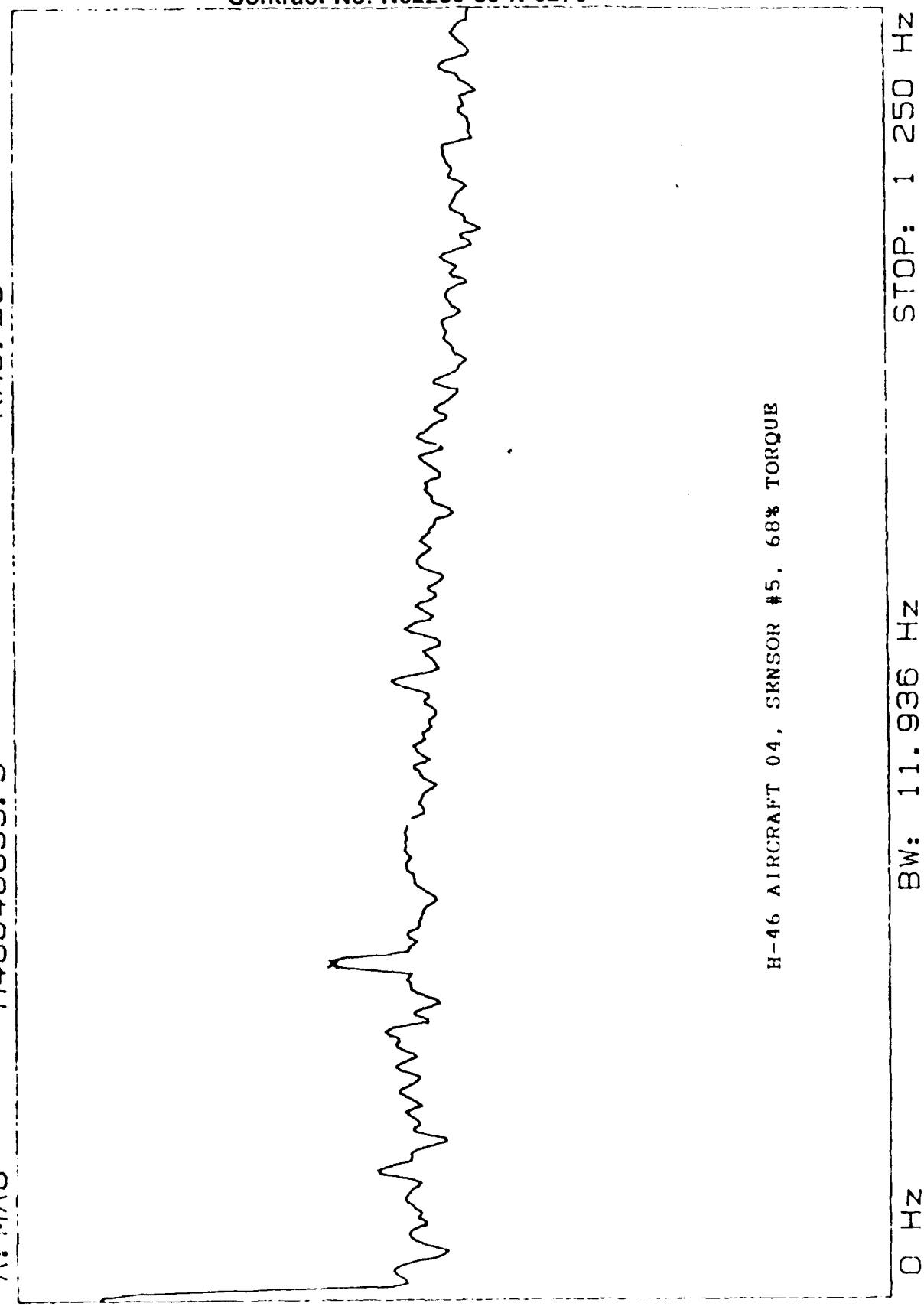
A: MAG
H46046835.3
RANGE: 9 dBV
STATUS: PAUSED
RMS: 25
9
dBV
10
dB
/DIV
-71
START: 0 Hz
X: 325 Hz
BW: 11.936 Hz
Y: -19.74 dBV
STOP: 1 250 Hz
H-46 AIRCRAFT 04, SENSOR #5, 68% TORQUE

Figure 22B

associated with the 1/rev and harmonics of the mix box input pinion gear. This occurs only at the lower torques of 17% to 28%. The fact that the second harmonic frequency at 650 Hz has the highest amplitude (approximately 20 db) may be an indication that this frequency is being strengthened by a source other than the pinion gear. The most likely candidate for this second 650 Hz source is a rolling element in the idler gear aft support bearing (refer to item 12 in Figure 13).

Figures 23, 24, and 25 are representative spectra at 17%, 42%, and 68% torque.

Mix Box #2 Input Idler Gear (Sensor Location #6)

Aircraft #01 exhibits strong spectral lines associated with the 1/rev and harmonics of the mix box input pinion gear. The 325 Hz 1/rev amplitudes of this pinion are in excess of 10 db above background levels at all torques except 68%, where it drops to just about 10 db. In addition, the amplitude of this spectral line and associated SWE levels were observed to fluctuate significantly while operating at a constant torque. Figures 26, 27, and 28 illustrate the spectral changes that were associated with SWE readings that ranged from 87,045 to 146,671 while operating at 25% torque. These abnormally high SWE fluctuations were only observed at the lower operating torques of 17% to 42%

Aircraft #04 also had a 325 Hz spectral line that was just over 10 db, but only at the minimum operating torque of 17%. There are three other spectral lines worthy of note in the data acquired from aircraft #04; 68 Hz, 126 Hz, and 50 Hz. The 68 Hz line corresponds to the outer race defect frequency of the planet bearing in the main transmission. This spectral line exceeded the 10 db limit only at 25% torque and is shown in Figures 29 and 30. The 126 Hz line never exceeds 10 db above background, but corresponds to the 1/rev of the idler gear assembly and the 1/rev of the blower drive gear assembly (refer to items 4 & 7 in Figure 11). This frequency could also be related to cage rubbing in one of the mix box input pinion bearings (refer to item 15 in Figure 13). The 50 Hz spectral line only exceeds 10 db at 50% torque (see Figure 31), and is most probably a cage rub frequency from one of the idler gear assembly bearings (refer to items 12 and 13 in Figure 13).

Figures 32, 33, and 34 are representative spectra at 17%, 42%, and 68% torque.

Mix Box #1 Input Idler Gear (Sensor Location #8)

No significant spectral lines more than 10 db above background levels were observed at any torque level on aircraft #04. The only clearly distinguishable spectral lines on this aircraft are at the 1/rev of the mix box input pinion gear. Aircraft #01 exhibits strong spectral lines associated with the 1/rev and harmonics of

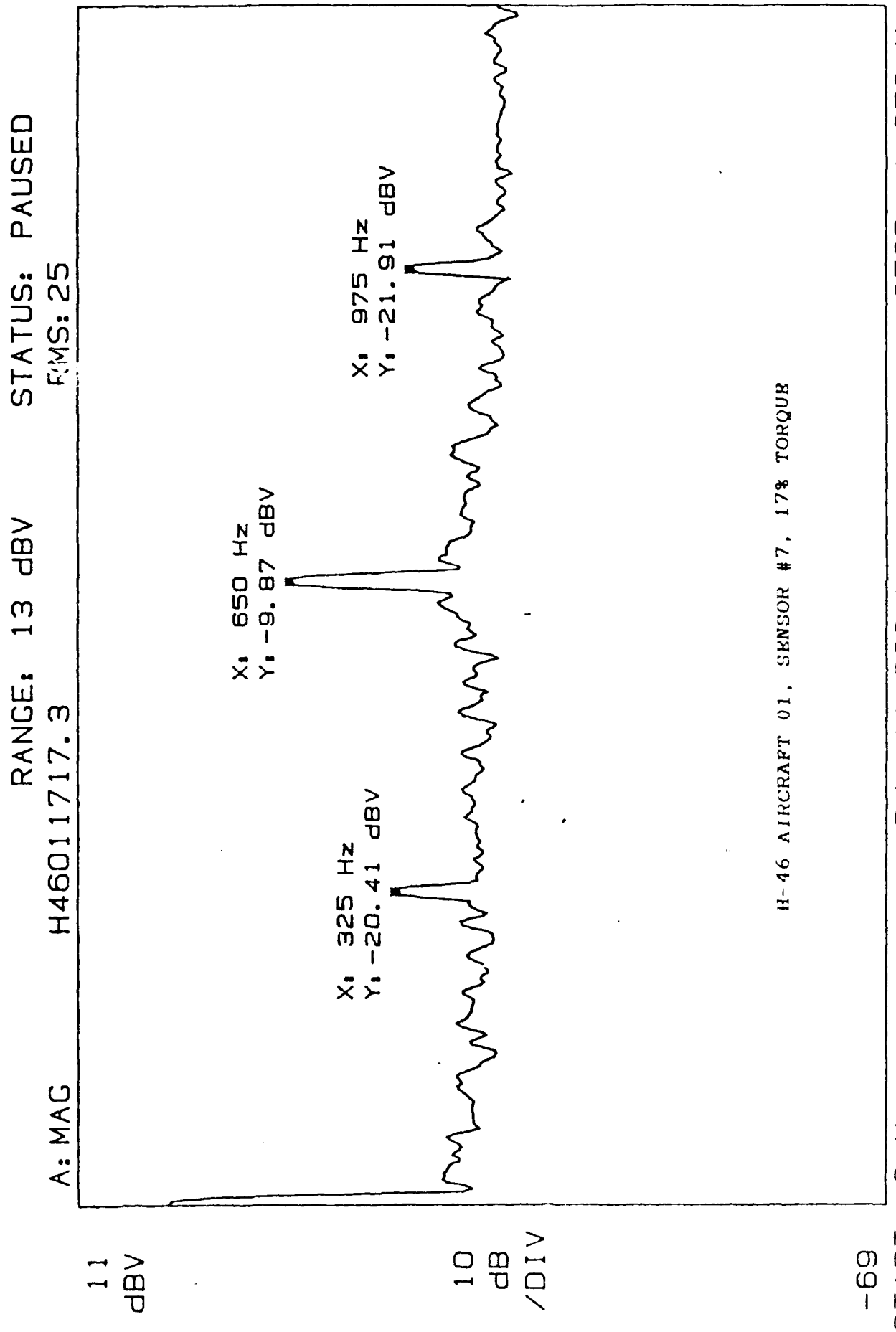
A: MAG
RANGE: 13 dBV
H46011717.3
STATUS: PAUSED
FMS: 25
X: 325 Hz
Y: -20.41 dBV
X: 650 Hz
Y: -9.87 dBV
X: 975 Hz
Y: -21.91 dBV
H-46 AIRCRAFT 01, SENSOR #7, 17% TORQUE
11 dBV
10 dB /DIV
-69
START: 0 Hz
X: 325 Hz
BW: 11.936 Hz
Y: -20.41 dBV
STOP: 1 250 Hz
THD: 10.80 dB

Figure 23A

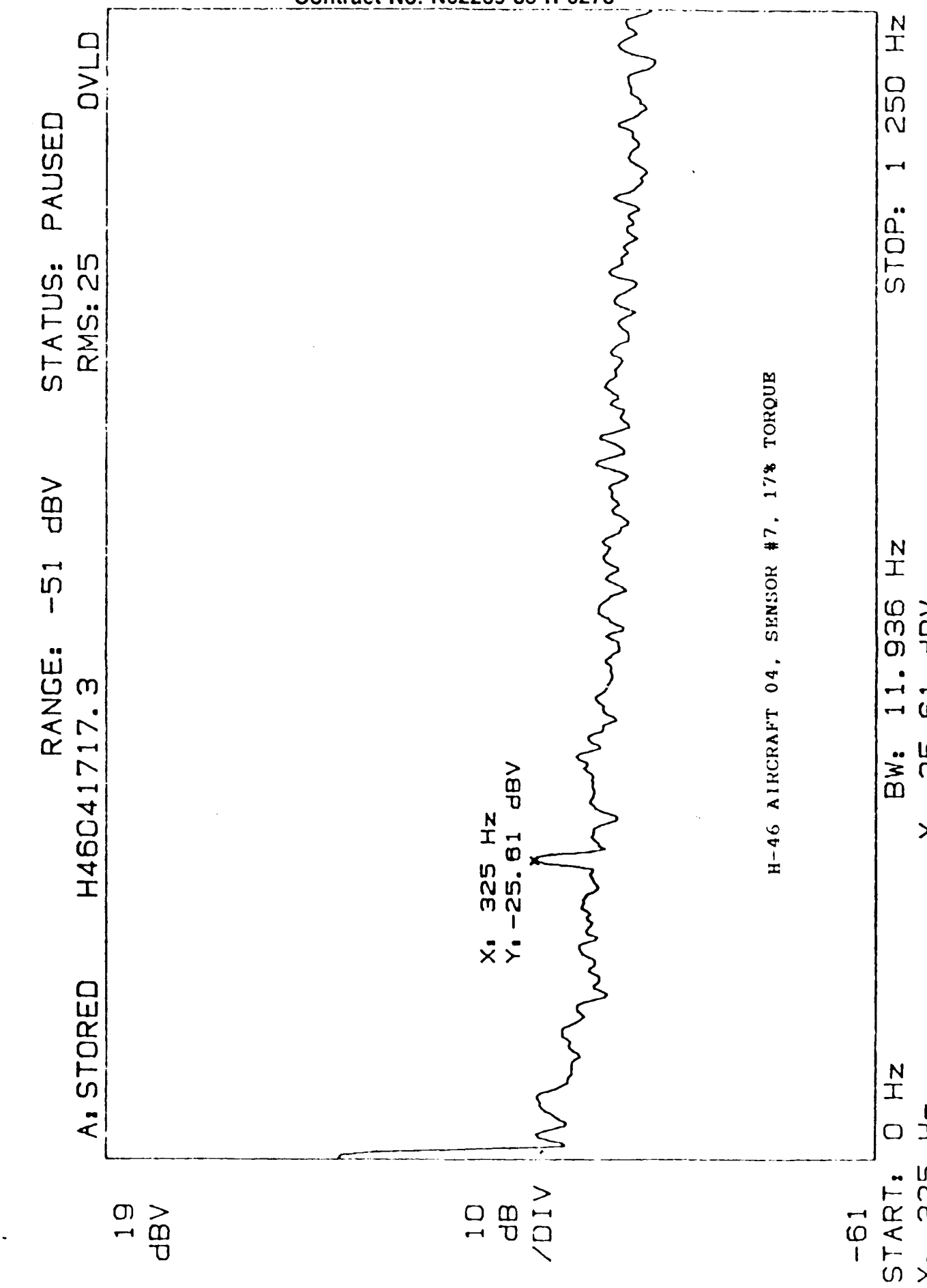
A: STORED
RANGE: -51 dBV
H46041717.3
STATUS: PAUSED
RMS: 25
OVLD
X: 325 Hz
Y: -25.61 dBV
H-46 AIRCRAFT 04, SENSOR #7, 17% TORQUE
19
dBV
10
dB
/DIV
-61
START: 0 Hz
X: 325 Hz
BW: 11.936 Hz
Y: -25.61 dBV
STOP: 1 250 Hz

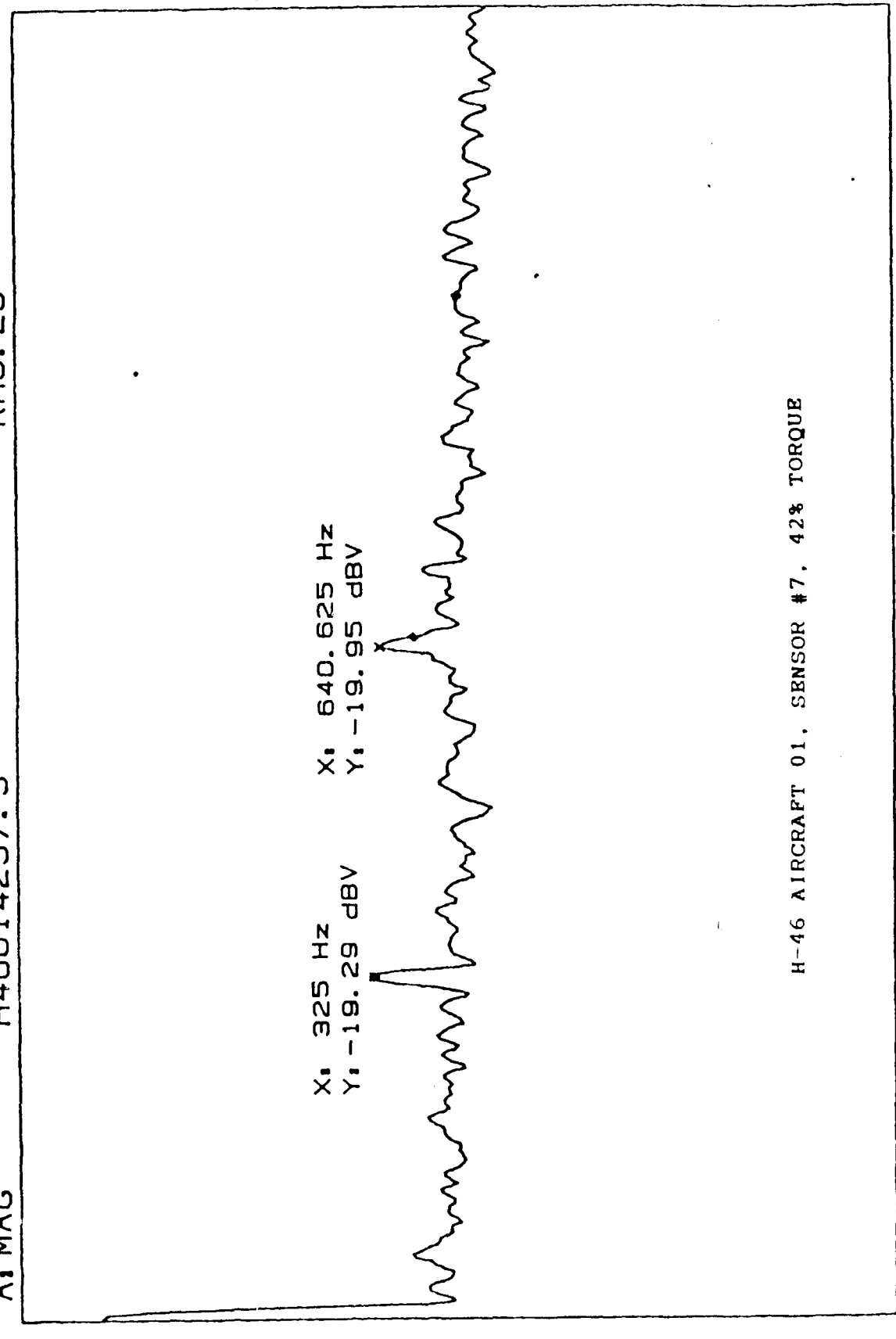
A: MAG
H46014257.3
RANGE: 13 dBV
STATUS: PAUSED
RMS: 25
X: 325 Hz
Y: -19.29 dBV
X: 640.625 Hz
Y: -19.95 dBV
H-46 AIRCRAFT 01, SENSOR #7, 42% TORQUE
13 dBV
10 dB /DIV
-67
START: 0 Hz
X: 325 Hz
BW: 11.936 Hz
Y: -19.29 dBV
STOP: 1 250 Hz
THD: -2.40 dB

Figure 24A

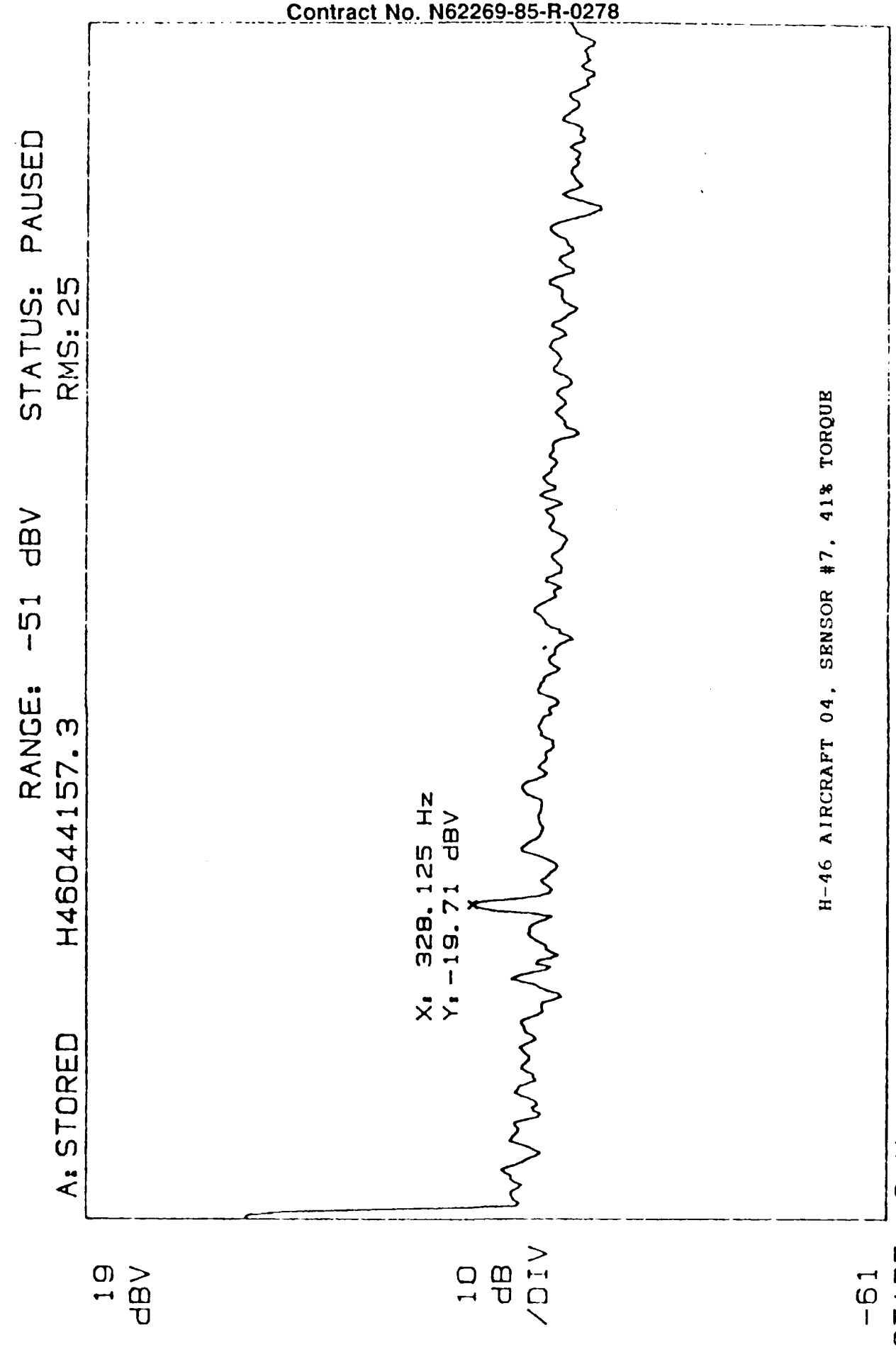
A: STORED
RANGE: -51 dBV
H46044157.3
STATUS: PAUSED
RMS: 25
X: 328.125 Hz
Y: -19.71 dBV
H-46 AIRCRAFT 04, SENSOR #7, 41% TORQUE
19
dBV
10
dB
/DIV
-61
START: 0 Hz
X: 328.125 Hz
BW: 11.936 Hz
Y: -19.71 dBV
STOP: 1 250 Hz

Figure 24B

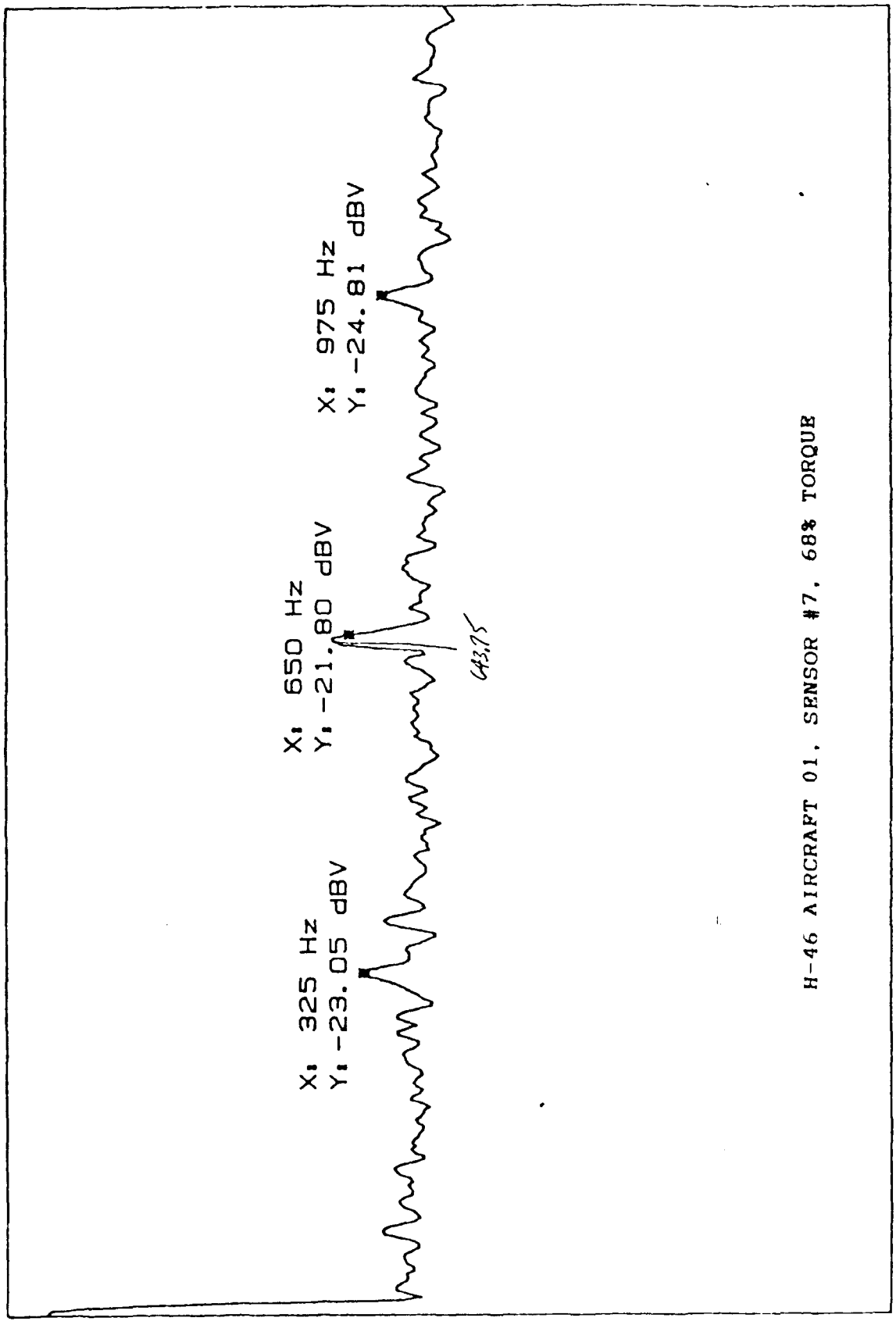
A: MAG
RANGE: 9 dBV
H46016837.3
STATUS: PAUSED
RMS: 25
OVLD
X: 325 Hz
Y: -23.05 dBV
X: 650 Hz
Y: -21.80 dBV
X: 975 Hz
Y: -24.81 dBV
43.75
H-46 AIRCRAFT 01, SENSOR #7, 68% TORQUE
3W: 11.936 Hz
Y: -23.05 dBV
THD: 3.01 dB
START: 0 Hz
X: 325 Hz
STOP: 1 250 Hz
9
dBV
10
dB
/DIV
-71

Figure 25A

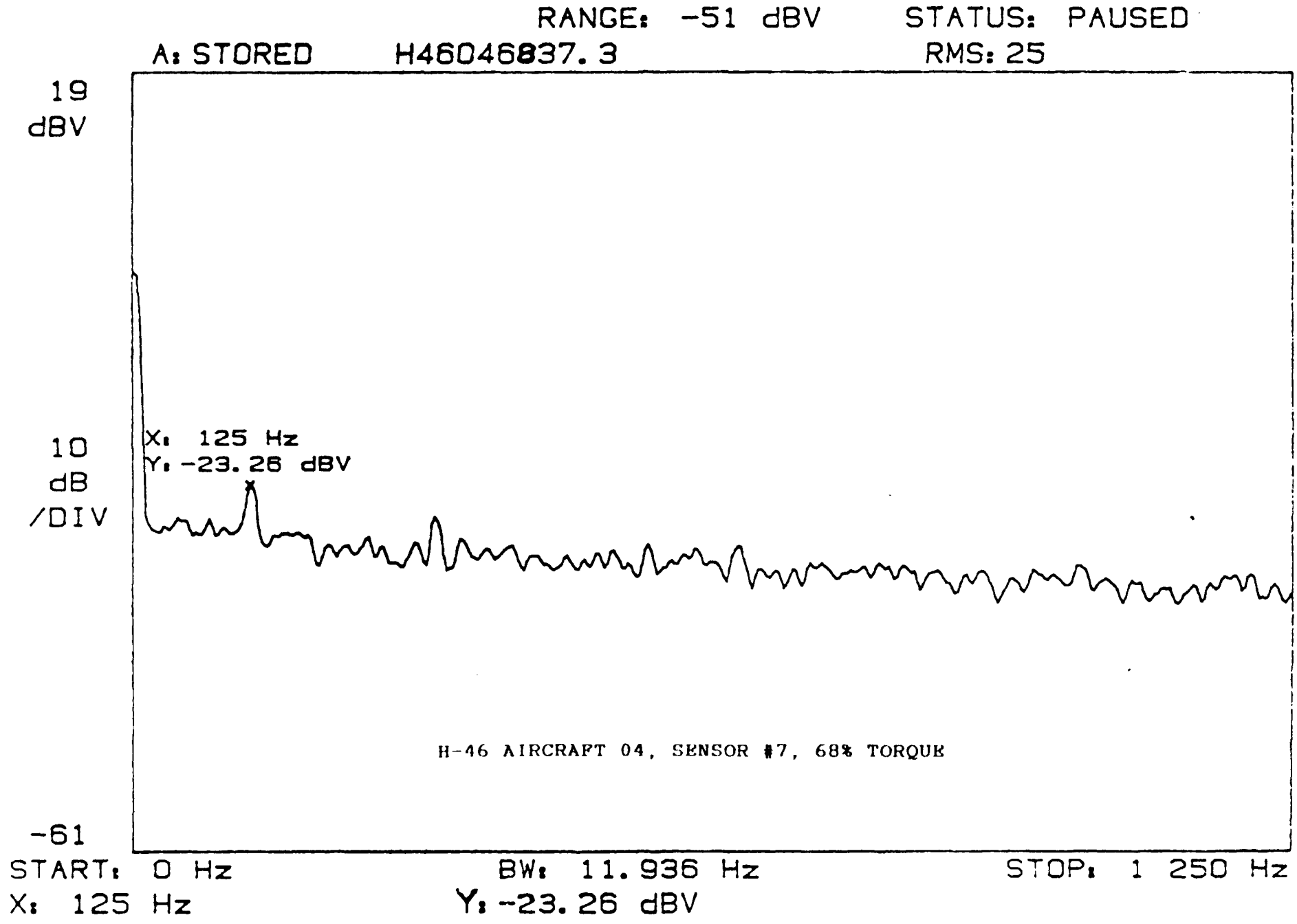
RANGE: -51 dBV
STATUS: PAUSED
A: STORED
H46046837.3
RMS: 25
19
dBV
10
dB
/DIV
-61
X: 125 Hz
Y: -23.26 dBV
H-46 AIRCRAFT 04, SENSOR #7, 68% TORQUE
START: 0 Hz
BW: 11.936 Hz
STOP: 1 250 Hz
X: 125 Hz
Y: -23.26 dBV

Figure 25B

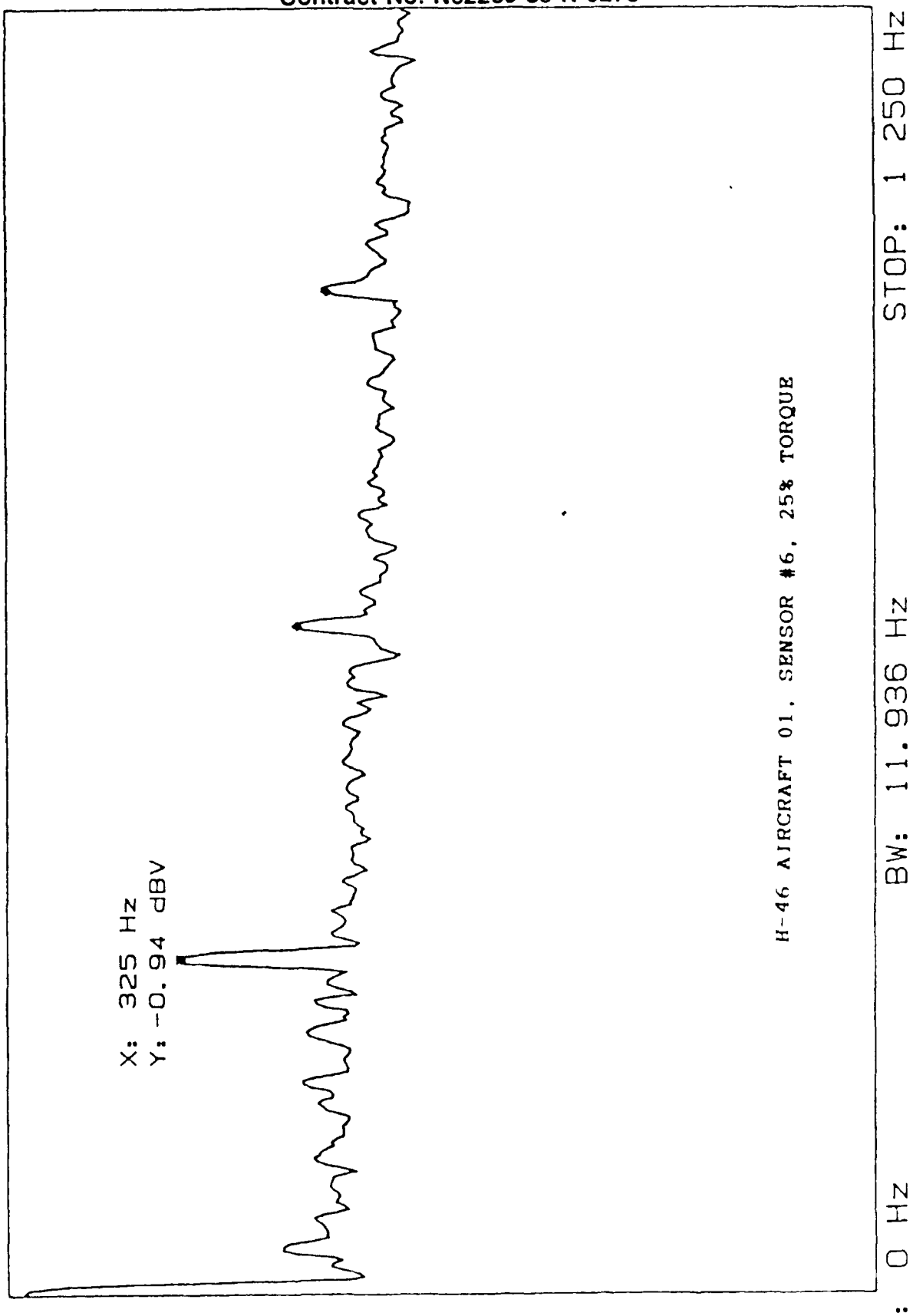
A: MAG
1H46012546.3
RANGE: -21 dBV
STATUS: PAUSED
RMS: 25
X: 325 Hz
Y: -0.94 dBV
H-46 AIRCRAFT 01, SENSOR #6, 25% TORQUE
15
dBV
10
dB
/DIV
-65
START: 0 Hz
X: 325 Hz
BW: 11.936 Hz
Y: -0.94 dBV
STOP: 1 250 Hz
THD: -9.05 dB

Figure 26

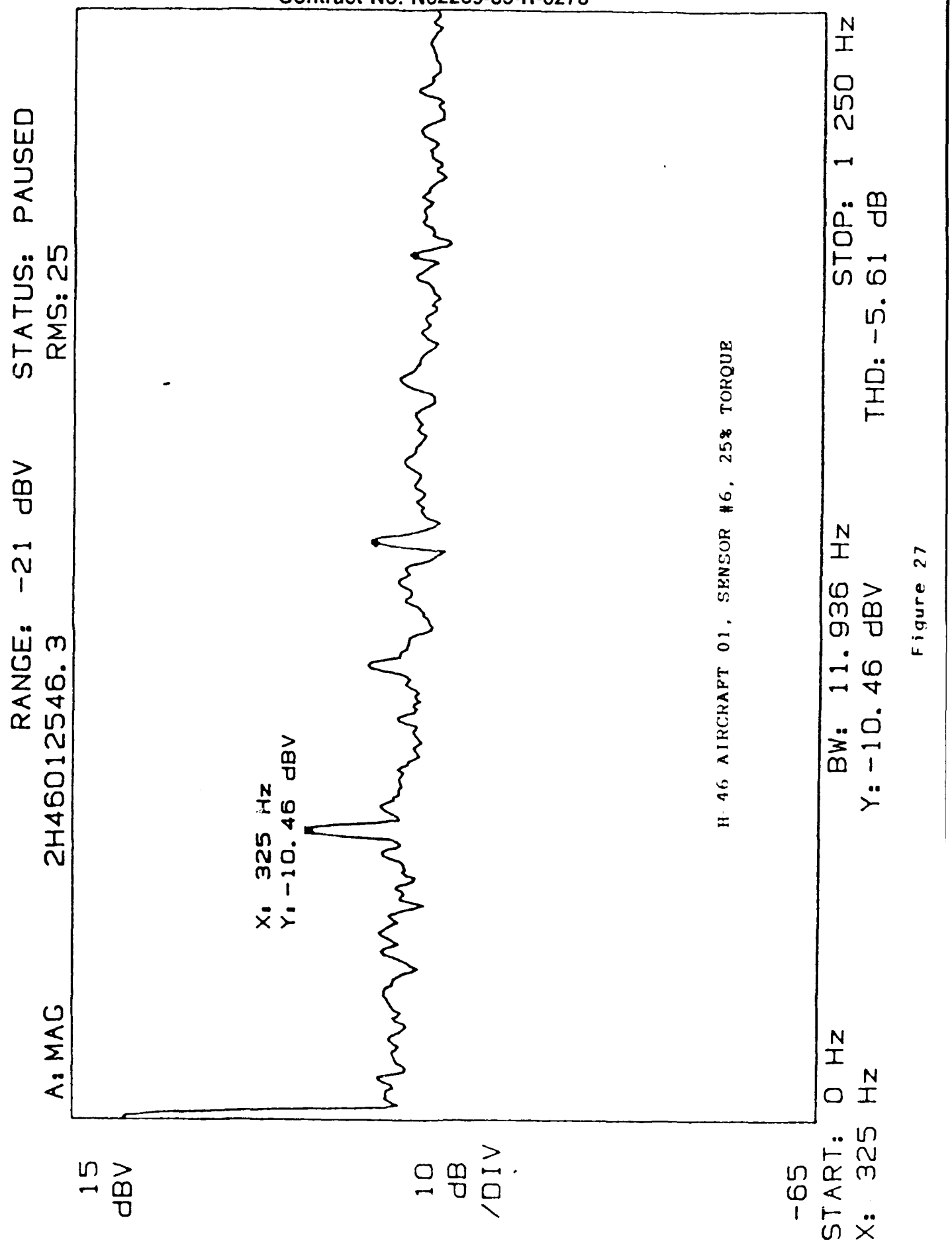
A: MAG
RANGE: -21 dBV
2H46012546.3
STATUS: PAUSED
RMS: 25
X: 325 Hz
Y: -10.46 dBV
15 dBV
10 dB /DIV
-65
START: 0 Hz
X: 325 Hz
BW: 11.936 Hz
Y: -10.46 dBV
STOP: 1 250 Hz
THD: -5.61 dB
H-46 AIRCRAFT 01, SENSOR #6, 25% TORQUE

Figure 27

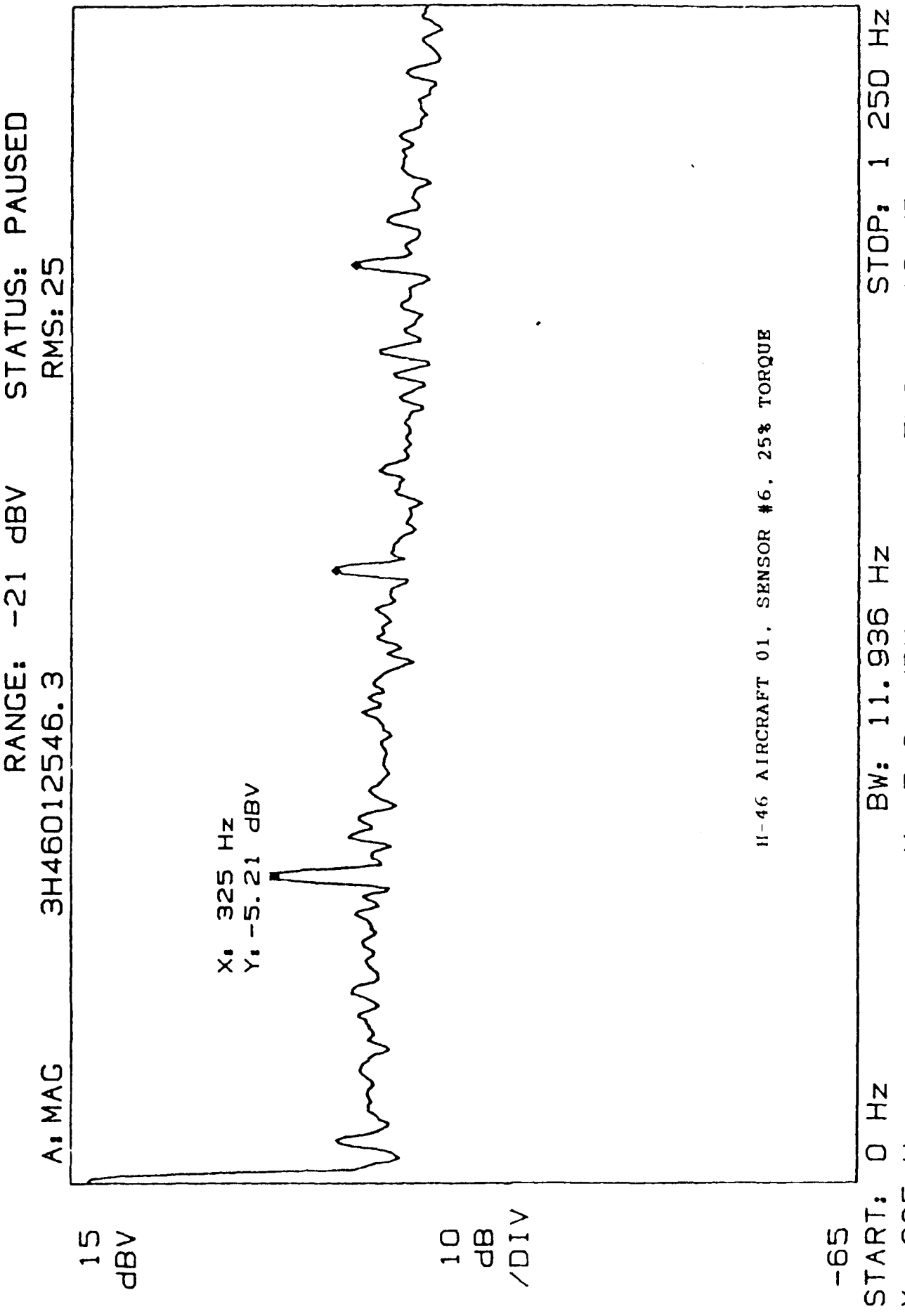
A: MAG
RANGE: -21 dBV
3H46012546.3
STATUS: PAUSED
RMS: 25
X: 325 Hz
Y: -5.21 dBV
H-46 AIRCRAFT 01, SENSOR #6, 25% TORQUE
15
dBV
10
dB
/DIV
-65
START: 0 Hz
X: 325 Hz
BW: 11.936 Hz
Y: -5.21 dBV
STOP: 1 250 Hz
THD: -4.13 dB

Figure 28

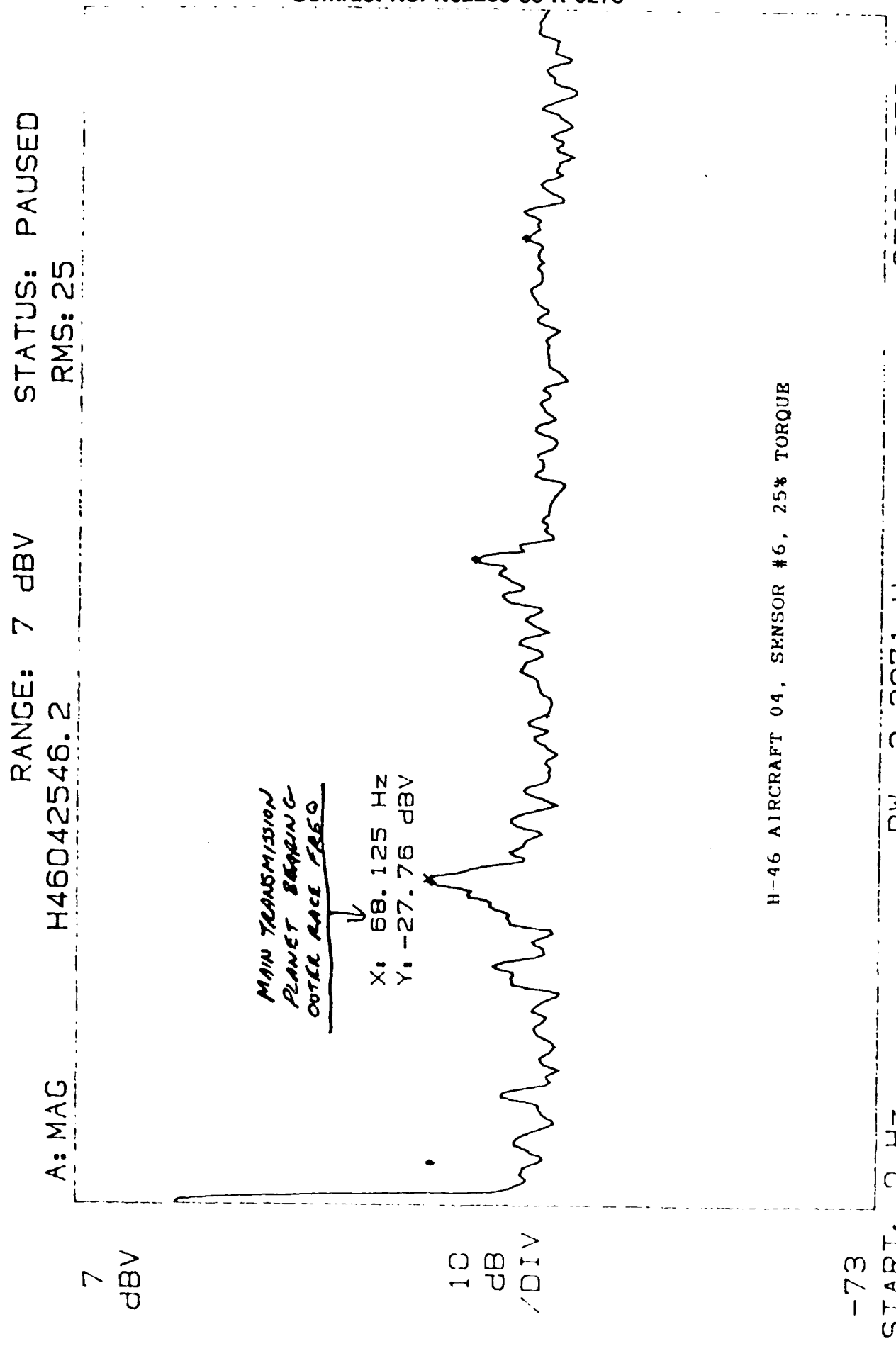

H-46 AIRCRAFT 04, SENSOR #6, 25% TORQUE

Figure 29

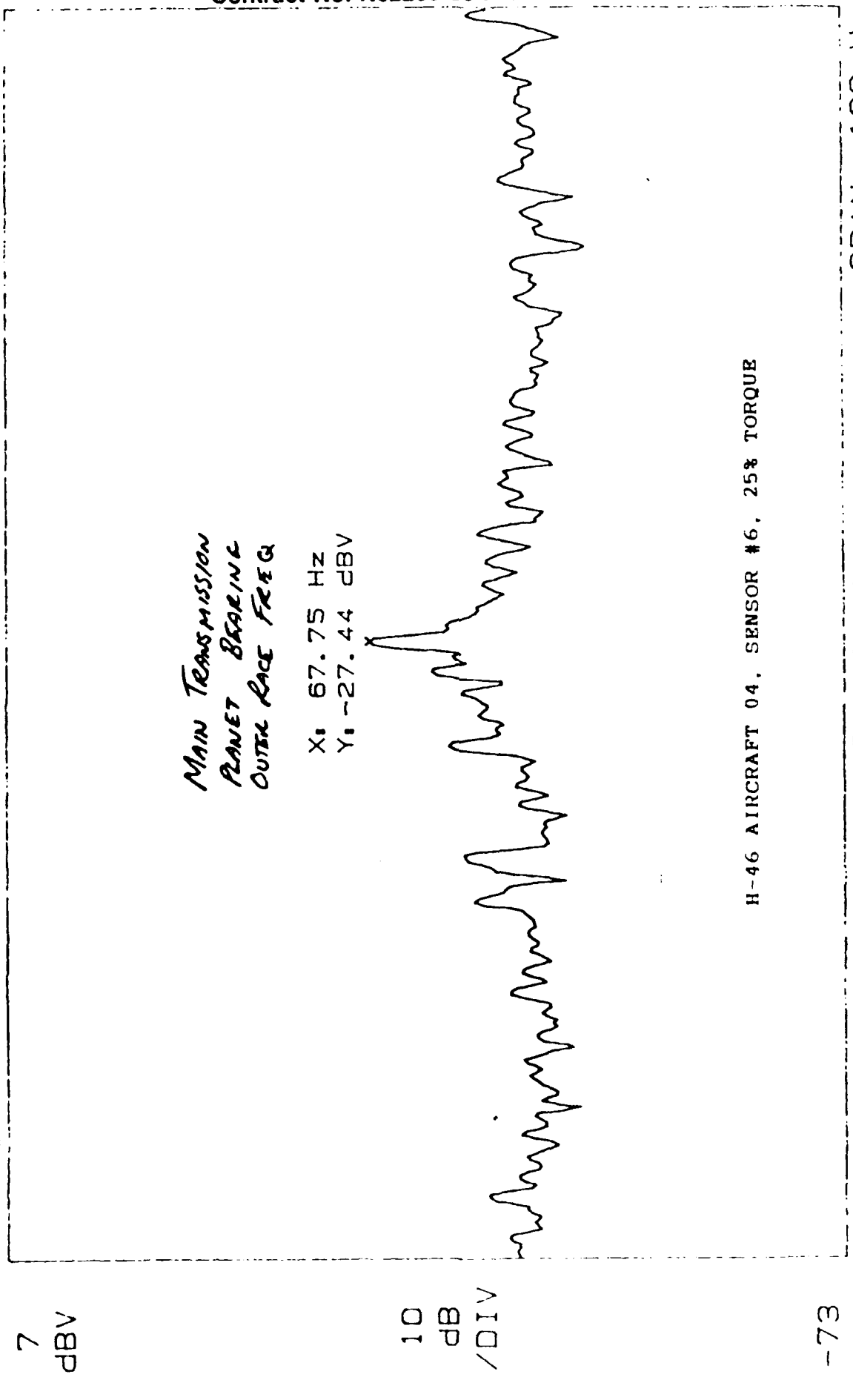
RANGE: 7 dBV
STATUS: PAUSED
H46042546.
RMS: 10
A: MAG
MAIN TRANSMISSION
PLANET BEARING
OUTER RACE FREQ
X: 67.75 Hz
Y: -27.44 dBV
7
dBV
10
dB
/DIV
-73
CENTER: 68.25 Hz
BW: 954.85 mHz
SPAN: 100 Hz
X: 67.75 Hz
Y: -27.44 dBV
H-46 AIRCRAFT 04, SENSOR #6, 25% TORQUE

Figure 30

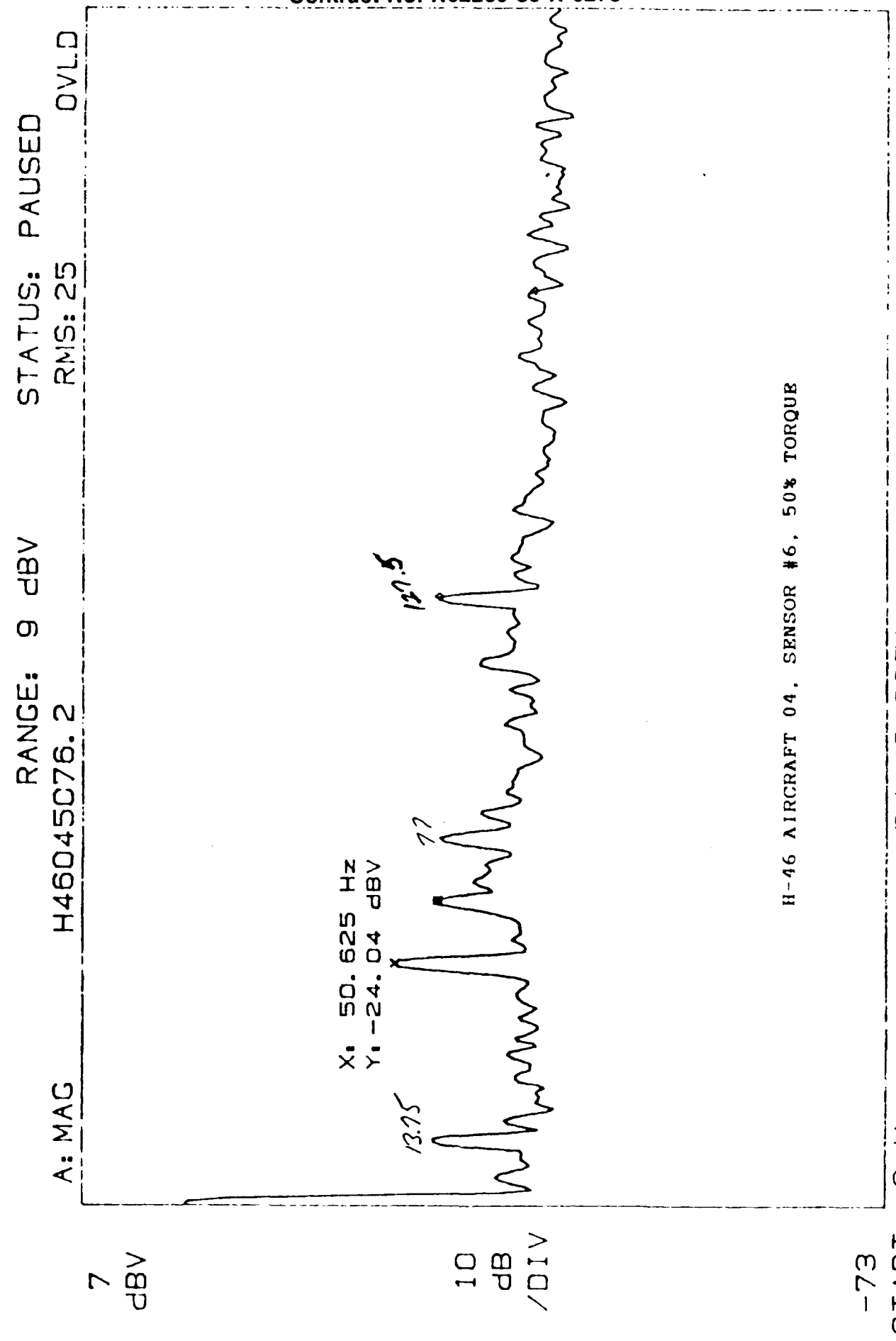
A: MAG
H46045076.2
RANGE: 9 dBV
STATUS: PAUSED
RMS: 25
OVLD
X: 50.625 Hz
Y: -24.04 dBV
13.75
77
120.5
H-46 AIRCRAFT 04, SENSOR #6, 50% TORQUE
7
dBV
10
dB
/DIV
-73
START: 0 Hz
X: 63.75 Hz
BW: 2.3871 Hz
Y: -28.28 dBV
STOP: 250 Hz
THD: 0.33 dB

Figure 31

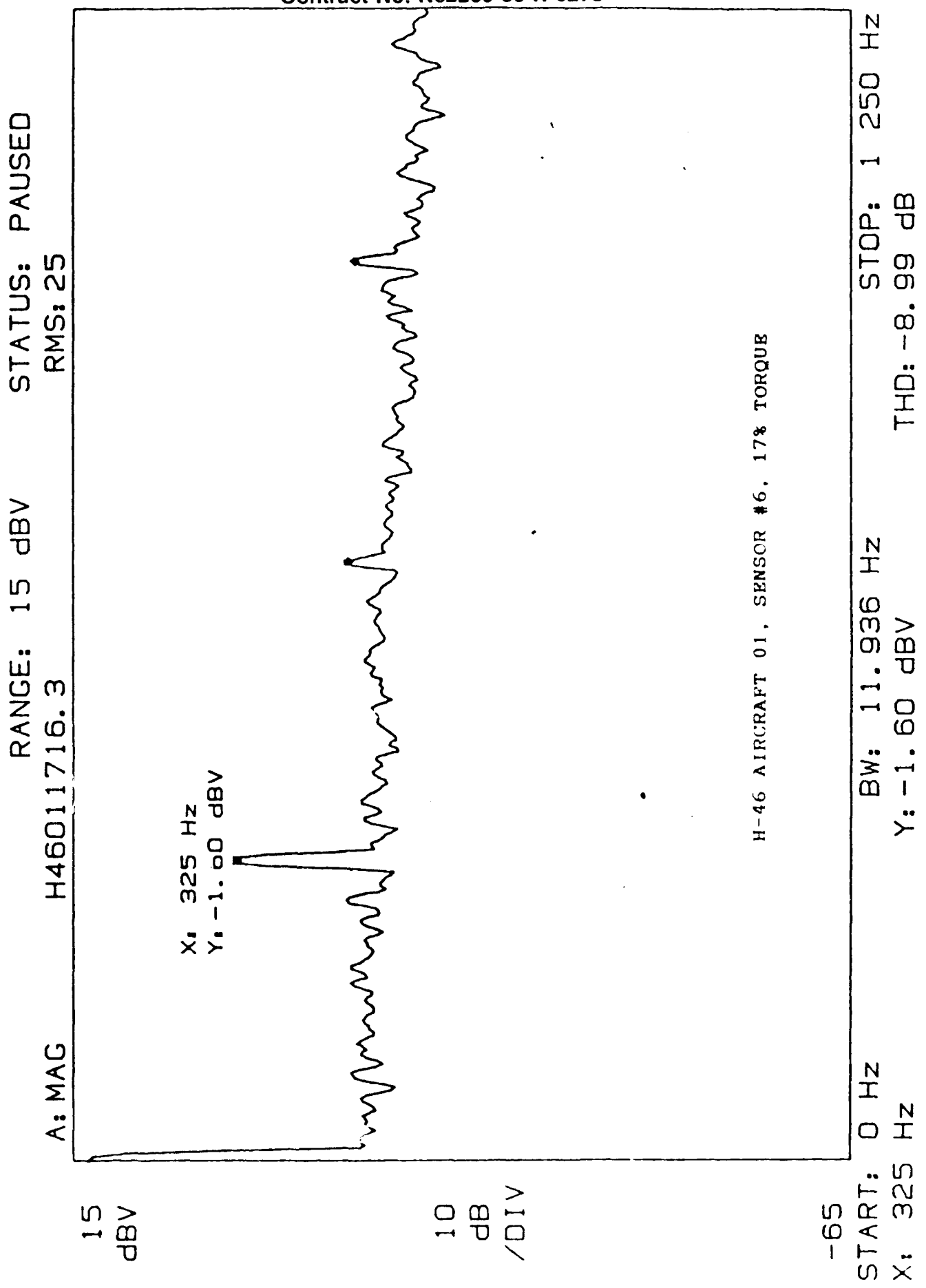
A: MAG
H46011716.3
RANGE: 15 dBV
STATUS: PAUSED
RMS: 25
X: 325 Hz
Y: -1.00 dBV
H-46 AIRCRAFT 01, SENSOR #6, 17% TORQUE
15 dBV
10 dB /DIV
-65
START: 0 Hz
X: 325 Hz
BW: 11.936 Hz
Y: -1.60 dBV
STOP: 1 250 Hz
THD: -8.99 dB

Figure 32A

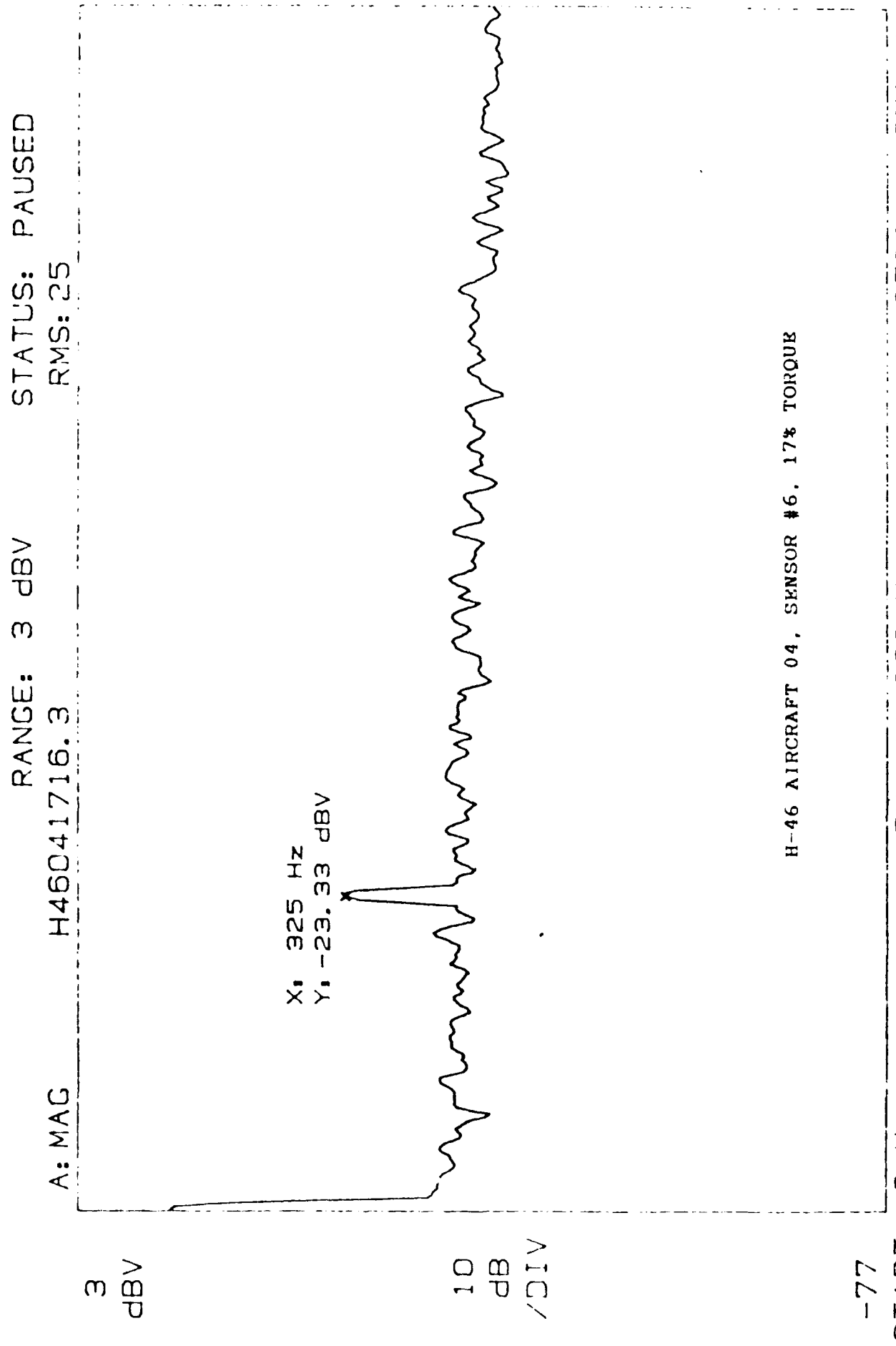
A: MAG
H46041716.3
RANGE: 3 dBV
STATUS: PAUSED
RMS: 25
X: 325 Hz
Y: -23.33 dBV
H-46 AIRCRAFT 04, SENSOR #6, 17% TORQUE
START: 0 Hz
X: 325 Hz
BW: 11.936 Hz
Y: -23.33 dBV
STOP: 1 250 Hz
3 dBV
10 dB /DIV
-77

Figure 32B

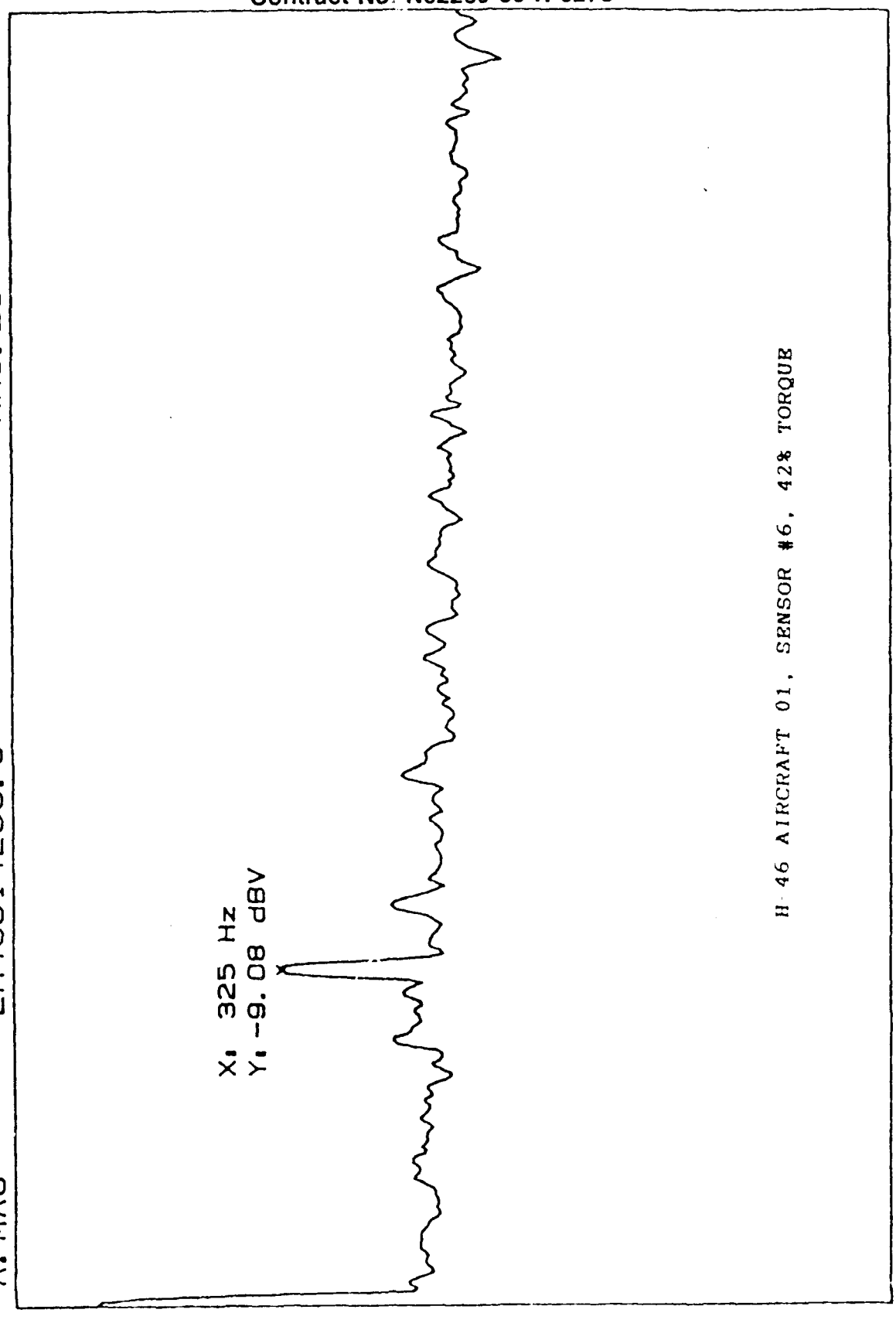
A: MAG
2H46014256.3
RANGE: -21 dBV
STATUS: PAUSED
RMS: 25
X: 325 Hz
Y: -9.08 dBV
H-46 AIRCRAFT 01, SENSOR #6, 42% TORQUE
15
dBV
10
dB
/DIV
-65
START: 0 Hz
X: 325 Hz
BW: 11.936 Hz
Y: -9.08 dBV
STOP: 1 250 Hz

Figure 33A

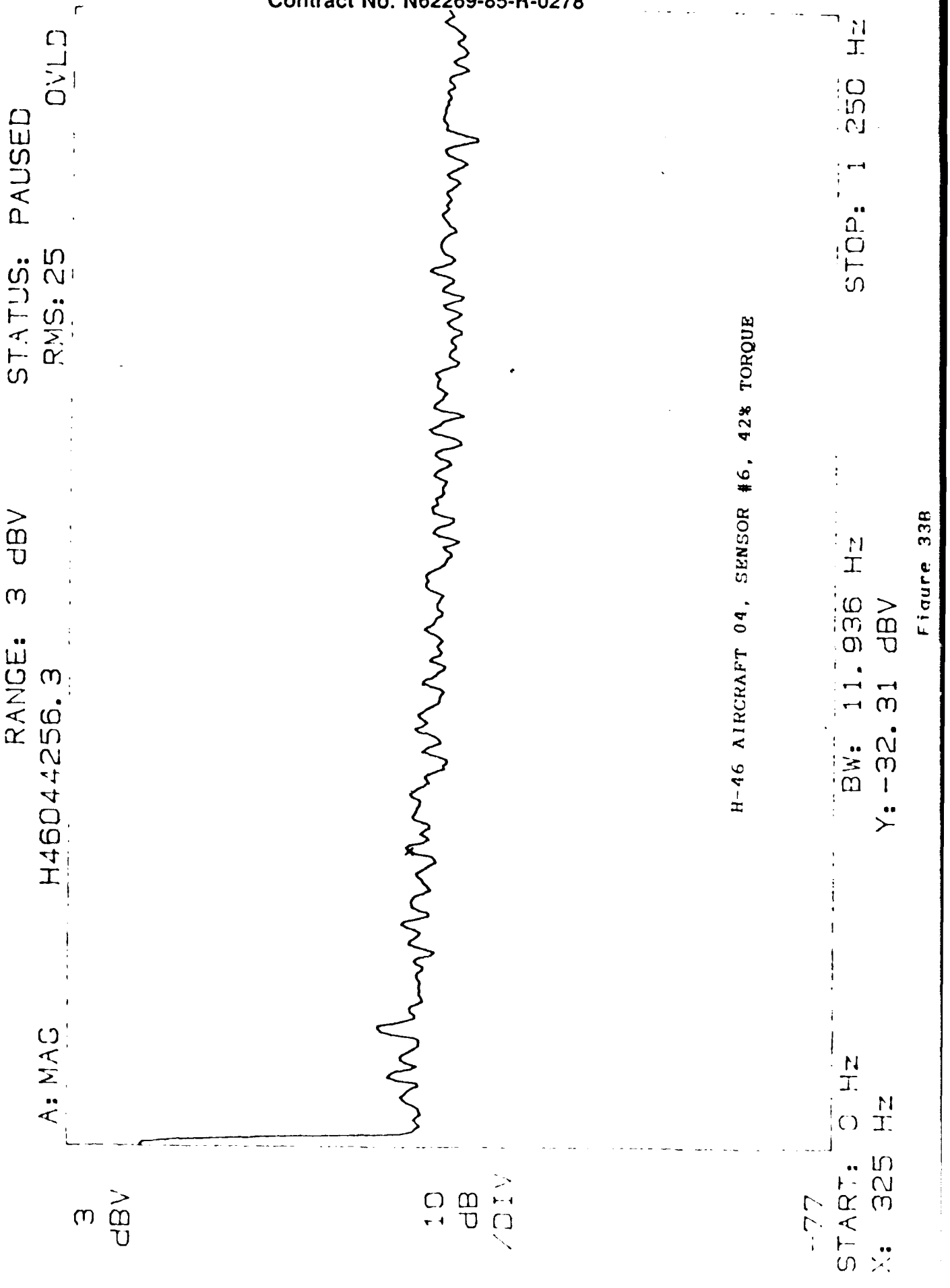

H-46 AIRCRAFT 04, SENSOR #6, 42% TORQUE

Figure 33B

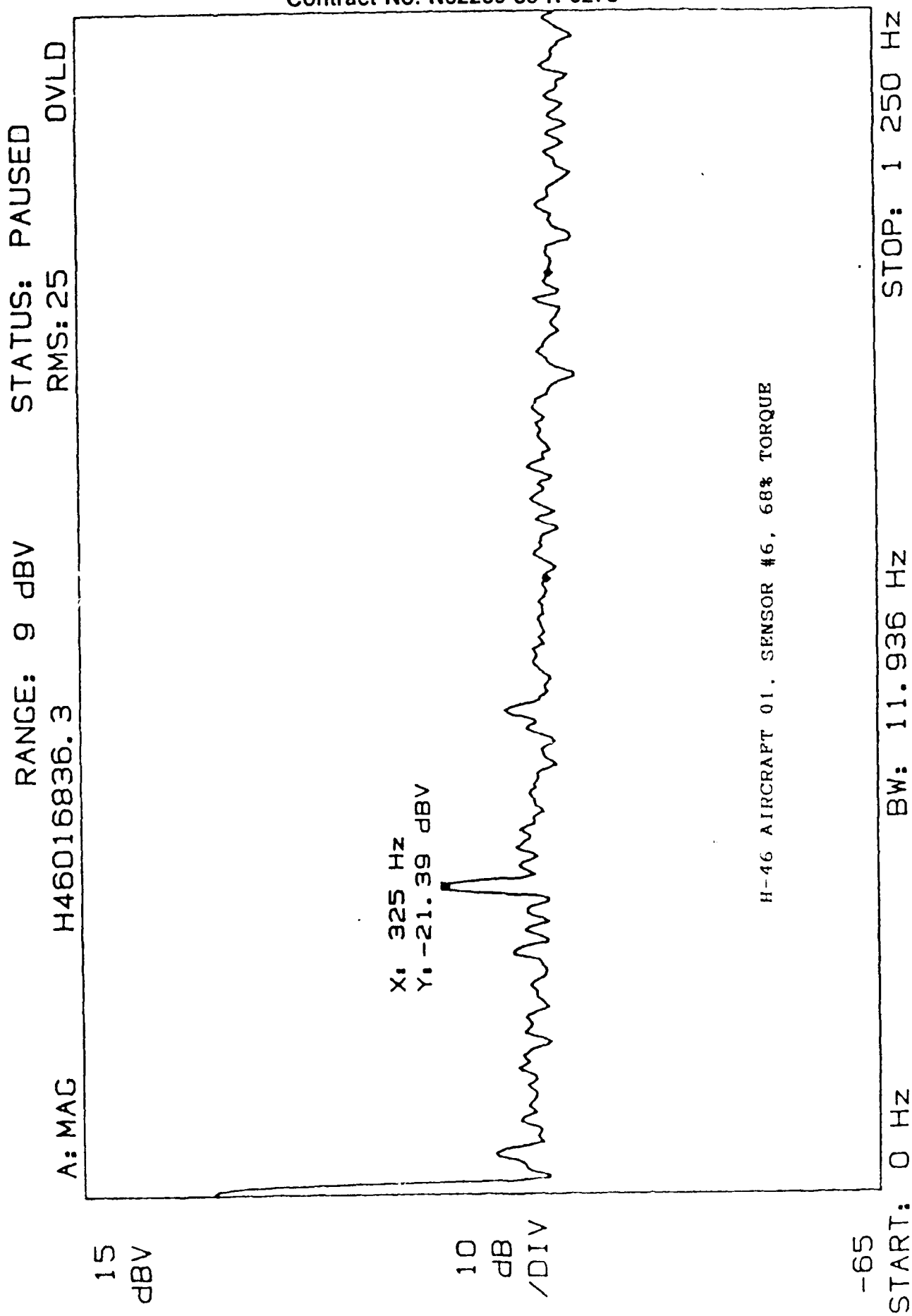
A: MAG
RANGE: 9 dBV
H46016836.3
STATUS: PAUSED
RMS: 25
OVLD
X: 325 Hz
Y: -21.39 dBV
H-46 AIRCRAFT 01, SENSOR #6, 68% TORQUE
15
dBV
10
dB
/DIV
-65
START: 0 Hz
X: 325 Hz
BW: 11.936 Hz
Y: -21.39 dBV
STOP: 1 250 Hz
THD: -7.77 dB

Figure 34A

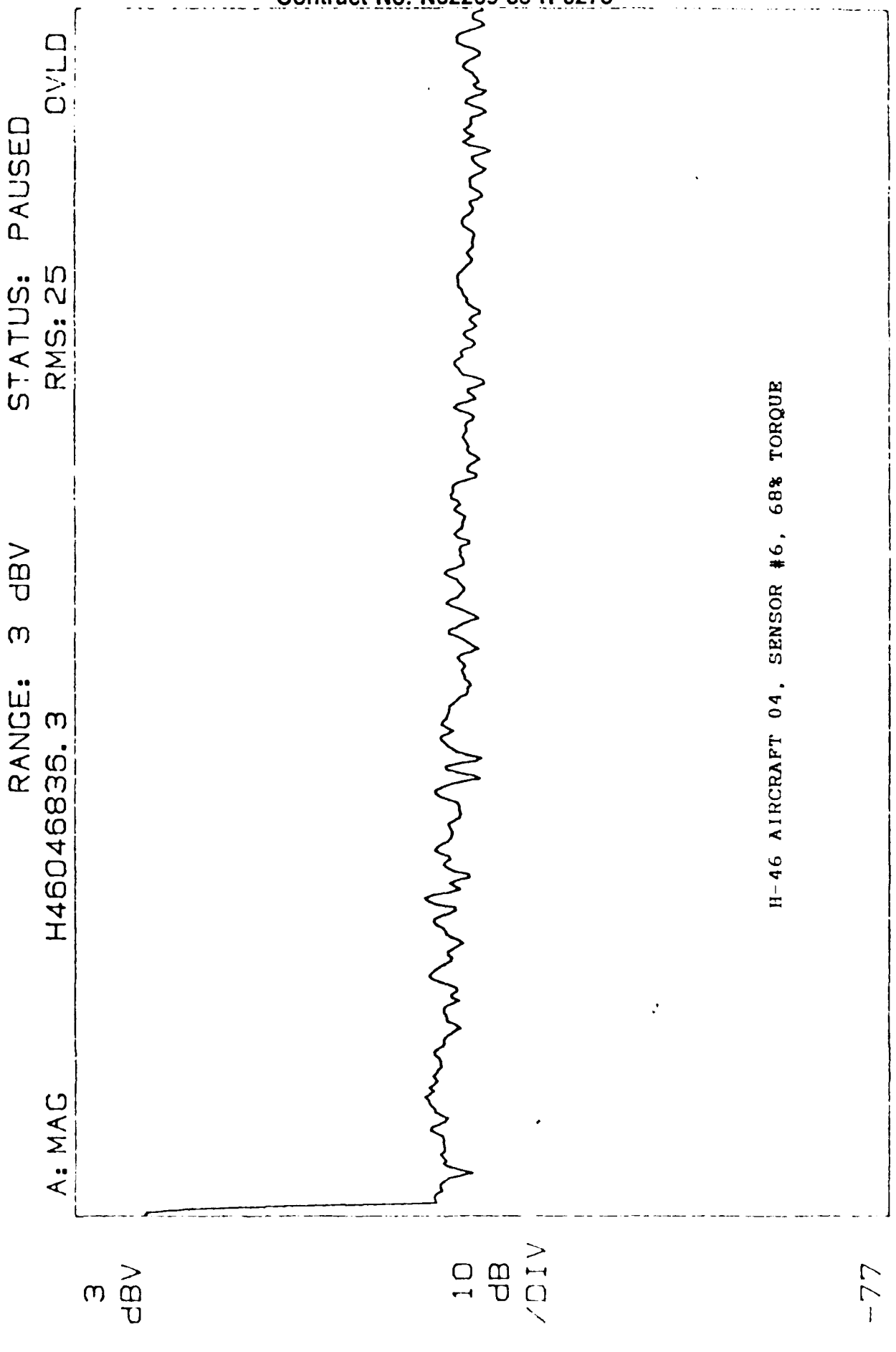

H-46 AIRCRAFT 04, SENSOR #6, 68% TORQUE

Figure 34B

the mix box input pinion gear, but this occurs only at the lower torques of 17% and 25%. Figures 35, 36, and 37 are representative spectra at 17%, 42%, and 68% torque.

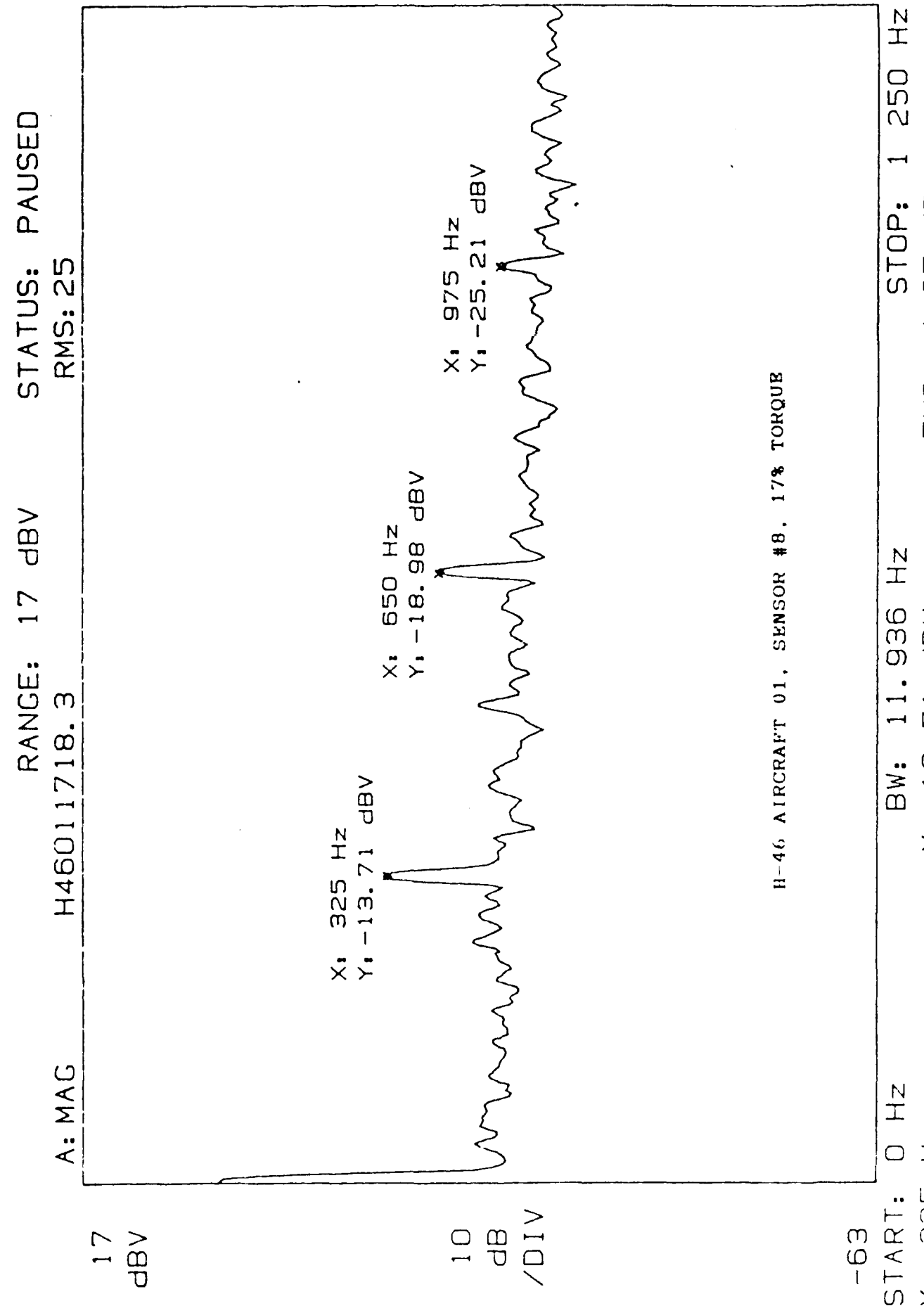
A: MAG
H46011718.3
RANGE: 17 dBV
STATUS: PAUSED
RMS: 25
X: 325 Hz
Y: -13.71 dBV
X: 650 Hz
Y: -18.98 dBV
X: 975 Hz
Y: -25.21 dBV
H-46 AIRCRAFT 01, SENSOR #8, 17% TORQUE
17 dBV
10 dB /DIV
-63
START: 0 Hz
X: 325 Hz
BW: 11.936 Hz
Y: -13.71 dBV
STOP: 1 250 Hz
THD: -4.35 dB

Figure 35A

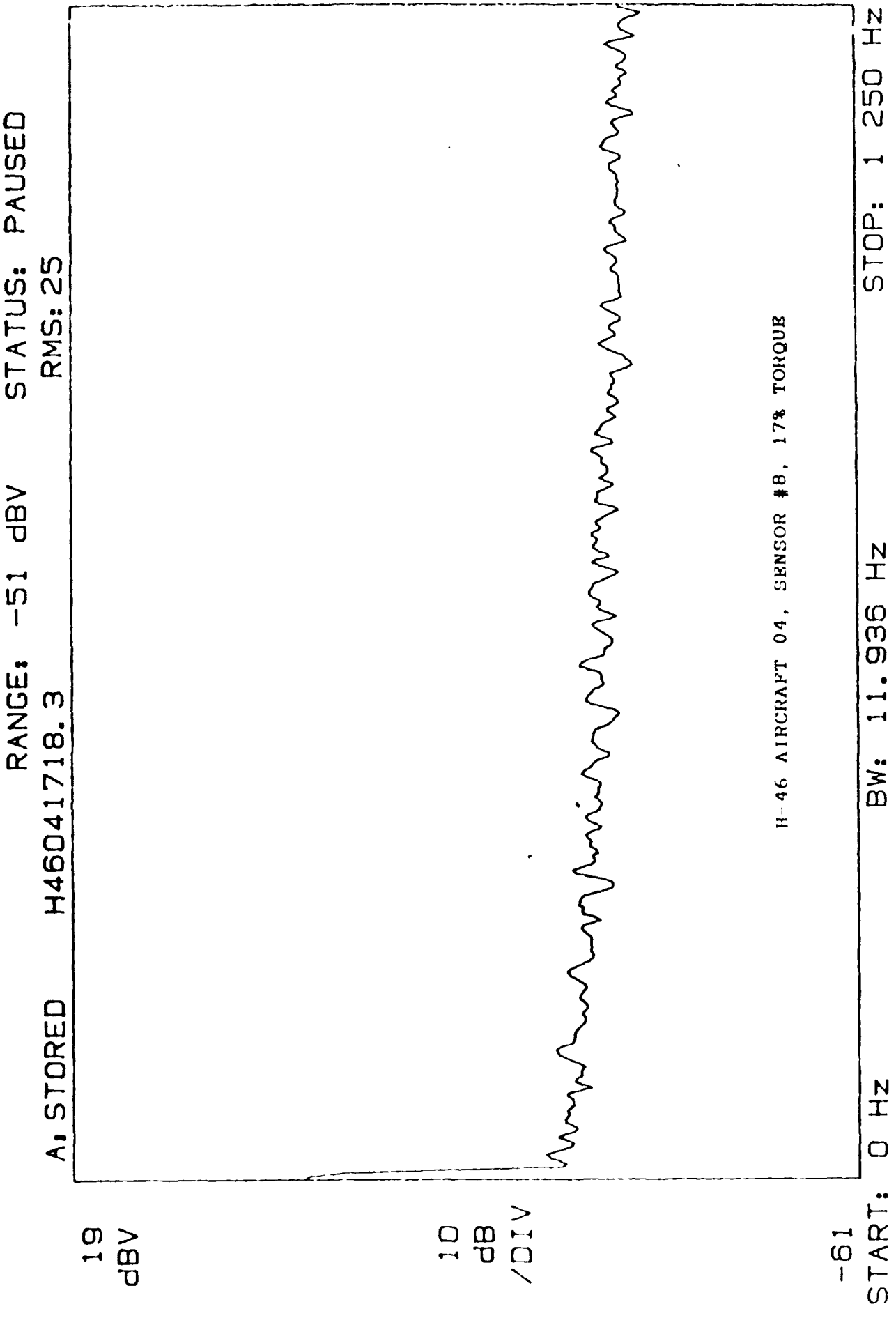
A, STORED
RANGE: -51 dBV
H46041718.3
STATUS: PAUSED
RMS: 25
19
dBV
10
dB
/DIV
-61
START: 0 Hz
BW: 11.936 Hz
STOP: 1 250 Hz
H-46 AIRCRAFT 04, SENSOR #8, 17% TORQUE

Figure 35B

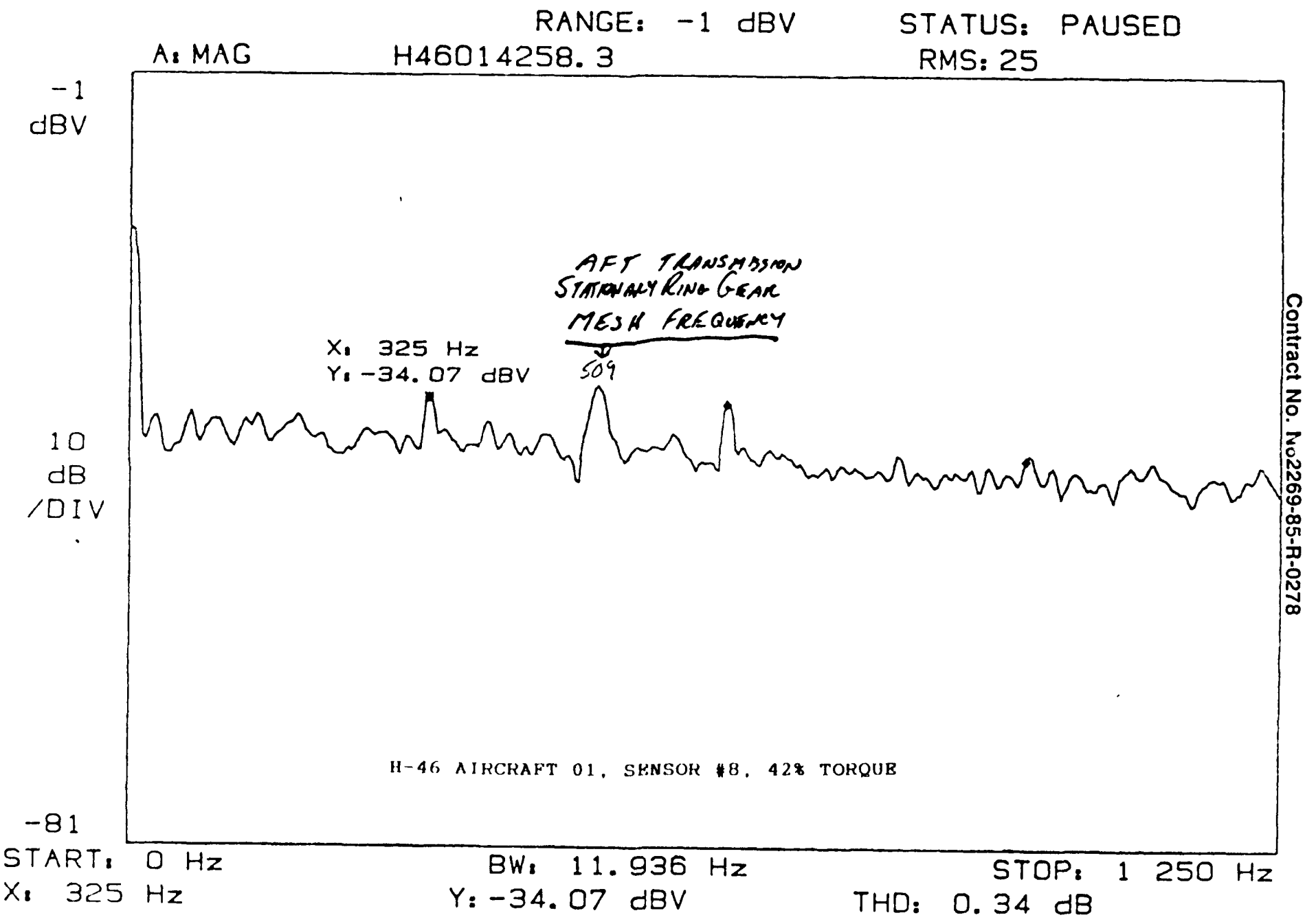

Report No. NADC-91069-60
Contract No. No2269-85-R-0278

Figure 36A

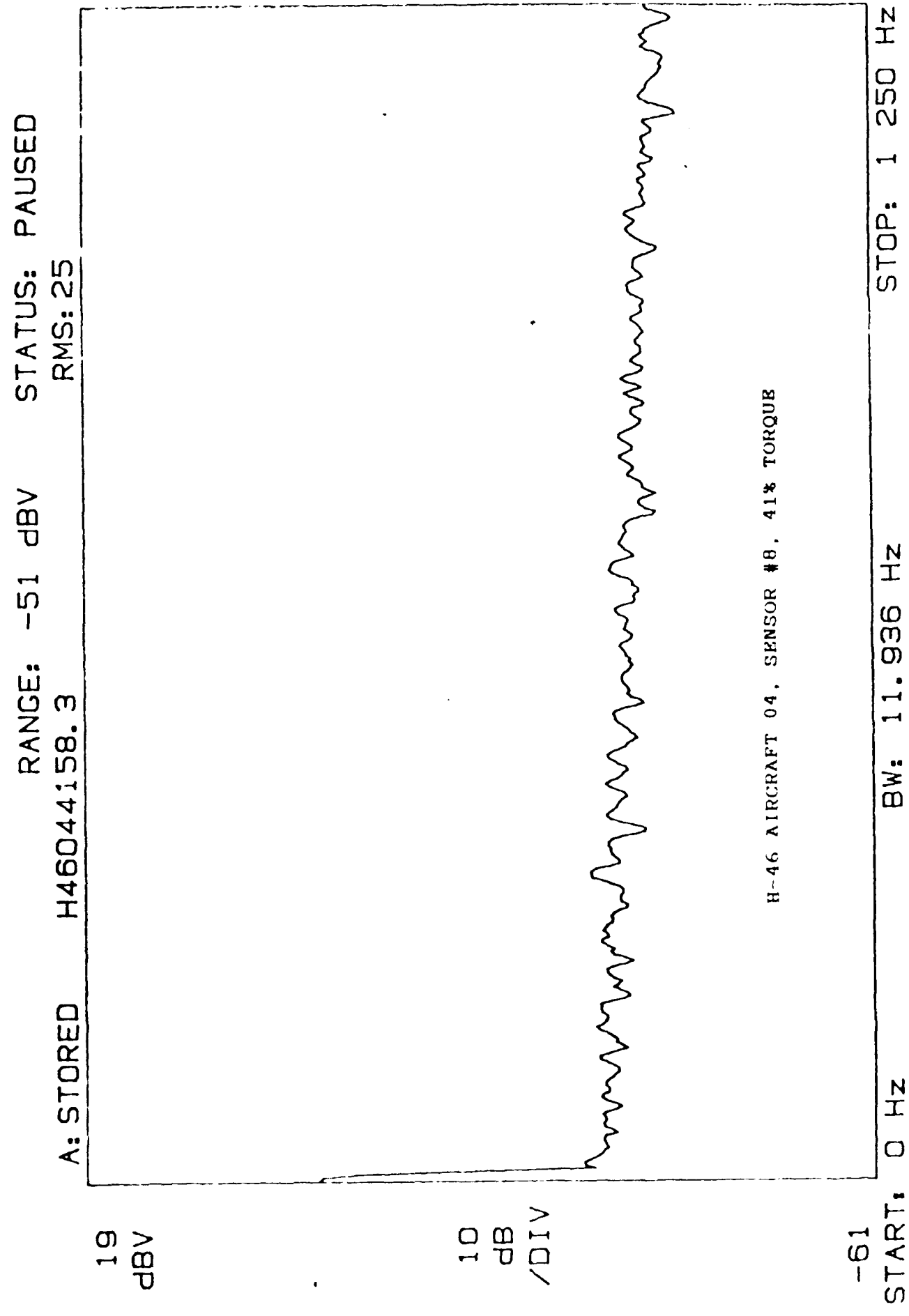
A: STORED
RANGE: -51 dBV
H46044158.3
STATUS: PAUSED
RMS: 25
19 dBV
10 dB /DIV
-61
START: 0 Hz
BW: 11.936 Hz
STOP: 1 250 Hz
H-46 AIRCRAFT 04, SENSOR #8, 41% TORQUE

Figure 36B

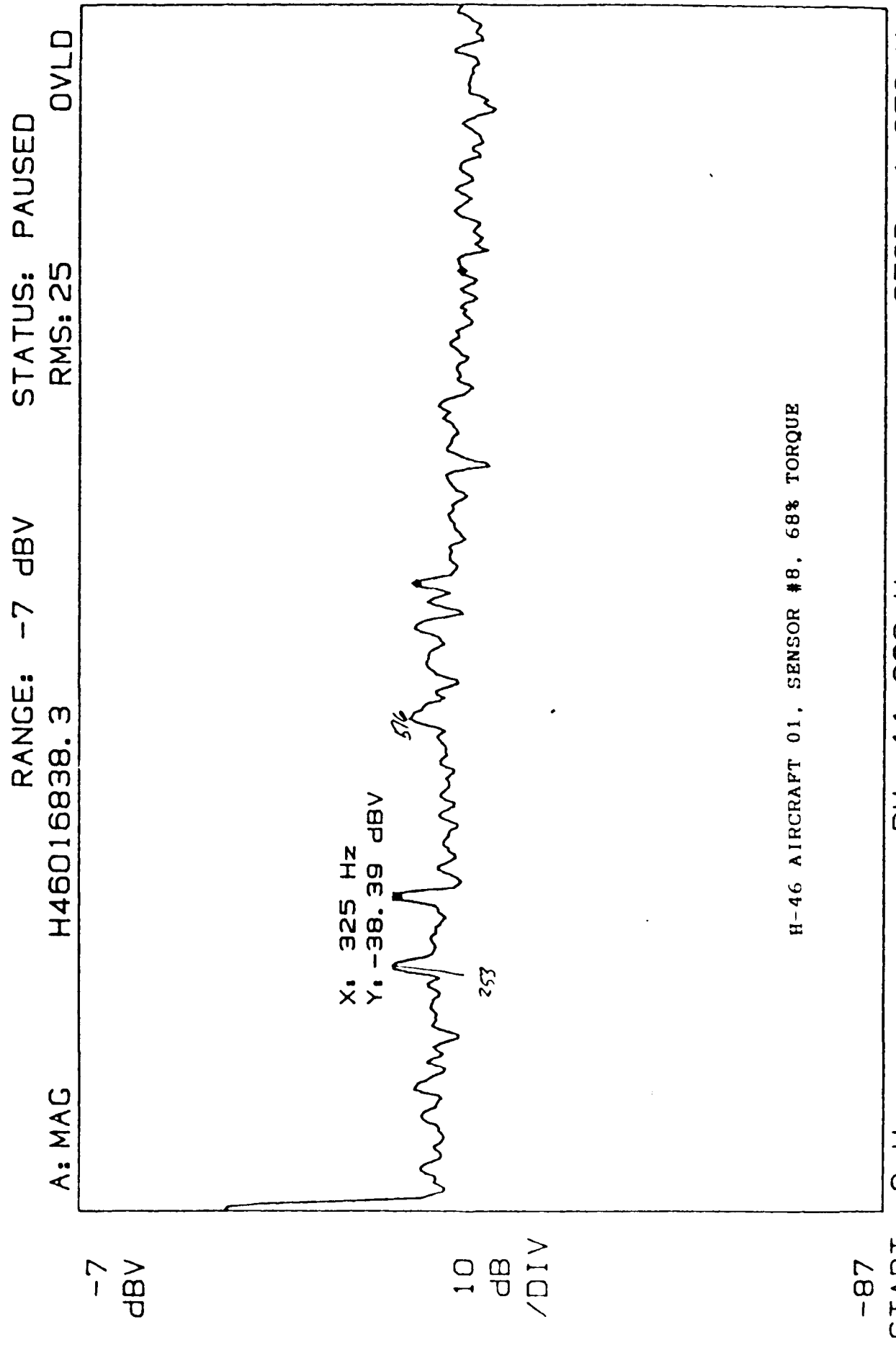
A: MAG
RANGE: -7 dBV
H46016838.3
STATUS: PAUSED
RMS: 25
OVLD
X: 325 Hz
Y: -38.39 dBV
5%
253
H-46 AIRCRAFT 01, SENSOR #8, 68% TORQUE
BW: 11.936 Hz
Y: -38.39 dBV
STOP: 1 250 Hz
THD: -0.58 dB
-7
dBV
10
dB
/DIV
-87
START: 0 Hz
X: 325 Hz

Figure 37A

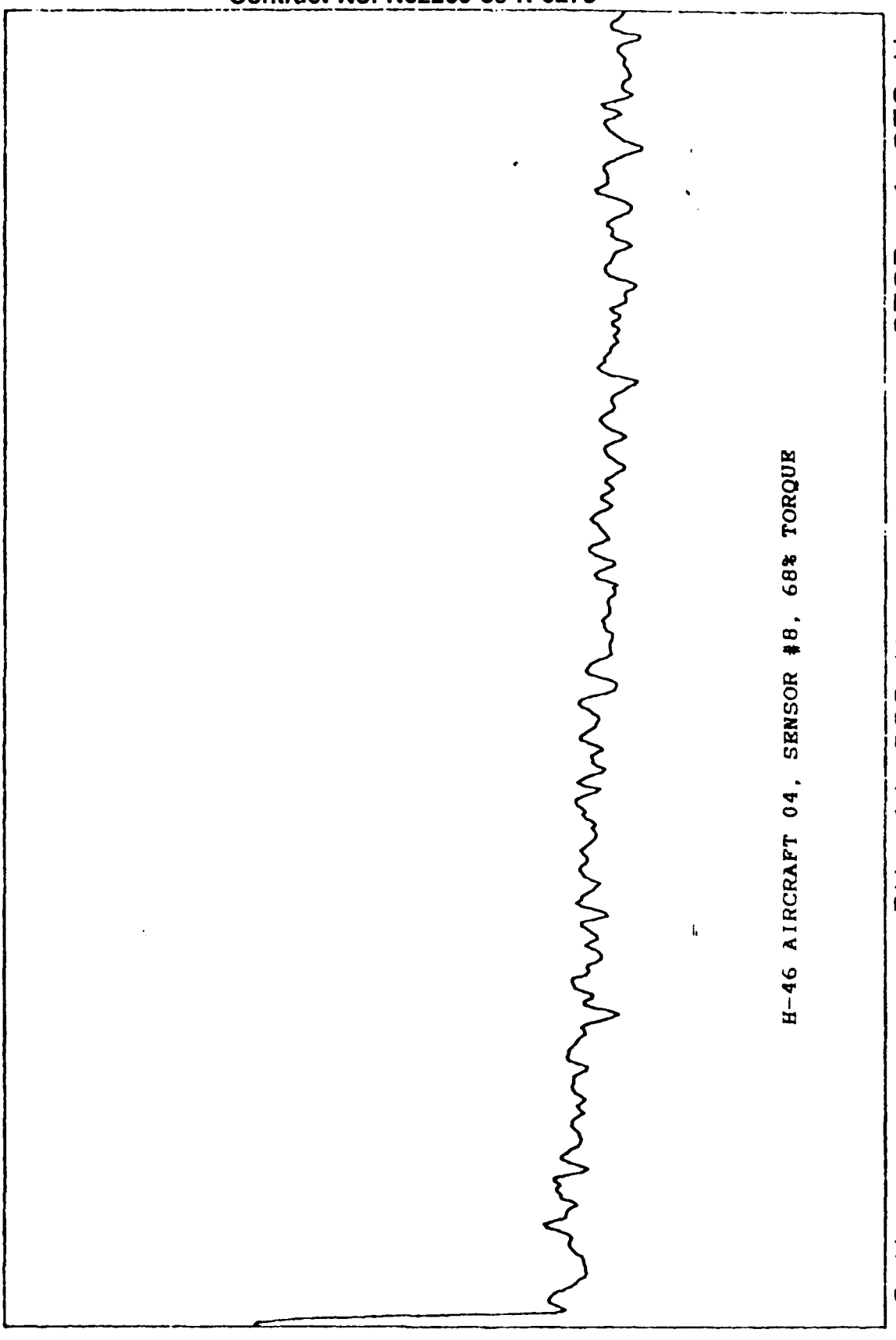
A: STORED
RANGE: -51 dBV
H46046838.3
STATUS: PAUSED
RMS: 25
19 dBV
10 dB /DIV
-61
START: 0 Hz
BW: 11.936 Hz
STOP: 1 250 Hz
H-46 AIRCRAFT 04, SENSOR #8, 68% TORQUE

Figure 378

4.0 OH-58 Main Rotor Transmission Data Analysis

4.1 Test Description and Sensor Locations

The OH-58 transmission was operated under load in a NASA-Lewis test cell. The input torque was from 3621 to 3662 in.-lbs. and the input speed varied from 6059 to 6066 RPM. Figure 38 illustrates the location of the four stress wave sensors that were installed on the OH-58 transmission during this test. Figures 39 and 40 illustrate the characteristic defect frequencies that were calculated for gears and bearings in this gearbox when operating at 6060 RPM.

No other details regarding the operation of, or maintenance actions on, the transmission are known to the writer at the time of this report's preparation.

4.2 Data Analysis

Tables VII through X are summaries of the SWE statistical data for each of the four sensor locations. These tables list the SWE statistical data as of the End Of Day (EOD) for each of the 28 days of testing along with the elapsed total operating hours since the beginning of the test. Figures 41 through 44 are bar-graph representations of the SWE as a function of time at each sensor location. The following is a narrative of the observed changes in the SWE and its spectral content, at each sensor location.

Day 0, Total Test Time = 1:25

Sensor #1 (Top Cover Bolt #1)

The mean SWE is 40,900 and the dominant spectral lines are all associated with two frequencies:

1. The frequency at which a planet gear passes a point on the stationary ring gear, 17.5 Hz; and

2. The mesh frequency for all the gears in the planetary gear system, 573 Hz.

There are also some small lines associated with the rotor shaft RPM, 5.79 Hz. The strongest spectral line is planet passage frequency of 17.5 Hz that is about 16 db above background levels and has two clearly evident harmonics. Figures 45A and 45B are representative spectra for this sensor location.

Sensor #2 (Top Cover Bolt #2)

The mean SWE is 100,602 and the dominant spectral lines are all associated with three frequencies:

NADC PCB Accelerometer Locations
NASA 500-hp Transmission Test Stand
NAPC Lubricants Program - OH-58A Transmission

#1,2,3,4 attached to NADC mounting brackets which attach to housing studs.

Tape ID: ADVLUBHF 1

Date: 9/89

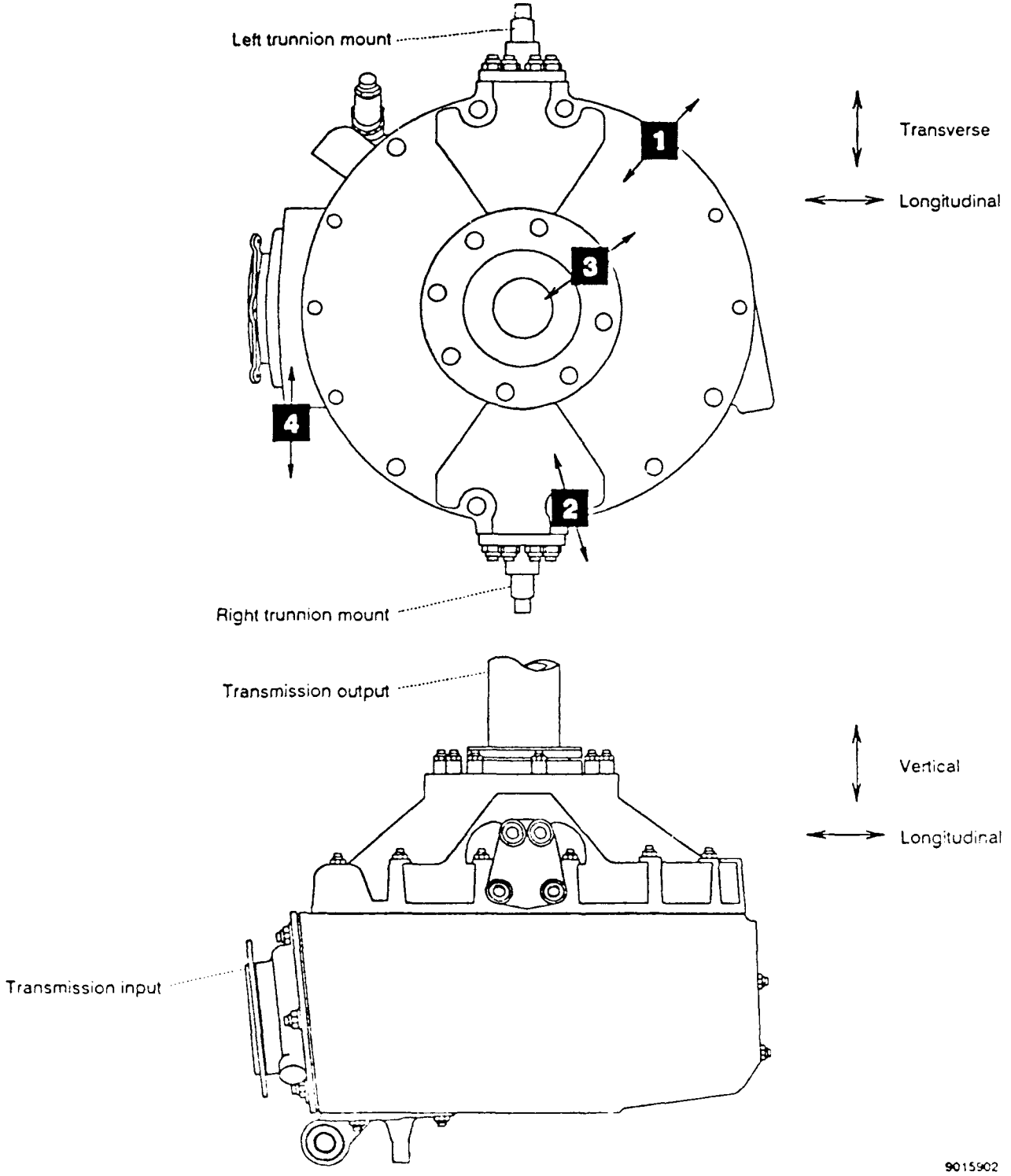

Figure 38 - OH-58 TRANSMISSION SENSOR LOCATIONS

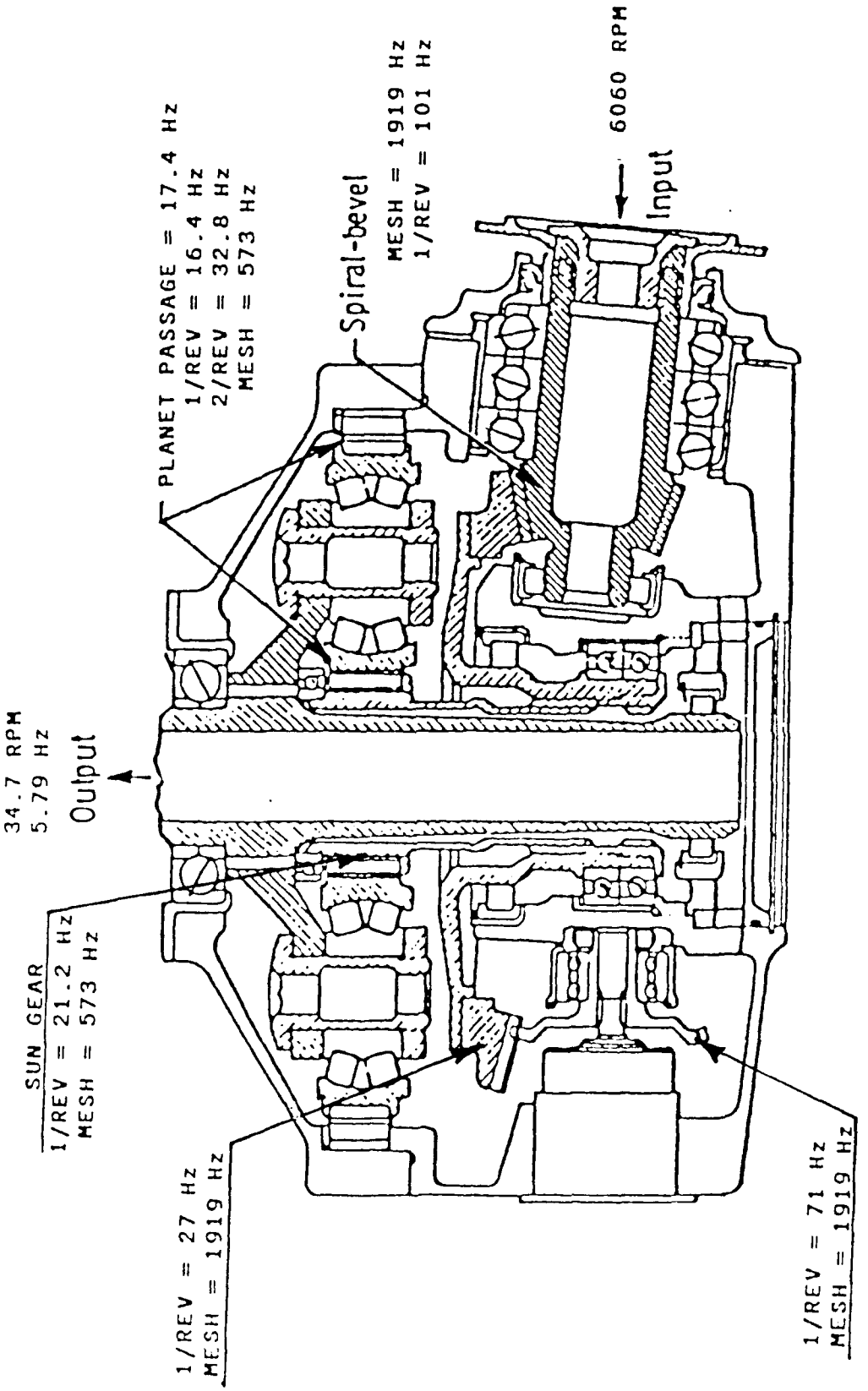

Figure 39 - OH-58 TRANSMISSION GEAR FREQUENCIES

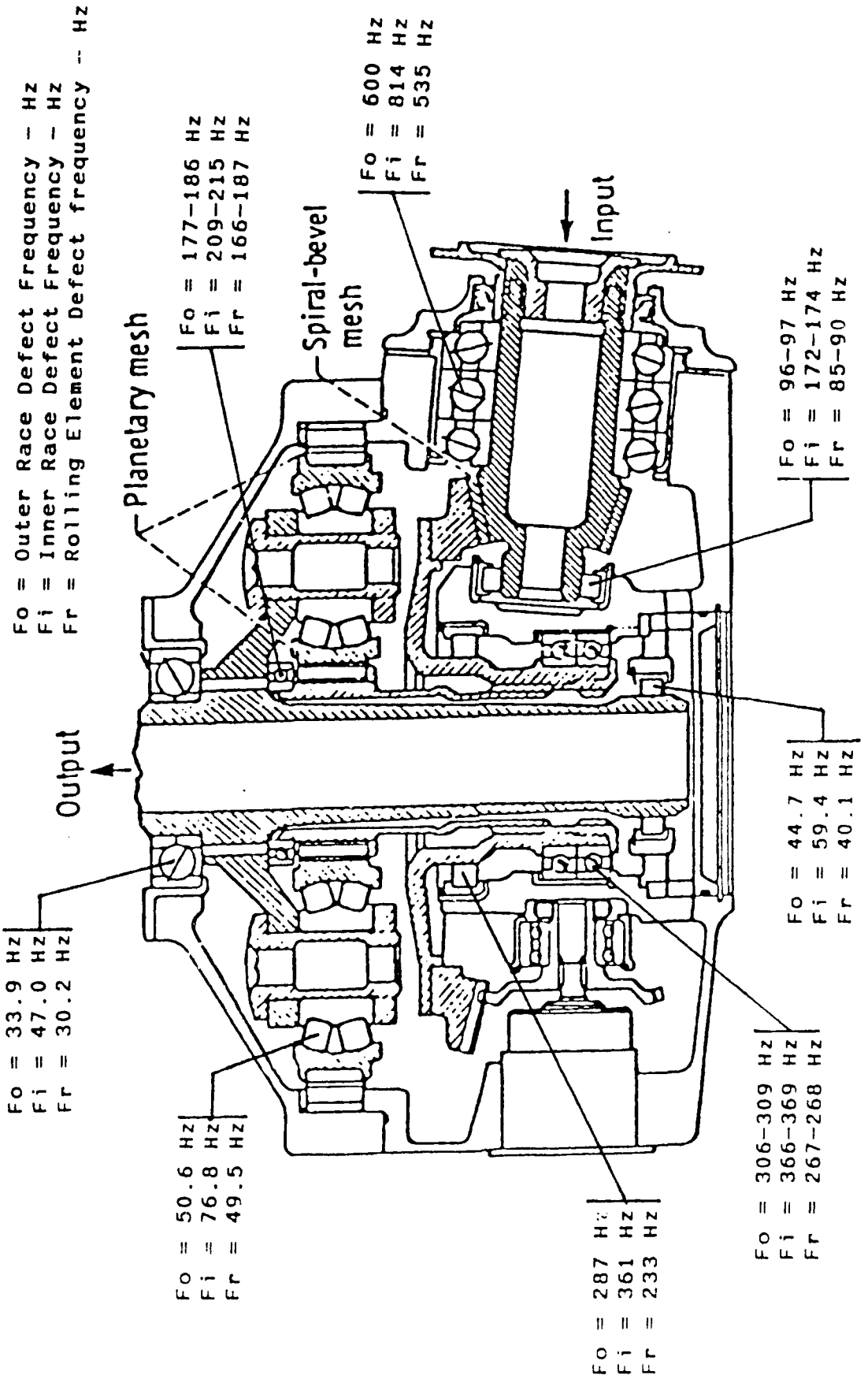

Figure 40 - OH-58 TRANSMISSION BEARING FREQUENCIES

TABLE VII

B-58 STATISTICAL SWB DATA, SENSOR #1

			SWE			
SENSOR #	HRS:MIN	PSL	MEAN	SIGMA	M-3SIG	EOD
1	001:25	3(6)	40900	305	41816	0
1	010:35	3	27586	104	27898	2
1	014:55	4-5	26372	43	26500	3
1	019:22	4-5	22503	44	22637	4
1	23:35	3-4(5)	27465	61	27648	5
1	31:10	3-4	26738	40	26858	6
1	39:52	3-4	29056	98	29350	7
1	48:14	3-4	29097	463	30487	8
1	55:52	3-4	28978	201	29582	9
1	62:31	4	47154	389	48321	10
1	69:14	4(5)	48841	404	50054	11
1	76:23	4(5)	56478	233	56176	12
1	83:20	4	55395	686	57454	13
1	87:18	4-5	44457	253	45216	14
1	90:46	4(5)	44676	357	45746	15
1	102:11	4-5	54036	519	55572	16
1	110:36	4-5	57953	755	60018	17
1	117:26	4-5	61217	1332	65497	18
1	125:02	4	49634	492	51110	19
1	133:02	4-5	58109	284	59913	20
1	136:18	4	58417	112	58754	21
1	143:55	4(5)	56405	384	57556	22
1	149:27	4	49256	152	49729	23
1	156:49	4	45424	138	45909	24
1	165:04	4	44836	134	45246	25
1	169:08	5	41447	749	43693	26
1	177:58	4-5	61144	234	61847	27
1	183:33	4-5	63807	1019	66863	28

TABLE VII
B-58 STATISTICAL SWE DATA, SENSOR #1

			SWE			
SENSOR #	HRS:MIN	PSL	MEAN	SIGMA	M+3SIG	EOD
1	001:25	3(6)	40900	305	41816	0
1	010:35	3	27586	104	27898	2
1	014:55	4-5	26372	43	26500	3
1	019:22	4-5	22503	44	22637	4
1	23:35	3-4(5)	27465	61	27648	5
1	31:10	3-4	26738	40	26858	6
1	39:52	3-4	29056	98	29350	7
1	48:14	3-4	29097	463	30487	8
1	55:52	3-4	28978	201	29582	9
1	62:31	4	47154	389	48321	10
1	69:14	4((5))	48841	404	50054	11
1	76:23	4(5)	55478	233	56176	12
1	83:20	4	55395	686	57454	13
1	87:18	4-5	44457	253	45216	14
1	90:46	4(5)	44676	357	45746	15
1	102:11	4-5	64036	512	65572	16
1	110:36	4-5	57953	755	60019	17
1	117:26	4-5	61317	1392	65493	18
1	125:02	4	49634	492	51110	19
1	133:02	4-5	59109	269	59915	20
1	136:18	4	53917	112	54254	21
1	143:55	4(5)	56405	384	57556	22
1	149:27	4	49238	162	49725	23
1	156:49	4	45924	194	46505	24
1	165:04	4	46838	136	47246	25
1	169:08	5	72447	749	74693	26
1	177:58	4-5	67144	349	68190	27
1	183:33	4-5	63807	1019	66863	28

TABLE VIII
H-58 STATISTICAL SWB DATA, SENSOR #2

			SWE			
SENSOR #	HRS:MIN	PSL	MEAN	SIGMA	M+3SIG	EOD
2	001:25	4-5	55148	388	56312	0
2	010:35	4(5)	38191	102	38497	2
2	014:55	4-5	48380	12960	87261	3
2	019:22	4-5	27117	101	27420	4
2	23:35	4	36749	153	37208	5
2	31:10	4	34356	89	34623	6
2	39:52	4	37785	172	38301	7
2	48:14	4	37085	548	38732	8
2	55:52	4	37133	63	37323	9
2	62:31	4-5	68701	353	69761	10
2	69:14	4-5	72717	189	73285	11
2	76:23	4-5	75131	146	75569	12
2	83:20	4-5	71136	249	71884	13
2	87:18	4.5	60457	171	60970	14
2	90:46	4-5	72877	629	74764	15
2	102:11	4-5	68336	133	68736	16
2	110:36	4-5	74788	229	75475	17
2	117:26	5	81673	491	83145	18
2	125:02	5	86126	1084	89377	19
2	133:02	5	81249	198	81845	20
2	136:18	5	78485	438	79799	21
2	143:55	5	64995	517	66546	22
2	149:27	5	64265	166	64764	23
2	156:49	5	63942	55	64107	24
2	165:04	5	63692	443	65021	25
2	169:08	4	58973	170	59485	26
2	177:58	4	58832	172	59349	27
2	183:33	4	58170	306	59087	28

TABLE IX
H-58 STATISTICAL SWE DATA, SENSOR #3

SENSOR #	HRS:MIN	PSL	SWE MEAN	SWE SIGMA	SWE M+3SIG	EOD
3	001:25		128485	13206	168104	0
3	010:35	4-5	23574	53	23733	2
3	014:55	4-5	25972	112	26307	3
3	019:22	4-5	10860	33	10959	4
3	23:35	4-5	20870	287	21731	5
3	31:10	4-5	18789	62	18975	6
3	39:52	4-5	20522	79	20759	7
3	48:14	4-5	20844	344	21876	8
3	55:52	4-5	20770	82	21014	9
3	62:31	5	14589	142	15016	10
3	69:14	5	13496	52	13651	11
3	76:23	5	14054	134	14455	12
3	83:20	5	13675	85	13930	13
3	87:18	4(5)	18629	87	18890	14
3	90:46	5	18148	92	18423	15
3	102:11	5	19026	50	19178	16
3	110:36	5	19305	69	19512	17
3	117:26	5	19267	105	19581	18
3	125:02	2-3	19631	46	19768	19
3	133:02	2-3(4)	19447	32	19541	20
3	136:18	2-3	18779	36	18888	21
3	143:55	2(3)	15446	32	15541	22
3	149:27	2(3)	15297	74	15508	23
3	156:49	2-3	15463	146	15901	24
3	165:04	2-3	15373	59	15550	25
3	169:08	2(3)	12229	34	12330	26
3	177:58	2	12028	21	12090	27
3	183:33	2	12202	83	12450	28

TABLE X
H-58 STATISTICAL SWE DATA, SENSOR #4

SENSOR #	HRS:MIN	PSL	SWE MEAN	SWE SIGMA	SWE M+3SIG	EOD
4	001:25	4-5(6)	100602	241	101324	0
4	010:35	4-5	86266	157	86736	2
4	014:55	4-5	86231	186	86789	3
4	019:22	4-5	90744	40	90865	4
4	23:35	4-5	86023	365	87119	5
4	31:10	4-5	82070	833	84567	6
4	39:52	4-5	86657	338	87671	7
4	48:14	4-5	90926	853	93486	8
4	55:52	4-5	93120	152	93576	9
4	62:31	5	98369	763	100657	10
4	69:14	5	93448	541	95070	11
4	76:23	5	93513	487	94975	12
4	83:20	5	94987	559	96665	13
4	87:18	4(5)	110274	2688	118339	14
4	90:46	5	115698	1356	119767	15
4	102:11	5	125275	294	126156	16
4	110:36	5	122345	423	123615	17
4	117:26	5	125665	97	125955	18
4	125:02	5	125475	331	126469	19
4	133:02	4	111742	218	112398	20
4	136:18	4(5-6)	112363	382	113508	21
4	143:55	5	119837	591	121609	22
4	149:27	4-5	111516	454	112877	23
4	156:49	4(5)	113529	1212	117165	24
4	165:04	4-5	118676	1141	122099	25
4	169:08	5(6)	131063	825	133538	26
4	177:58	5-6	162056	731	164250	27
4	183:33	5-6	162336	525	163911	28

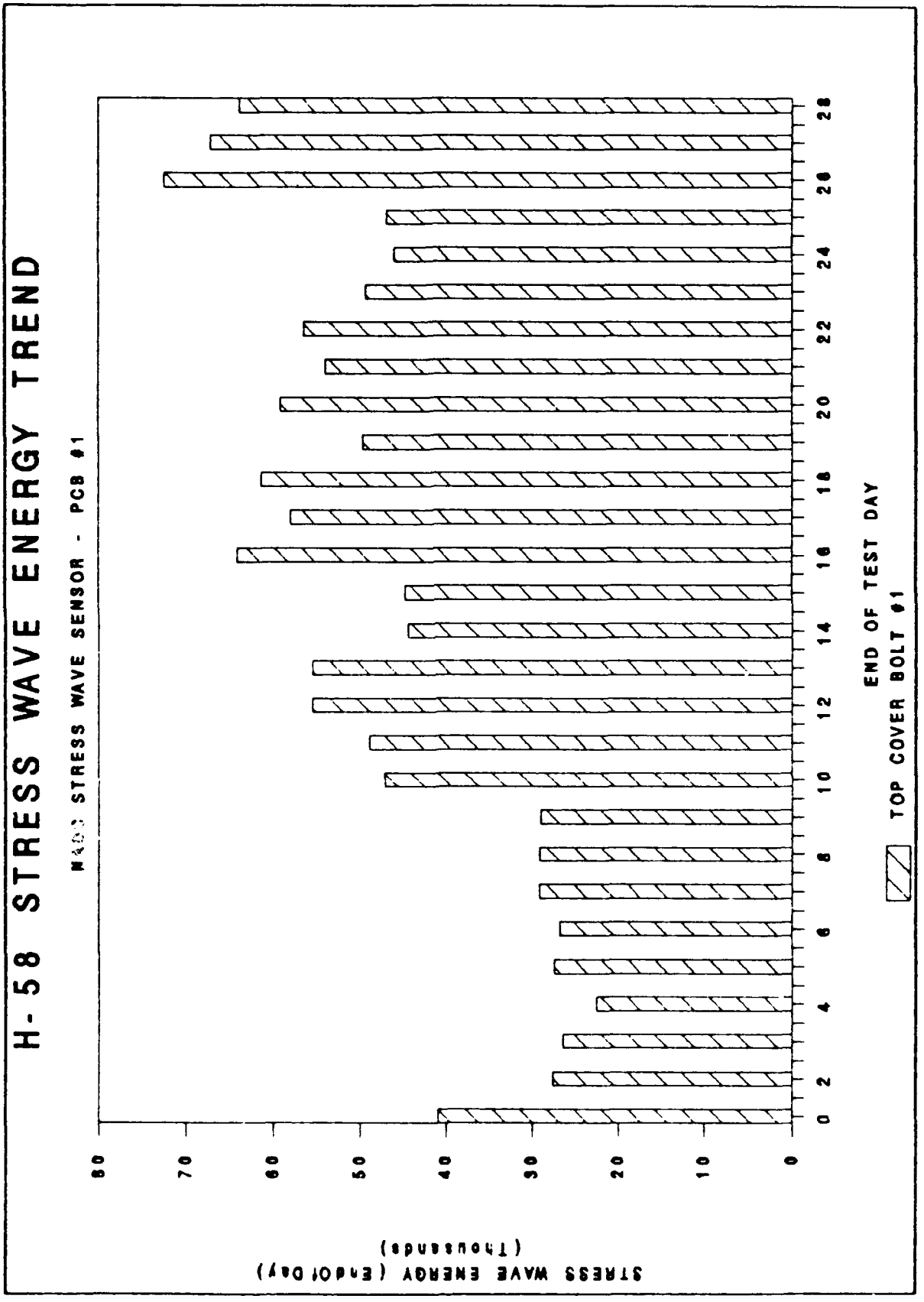
H-58 STRESS WAVE ENERGY TREND
STRESS WAVE SENSOR - PCB #1
STRESS WAVE ENERGY (End/Day)
(Thousands)
0
10
20
30
40
50
60
70
80
0
2
4
6
8
10
12
14
16
18
20
22
24
26
28
END OF TEST DAY
TOP COVER BOLT #1

Figure 41

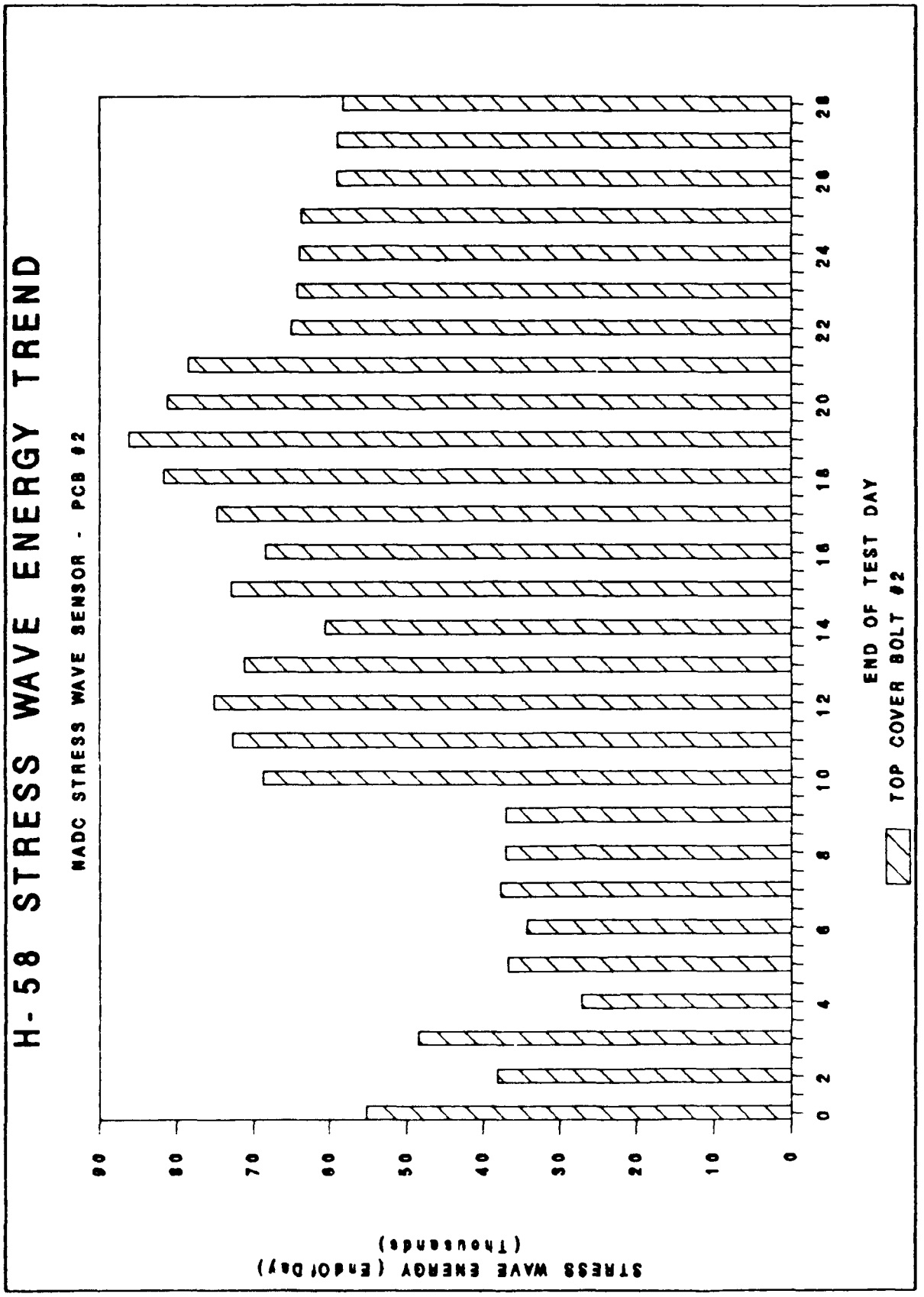
H-58 STRESS WAVE ENERGY TREND
NADC STRESS WAVE SENSOR - PCB #2
STRESS WAVE ENERGY (End/Day)
(Thousands)
0
10
20
30
40
50
60
70
80
90
0 2 4 6 8 10 12 14 16 18 20 22 24 26 28
END OF TEST DAY
TOP COVER BOLT #2

Figure 42

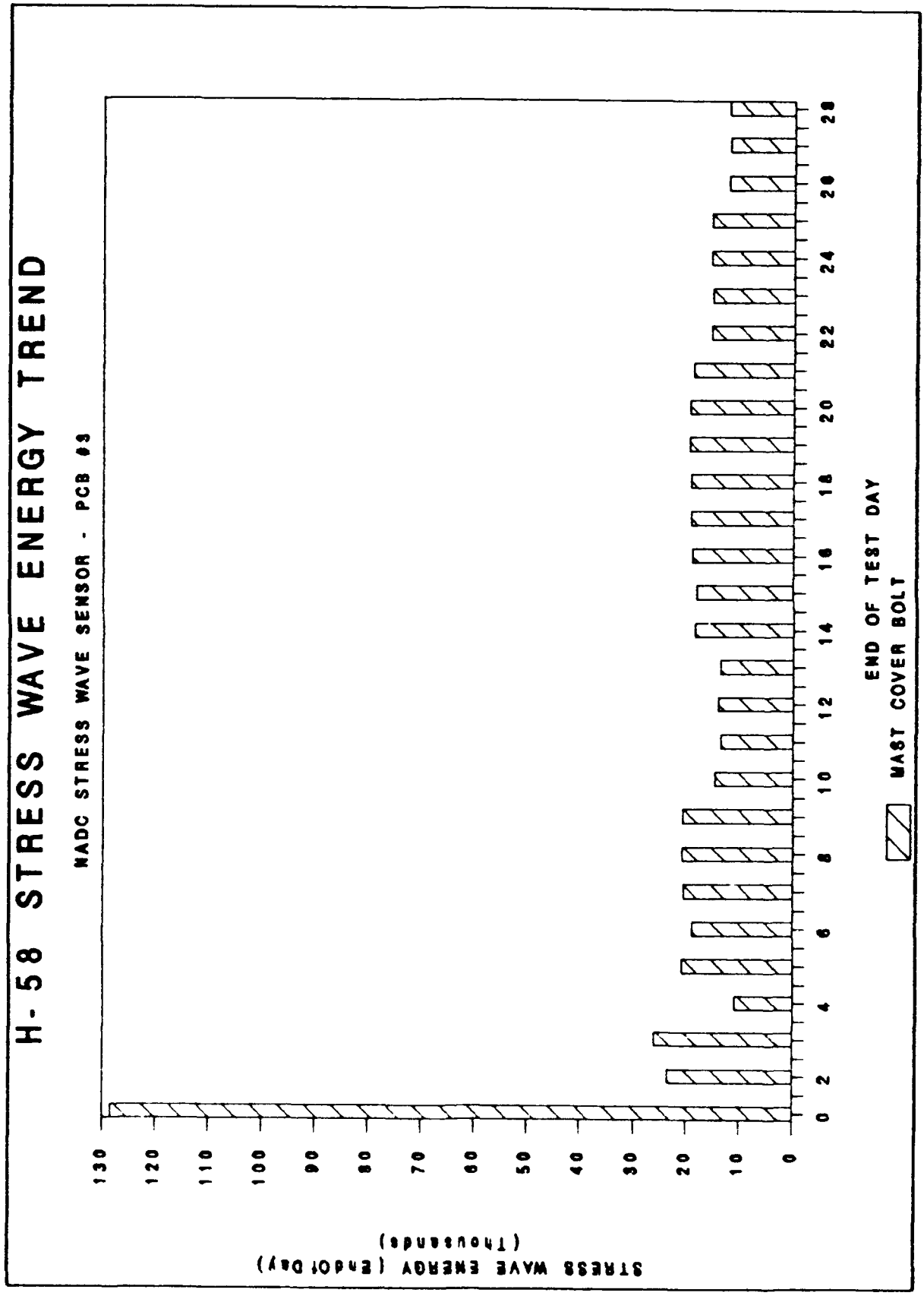
H-58 STRESS WAVE ENERGY TREND
NADC STRESS WAVE SENSOR - PCB #3
STRESS WAVE ENERGY (Endot Day)
(Thousands)
0
10
20
30
40
50
60
70
80
90
100
110
120
130
0 2 4 6 8 10 12 14 16 18 20 22 24 26 28
END OF TEST DAY
MAST COVER BOLT

Figure 43

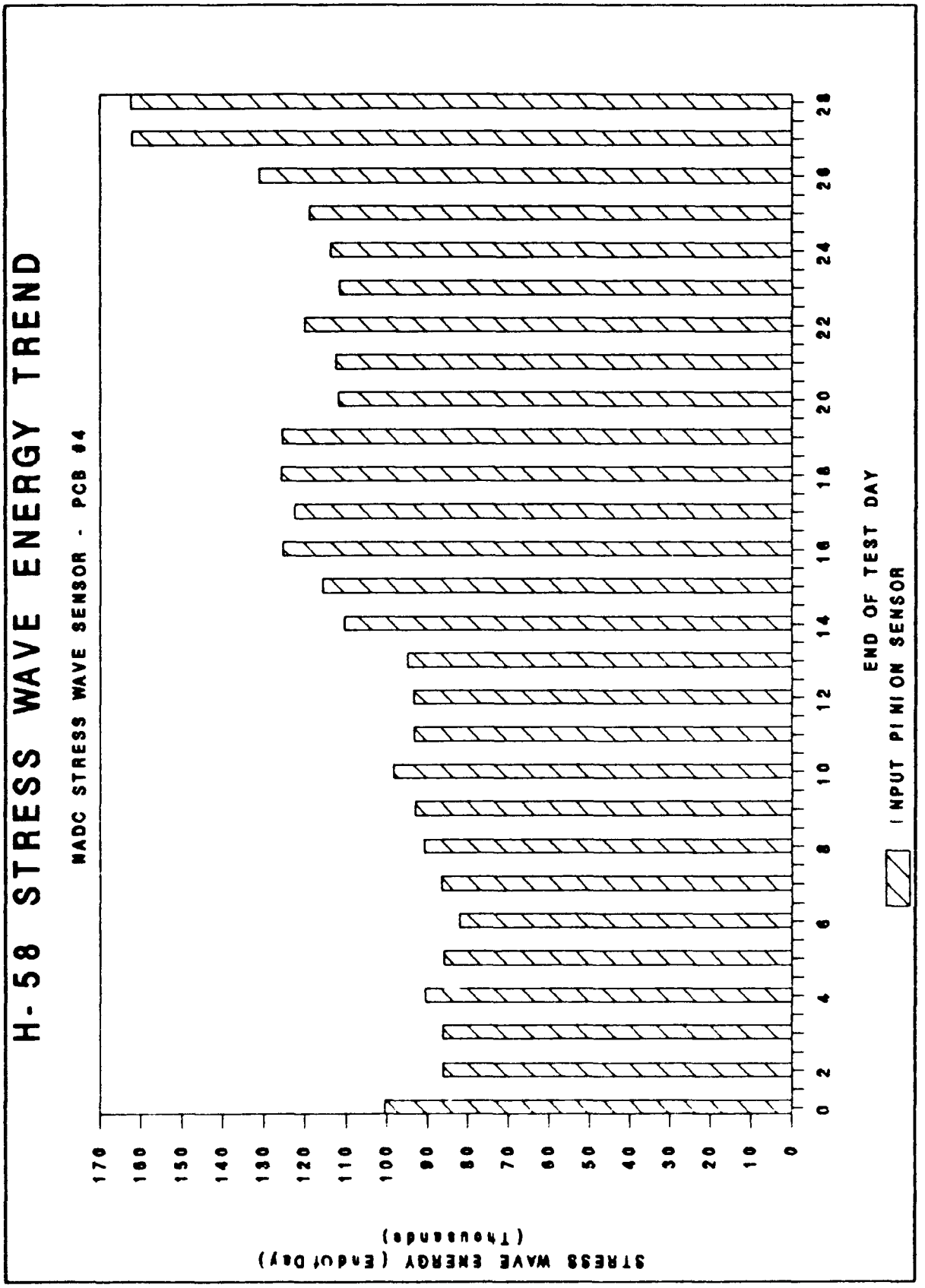
H-58 STRESS WAVE ENERGY TREND
NADC STRESS WAVE SENSOR - PCB #4
STRESS WAVE ENERGY (End of Day)
(Thousands)
170
160
150
140
130
120
110
100
90
80
70
60
50
40
30
20
10
0
0 2 4 6 8 10 12 14 16 18 20 22 24 26 28
END OF TEST DAY
INPUT PINION SENSOR

Figure 44

Table XI

H-58 Power Spectral Density Identification Code

At the top of each Power Spectral Density sheet is an identification code of the form:

H581/183:33

This code can be interpreted as follows:

Character No.	Meaning
1-3	58 = aircraft type
4	1 = sensor location number
5	/ = no meaning
6-11	183:33 = cumulative test time, HRS:MIN

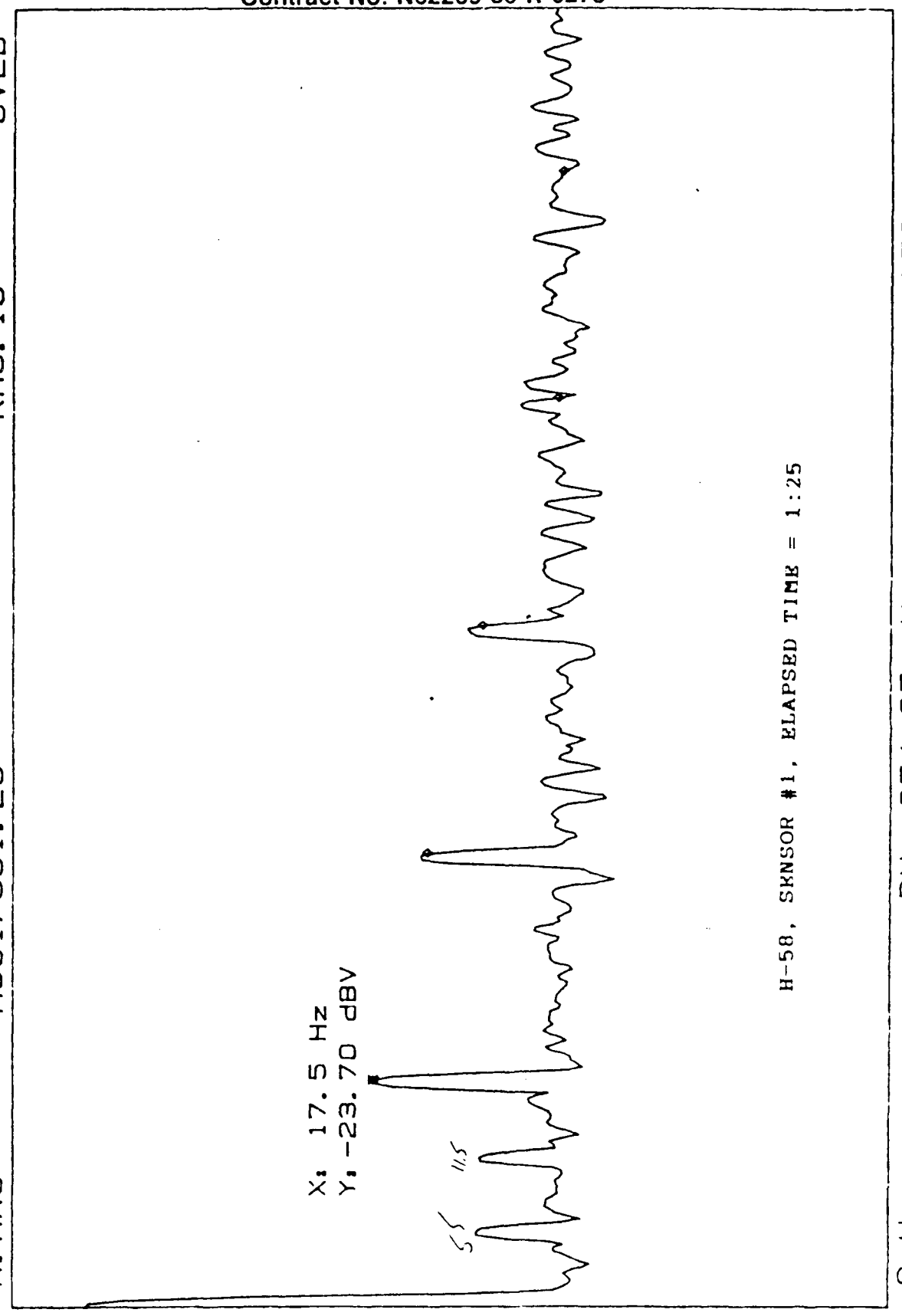
A: MAG
RANGE: 9 dBV
H581/001:25
STATUS: PAUSED
RMS: 10
OVLD
X: 17.5 Hz
Y: -23.70 dBV
H-58, SENSOR #1, ELAPSED TIME = 1:25
BW: 954.85 mHz
Y: -23.70 dBV
STOP: 100 Hz
THD: -3.25 dB
9
dBV
10
dB
/DIV
-71
START: 0 Hz
X: 17.5 Hz

Figure 45A

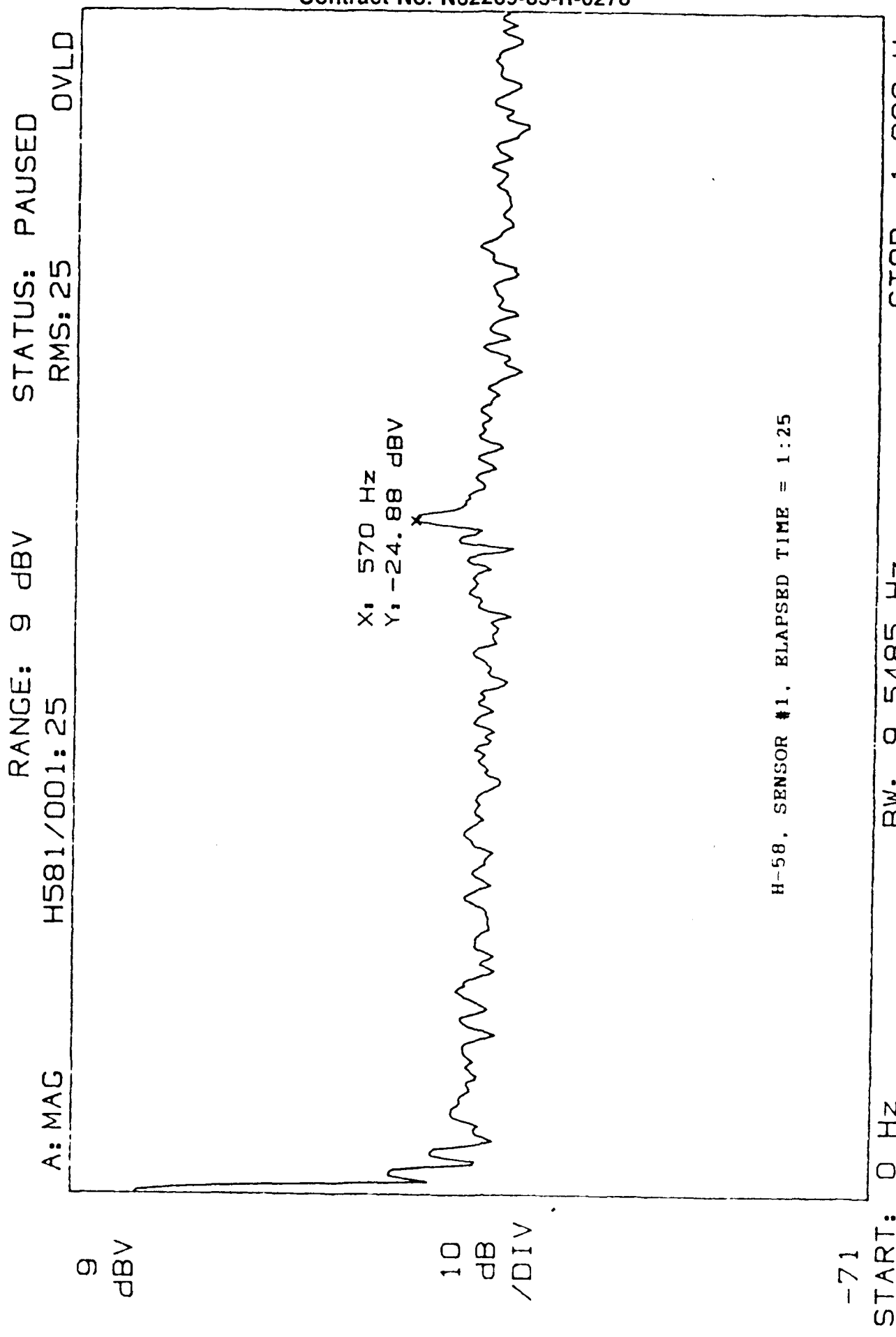
A: MAG
RANGE: 9 dBV
H581/001:25
STATUS: PAUSED
RMS: 25
OVLD
X: 570 Hz
Y: -24.88 dBV
H-58, SENSOR #1, ELAPSED TIME = 1:25
9
dBV
10
dB
/DIV
-71
START: 0 Hz
X: 570 Hz
BW: 9.5485 Hz
Y: -24.88 dBV
STOP: 1 000 Hz

Figure 45B

1. The planet gear passage frequency, 17.5 Hz;

2. The rotor shaft 1/rev, 5.79 Hz; and

3. The mesh frequency for all the gears in the planetary gear system, 573 Hz.

The lines associated with the rotor shaft RPM, 5.79 Hz, are more of a factor than at location #1, with an 11 db fundamental and numerous harmonics that form side bands with 17.5 Hz and its harmonics. The strongest spectral line is planet passage frequency of 17.5 Hz that is about 21 db above background levels and also has clearly evident harmonics. Figures 46A and 46B are representative spectra for this sensor location.

Sensor # 3 (Mast Cover Bolt)

The mean SWE is 128,485 and the dominant spectral lines are associated with two frequencies:

1. The planet gear passage frequency, 17.5 Hz; and

2. The rotor shaft 1/rev, 5.79 Hz.

Both of these frequencies are about 11 db above background levels. Figures 47A and 47B are representative spectra for this sensor location.

Sensor # 4 (Input Pinion Housing)

The mean SWE is 100,602 and the dominant spectral lines are associated with two frequencies:

1. The planet gear passage frequency, 17.5 Hz; and

2. The input pinion gear shaft 1/rev, 101 Hz.

The planet gear passage frequency is about 10 db above background levels. Figures 48A and 48B are representative spectra for this sensor location.

Day 2, Total Test Time = 10:35

Sensor #1 (Top Cover Bolt #1)

The mean SWE has dropped to 26,372 and the dominant spectral lines are all associated with the same two frequencies:

1. The planet gear passage frequency, 17.5 Hz; and

2. The mesh frequency for all the gears in the planetary gear system, 573 Hz.

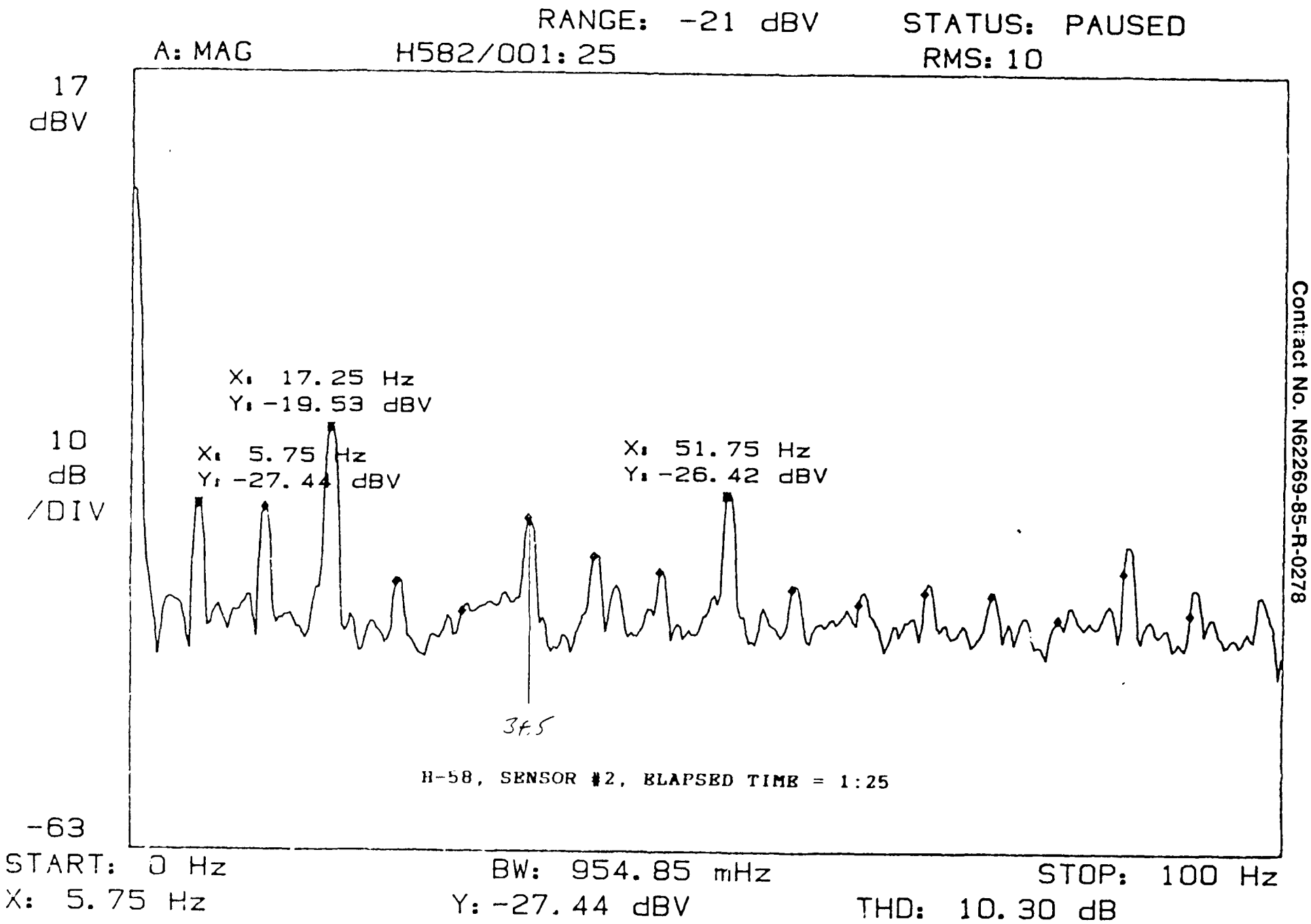

Figure 46A

Report No. NADC-91069-60
Contract No. N62269-85-R-0278

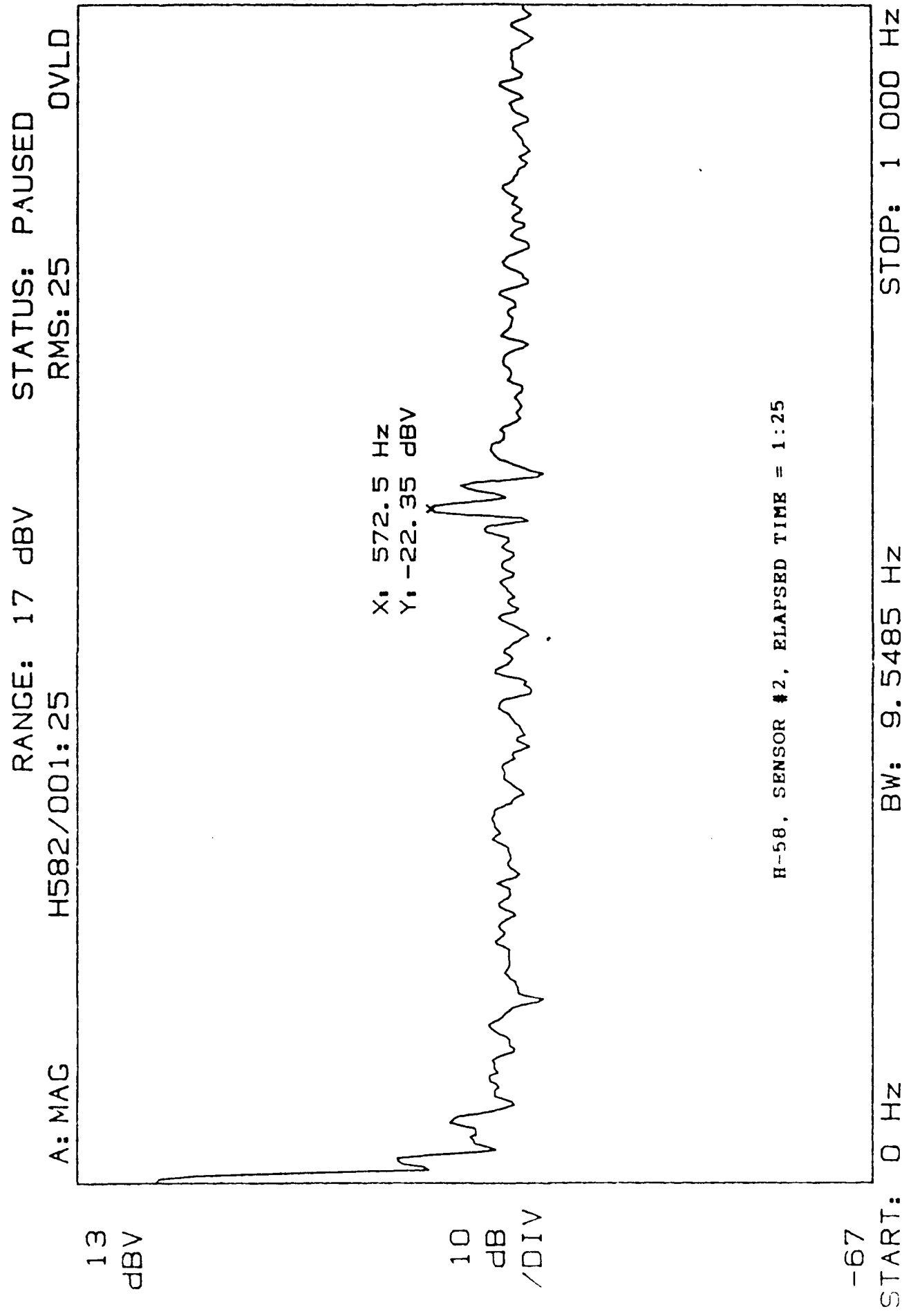
A: MAG
RANGE: 17 dBV
H582/001:25
STATUS: PAUSED
RMS: 25
OVLD
X: 572.5 Hz
Y: -22.35 dBV
H-58, SENSOR #2, ELAPSED TIME = 1:25
13
dBV
10
dB
/DIV
-67
START: 0 Hz
X: 572.5 Hz
BW: 9.5485 Hz
Y: -22.35 dBV
STOP: 1 000 Hz

Figure 46B

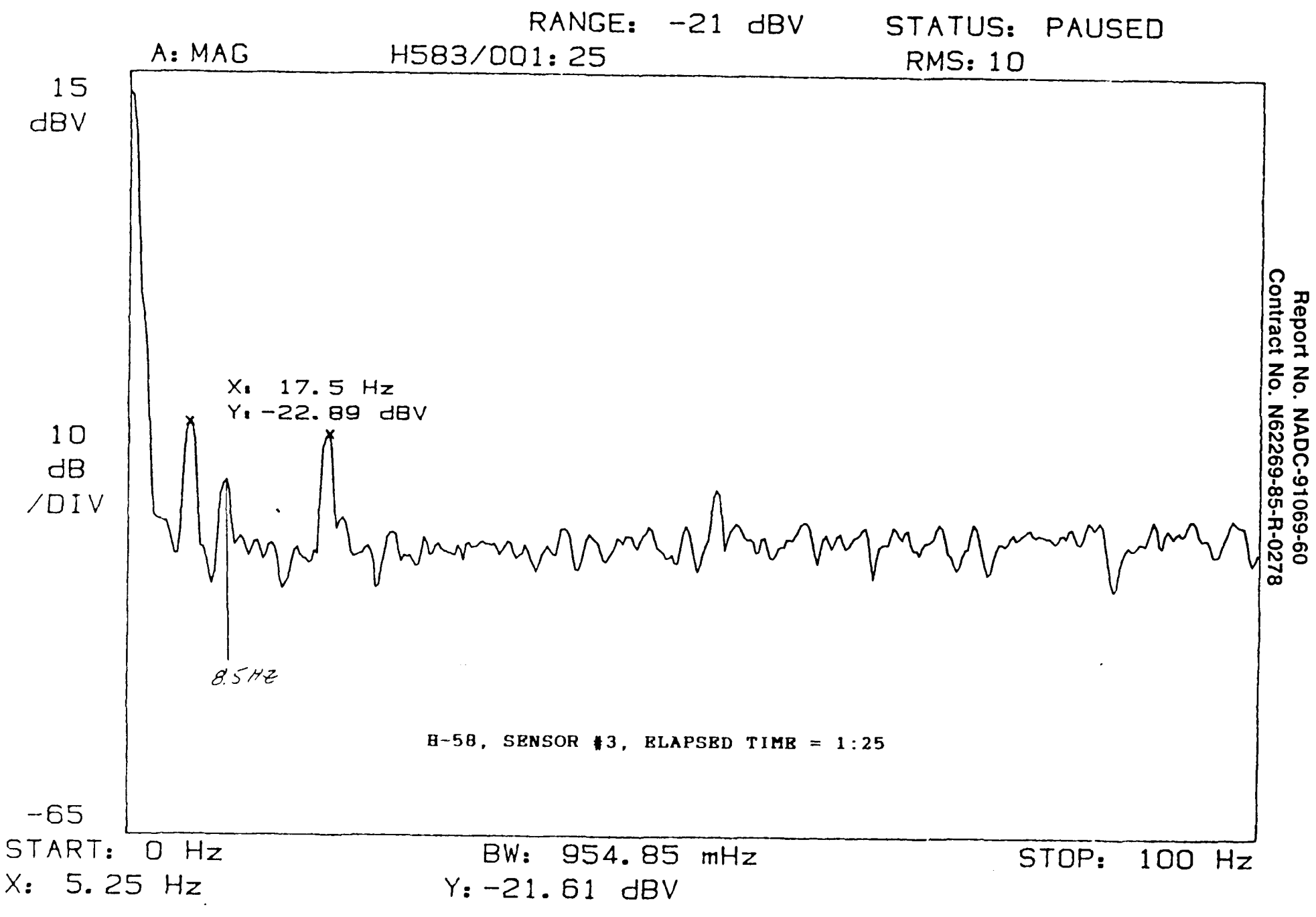
RANGE: -21 dBV
STATUS: PAUSED
A: MAG
H583/001: 25
RMS: 10
15
dBV
X: 17.5 Hz
Y: -22.89 dBV
10
dB
/DIV
8.5HZ
H-58, SENSOR #3, ELAPSED TIME = 1:25
-65
START: 0 Hz
BW: 954.85 mHz
STOP: 100 Hz
X: 5.25 Hz
Y: -21.61 dBV

Figure 47A

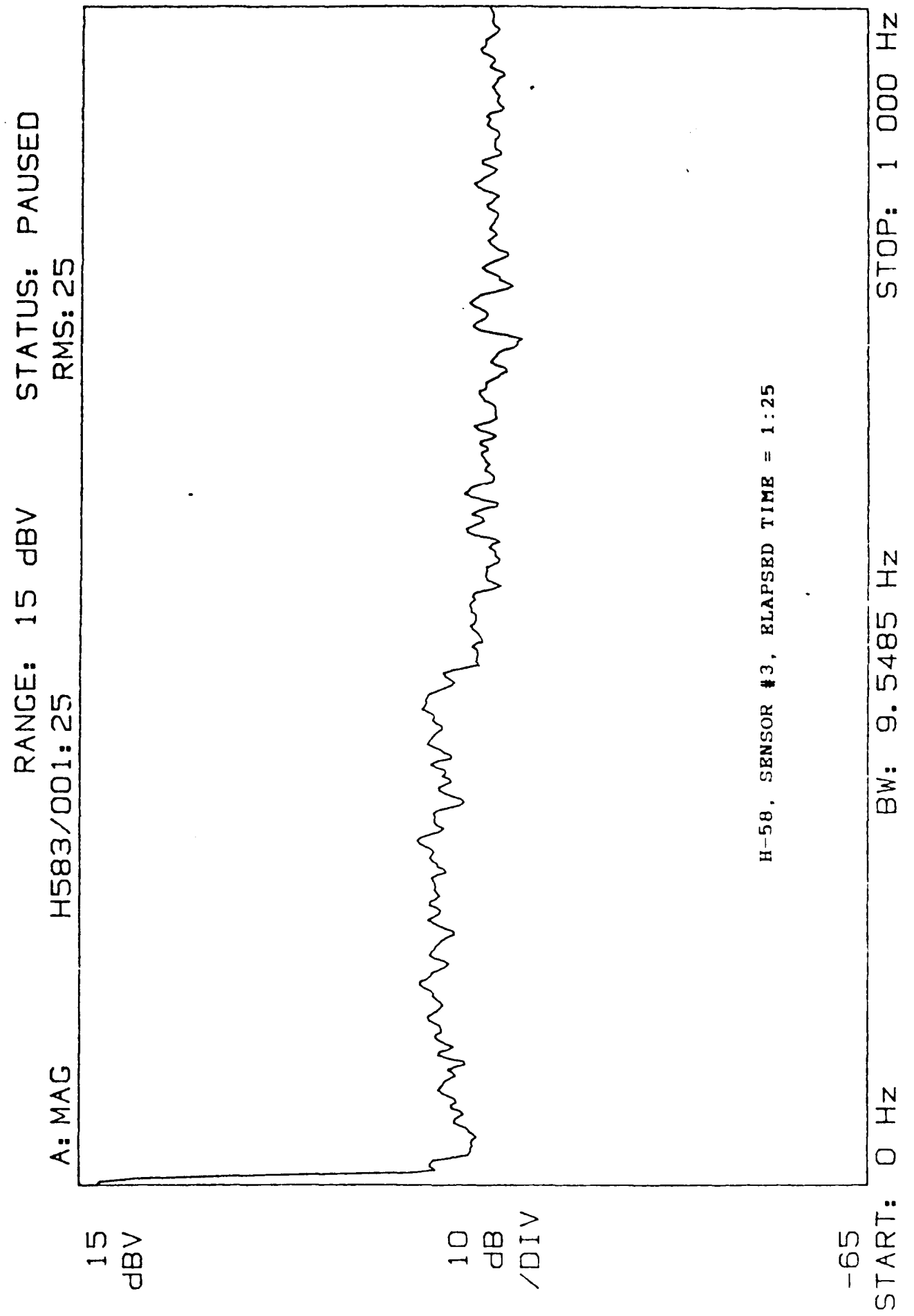
A: MAG
H583/001: 25
RANGE: 15 dBV
STATUS: PAUSED
RMS: 25
15 dBV
10 dB /DIV
-65
START: 0 Hz
BW: 9.5485 Hz
STOP: 1 000 Hz
H-58, SENSOR #3, ELAPSED TIME = 1:25

Figure 47B

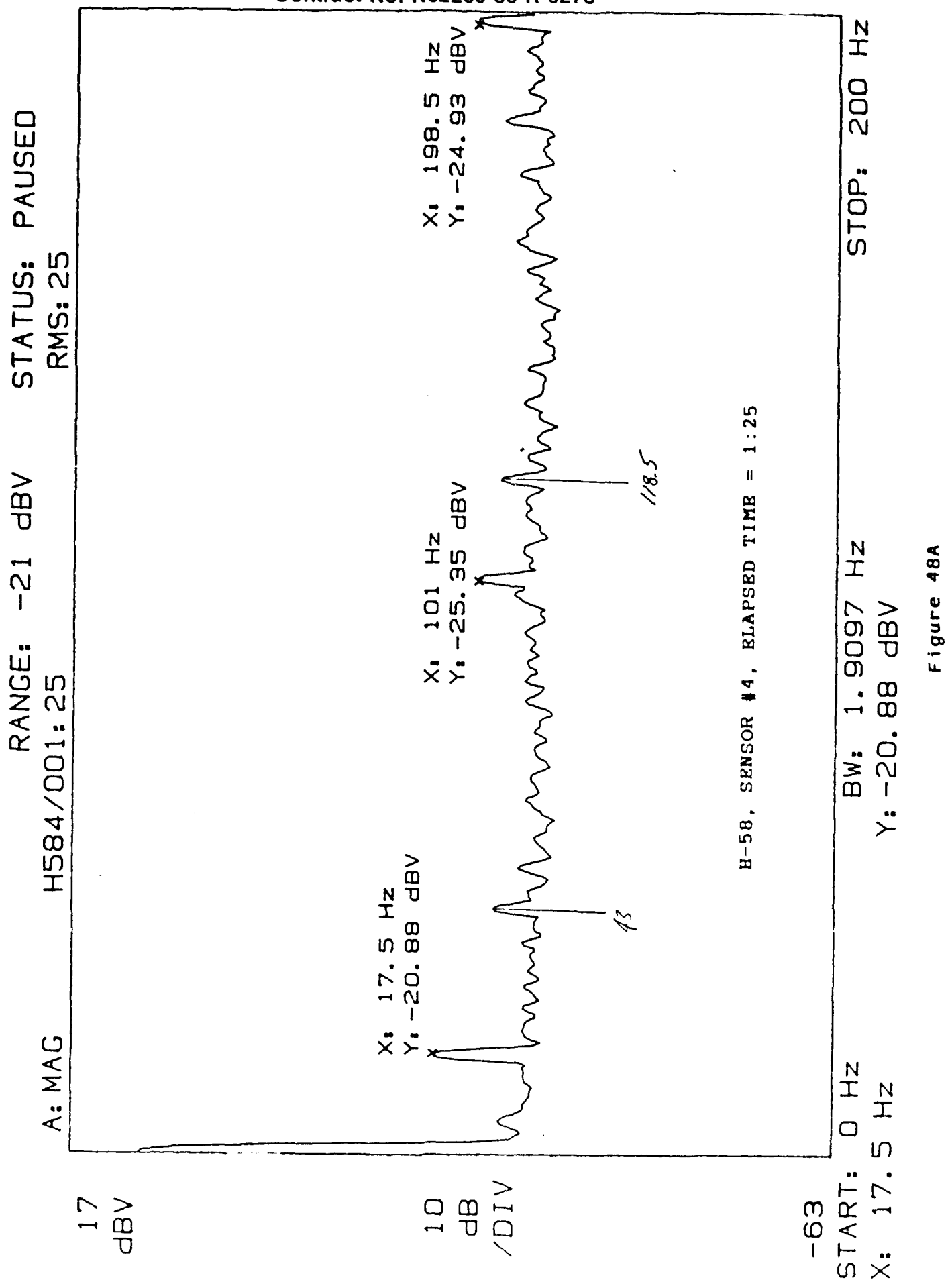
A: MAG
RANGE: -21 dBV
H584/001:25
STATUS: PAUSED
RMS: 25
X: 198.5 Hz
Y: -24.93 dBV
X: 101 Hz
Y: -25.35 dBV
X: 17.5 Hz
Y: -20.88 dBV
118.5
43
H-58, SENSOR #4, ELAPSED TIME = 1:25
17
dBV
10
dB
/DIV
-63
START: 0 Hz
X: 17.5 Hz
BW: 1.9097 Hz
Y: -20.88 dBV
STOP: 200 Hz

Figure 48A

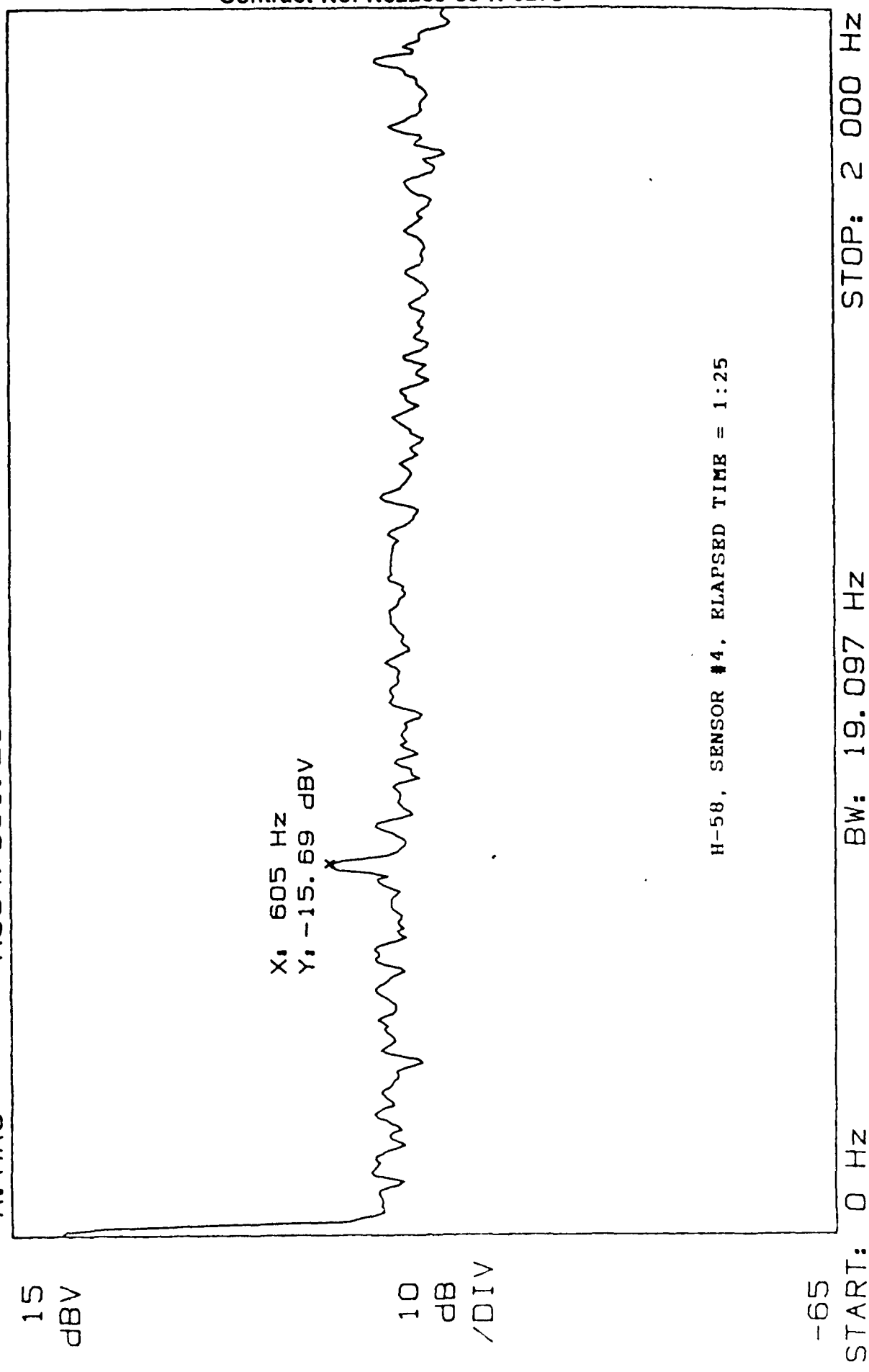
A: MAG
RANGE: 15 dBV
H584/001:25
STATUS: PAUSED
RMS: 25
X: 605 Hz
Y: -15.69 dBV
H-58, SENSOR #4, ELAPSED TIME = 1:25
15
dBV
10
dB
/DIV
-65
START: 0 Hz
X: 605 Hz
BW: 19.097 Hz
Y: -15.69 dBV
STOP: 2 000 Hz

Figure 48B

The planetary gear mesh frequency is about 10 db above background levels. There are also some 10 db lines associated with the rotor shaft RPM, 5.79 Hz. The strongest spectral line is at the planet passage frequency of 17.5 Hz that is about 20 db above background levels and has four clearly evident harmonics. Figures 49 and 50 are representative spectra for this sensor location.

Sensor #2 (Top Cover Bolt #2)

The mean SWE has dropped to 38,191 and the dominant spectral lines are all still associated with three frequencies:

1. The planet gear passage frequency, 17.5 Hz;

2. The rotor shaft 1/rev, 5.79 Hz; and

3. The mesh frequency for all the gears in the planetary gear system, 573 Hz.

The lines associated with the rotor shaft RPM, 5.79 Hz, are fluctuating over a range of from 0-13 db and the 17.5 hz line varies from 16-21 db as shown in Figure 51. The planetary gear mesh frequency is also variable from 2-10 db above background levels (see Figure 52).

Sensor # 3 (Mast Cover Bolt)

The mean SWE has dropped dramatically from 128,485 to 23,574 and the dominant spectral lines are associated with two frequencies:

1. The planet gear passage frequency, 17.5 Hz; and

2. The rotor shaft 1/rev, 5.79 Hz.

The rotor shaft 1/rev remains about the same at 10 db, but the 17.5 hz line has grown to about 15 db. Planetary gear mesh is also present, but at less than a 10 db amplitude. Figures 53 and 54 are representative spectra for this sensor location.

Sensor # 4 (Input Pinion Housing)

The mean SWE is 86,266 and there are no spectral lines over 10 db in amplitude.

<u>Day 3, Total Test Time = 14:55</u>

Sensor #1 (Top Cover Bolt #1)

The mean SWE remains almost the same at 26,372 and the dominant spectral lines are all associated with the same two frequencies:

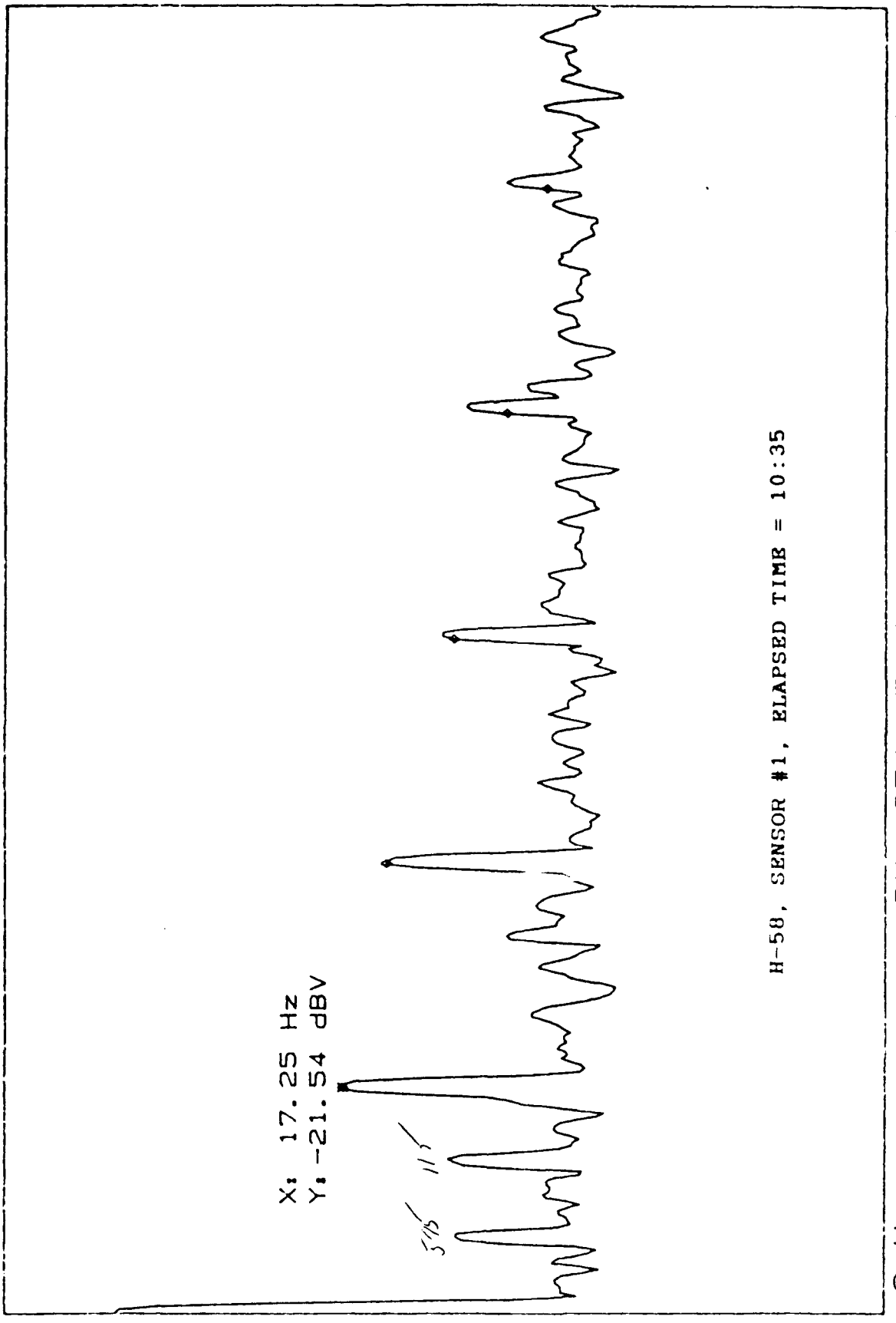
A: MAG
H581/010:35
RANGE: 9 dBV
STATUS: PAUSED
RMS: 10
X: 17.25 Hz
Y: -21.54 dBV
H-58, SENSOR #1, ELAPSED TIME = 10:35
BW: 954.85 mHz
Y: -21.54 dBV
THD: -2.52 dB
START: 0 Hz
X: 17.25 Hz
STOP: 100 Hz
9
dBV
10
dB
/DIV
-71

Figure 49

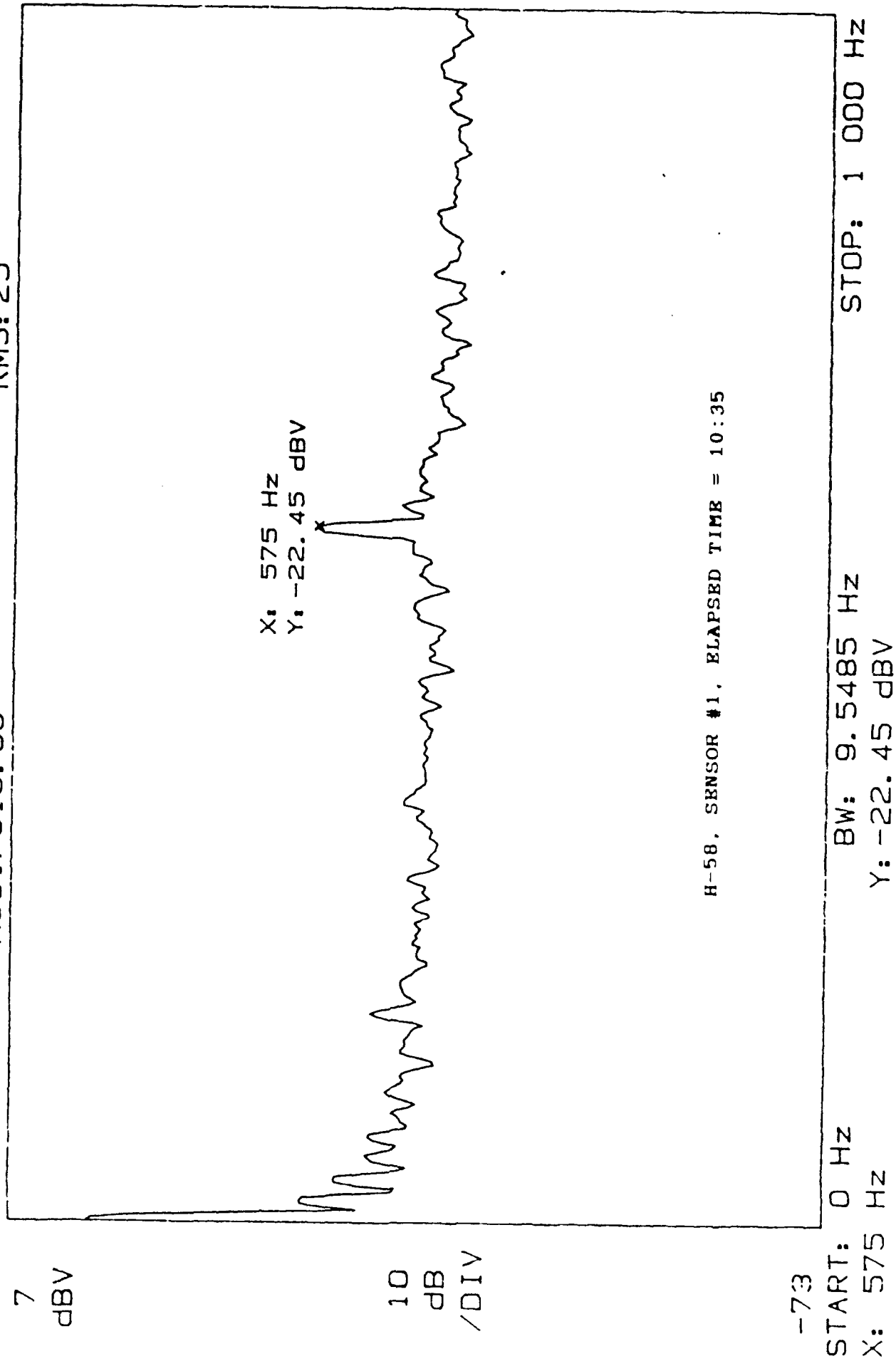
A: MAG
RANGE: 7 dBV
H581/010:35
STATUS: PAUSED
RMS: 25
X: 575 Hz
Y: -22.45 dBV
H-58, SENSOR #1, ELAPSED TIME = 10:35
7
dBV
10
dB
/DIV
-73
START: 0 Hz
X: 575 Hz
BW: 9.5485 Hz
Y: -22.45 dBV
STOP: 1 000 Hz

Figure 50

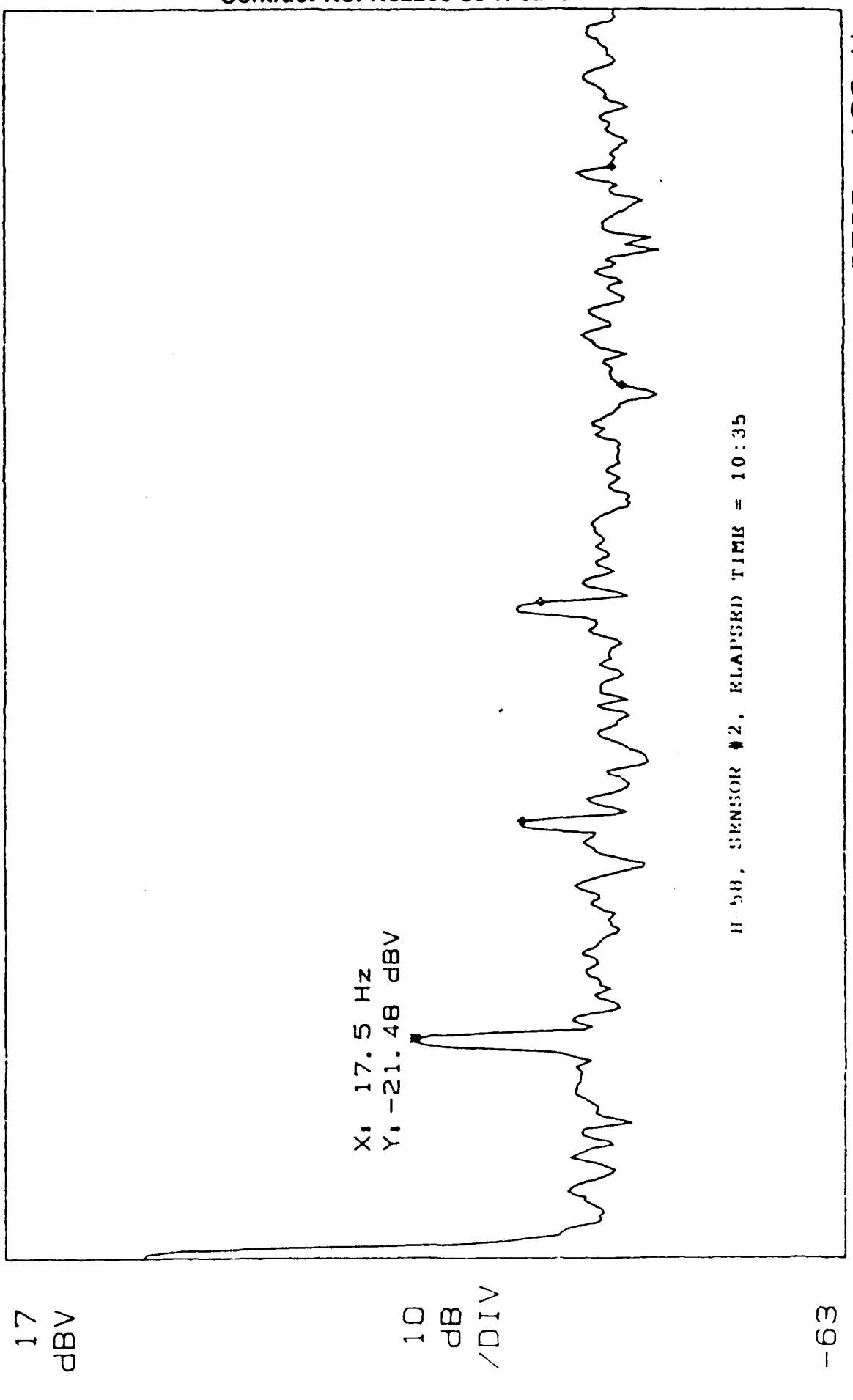
A: MAG
H582/010: 35
RANGE: 17 dBV
STATUS: PAUSED
RMS: 10
X: 17.5 Hz
Y: -21.48 dBV
17
dBV
10
dB
/DIV
-63
START: 0 Hz
X: 17.5 Hz
BW: 954.85 mHz
Y: -21.48 dBV
STOP: 100 Hz
THD: -7.61 dB

Figure 51A

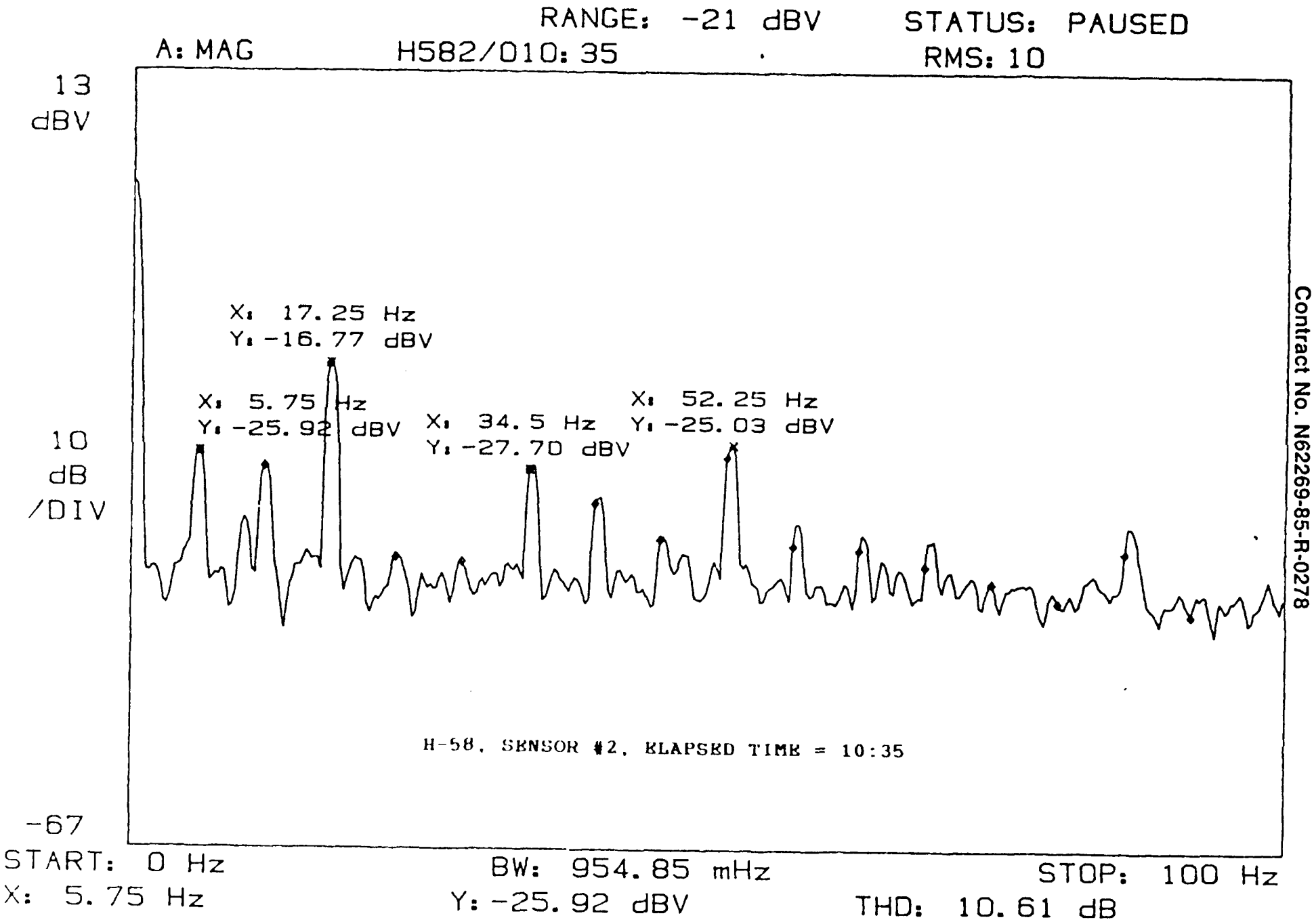

Figure 51B

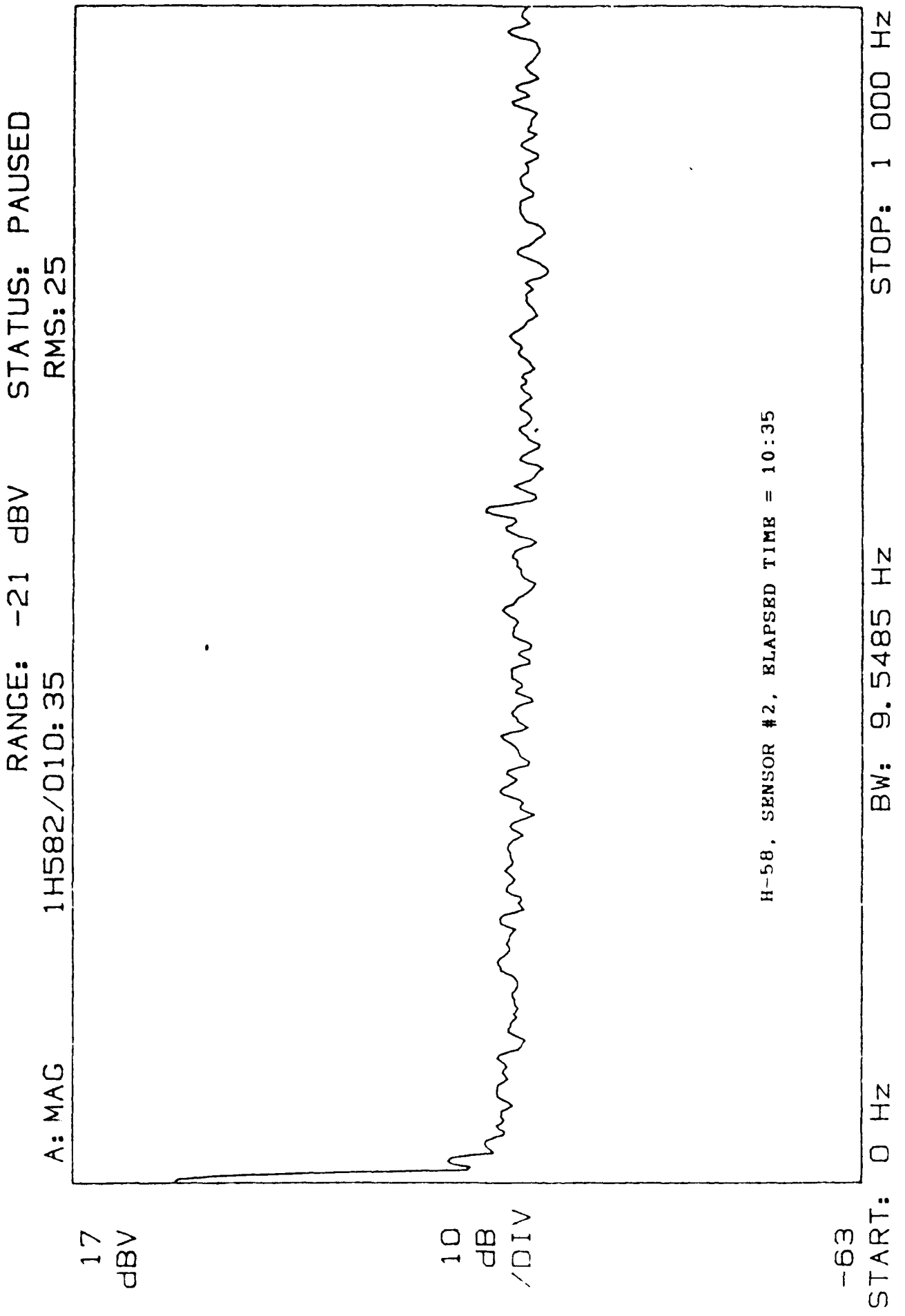
A: MAG
RANGE: -21 dBV
1H582/010:35
STATUS: PAUSED
RMS: 25
17 dBV
10 dB /DIV
-63
START: 0 Hz
BW: 9.5485 Hz
STOP: 1 000 Hz
H-58, SENSOR #2, ELAPSED TIME = 10:35

Figure 52A

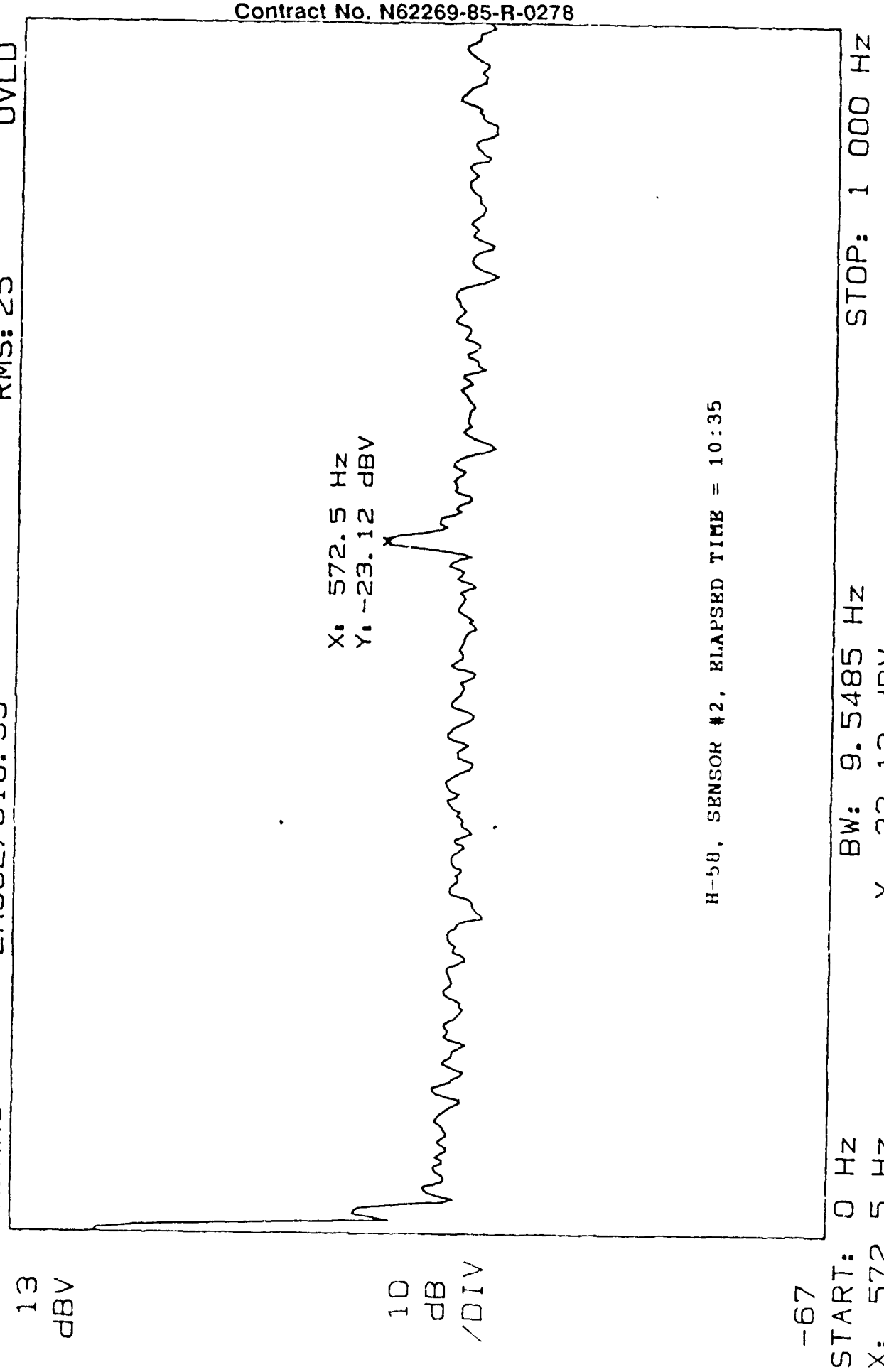
A: MAG
RANGE: -21 dBV
2H582/010:35
STATUS: PAUSED
RMS: 25
OVLD
X: 572.5 Hz
Y: -23.12 dBV
H-58, SENSOR #2, ELAPSED TIME = 10:35
13
dBV
10
dB
/DIV
-67
START: 0 Hz
X: 572.5 Hz
BW: 9.5485 Hz
Y: -23.12 dBV
STOP: 1 000 Hz

Figure 52B

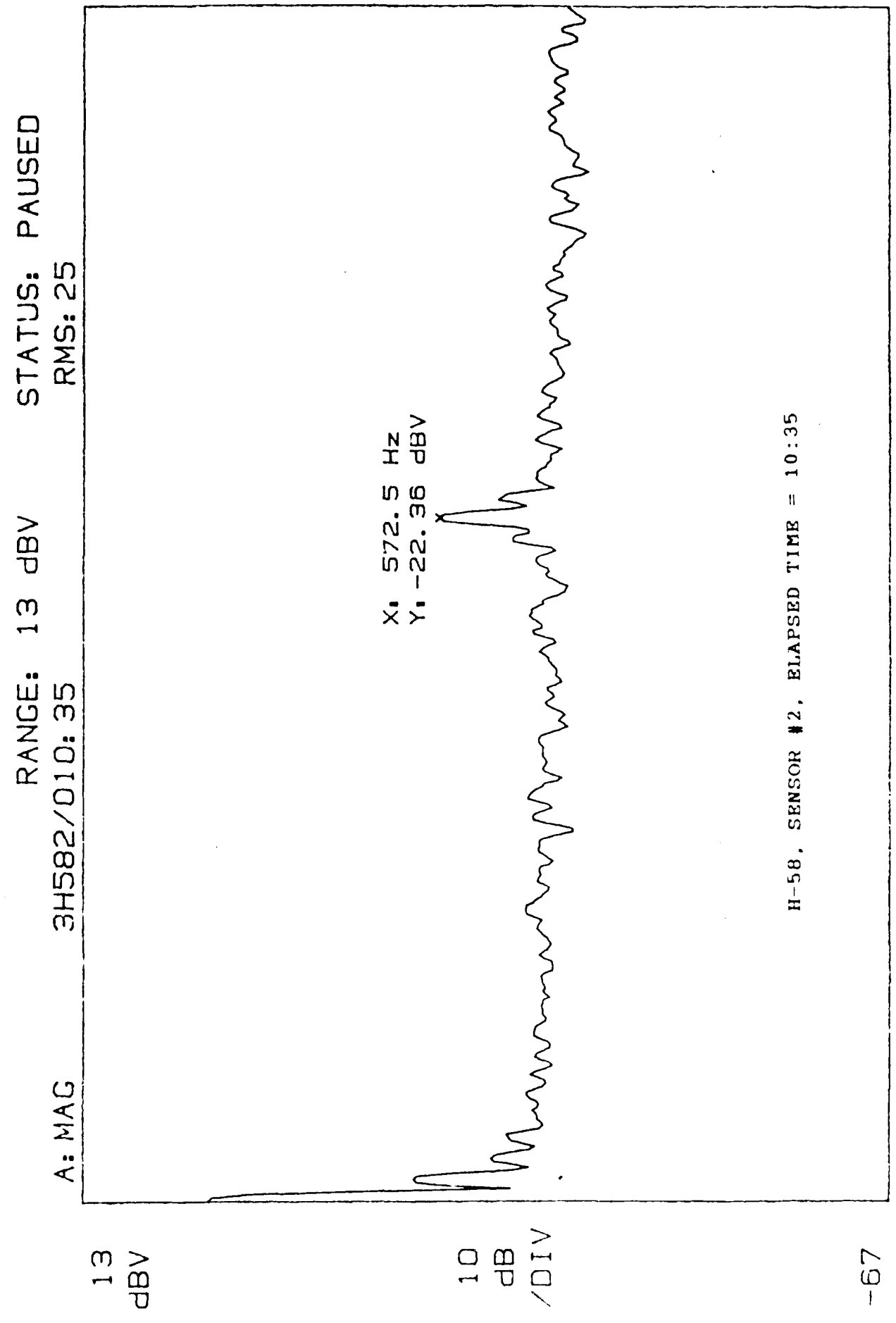
A: MAG
RANGE: 13 dBV
3H582/010: 35
STATUS: PAUSED
RMS: 25
X: 572.5 Hz
Y: -22.36 dBV
H-58, SENSOR #2, ELAPSED TIME = 10:35
13
dBV
10
dB
/DIV
-67
START: 0 Hz
X: 572.5 Hz
BW: 9.5485 Hz
Y: -22.36 dBV
STOP: 1 000 Hz

Figure 52c

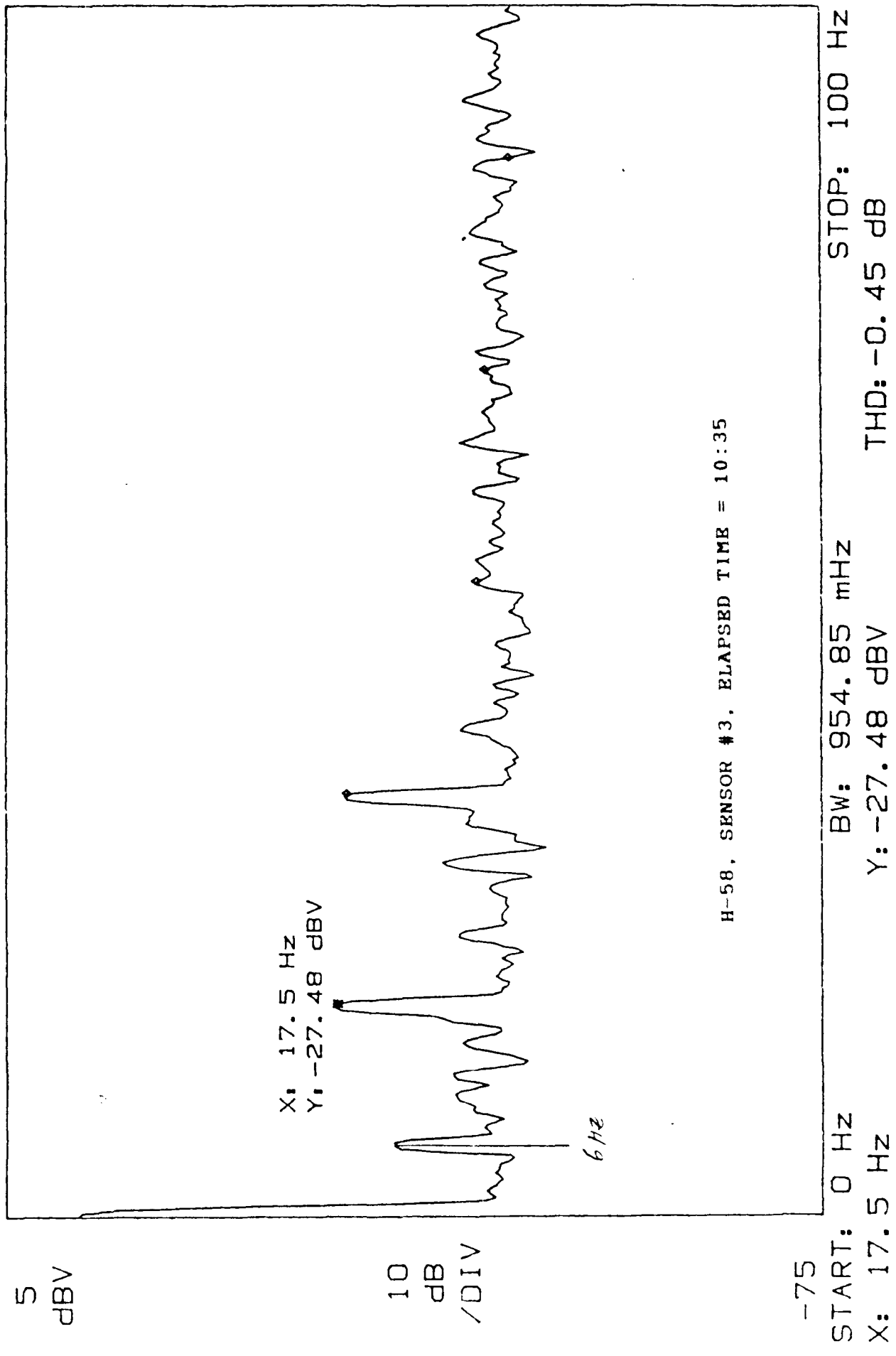
A: MAG
RANGE: -21 dBV
H583/010:35
STATUS: PAUSED
RMS: 10
OVLD
X: 17.5 Hz
Y: -27.48 dBV
6Hz
H-58, SENSOR #3, ELAPSED TIME = 10:35
5 dBV
10 dB /DIV
-75
START: 0 Hz
X: 17.5 Hz
BW: 954.85 mHz
Y: -27.48 dBV
STOP: 100 Hz
THD: -0.45 dB

Figure 53

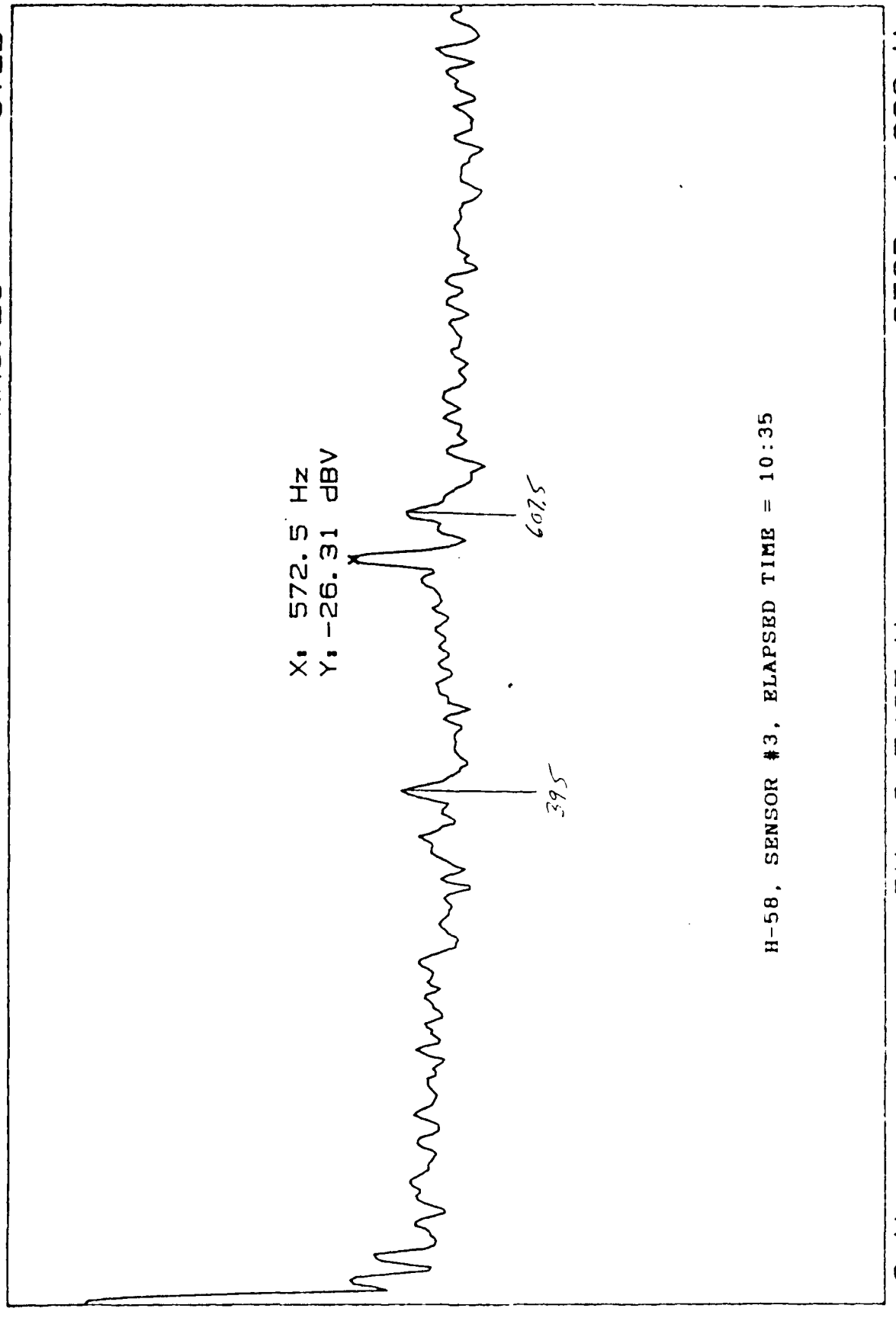
A: MAG
H583/010: 35
RANGE: 5 dBV
STATUS: PAUSED
RMS: 25
OVLD
X: 572.5 Hz
Y: -26.31 dBV
6025
395
H-58, SENSOR #3, ELAPSED TIME = 10:35
5 dBV
10 dB /DIV
-75
START: 0 Hz
X: 572.5 Hz
BW: 9.5485 Hz
Y: -26.31 dBV
STOP: 1 000 Hz

Figure 54

1. The planet gear passage frequency, 17.5 Hz; and

2. The mesh frequency for all the gears in the planetary gear system, 573 Hz.

The planetary gear mesh frequency is about 7 db above background levels. The strongest spectral line is at the planet passage frequency of 17.5 Hz. It is about 20 db above background levels and has four clearly evident harmonics.

Sensor #2 (Top Cover Bolt #2)

The mean SWE has increased to 48,380.

Sensor # 3 (Mast Cover Bolt)

The mean SWE is 25,972 and the dominant spectral lines are associated with two frequencies:

1. The planet gear passage frequency, 17.5 Hz; and

2. The planetary gear mesh frequency, 573 Hz.

Figures 55 and 56 illustrate 17.5 Hz side bands around the gear mesh frequency.

Sensor # 4 (Input Pinion Housing)

The mean SWE is 86,231 and there are no spectral lines over 10 db in amplitude.

Day 4, Total Test Time = 19:22

Sensor #1 (Top Cover Bolt #1)

The mean SWE decreased slightly to 22,503 and the dominant spectral lines are all associated with the same two frequencies:

1. The planet gear passage frequency, 17.5 Hz; and

2. The mesh frequency for all the gears in the planetary gear system, 573 Hz.

The planetary gear mesh frequency is about 10 db above background levels. The strongest spectral line is at the planet passage frequency of 17.5 Hz. It is about 20 db above background levels.

Sensor #2 (Top Cover Bolt #2)

The mean SWE has dropped from 48,380 to 27,117 and the dominant spectral lines are:

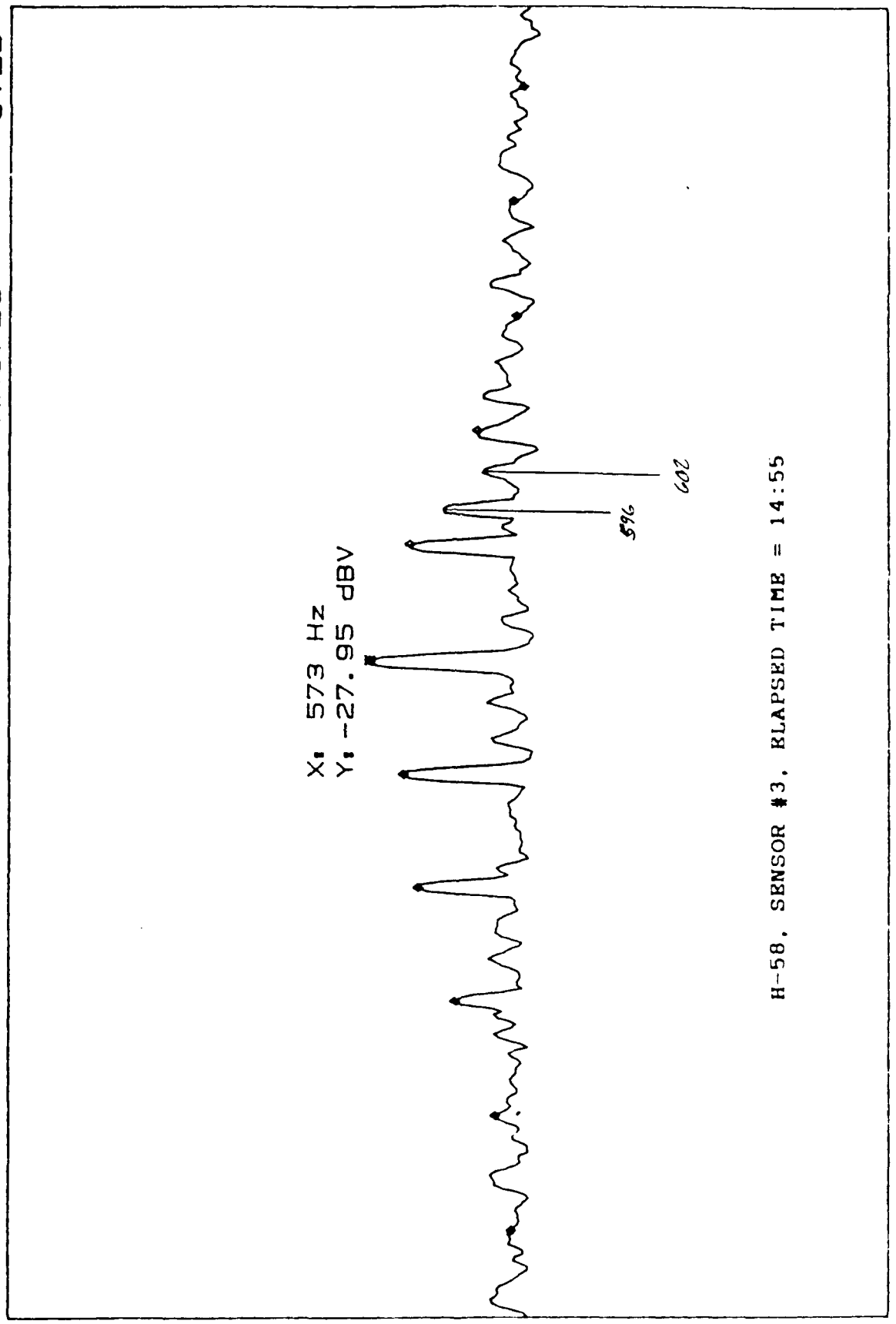
RANGE: -1 dBV
STATUS: PAUSED
H583/014:55
RMS: 25
OVLD
A: MAG
X: 573 Hz
Y: -27.95 dBV
H-58, SENSOR #3, ELAPSED TIME = 14:55
5 dBV
10 dB /DIV
-75
CENTER: 572.5 Hz
BW: 1.9097 Hz
SPAN: 200 Hz
X: 573 Hz
Y: -27.95 dBV
SB: 2.65 dB

Figure 55

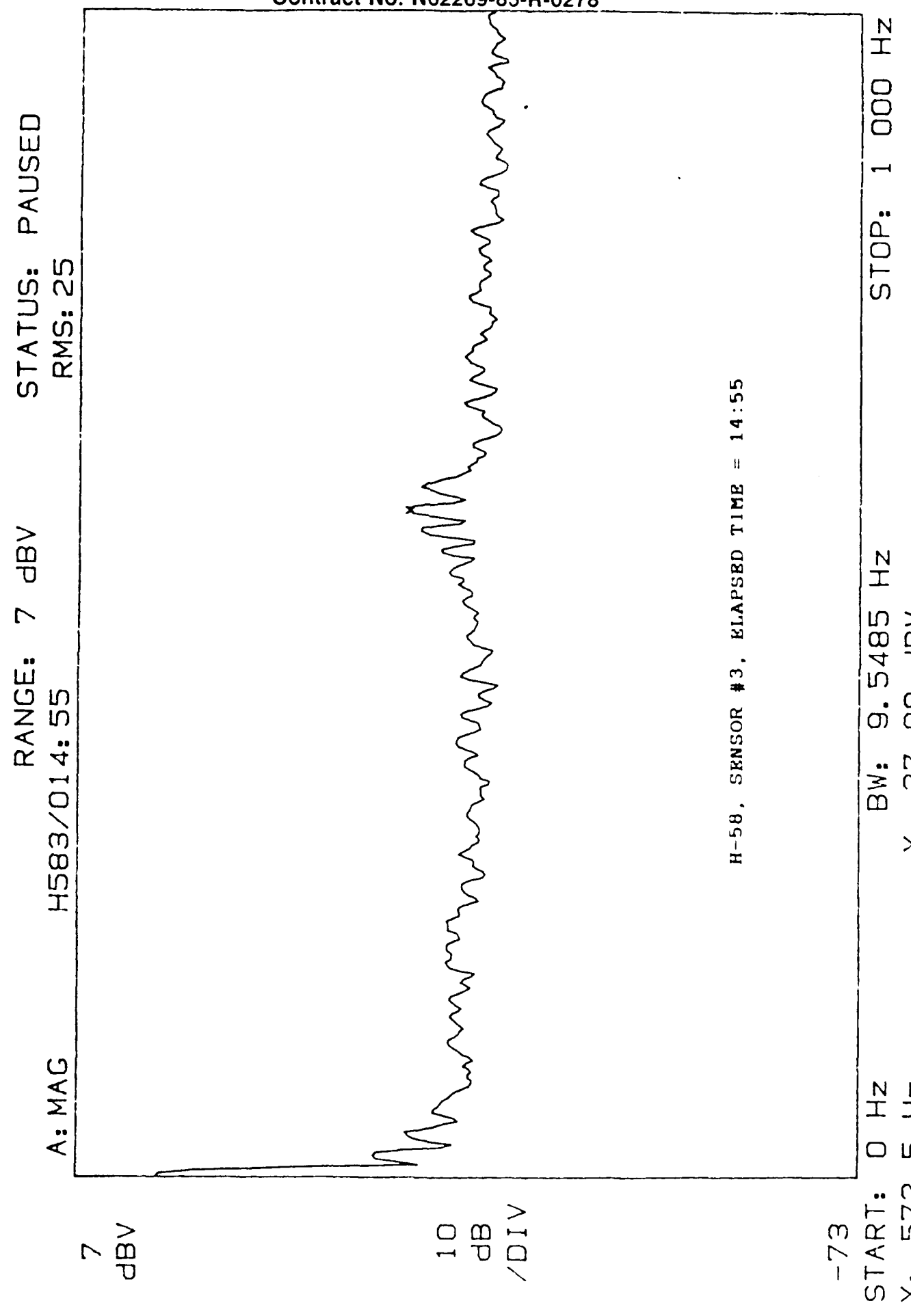
A: MAG
H583/014:55
RANGE: 7 dBV
STATUS: PAUSED
RMS: 25
H-58, SENSOR #3, ELAPSED TIME = 14:55
7
dBV
10
dB
/DIV
-73
START: 0 Hz
BW: 9.5485 Hz
STOP: 1 000 Hz
X: 572.5 Hz
Y: -27.08 dBV

1. The planet gear passage frequency, 17.5 Hz; and

2. The planetary gear mesh frequency, 573 Hz.

The 17.5 Hz line is 20 db above background levels and has four harmonics. The gear mesh is only about 6 db above background levels.

Sensor # 3 (Mast Cover Bolt)

The mean SWE has dropped from 25,972 to 10,860 and there are no significant spectral lines.

Sensor # 4 (Input Pinion Housing)

The mean SWE is 90,744 and there are no spectral lines over 10 db in amplitude.

Day 5, Total Test Time = 23:35

Sensor #1 (Top Cover Bolt #1)

The mean SWE increased slightly to 27,465 and the dominant spectral lines are all associated with the same two frequencies:

1. The planet gear passage frequency, 17.5 Hz; and

2. The mesh frequency for all the gears in the planetary gear system, 573 Hz.

The planetary gear mesh frequency is about 6 db above background levels. The strongest spectral line is at the planet passage frequency of 17.5 Hz. It is about 20 db above background levels and has four clearly evident harmonics.

Sensor #2 (Top Cover Bolt #2)

The mean SWE has increased gradually to 36,749 and the dominant spectral lines are:

1. The planet gear passage frequency, 17.5 Hz; and

2. The planetary gear mesh frequency, 573 Hz.

The 17.5 Hz line is 20 db above background levels and has three harmonics. The gear mesh is 10 db above background levels.

Sensor # 3 (Mast Cover Bolt)

The mean SWE has increased from 10,860 to 20,870. The 17.5 Hz spectral line has grown to 10 db and has three harmonics.

Sensor # 4 (Input Pinion Housing)

The mean SWE is 86,023 and there are no spectral lines over 10 db in amplitude.

Days 6-9, Total Test Time = 55:52

Sensor #1 (Top Cover Bolt #1)

The mean SWE increased slightly to 28,978 and the dominant spectral lines are all associated with the same two frequencies:

1. The planet gear passage frequency, 17.5 Hz; and

2. The mesh frequency for all the gears in the planetary gear system, 573 Hz.

The planetary gear mesh frequency is about 10 db above background levels. The strongest spectral line is at the planet passage frequency of 17.5 Hz. It is about 21 db above background levels and has four clearly evident harmonics.

Sensor #2 (Top Cover Bolt #2)

The mean SWE has increased gradually to 37,133 and the dominant spectral lines are:

1. The planet gear passage frequency, 17.5 Hz; and

2. The planetary gear mesh frequency, 573 Hz.

The 17.5 Hz line is 20 db above background levels and has three harmonics. The gear mesh is 11 db above background levels.

Sensor # 3 (Mast Cover Bolt)

The mean SWE has remained relatively constant and is at 20,770. The 17.5 Hz spectral line has grown to 11 db and has an equally strong 2nd harmonic at 52 Hz. An 11 db line has also developed at the rotor shaft 1/rev (5.75 Hz) and at 10 Hz.

Sensor # 4 (Input Pinion Housing)

The mean SWE has gradually increased to 93,120 and there are no spectral lines over 10 db in amplitude. A small 4-5 db spectral line is sometimes present at 595 Hz. This is the outer race defect frequency for the input pinion triplex ball bearing.

Day 10, Total Test Time = 62:31

Sensor #1 (Top Cover Bolt #1)

The mean SWE increased from 28,978 to 51,374 and the dominant spectral lines are all associated with the same two frequencies:

1. The planet gear passage frequency, 17.5 Hz; and

2. The mesh frequency for all the gears in the planetary gear system, 573 Hz.

The planetary gear mesh frequency is about 11 db above background levels. The strongest spectral line is at the planet passage frequency of 17.5 Hz. It is about 20 db above background levels and has four clearly evident harmonics. Other significant spectral lines are present at the rotor shaft 1/rev and at 9.75 Hz.

Sensor #2 (Top Cover Bolt #2)

The mean SWE has increased from 37,133 to 68,701 and the dominant spectral lines are:

1. The planet gear passage frequency, 17.5 Hz;

2. The planetary gear mesh frequency, 573 Hz;

3. The rotor shaft 1/rev, 5.75Hz; and

4. 9.75 Hz from an unknown source.

The 17.5 Hz line is 13 db above background levels and has four harmonics. The gear mesh is 10 db above background levels. The 5.75Hz and 9.75 Hz lines are also at about 10 db.

Sensor # 3 (Mast Cover Bolt)

The mean SWE increased from 20,870 to 33,633 and then settled back to 14,589 at 62:31 total test time. All spectral lines have fallen to less than 10 db above background levels.

Sensor # 4 (Input Pinion Housing)

The mean SWE increased from 93,120 to 104,574 and then settled back to 98,369 at 62:31 total test time. A 13 db spectral line has appeared at the planet passage frequency of 17.5 Hz and at the input pinion 1/rev. There is a comparable amplitude 1st harmonic of the input pinion 1/rev and an 11 db line at the input pinion gear mesh frequency of 1915 Hz. A small 3-4 db spectral line is present at 600 Hz. This is the outer race defect frequency for the input pinion triplex ball bearing. Figures 57 and 58 illustrate these spectral changes.

Day 12, Total Test Time = 76:23

Sensor #1 (Top Cover Bolt #1)

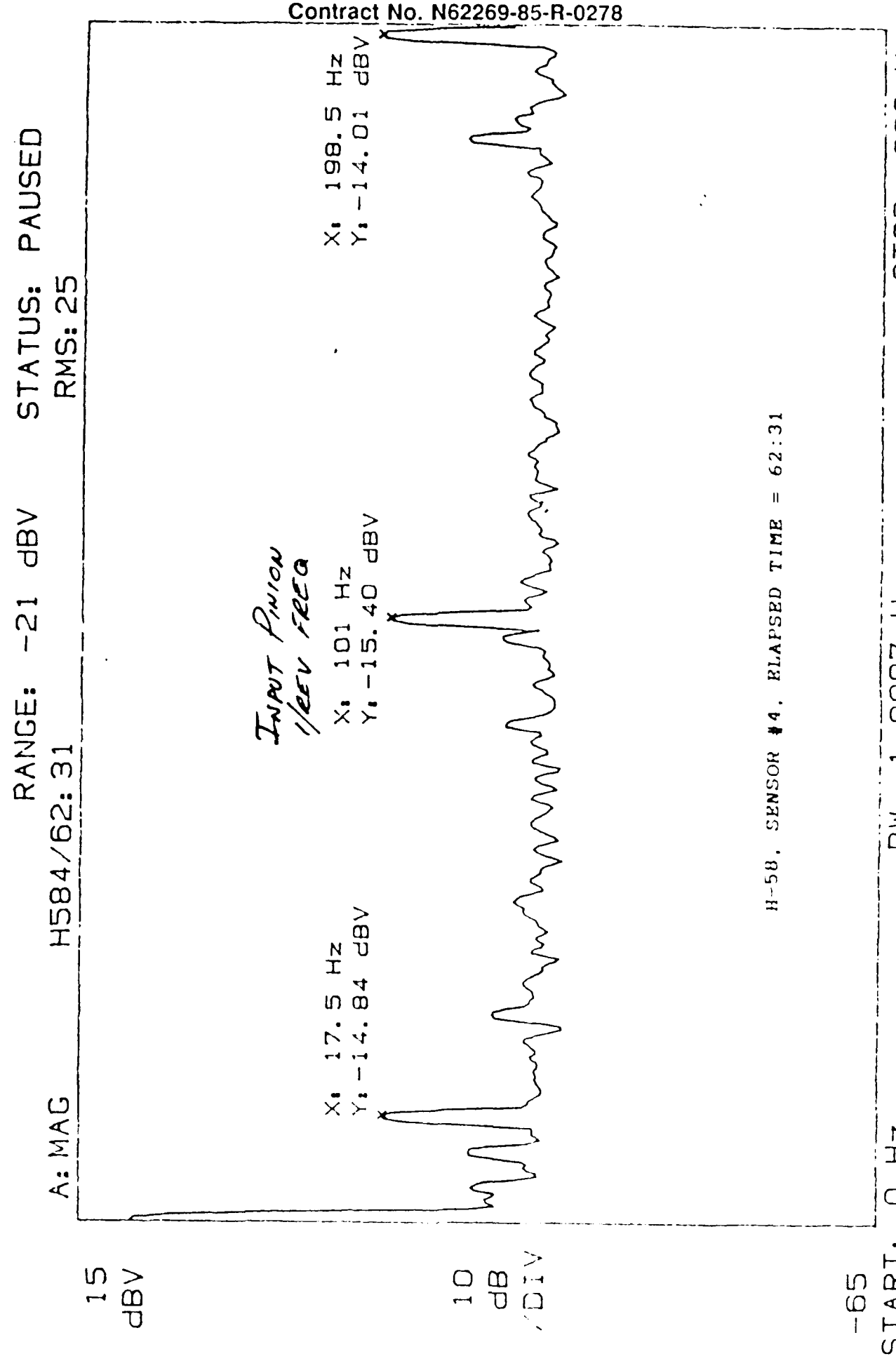
RANGE: -21 dBV
STATUS: PAUSED
A: MAG
H584/62: 31
RMS: 25
X: 198.5 Hz
Y: -14.01 dBV
INPUT PINION
1/REV FREQ
X: 101 Hz
Y: -15.40 dBV
X: 17.5 Hz
Y: -14.84 dBV
H-58, SENSOR #4, ELAPSED TIME = 62:31
15
dBV
10
dB
/DIV
-65
START: 0 Hz
X: 198.5 Hz
BW: 1.9097 Hz
Y: -14.01 dBV
STOP: 200 Hz

Figure 57

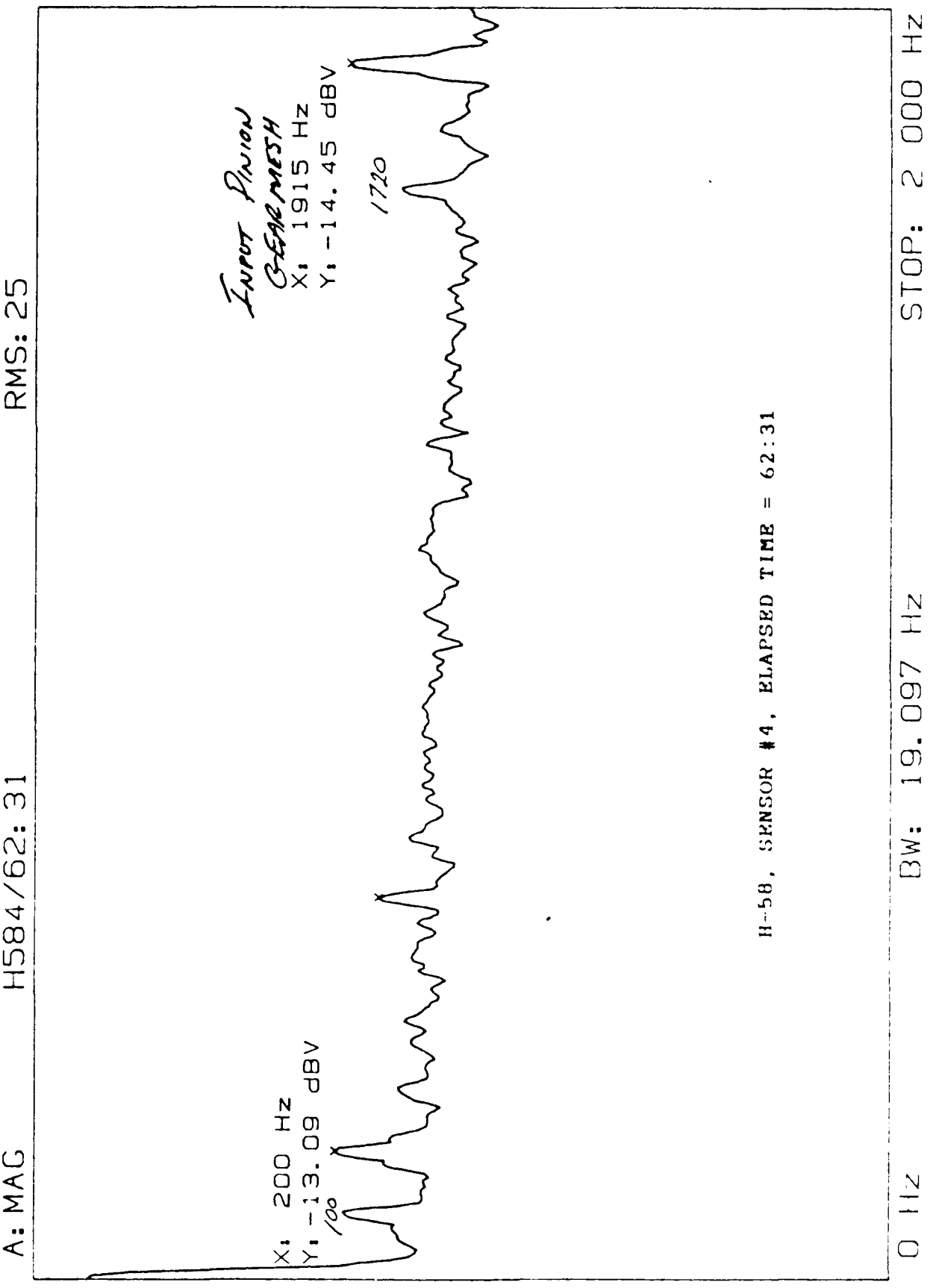
RANGE: 15 dBV
STATUS: PAUSED
A: MAG
H584/62:31
RMS: 25
INPUT PINION GEAR MESH
X: 1915 Hz
Y: -14.45 dBV
1720
X: 200 Hz
Y: -13.09 dBV
100
H-58, SENSOR #4, ELAPSED TIME = 62:31
15 dBV
10 dB /DIV
-65
START: 0 Hz
/: 600 Hz
BW: 19.097 Hz
Y: -17.18 dBV
STOP: 2 000 Hz

Figure 58

The mean SWE increased from 51,374 to 55,478 and the dominant spectral lines are all associated with the same two frequencies:

1. The planet gear passage frequency, 17.5 Hz; and

2. The mesh frequency for all the gears in the planetary gear system, 573 Hz.

The planetary gear mesh frequency is about 10 db above background levels. The strongest spectral line is at the planet passage frequency of 17.5 Hz. It is about 21 db above background levels and has four clearly evident harmonics. Other significant spectral lines are present at the rotor shaft 1/rev and at 10 Hz.

NOTE: The data sheets provided by government personnel indicate that this sensor was disconnected at this time due to a "17 Hz oscillation". This does not agree with the data on tape which appears valid and quite similar to data acquired both before and after the alleged disconnection of sensor #1.

Sensor #2 (Top Cover Bolt #2)

The mean SWE has increased from 68,701 to 75,131 and the dominant spectral lines are:

1. The planet gear passage frequency, 17.5 Hz;

2. The planetary gear mesh frequency, 573 Hz;

3. The rotor shaft 1/rev, 5.75Hz; and

4. 9.75 Hz from an unknown source.

The 17.5 Hz line is 16 db above background levels and has four harmonics. The gear mesh is 10 db above background levels. The 5.75Hz and 9.75 Hz lines are also at about 10 db.

Sensor # 3 (Mast Cover Bolt)

The mean SWE is relatively unchanged at 14,054. The 17.5 Hz spectral line is up to 10 db and the rotor shaft 1/rev is about 6 db above background levels.

Sensor # 4 (Input Pinion Housing)

The mean SWE is essentially unchanged at 93,513. The planet passage frequency of 17.5 Hz is at 16 db and the input pinion 1/rev is about 12 db above background. There is a comparable amplitude 1st harmonic of the input pinion 1/rev and an 8 db line at the input pinion gear mesh frequency of 1915 Hz. A small 3 db spectral line is present at 600 Hz. This is the outer race defect frequency for the input pinion triplex ball bearing.

Day 13, Total Test Time = 83:20

Sensor #1 (Top Cover Bolt #1)

The mean SWE is about the same at 55,395 and the dominant spectral lines are all associated with the same two frequencies:

1. The planet gear passage frequency, 17.5 Hz; and

2. The mesh frequency for all the gears in the planetary gear system, 573 Hz.

The planetary gear mesh frequency is about 8 db above background levels. The strongest spectral line is at the planet passage frequency of 17.5 Hz. It is about 21 db above background levels and has four clearly evident harmonics. Other significant spectral lines are present at the rotor shaft 1/rev and at 10 Hz.

Sensor #2 (Top Cover Bolt #2)

The mean SWE has decreased from 75,131 to 71,136 and the dominant spectral lines are:

1. The planet gear passage frequency, 17.5 Hz;

2. The planetary gear mesh frequency, 573 Hz;

3. The rotor shaft 1/rev, 5.75Hz; and

4. 9.75 Hz from an unknown source.

The 17.5 Hz line is 16 db above background levels and has four harmonics. The gear mesh is 10 db above background levels and has several 17.25 Hz side bands. The 5.75Hz and 9.75 Hz lines are also at about 10 db. Figures 59, 60, and 61 show these spectral features.

Sensor # 3 (Mast Cover Bolt)

The mean SWE is relatively unchanged at 13,765. The 17.5 Hz spectral line is up to 10 db and there are no other apparent spectral features.

Sensor # 4 (Input Pinion Housing)

The mean SWE is up slightly at 93,513. The planet passage frequency of 17.5 Hz is at 15 db and the input pinion 1/rev is about 12 db above background. There is a comparable amplitude 1st harmonic of the input pinion 1/rev and an 8 db line at the input pinion gear mesh frequency of 1915 Hz. A very small 2 db spectral line is present at 600 Hz. This is the outer race defect frequency for the input pinion triplex ball bearing.

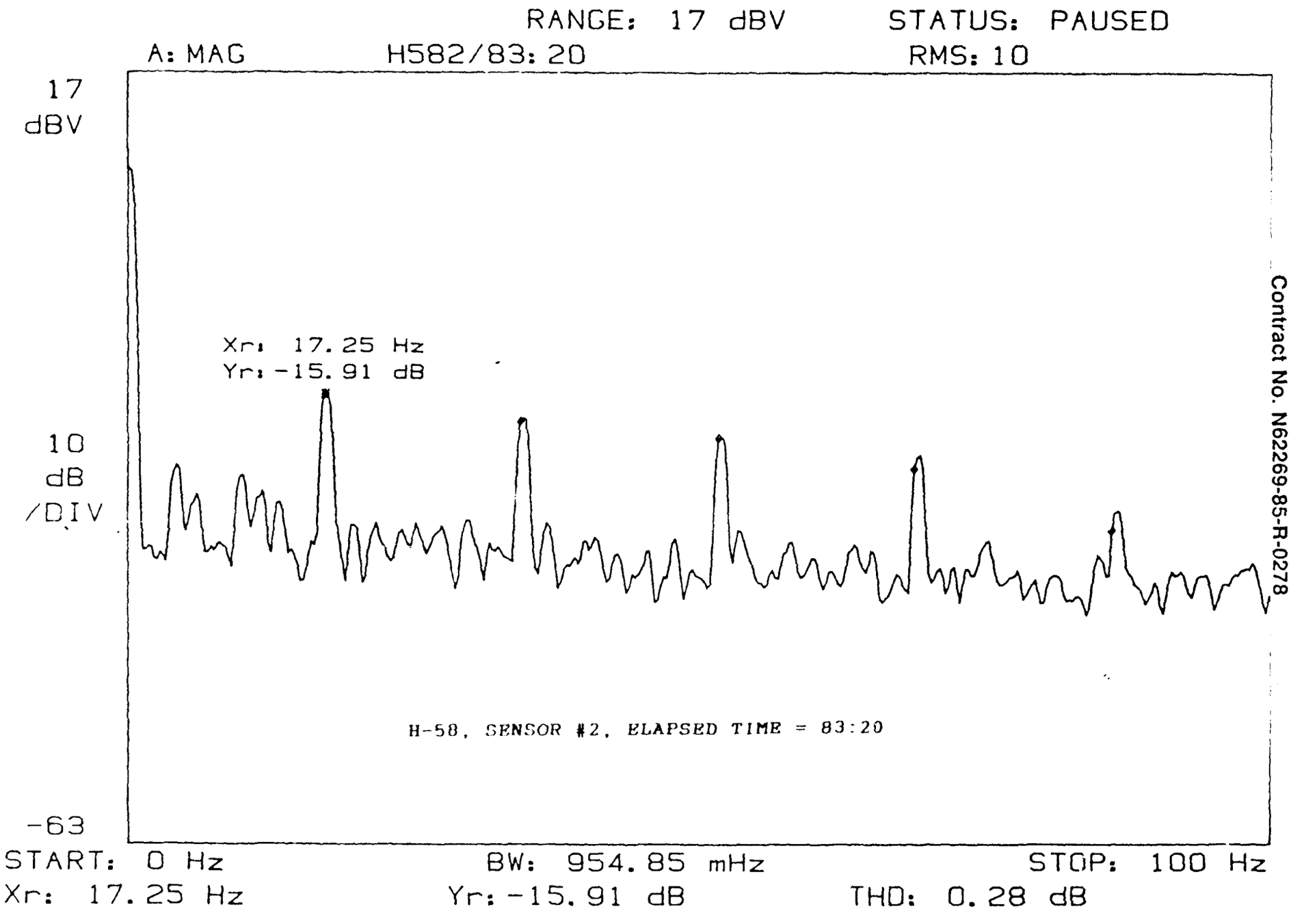

Report No. NADC-91069-60
Contract No. N62269-85-R-0278

Figure 59

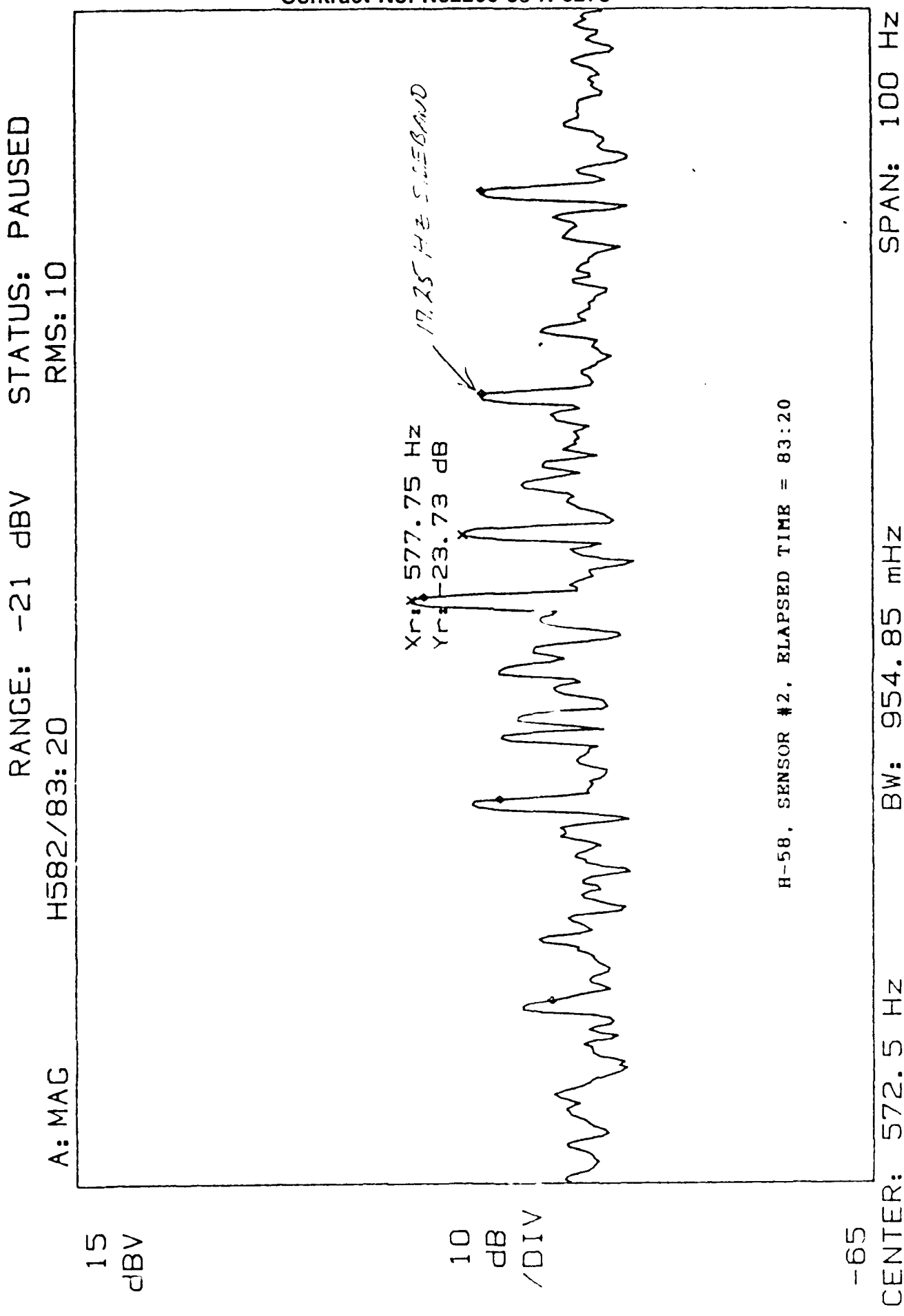
RANGE: -21 dBV
STATUS: PAUSED
A: MAG
H582/83: 20
RMS: 10
17.25 Hz SIDEBAND
Xr: 577.75 Hz
Yr: 23.73 dB
H-58, SENSOR #2, ELAPSED TIME = 83:20
15 dBV
10 dB /DIV
-65
CENTER: 572.5 Hz
BW: 954.85 mHz
SPAN: 100 Hz
Xr: 572.25 Hz
Yr: -18.60 dB
SB: -1.28 dB

Figure 60

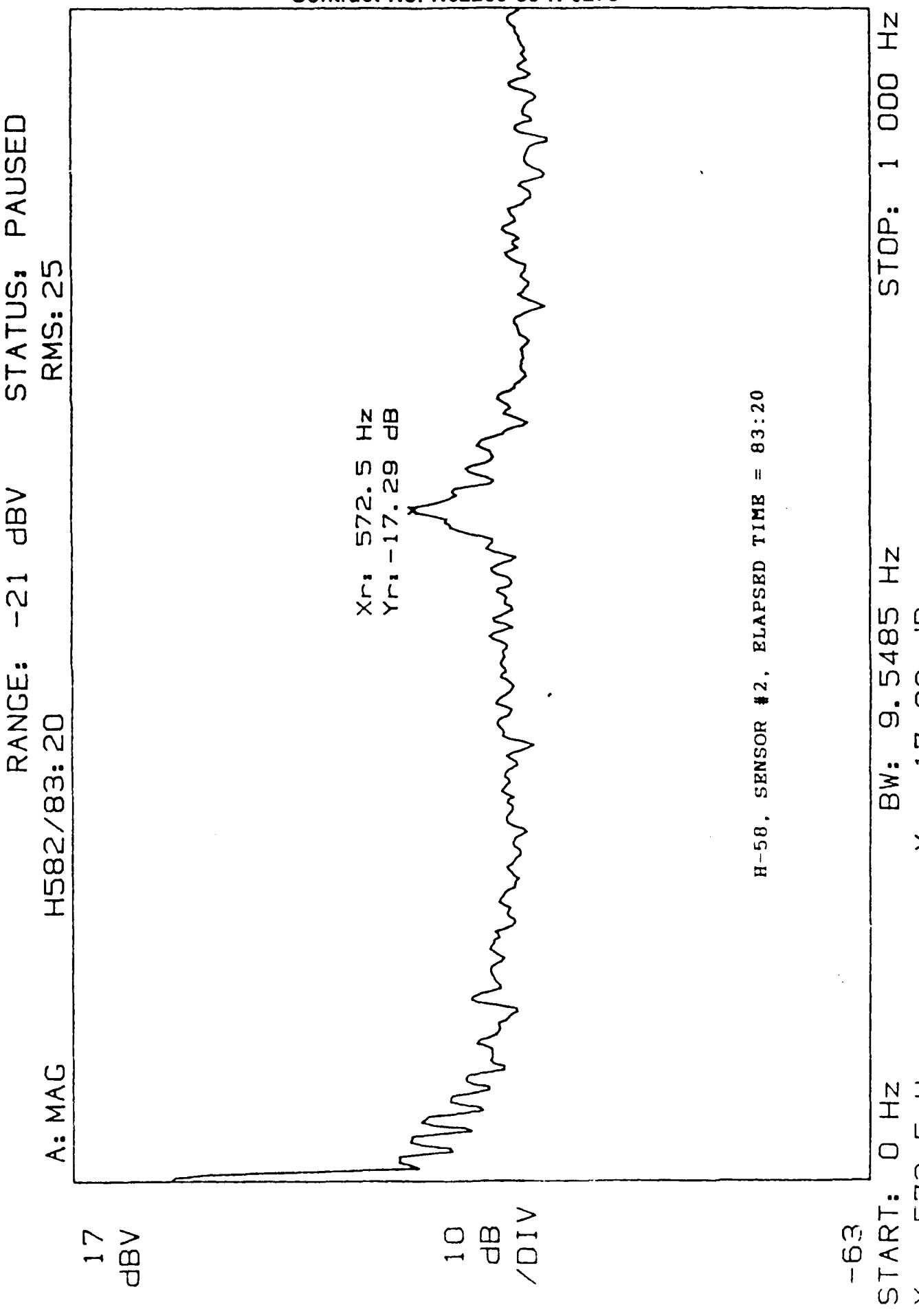
RANGE: -21 dBV
STATUS: PAUSED
H582/83:20
RMS: 25
A: MAG
Xr: 572.5 Hz
Yr: -17.29 dB
H-58, SENSOR #2, ELAPSED TIME = 83:20
17
dBV
10
dB
/DIV
-63
START: 0 Hz
BW: 9.5485 Hz
STOP: 1 000 Hz
Xr: 572.5 Hz
Yr: -17.29 dB

Figure 61

Day 14, Total Test Time = 87:18

Sensor #1 (Top Cover Bolt #1)

The mean SWE has dropped from 55,395 to 44,457 but the dominant spectral lines are all associated with the same two frequencies:

1. The planet gear passage frequency, 17.5 Hz; and

2. The mesh frequency for all the gears in the planetary gear system, 573 Hz.

The planetary gear mesh frequency is about 10 db above background levels. The strongest spectral line is at the planet passage frequency of 17.5 Hz. It is about 13 db above background levels and has four clearly evident harmonics. One other 10 db spectral line is present at 10 Hz.

Sensor #2 (Top Cover Bolt #2)

The mean SWE has decreased from 71,136 to 60,457 and the dominant spectral lines are:

1. The planet gear passage frequency, 17.5 Hz;

2. The planetary gear mesh frequency, 573 Hz;

3. The rotor shaft 1/rev, 5.75Hz; and

4. 9.75 Hz from an unknown source.

The 17.5 Hz line is 16 db above background levels and has four harmonics. The gear mesh is 5 db above background levels but was 10 db above at the start of the day (Total Time = 84:18). The 5.75Hz line also dropped from 12 db at the star of the days testing to about 6 db at the end of the day.

Sensor # 3 (Mast Cover Bolt)

The mean SWE increased from 13,765 to 18,629. The 17.5 Hz spectral line is up to 13 db (10 db at the start of the day) and there are three apparent harmonics. The rotor shaft 1/rev started the day at 12 db but decreased to about 3 db by the end of the day.

Sensor # 4 (Input Pinion Housing)

The mean SWE increased from 93,513 to 110,274 (113,343 at the start of the day). There are no spectral lines at 10 db or above background levels, but 6 db features are apparent at 600 Hz and at 1800 Hz.

Day 16, Total Test Time = 102:11

Sensor #1 (Top Cover Bolt #1)

The mean SWE has increased from 44,457 to 64,036 but the dominant spectral lines are all associated with the 17.25 Hz planet gear passage frequency. The planetary gear mesh frequency is about 3 db above background levels. The strongest spectral line is at the planet passage frequency of 17.5 Hz. It is about 20 db above background levels and has three clearly evident harmonics.

Sensor #2 (Top Cover Bolt #2)

The mean SWE increased from 60,457 to 72,877 on day 15 and then dropped to 68,366 by the end of testing on day 16. The dominant spectral lines are:

1. The planet gear passage frequency, 17.25 Hz;
2. The planetary gear mesh frequency, 573 Hz;
3. The rotor shaft 1/rev, 5.75Hz; and
4. 9.75 Hz from an unknown source.

The 17.5 Hz line is 13 db above background levels and has four harmonics. The gear mesh is 10 db above background stress wave energy.

Sensor # 3 (Mast Cover Bolt)

The mean SWE increased from 18,629 to 19,026. The 17.25 Hz spectral line is still at 13 db and there are three apparent harmonics. The 9.75 Hz frequency from an unknown source is at 11 db above background levels.

Sensor # 4 (Input Pinion Housing)

The mean SWE increased from 110,274 to 125,275. There are four spectral lines at 10 db or above background levels. The 17.5 Hz line has an amplitude of 12 db. The input pinion 1/rev and its harmonic(?) are about 12 db above background levels. The amplitude of the input pinion gear mesh spectral line is 10 db.

Day 19, Total Test Time = 125:02

Sensor #1 (Top Cover Bolt #1)

The mean SWE has decreased from 64,036 to 49,634. The dominant spectral lines are all associated with the 17.25 Hz planet gear passage frequency. The planetary gear mesh frequency is about 11 db above background levels. The strongest spectral line is at the

planet passage frequency of 17.25 Hz. It is about 12 db above background levels and has three clearly evident harmonics. The 10 Hz spectral line of unknown origin is also present at a 10 db amplitude.

Sensor #2 (Top Cover Bolt #2)

The mean SWE increased from 68,336 on day 16 to 97,439 at the start of testing on day 19 and then dropped to 86,126 by the end of testing on day 19. The dominant spectral lines are:

1. The planet gear passage frequency, 17.25 Hz;

2. 83.5 Hz from an unknown source; and

3. The input pinion 1/rev, 100 Hz.

The 17.5 Hz line is 20 db above background levels and has three harmonics. The 83.5 Hz frequency from an unknown source is at 13 db above background levels. The 100 Hz input pinion 1/rev is at 10 db and has 17.25 Hz side bands.

Sensor # 3 (Mast Cover Bolt)

The mean SWE increased from 19,026 at the end of day 16 to 38,165 during the first hour of testing on day 19, then dropped back to 19,631 by the end of day 19. The 17.25 Hz spectral line is still at 13 db and there are 1st and 3rd harmonics. The planetary gear mesh frequency is evident but has an amplitude of only 6 db.

Sensor # 4 (Input Pinion Housing)

The mean SWE remained steady and finished the day at 125,475. There are three spectral lines at 10 db or above background levels. The 17.5 Hz line has an amplitude of 11 db. The input pinion 1/rev and its harmonic(?) are at about 10 db above background levels.

Day 21, Total Test Time = 136:18

Sensor #1 (Top Cover Bolt #1)

The mean SWE increased from 49,634 on day 19 to 59,109 on day 20 and then dropped back to 53,917 by the end of day 21. The dominant spectral lines are all associated with the 17.25 Hz planet gear passage frequency. The planetary gear mesh frequency is about 10 db above background levels. The planet passage frequency of 17.25 Hz is about 10 db above background levels and has three clearly evident harmonics. The 9.75 Hz spectral line of unknown origin is also present at a 10 db amplitude.

Sensor #2 (Top Cover Bolt #2)

The mean SWE decreased from 86,126 at the end of testing on day 19 to 78,485 by the end of day 21. The dominant spectral lines are:

1. The planet gear passage frequency, 17.25 Hz;
2. 83.5 Hz from an unknown source;
3. The input pinion 1/rev, 100 Hz, and
4. The rotor shaft 1/rev, 5.75 Hz.

The 17.5 Hz line is 13 db above background levels and has four identifiable harmonics. The 83.5 Hz frequency from an unknown source is at 13 db above background levels. The 100 Hz input pinion 1/rev is at 6 db and has 17.25 Hz side bands. The amplitude of the rotor shaft 1/rev is 10 db.

Sensor # 3 (Mast Cover Bolt)

The mean SWE decreased from 19,631 at the end of day 19 to 18,779 during the last testing on day 21. The 17.25 Hz spectral line is still at 13 db and there are three harmonics. The planetary gear mesh frequency is evident but has an amplitude of only 6 db.

Sensor # 4 (Input Pinion Housing)

The mean SWE decreased to 112,363. All spectral lines except 600 Hz and its harmonics have disappeared. The 600 Hz frequency has an amplitude of only 8 db above background, and two harmonics that are 2-3 db each. 600 Hz is the ball passage frequency over a point on the outer race of the input pinion triplex bearing.

Day 25, Total Test Time = 165:04

Sensor #1 (Top Cover Bolt #1)

The mean SWE increased from 53,917 on day 21 to 56,405 on day 22 and then dropped back to 46,838 by the end of day 25. The dominant spectral lines are all associated with the planetary gear system frequencies. The planetary gear mesh frequency is about 12 db above background levels. The strongest spectral line, at the planet passage frequency of 17.25 Hz, is about 22 db above background levels and has four clearly evident harmonics. The 9.75 Hz spectral line of unknown origin and the rotor shaft 1/rev are also present at a 10-11 db amplitude.

Sensor #2 (Top Cover Bolt #2)

The mean SWE decreased from 78,485 at the end of testing on day 21 to 64,995 by the end of day 22. It then remained relatively

unchanged for three days, finishing day 25 at 63,692. The spectral features also remained very stable during this period. The dominant spectral lines are:

1. The planet gear passage frequency, 17.25 Hz;

2. The planetary gear mesh frequency, 573 Hz;

3. The rotor shaft 1/rev, 5.75 Hz, and

4. the 9.75 Hz frequency of unknown origin.

The 17.5 Hz line is 16 db above background levels and has four identifiable harmonics. The planetary gear mesh frequency has a 12 db amplitude and the rotor shaft 1/rev is at 11 db. The 9.75 Hz frequency from an unknown source is at 10 db above background levels. Figures 62, 63, and 64 illustrate the spectral features during this 4 day period, including 17.5 Hz side bands about the planetary gear mesh frequency.

Sensor # 3 (Mast Cover Bolt)

The mean SWE decreased from 18,779 at the end of day 21 to 15,446 during the last testing on day 22. It then remained relatively unchanged for three days, finishing day 25 at 15,373. The amplitude of the 17.25 Hz spectral line varied from undetectable to 11 db and finished day 25 at about 8 db. The planetary gear mesh frequency amplitude also fluctuated from a maximum of 10 db to a minimum of 6 db where it finished on day 25. There was no significant harmonic content in either of these frequencies.

Sensor # 4 (Input Pinion Housing)

The mean SWE increased from 112,363 to 119,837 during testing on day 22, then fell back down to 111,516 on the next day. The SWE then increased slowly for the remainder of this 4 day period and finished day 25 at 118,676. A significant change in spectral features accompanied the SWE increase on day 22. Figures 65 and 66 show these spectral changes which included lines of 10 db or greater at the planet passage frequency, the input pinion gear 1/rev, and the input pinion gear mesh. When the SWE level fell during operation the following day, all these frequencies disappeared and the spectrum returned to the way it was on day 21. Figures 67 and 68 are the spectra obtained at the end of day 25. All spectral lines except 600 Hz and its harmonics have disappeared. The 600 Hz frequency has an amplitude of only 8 db above background, and two harmonics that are 2-3 db each. 600 Hz is the ball passage frequency over a point on the outer race of the input pinion triplex bearing.

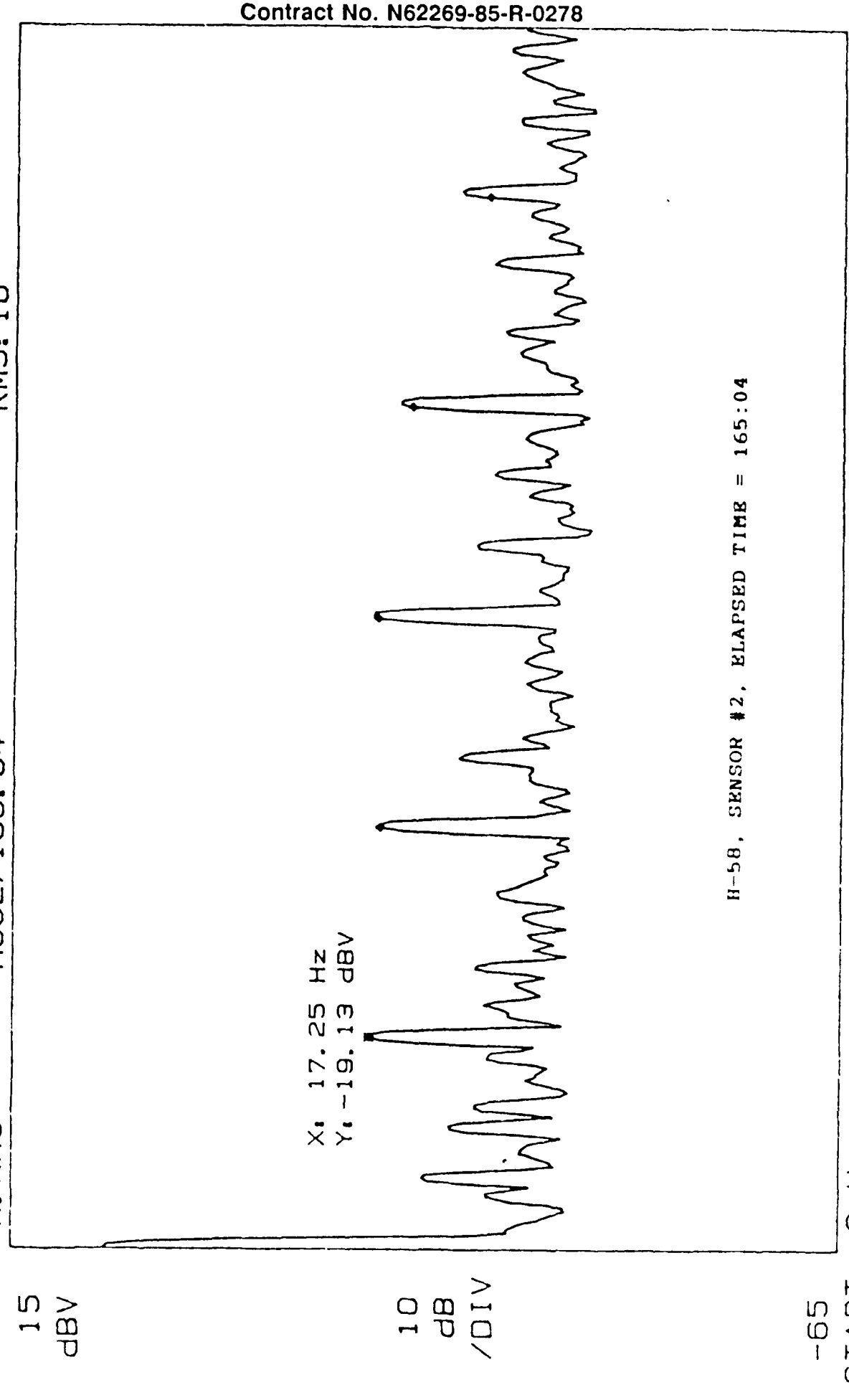
A: MAG
RANGE: 15 dBV
H582/165:04
STATUS: PAUSED
RMS: 10
X: 17.25 Hz
Y: -19.13 dBV
H-58, SENSOR #2, ELAPSED TIME = 165:04
15 dBV
10 dB /DIV
-65
START: 0 Hz
X: 17.25 Hz
BW: 954.85 mHz
Y: -19.13 dBV
STOP: 100 Hz
THD: 3.28 dB

Figure 62

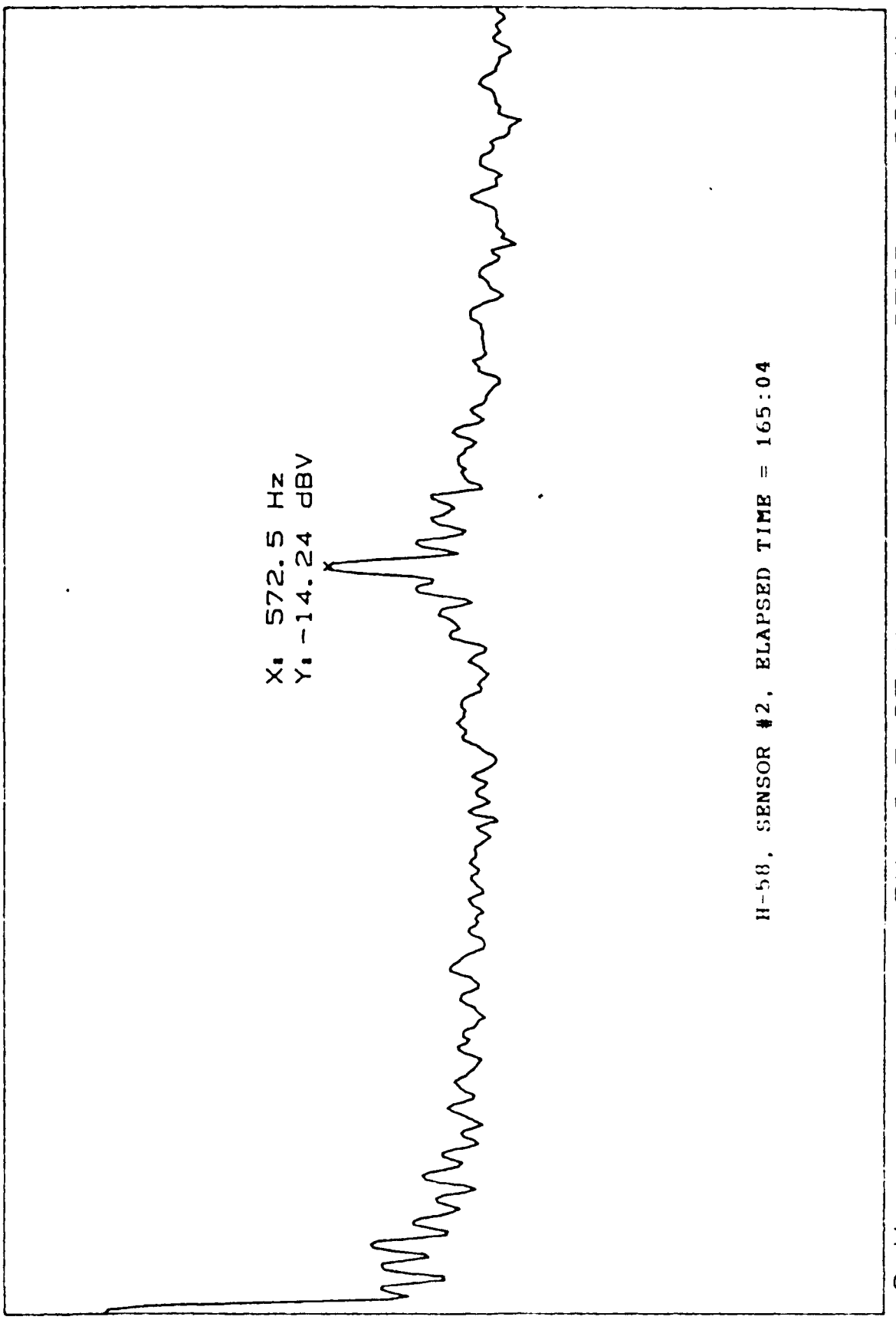
A: MAG
RANGE: 15 dBV
H582/165:04
STATUS: PAUSED
RMS: 25
X: 572.5 Hz
Y: -14.24 dBV
H-58, SENSOR #2, ELAPSED TIME = 165:04
15 dBV
10 dB /DIV
-65
START: 0 Hz
X: 572.5 Hz
BW: 9.5485 Hz
Y: -14.24 dBV
STOP: 1 000 Hz

Figure 63

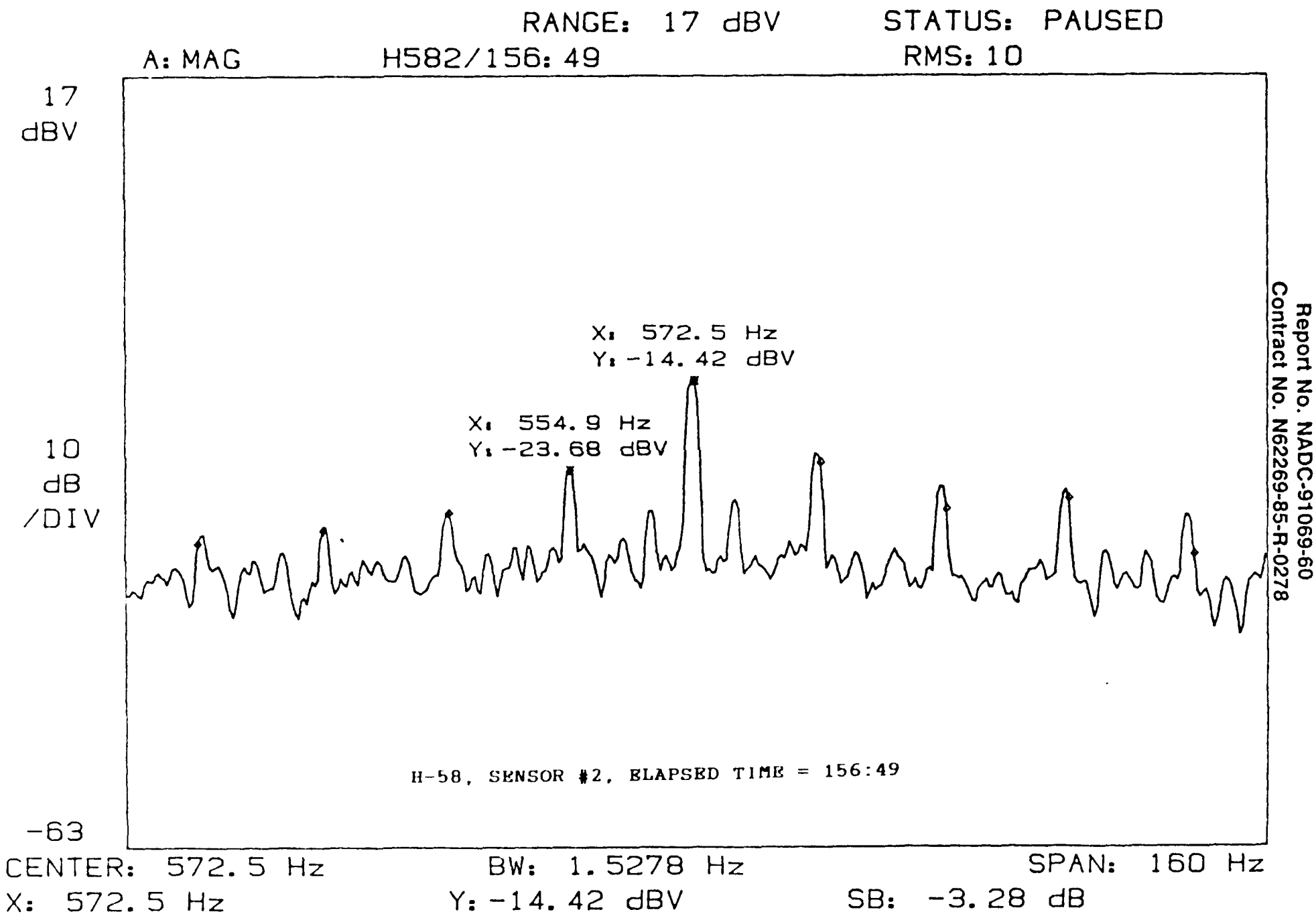

Report No. NADC-91069-60
Contract No. N62269-85-R-0278

Figure 64

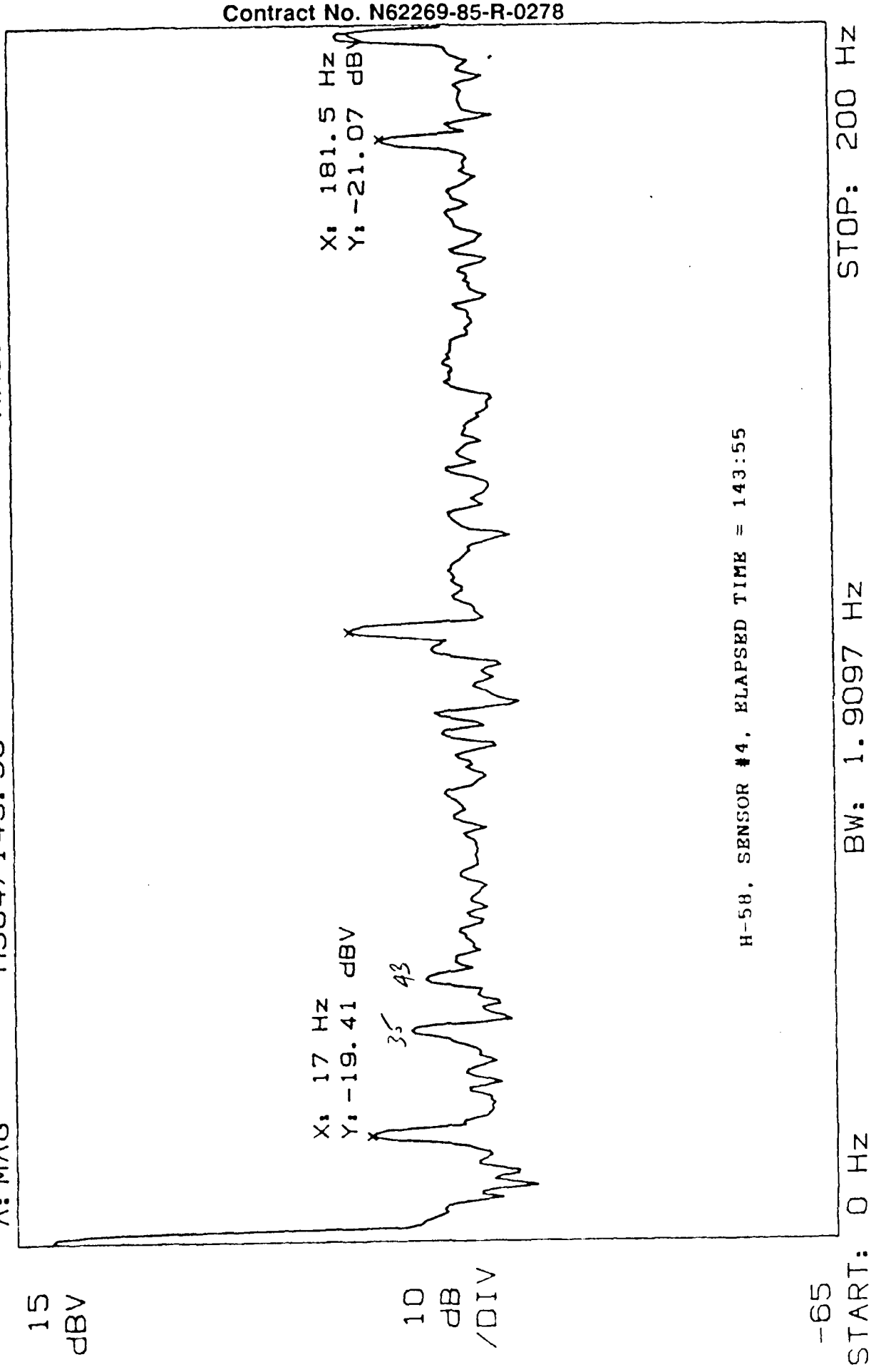
A: MAG
RANGE: 15 dBV
H584/143:55
STATUS: PAUSED
RMS: 10
X: 181.5 Hz
Y: -21.07 dBV
X: 17 Hz
Y: -19.41 dBV
35
43
H-58, SENSOR #4, ELAPSED TIME = 143:55
BW: 1.9097 Hz
Y: -17.57 dBV
NO FUND
15 dBV
10 dB /DIV
-65
START: 0 Hz
STOP: 200 Hz
X: 100.5 Hz

Figure 65

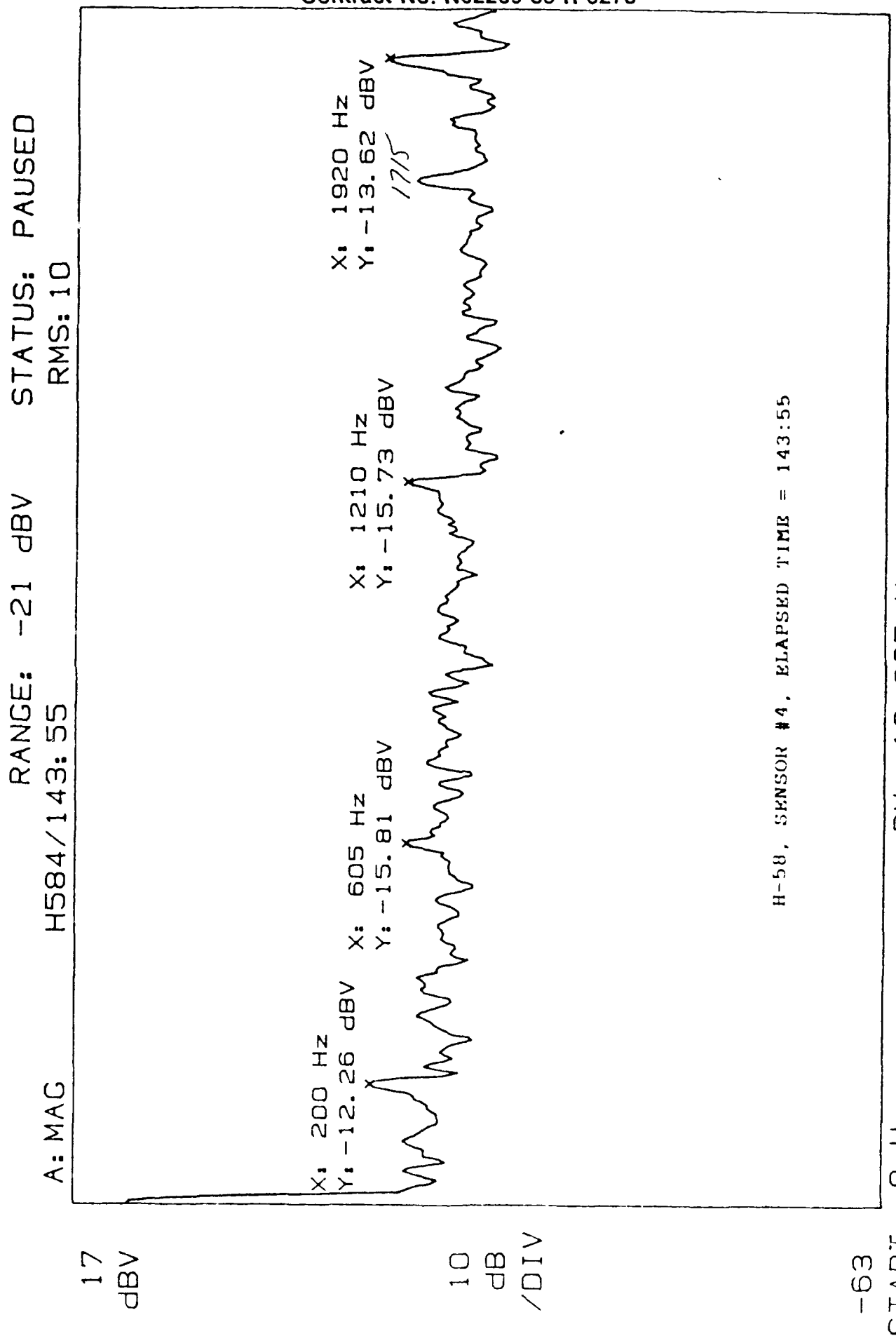
A: MAG
RANGE: -21 dBV
H584/143:55
STATUS: PAUSED
RMS: 10
X: 200 Hz
Y: -12.26 dBV
X: 605 Hz
Y: -15.81 dBV
X: 1210 Hz
Y: -15.73 dBV
X: 1920 Hz
Y: -13.62 dBV
H-58, SENSOR #4, ELAPSED TIME = 143:55
17
dBV
10
dB
/DIV
-63
START: 0 Hz
X: 1920 Hz
BW: 19.097 Hz
Y: -13.62 dBV
STOP: 2 000 Hz

Figure 66

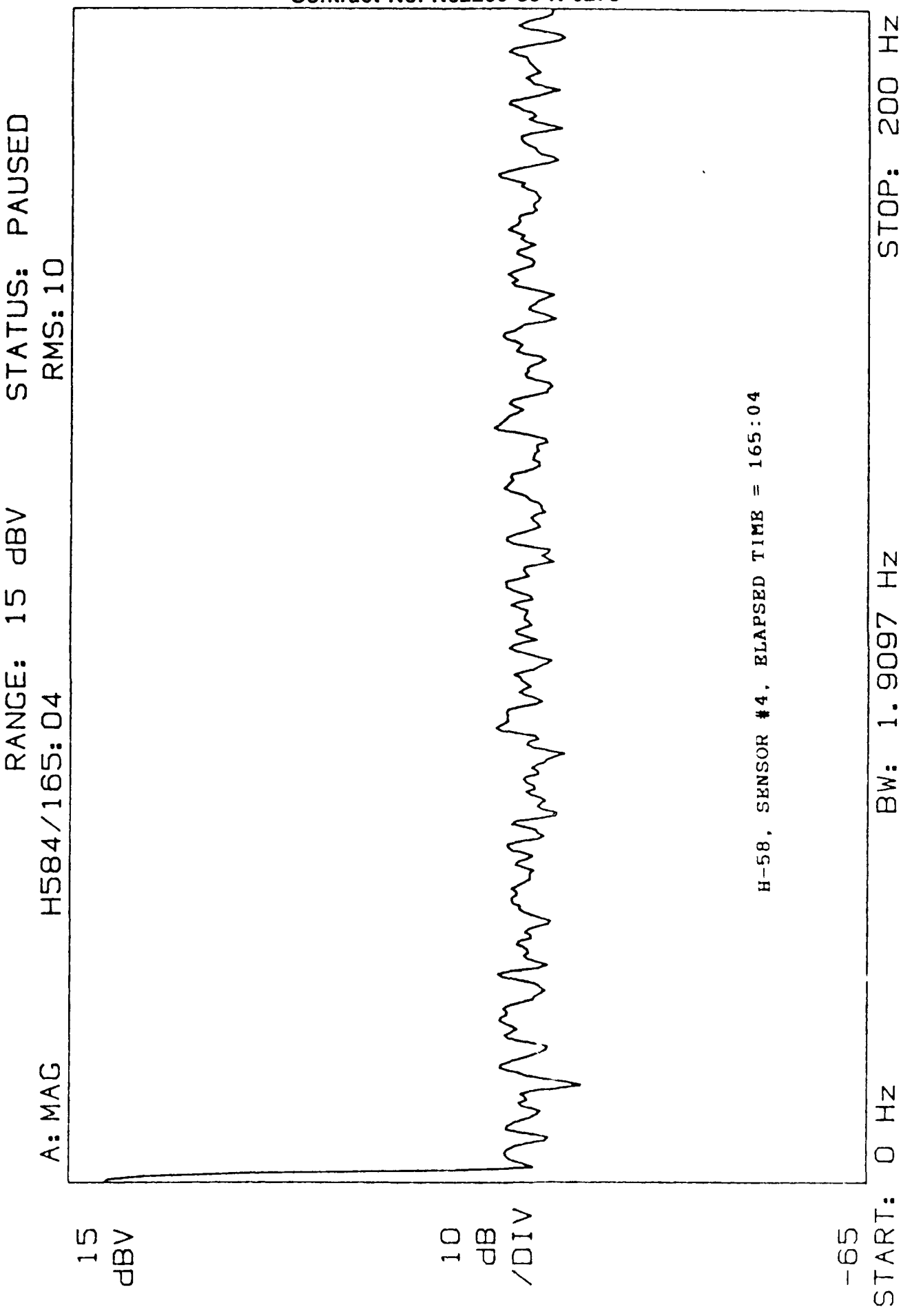
A: MAG
RANGE: 15 dBV
H584/165: 04
STATUS: PAUSED
RMS: 10
15 dBV
10 dB /DIV
-65
START: 0 Hz
BW: 1.9097 Hz
STOP: 200 Hz
H-58, SENSOR #4, ELAPSED TIME = 165:04

Figure 67

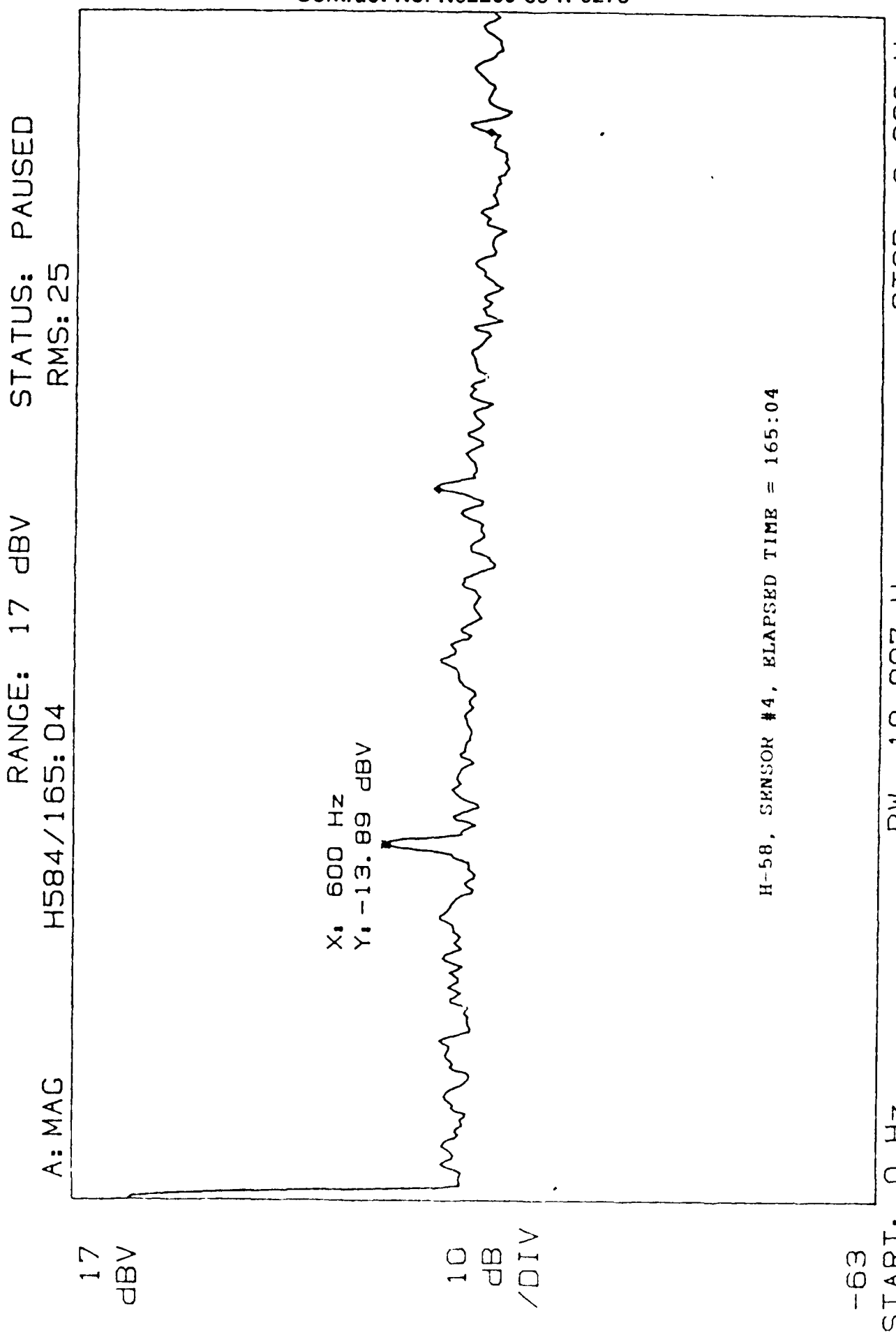
A: MAG
RANGE: 17 dBV
H584/165:04
STATUS: PAUSED
RMS: 25
X: 600 Hz
Y: -13.89 dBV
H-58, SENSOR #4, ELAPSED TIME = 165:04
17
dBV
10
dB
/DIV
-63
START: 0 Hz
X: 600 Hz
BW: 19.097 Hz
Y: -13.89 dBV
STOP: 2 000 Hz
THD: -3.67 dB

Figure 68

Day 26, Total Test Time = 169:08

Sensor #1 (Top Cover Bolt #1)

The mean SWE increased from 46,838 on day 25 to 72,447 on day 26. The spectral characteristics changed dramatically in conjunction with this rapid increase in SWE. The dominant spectral feature became a 21 db, 23 Hz spectral line and its harmonics. Figure 69 illustrates this feature. This 23 Hz frequency is very close to the 1/rev of the sun gear. The 1st harmonic of the rotor shaft 1/rev and the planet passage frequency are also over 10 db in amplitude, although their fundamental frequencies are at low amplitude. Figure 70 shows the 568 hz line associated with the planetary gear mesh,and figure 71 shows the 23 Hz side bands formed around this frequency.

Sensor #2 (Top Cover Bolt #2)

The mean SWE decreased from 63,692 at the end of testing on day 25 to 58,973 by the end of day 26. The spectral characteristics show a dramatic change, similar to that displayed by sensor #1. The only significant spectral line is at 23 Hz and its harmonics. Furthermore, the strongest spectral line is at the 3/rev of the sun gear, which is the frequency at which a point on the sun gear contacts the three planet gears. Figures 72 and 73 illustrate these features.

Sensor # 3 (Mast Cover Bolt)

The mean SWE decreased from 15,373 at the end of day 25 to 12,229 during the last testing on day 26. All significant spectral characteristics disappeared.

Sensor # 4 (Input Pinion Housing)

The mean SWE increased from 118,676 to 131063 during testing on day 26. There are no spectral lines of 10 db or more in amplitude, but the 23.5 hz sun gear frequency is a new feature with an amplitude of about 8 db. The input pinion 1/rev at 101 Hz is also present along with its associated (harmonic ?) 193 Hz spectral line.

Day 28, Total Test Time = 183:33

Sensor #1 (Top Cover Bolt #1)

The mean SWE decreased from 72,447 on day 26 to 63,807 on day 28. The dominant spectral feature remains a 21 db, 23 Hz spectral line and its harmonics. Figure 74 illustrates this feature. Figure 75 shows the 568 hz line associated with the planetary gear mesh, and figure 76 shows the 23 Hz side bands formed around this frequency.

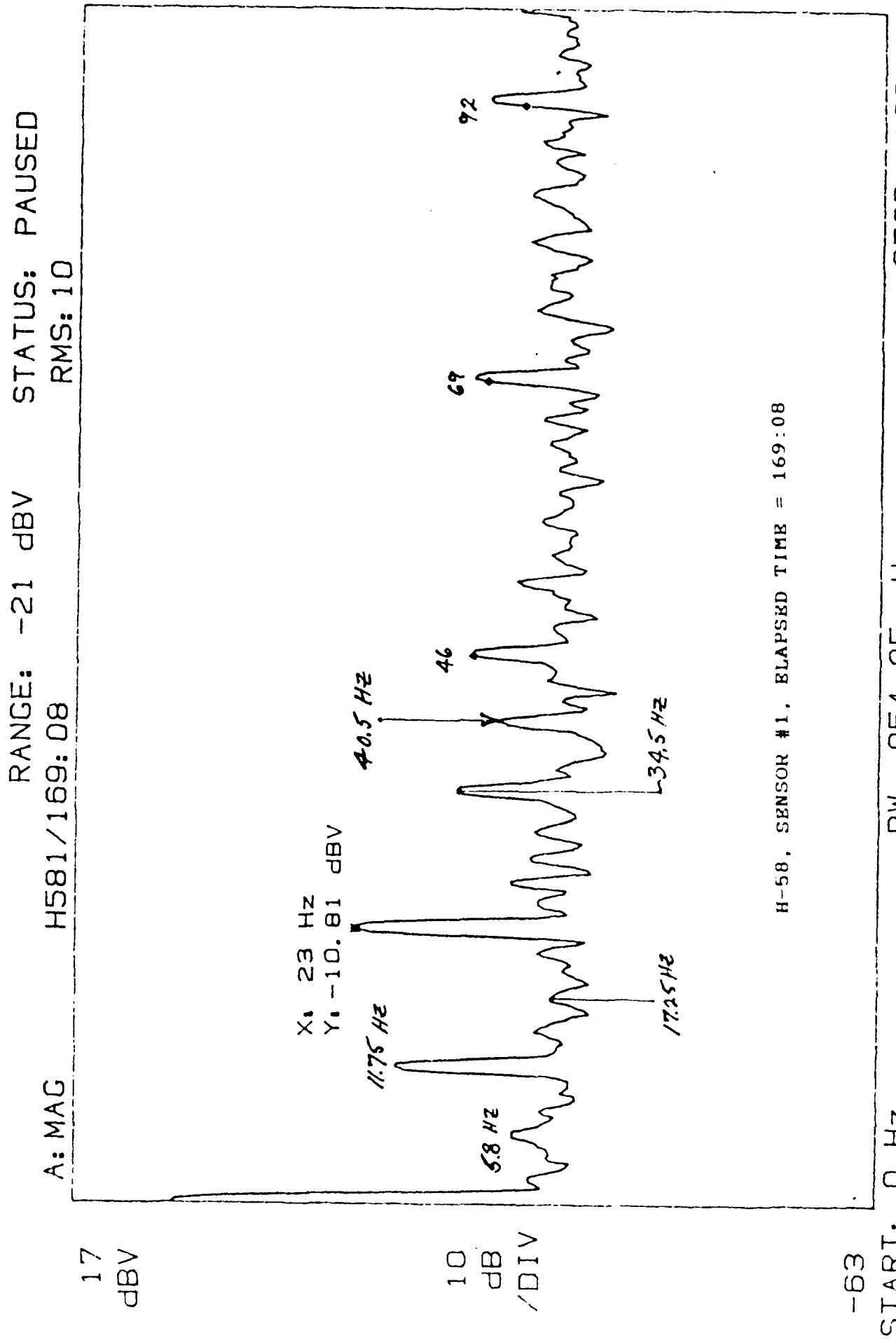
A: MAG
H581/169: 08
RANGE: -21 dBV
STATUS: PAUSED
RMS: 10
X: 23 Hz
Y: -10.81 dBV
40.5 Hz
46
69
92
11.75 Hz
5.8 Hz
34.5 Hz
17.25 Hz
H-58, SENSOR #1, ELAPSED TIME = 169:08
17 dBV
10 dB/DIV
-63
START: 0 Hz
X: 23 Hz
BW: 954.85 mHz
Y: -10.81 dBV
STOP: 100 Hz
THD: -8.41 dB

Figure 69

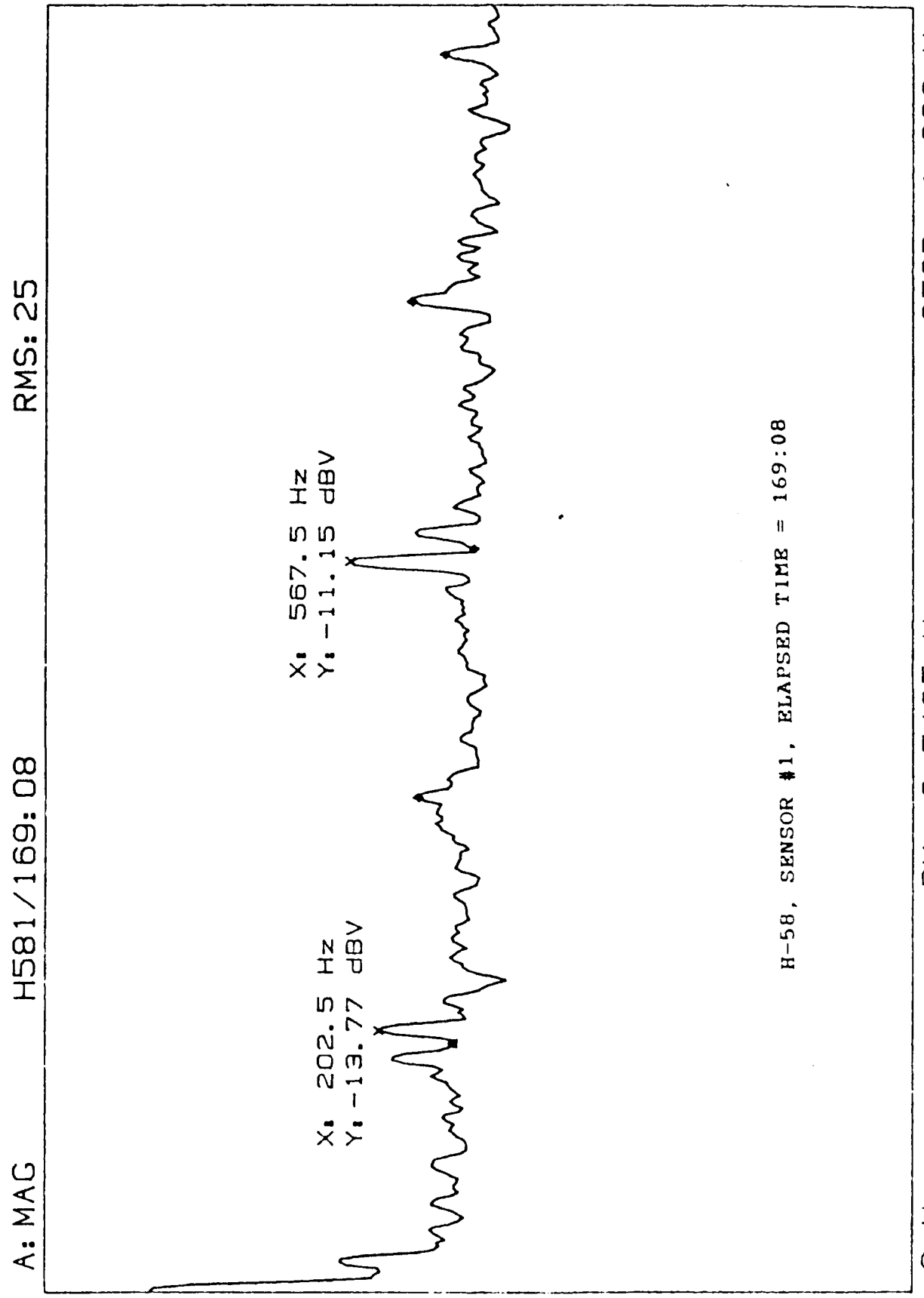
A: MAG
RANGE: 17 dBV
H581/169: 08
STATUS: PAUSED
RMS: 25
X: 567.5 Hz
Y: -11.15 dBV
X: 202.5 Hz
Y: -13.77 dBV
H-58, SENSOR #1, ELAPSED TIME = 169:08
17 dBV
10 dB /DIV
-63
START: 0 Hz
X: 192.5 Hz
BW: 9.5485 Hz
Y: -20.48 dBV
STOP: 1 000 Hz
THD: 7.96 dB

Figure 70

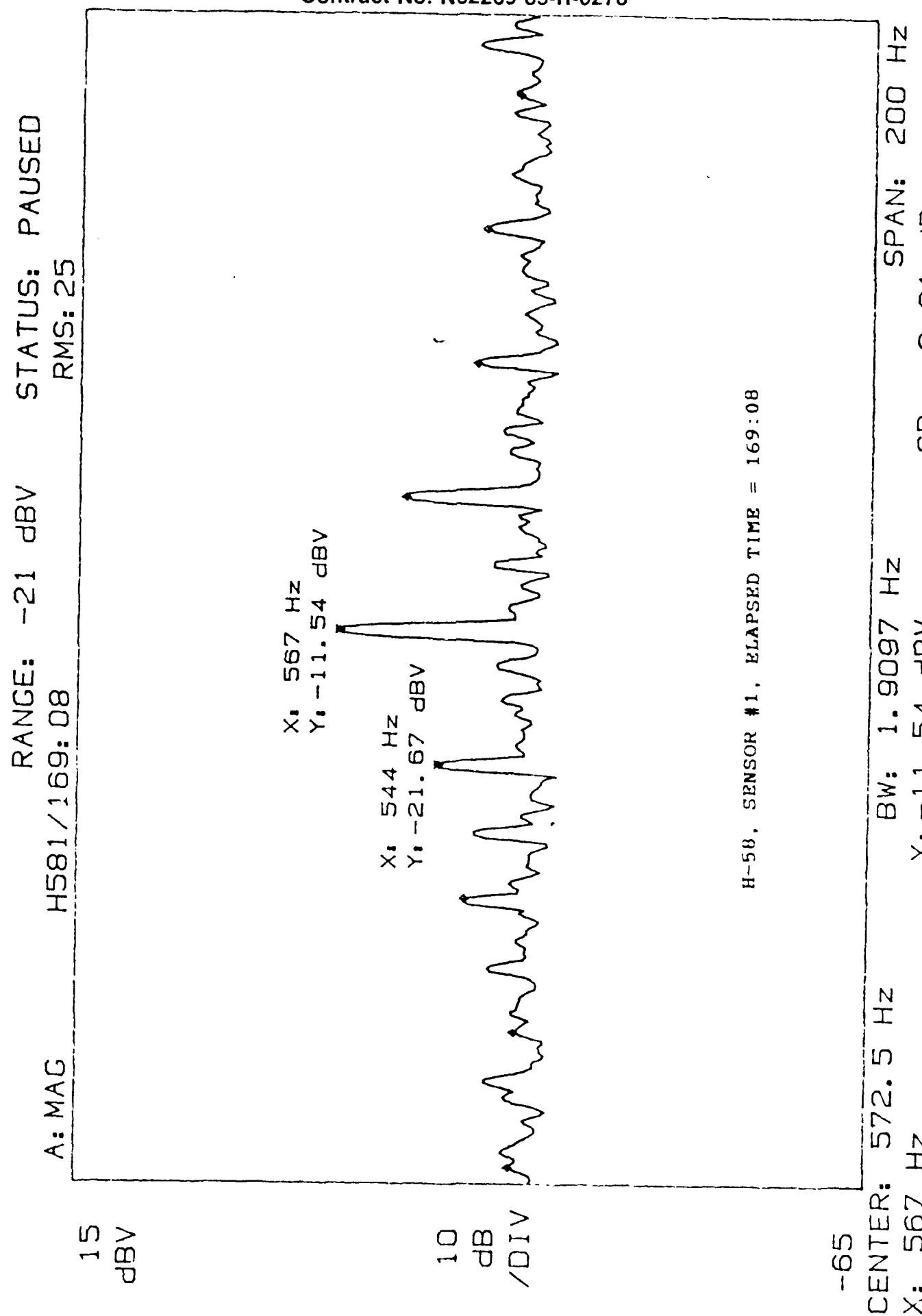
A: MAG
RANGE: -21 dBV
H581/169:08
STATUS: PAUSED
RMS: 25
X: 567 Hz
Y: -11.54 dBV
X: 544 Hz
Y: -21.67 dBV
H-50, SENSOR #1, ELAPSED TIME = 169:08
15 dBV
10 dB /DIV
-65
CENTER: 572.5 Hz
X: 567 Hz
BW: 1.9097 Hz
Y: -11.54 dBV
SPAN: 200 Hz
SB: -3.01 dB

Figure 71

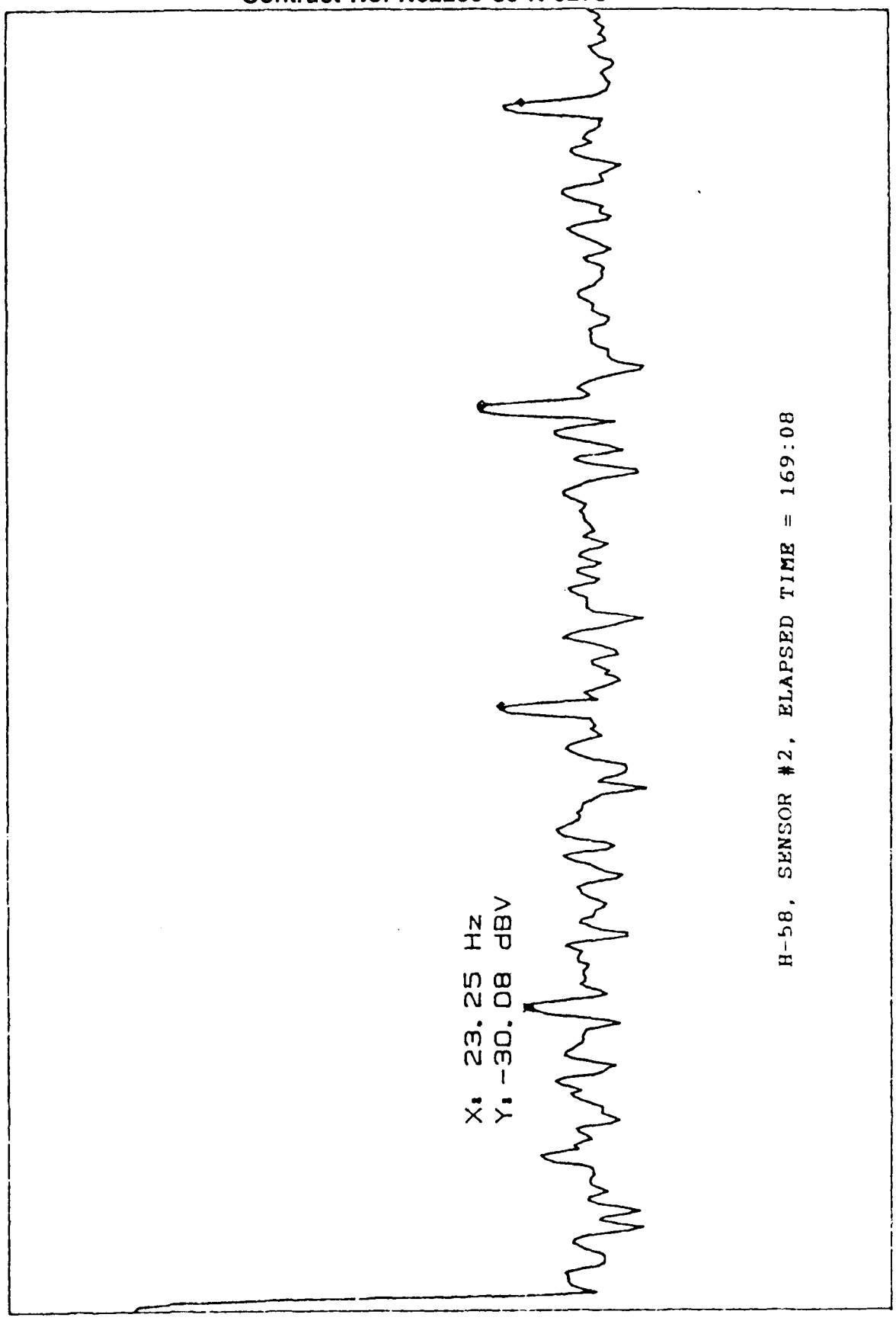
A: MAG
RANGE: -21 dBV
H582/169: 08
STATUS: PAUSED
RMS: 10
X: 23.25 Hz
Y: -30.08 dBV
H-58, SENSOR #2, ELAPSED TIME = 169:08
17
dBV
10
dB
/DIV
-63
START: 0 Hz
X: 23.25 Hz
BW: 954.85 mHz
Y: -30.08 dBV
STOP: 100 Hz
THD: 7.20 dB

Figure 72

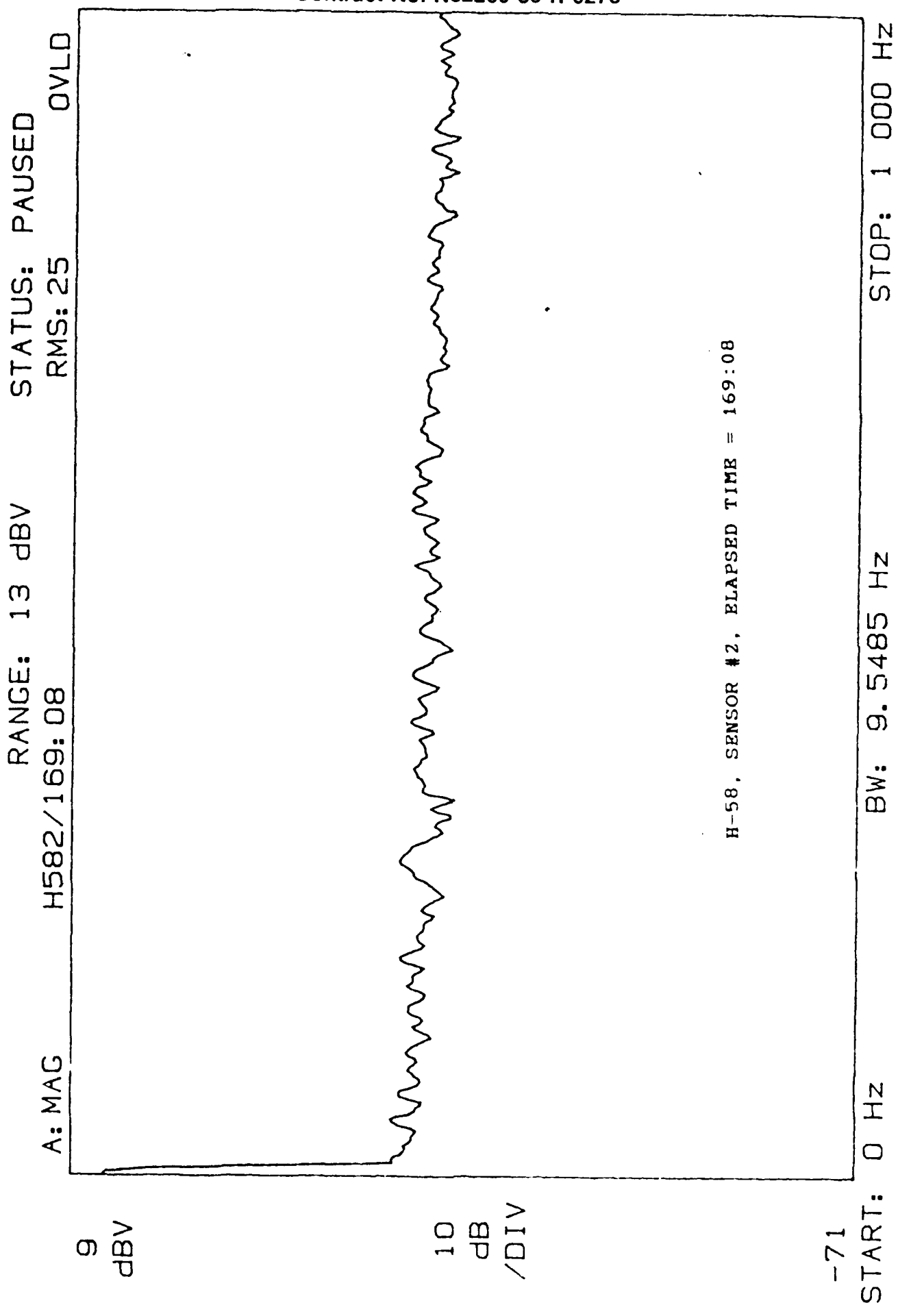
A: MAG
RANGE: 13 dBV
H582/169: 08
STATUS: PAUSED
RMS: 25
OVLD
9
dBV
10
dB
/DIV
-71
START: 0 Hz
BW: 9.5485 Hz
STOP: 1 000 Hz
H-58, SENSOR #2, ELAPSED TIME = 169:08

Figure 73

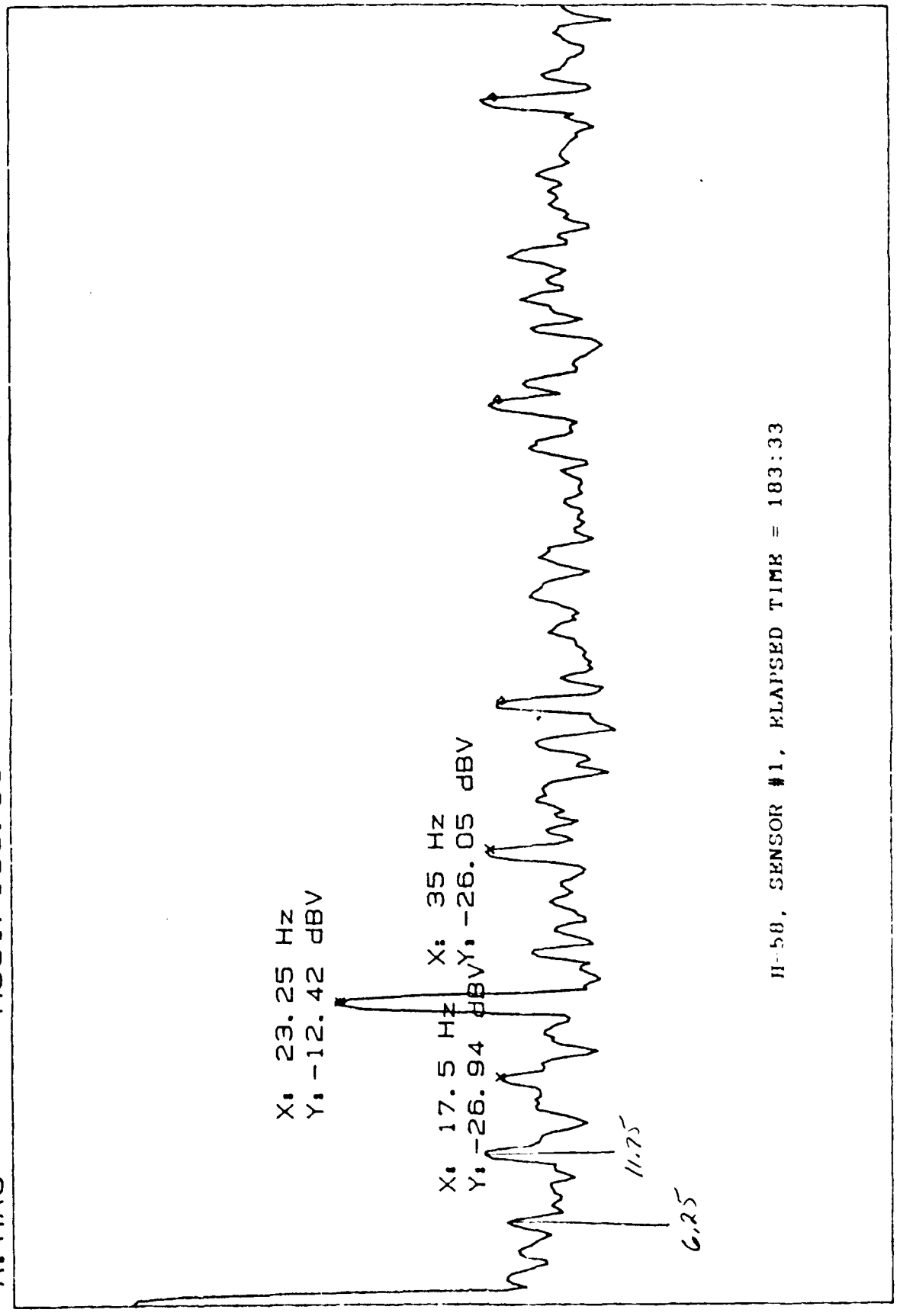
A: MAG
RANGE: ±81dBV
H581/183:33
STATUS: PAUSED
RMS: 10
X: 23.25 Hz
Y: -12.42 dBV
X: 35 Hz
Y: -26.05 dBV
X: 17.5 Hz
Y: -26.94 dBV
11.25
6.25
H-58, SENSOR #1, ELAPSED TIME = 183:33
BW: 954.85 mHz
Y: -12.42 dBV
STOP: 100 Hz
THD: -9.76 dB
17
dBV
10
dB
/DIV
-63
START: 0 Hz
X: 23.25 Hz

Figure 74

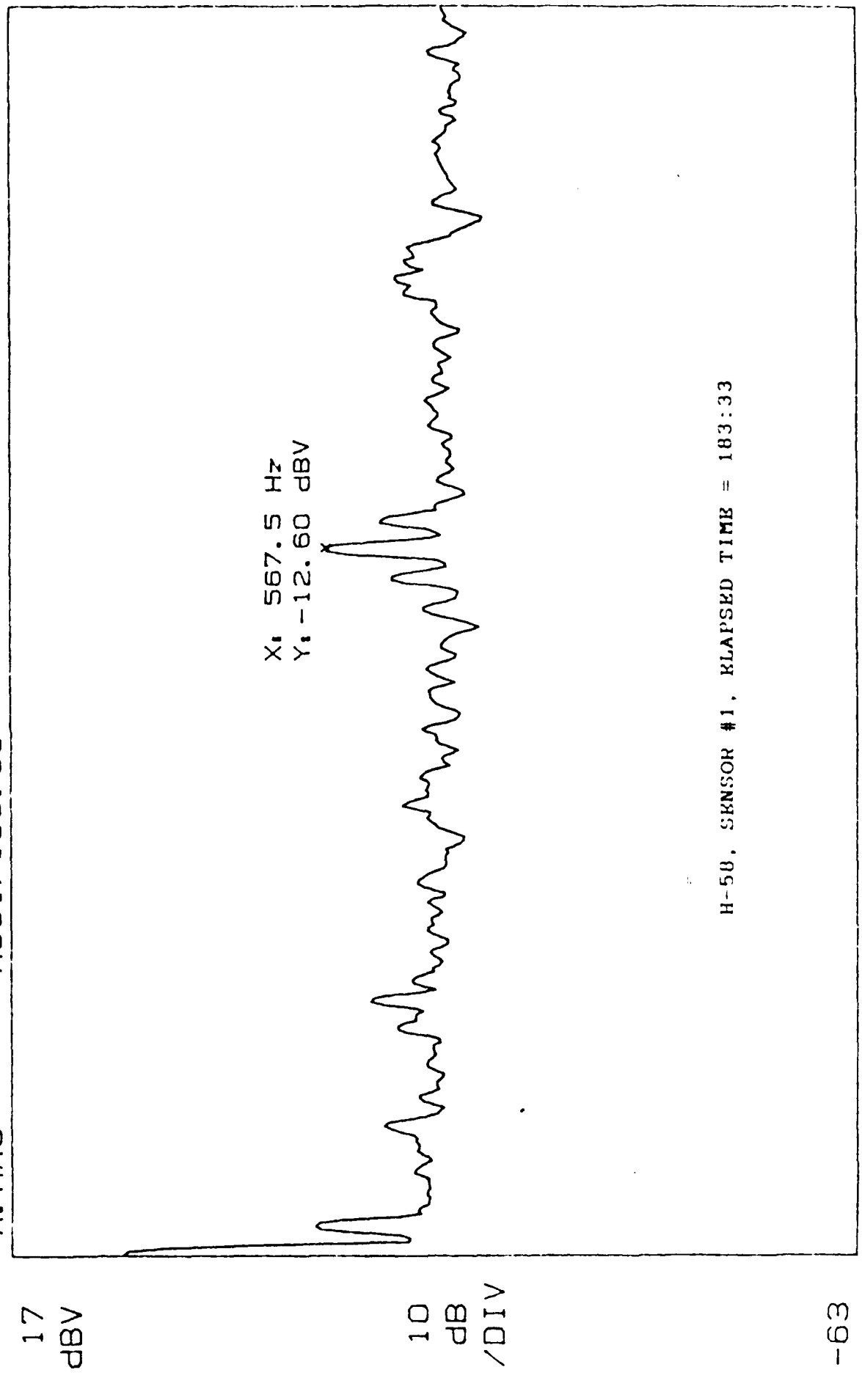
A: MAG
RANGE: -21 dBV
H581/183:33
STATUS: PAUSED
RMS: 25
X: 567.5 Hz
Y: -12.60 dBV
H-58, SENSOR #1, ELAPSED TIME = 183:33
17
dBV
10
dB
/DIV
-63
START: 0 Hz
X: 567.5 Hz
BW: 9.5485 Hz
Y: -12.60 dBV
STOP: 1 000 Hz

Figure 75

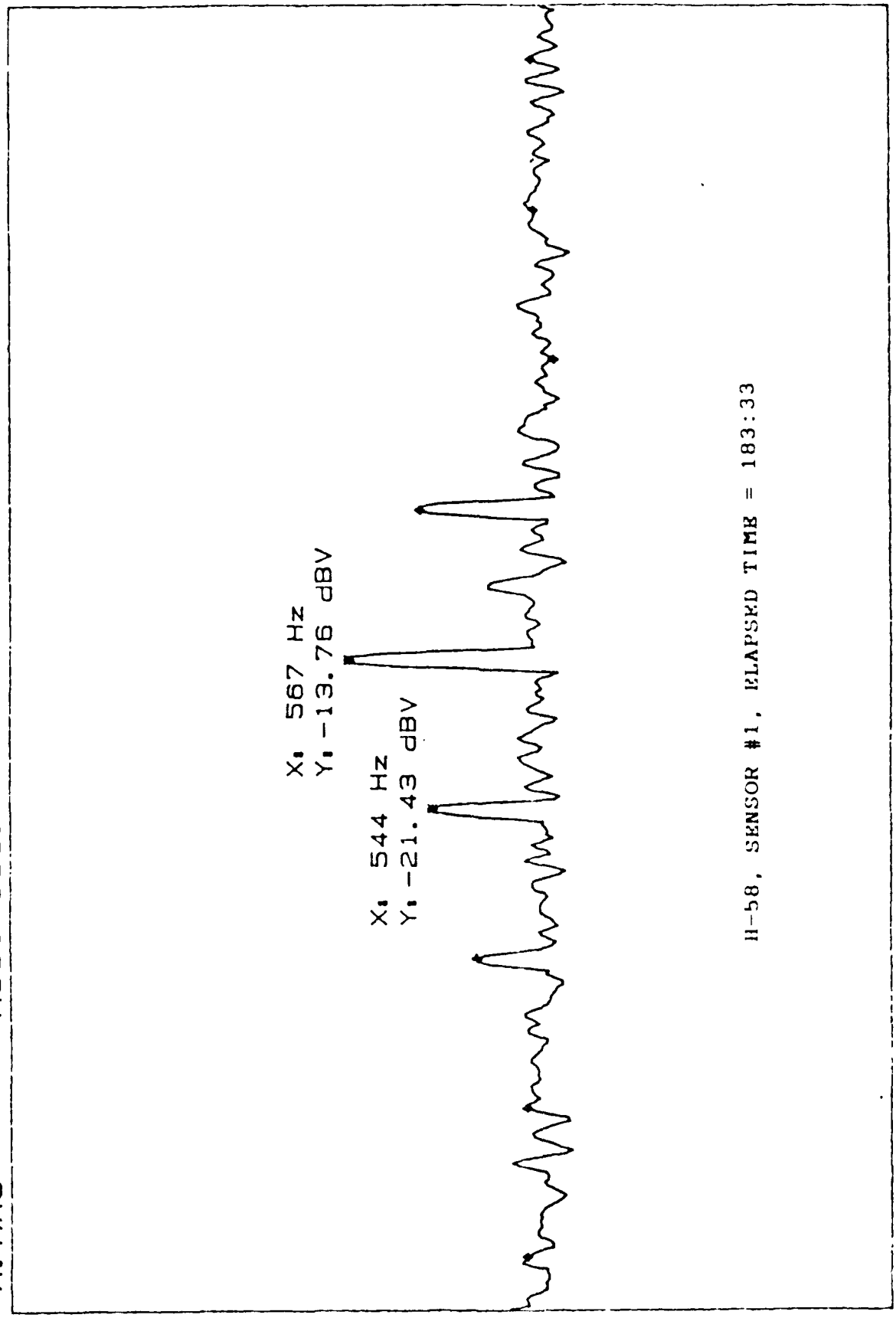
RANGE: -21 dBV
STATUS: PAUSED
H581/183:33
RMS:25
A: MAG
X: 567 Hz
Y: -13.76 dBV
X: 544 Hz
Y: -21.43 dBV
H-58, SENSOR #1, ELAPSED TIME = 183:33
17
dBV
10
dB
/DIV
-63
CENTER: 567 Hz
BW: 1.9097 Hz
SPAN: 200 Hz
X: 567 Hz
Y: -13.76 dBV
SB: -2.54 dB

Figure 76

Sensor #2 (Top Cover Bolt #2)

The mean SWE remained essentially constant from day 26 through day 28. The only significant spectral line is at 23 Hz and its harmonics.

Sensor # 3 (Mast Cover Bolt)

The mean SWE remained essentially constant from day 26 through day 28. There are no spectral lines with an amplitude of 10 db or more, but a 6 db 23 Hz frequency is also present at this sensor location.

Sensor # 4 (Input Pinion Housing)

The mean SWE increased from 131,063 to 162,336 during the last two days of testing. There are four spectral lines of 10 db or more in amplitude: the 23.5 Hz sun gear frequency at 13 db, the 101 Hz input pinion 1/rev at 13 db, the 1920 Hz input pinion gear mesh at 11 db, and the 570 Hz planetary gear mesh at 10 db.

5.0 Conclusions and Recommendations

5.1 CH-46 Input Pinion Anomaly

Conclusions

Due to the limited amount of data obtained, it is not realistic to draw firm conclusions on this issue. It appears as though the "peaking" of SWE readings during taxi operations with the nose gear raised off the ground is associated with either the blower drive gear assembly or the idler gear assembly in the mix box. Of these two possibilities, the blower drive gear assembly seems to be the most likely cause. It is hypothesized that small amounts of fuselage structural bending are caused by exerting more collective pitch and lifting forces on the front of the CH-46 tandem rotor helicopter. This structural bending the causes a small amount of misalignment between the oil cooler blower and its related drive gear assembly in the mix box. Misalignment typically results in cyclic loading of the gear at its 1/rev frequency, in this case 126 Hz. Both this 1/rev frequency and the SWE increased and decreased at the same time on aircraft #04. This fact is the strongest piece of evidence to support this hypothesis. Some perplexing questions on this issue remain:

1. Why would this misalignment of the blower drive assembly, which is located at the top center of the mix box, be observable at transmission input pinion but not at other points on the mix box ?

2. Why was this "peaking" phenomenon not observed on the #01 aircraft ?

Regardless of the uncertainty associated with the above, it can be stated that at no time has this SWE "peaking" with the nose high attitude been related to the 1/rev of the transmission input pinion/quill shaft nor any of the characteristic defect frequencies of its support bearings.

On aircraft #01 there was a considerable amount of SWE at the 1/rev frequency of the mix box input pinion gear. This was most evident on the number 2 side of the mix box and was a much more dominant spectral characteristic on aircraft #01 than on aircraft #02. This may be related to why "peaking" could not be observed on aircraft #01 since the amounts of SWE generated by input pinion imbalance or misalignment could obscure the SWE from misalignment of the slower speed blower drive gear. Unfortunately, the difference in tape recorder gains make it impossible to directly compare SWE data from the mix box sensor locations to see if aircraft #01 had higher SWE levels than aircraft #02. If aircraft #01 did have higher SWE levels than aircraft #02, it could be the answer to question 2 above. Another possible factor in answering question 2 would be any differences between aircraft in the basic alignment of the oil cooler blower and the mix box.

Recommendations

1. The data collection on aircraft #01, or another H-46 of the same model should be repeated using the same gain settings as used on aircraft #04.

2. When accomplishing recommendation number 1, an additional sensor should be mounted on the mix box housing in the vicinity of the blower drive assembly.

Implementation of the above recommendations will assist in answering both questions 1 and 2.

5.2 OH-58 Advanced Lubrication Testing

Conclusions

The numerous changes in SWE and their correlation with changes in gear and bearing spectral characteristics clearly demonstrate the ability of Stress Wave Analysis to monitor the condition of dynamic components in helicopter transmissions. The specific spectral characteristics observed in conjunction with SWE trends indicate that several different types of discrepant conditions developed during the 28 days of testing. These discrepancies include:

1.) Planet gear/bearing assembly damage or damage to the teeth on the stationary ring gear of the planetary gear system.

2.) Damage to the sun gear located at the center of the planetary gear system.

3.) Probable damage to the input pinion gear and one or more of the outer races of its triplex bearing. The changing amplitudes of the input pinion 1/rev in conjunction with fluctuations in the SWE level, as well as the relatively low amplitudes of the bearing outer race frequencies, are indicative of pieces of metallic debris becoming cold worked onto the surface of the gear teeth and bearing race.

4.) While there is no evidence of damage to the mast bearing, its extremely high initial SWE reading is indicative of a problem that quickly "worked itself out". This could have been a short term lubrication problem, skidding of bearing rolling elements, or a rubbing between some rotating and non-rotating structures that ceased after "wear in".

5.) At several locations and at several times during the 28 days of testing, evidence was present to indicate the presence of particulate debris becoming entrapped and

cold worked onto the contact surfaces of gears and bearings.

Recommendations

1.) The observations documented in this report should be correlated with the debris indications from chip detectors during the 28 days of testing.

2.) The observations documented in this report should be correlated with maintenance actions taken during the 28 days of testing.

3.) The observations documented in this report should be correlated with the results of disassembly inspection reports generated during the 28 days of testing.

DISTRIBUTION LIST (Continued)
Report No. NADC-91069-60

No. of Copies

Liberty Technology Center, Inc.
Lee Park, 1100 E. Hector Street
Conshohocken, PA 19428
Mr. M. Dowling 1

Diagnostic Equipment Development, Inc.
6899 N.E. 7th Ave.
Boca Raton, FL 33487
Mr. D. Board 1

Monitoring Technology Corporation
2779 Hartland Rd.
Falls Church, VA 22043
Dr. E. Page 1

Technology Integration and Development Group, Inc.
One Progress Road
Billerica, MA 01821
Mr. N. Higbie 1

Dynamic Instruments, Inc.
9440 Carroll Park Drive
San Diego, CA 92121-2256
Mr. H. Ness 1

Franklin Research Center
Valley Forge Corporate Center
2600 Monroe Boulevard
Norristown, PA 19403
Mr. M. Neary 1

Defense Technical Information Center
ATTN: DTIC-FDAB
Cameron Station BG5
Alexandria, VA 22304-6145

Center for Naval Analysis
4401 Fort Avenue
P.O. Box 16268
Alexandria, VA 22302-0268 1

DISTRIBUTION LIST
Report No. NADC-91069-60

	No. of Copies
Naval Air Development Center Warminster, PA 18974-5000	
Code 6061, Tony DeGennaro	12
Code 8131	2
David Taylor Research Center Annapolis, MD 21402-5067	
Code 272Z, Mr. B. Nickerson	2
David Taylor Research Center Bethesda, MD 20084-5000	
Code 187, Mr. R. Ploe	2
Code 18071, Mr. J. Chesley	2
Naval Air Test Center Patuxent River, MD 20670-5304	
RWATD, Code RW82B, Mr. M. Hollins	1
Naval Aviation Depot Naval Air Station Pensacola, FL 32508-5300	
PSD, Code 310, Mr. Bill Sullivan	1
NASA, Lewis Research Center Cleveland, OH 44135	
Code 2730, MS77-10, Mr. D. Townsend	2
U.S. Army Aviation Research & Technology Activity Advanced Aviation Technology Directorate, (AVSCOM) Ft. Eustis, VA 23604-5577	
SAVRT-TY-AFR, Mr. H. Young	1
Army Tank Automotive Command Warren, MI 48397-5000	
AMSTA-RVD, R.J. Watts	1
Bell Helicopter Textron P.O. Box 482 Fort Worth, TX 76101	
Structural Dynamics, Mr. W. Wilson	1
Boeing Helicopter P.O. Box 16858 Philadelphia, PA 19142	
Structural Dynamics, Mr. J. Rose	1